Mass spectrometry for measuring protein secretion from insulin sensitive tissues during obesity

Lindsay Edward Wu

Thesis submitted in partial fulfilment of the requirements for the degree of

Doctor of Philosophy

Performed at the

Garvan Institute of Medical Research

In collaboration with the

Bioanalytical Mass Spectrometry Facility,

University of New South Wales

Supervisor: **Professor David E. James** Garvan Institute of Medical Research

Co-supervisor: **Professor Michael Guilhaus** University of New South Wales

1st February, 2010

ORIGINALITY STATEMENT

‘I hereby declare that this submission is my own work and to the best of my knowledge it contains no materials previously published or written by another person, or substantial proportions of material which have been accepted for the award of any other degree or diploma at UNSW or any other educational institution, except where due acknowledgement is made in the thesis. Any contribution made to the research by others, with whom I have worked at UNSW or elsewhere, is explicitly acknowledged in the thesis. I also declare that the intellectual content of this thesis is the product of my own work, except to the extent that assistance from others in the project's design and conception or in style, presentation and linguistic expression is acknowledged.’

Signed …….....

Date …….....

Table of Contents

TABLE OF CONTENTS 2
SUMMARY 5
ACKNOWLEDGEMENTS 7
PUBLICATIONS & PRESENTATIONS 8
LIST OF FIGURES 9
ABBREVIATIONS 14

CHAPTER 1 17

The type 2 diabetes epidemic 18
Historical diagnosis of type 2 diabetes 20
Type 2 diabetes and insulin resistance 21
Insulin resistance and type 2 diabetes 27
Adipokines in insulin resistance 29
Mass spectrometry and identification of secreted proteins 36
Adipokine identification by mass spectrometry 40
Improvement on previous studies 47
Aims of investigation 49

CHAPTER 2 51

Abstract 52
Introduction 53
Methods 56
Cell culture 56
Conditioned media experiments 58
Glycoprotein purification 58
Protein visualisation 59
Amino acid isotopes 59
Mass spectrometry 60
Results 63
Glycoprotein purification reduces cytoplasmic contamination in conditioned media samples. 63
Secretome of insulin sensitive tissues 69
Survey of hepatocyte secretome 78
Survey of skeletal muscle secretome 85
Use of SILAC to probe rates of protein synthesis and secretion 89
Protein secretion during perturbed states 93
Adipokine secretion during insulin resistance 93
Partial SILAC labelling for measuring effects of palmitate on hepatocyte protein secretion 109
Discussion 120

CHAPTER 3 128

Summary 129
Introduction 130
Methods 132

Animal maintenance and experimental protocols 132
Hyperinsulinemic-euglycemic clamps 133
Glucose uptake 133
Cell Culture 134
Conditioned Media experiments 134
Production of recombinant PEDF 135
Lipolysis 135
ConA affinity chromatography 135
Mass spectrometry 136
Cell fractionation 136
Immunofluorescent analysis 137
Muscle lipids 138
qRT-PCR 138
Plasma hormone and metabolite analysis 138
Statistical analysis 138
Immunoblot analysis 139
Results *140*
Identification of the adipocyte secretome by mass spectrometry 140
Adipose tissue and plasma PEDF levels are elevated in obesity 140
PEDF regulates glucose metabolism in skeletal muscle and liver 145
PEDF induces proinflammatory signaling and impairs insulin signalling 149
Prolonged PEDF administration in lean mice causes ectopic lipid deposition and insulin resistance 151
PEDF neutralization in obese, insulin resistant mice improves insulin sensitivity 154
Identity of the PEDF receptor 159
Discussion *164*

CHAPTER 4 169

Introduction *171*
Methods *178*
Materials and buffers 178
Animals 179
Preparation of Anti-CD31 antibody-coated magnetic beads 180
Adipose tissue explants 180
Preadipocyte and endothelial cell isolation and culture 180
Lectin affinity chromatography 182
Amino acid isotopes 183
Mass spectrometry 183
Results *185*
Discussion *201*

CHAPTER 5 207

Abstract *208*
Introduction *209*
Methods *212*
SILAC labelling 212
Mass spectrometry 213
Hypoxia 214
Conditioned media experiments 215
Islet isolation 215
RT-PCR 216

Antibodies, ELISA ... 216
Results ... *218*
Hypoxic adipocyte conditioned media potentiates GSIS ... 218
Identification of FABP4 as an hypoxia regulated secretory protein ... 220
FABP4 enhances β-cell function ... 229
Metabolic poisons stimulate FABP4 secretion ... 233
Non-classical secretion of FABP4 ... 234
Potential modification of FABP4 by 4-hydroxynonenal ... 240
Discussion ... *242*

CHAPTER 6 ... 259

Glycoprotein purification and quantitative mass spectrometry for investigating secretory changes during disease ... 260
Future applications of technique ... 261
Future developments of technique ... 262
3T3-L1 adipocytes versus white adipose tissue explants ... 263
Notable absences from the adipocyte secretome ... 265
FABP4 – future investigations ... 272
Non-classical protein secretion ... 272
Mechanism of action for FABP4 ... 276
Adipose tissue as an endocrine organ? ... 277
Final conclusions ... 278
LIST OF REFERENCES ... 280

Summary

Due to the accessibility of the serum relative to other areas of the body, secretory proteins afford the best opportunity for diagnosis and treatment of disease. Identification of secretory proteins from cell culture conditioned media samples via a mass spectrometry approach has been attempted in the past. Contamination of conditioned media with non-secretory proteins released by necrotic cells dilutes the detection of low-abundance secretory proteins and has thwarted these previous attempts. To circumvent this problem, a lectin affinity chromatography approach was used to exploit N-glycosylation, a post-translational modification common to secretory proteins but largely absent from non-secretory proteins. This approach was used to survey the secretome of multiple insulin sensitive tissues with a focus on adipocytes, which play an integral role in the endocrine system. The anti-angiogenic molecule pigment epithelial derived factor was identified as an adipocyte secretory factor, and an important role for this protein in obesity induced insulin resistance was ascertained.

Lectin affinity chromatography was combined with partial metabolic labelling and mass spectrometry to quantitatively measure protein secretion from tissue explants and primary cultures. This allowed a direct comparison of the secretory abilities of visceral and subcutaneous adipose tissue and their constituent cell types, including endothelial cells, for which little is known of their secretory repertoire. Intrinsic differences in secretory ability were observed between visceral and subcutaneous derived samples, which may help explain the metabolically deleterious effects of visceral, but not subcutaneous, adipose tissue.

Finally in this investigation, conditioned media experiments were used in combination with quantitative mass spectrometry to identify a role for hypoxia-mediated secretion of fatty acid binding protein 4 in the adipocyte – β cell axis. This observation fills an important gap in knowledge regarding insulin measurements during obesity, as it indicates the elevated levels of insulin observed during obesity are not simply due to compensation for insulin resistance. This work has uncovered yet another important endocrine role for adipose tissue. From this work it is becoming clear that insulin levels should not be taken at face value, and are the result of an inter-organ communication network.

Acknowledgements

This thesis would not have been possible without the help and support of many people.

My PhD supervisor Professor David James was a constant source of advice, support and intellectual inspiration. I thoroughly enjoyed our regular conversations and the extraordinarily frank, constructive criticisms that he provided. I am thankful for the confidence he has placed in me, and am hopeful that I have fulfilled his expectations. David's passion for science is an inspiration to younger scientists like me.

Throughout the course of my PhD, I received advice and assistance from members of the Diabetes and Obesity department, including Dr. Georg Ramm, Dr. Jacqueline Stöckli, Dr. Mark Larance and Dr. Kyle Hoehn, for which I am grateful. From the Bioanalytical Mass Spectrometry Facility at UNSW, I received advice and assistance from Dr. Mark Raftery and Dr. Anne Poljak, for which I am again very grateful.

I am thankful to Dr. Matthew Watt and his lab for their collaborative effort in work on PEDF. I am also thankful to a fellow student, Dr. Samantha Hocking, for her collaboration on depot-specific adipose tissue protein secretion. The most exciting work in this thesis regarding the adipo-insular axis arose out of a conversation at the pub with Dr. James Cantley, and I have greatly enjoyed our work, intellectual exchanges and friendship. I look forward to pursuing this project with him further.

My friends and family have provided great moral support to me through my PhD. I would like to thank the regular Friday night Green Park Hotel crowd (past and present) from the department, including Alex Rowland, Kyle Hoehn, Jacqueline Stöckli, Georg Ramm, Mark Larance, James Canley, Amanda Preston, and David James. I would like to thank my parents for their support and for instilling a healthy (but balanced) Chinese work ethic. Perhaps most importantly, I would like to thank my long suffering partner, Stefanie Mikolaizak, with whom we are excitedly expecting our first child later this year. I hope that my absence from you late at night and on weekends will all be worth it in the end.

My PhD was put on hold for three months due to a spinal injury resulting from a rock-climbing accident. I am thankful to my parents for patiently waiting by my bedside while my vertebrae healed, to the friends and family that cheered my spirits in hospital and to Stef as she helped my physical recovery from the accident.

My thoughts are with the family of my co-supervisor, Professor Michael Guilhaus, who passed away last year at too early an age. The passing of this talented, energetic individual reminds us of the reason we are engaged in science. Although basic discovery brings a nation its prestige, and brings an incredible thrill to the scientist fortunate enough to be at the bench, it is through science that real improvements in the human condition are made.

In the past year, our family has lost my grandmother Chin-Hwa Wu, my grandfather Tse-Ngo Wu, and my grandfather Albert Edward Creighton. Along with my passed grandmother Rita Mary Creighton, they were very proud of me and of my family. I miss them, and hereby devote this thesis to their memories.

Publications & Presentations

Crowe S, Wu LE*, Economou C, Turpin SM, Matzaris M, Hoehn KL, Hevener AL, James DE, Duh EJ, Watt MJ. Pigment Epithelial Derived Factor Contributes to Insulin Resistance in Obesity. **Cell Metabolism** 10:1 40-47, 2009. *Equal first author.

Hocking SL, Wu LE*, Guilhaus M, Chisholm DJ, James DE. Instrinsic depot-specific differences in the secretome of adipose tissue, preadipocytes and adipose derived microvascular endothelial cells. Accepted for publication in **Diabetes**. *Equal first author

Hoehn KL, Hohnen-Behrens C, Cederberg A, Wu LE, Turner N, Yuasa T, Ebina Y, James DE. IRS-1-Independent Defects Define Major Nodes of Insulin Resistance. **Cell Metabolism** 7:5 421-433, 2008.

Wu LE, Cantley J, Buchfield JG, James DE. Non-classical secretion of adipocyte fatty acid binding protein. Accepted as poster presentation for 2010 Hunter Cell Biology Meeting to be held in the Hunter Valley, NSW Australia.

Wu LE, Hocking SL, Guilhaus M, Chisholm DJ, James DE. Quantitative Proteomic Survey of Adipokines Secreted from Subcutaneous and Visceral fat depots. Oral presentation in Pincus Taft Young Investigator Finalist session at 2009 Australian Diabetes Society meeting, Adelaide, South Australia.

Wu LE, Raftery M, Guilhaus M, James DE. Proteomic Survey of Myokines Secreted from L6 Myotubes. Poster presentation at 2009 Australian Diabetes Society meeting, Adelaide, South Australia.

Wu LE, Larance ML, Raftery M, Guilhaus M, James DE. Proteomic survey of adipokine secretion during insulin resistance. Poster presentation at 2009 American Diabetes Association meeting, New Orleans Louisiana USA.

List of Figures

Chapter 1 – General Introduction

Figure 1. Projected increases in prevalence of type 2 diabetes.

Figure 2. Glucose homeostasis and insulin stimulated glucose transport.

Figure 3. From the original description of the ob/ob mouse line.

Figure 4. Modified CILAIR workflow for comparing protein synthesis and secretion from two different samples.

Chapter 2 – Measuring Protein Secretion from Insulin Sensitive Tissues

Figure 1. Optimisation of ConA pulldown.

Figure 2. Secretion of a majority of protein species is insulin sensitive.

Figure 3. Con A affinity purification enriches for BFA sensitive secretory proteins from conditioned media to the exclusion of cytosolic proteins.

Figure 4. Secretory profile of 3T3-L1 fibroblasts and differentiated adipocytes.

Table 1. Adipocyte secretory factors identified.

Figure 5. Comparison of published studies for identifying secreted proteins in conditioned media using mass spectrometry.

Figure 6. Secretory profile of primary hepatocytes.

Table 2. Hepatocyte secretory proteins.

Figure 7. Secretory profile of L6 myotubes.

Table 3. Myotube secretory proteins.

Table 4. Use of stable isotopes and mass spectrometry for determining rates of protein synthesis.

Figure 8. Insulin resistance models alter secretion profile of 3T3-L1 adipocytes.

Table 5. Insulin resistance models alter adipokine secretion.

Figure 9. Adipocyte conditioned media displays paracrine effects towards insulin sensitivity.

Figure 10. PRLTS sequence shares identity with ligand binding domain of PDGF receptor β subunit.

Figure 11. PRLTS is predicted to have a signal peptide with peptide cleavage between residues 21 and 22.

Figure 12. PRLTS expression increases during adipogenesis, whilst expression of pro-angiogenic proteins decreases.

Figure 13. Flk-1 (VEFGR2) antisera recognise a protein species of 30 kDa that increases with angiogenesis.

Figure 14. Tissue distribution of PRLTS reveals expression in WAT.

Figure 15. PRLTS staining in adipocytes.

Table 6. PRLTS is upregulated during TNFα treatment.

Figure 16. Palmitate treatment alters secretion of proteins from hepatocytes.

Table 7. Quantitative proteomic comparison of protein secretion from primary hepatocytes during chronic palmitate treatment.

Table 8. Quantitative proteomic comparison of protein secretion from Huh7 hepatomas during hepatitis C infection.

Figure 17. Glycoprotein enrichment increases the detection of secretory proteins

Figure 18. Overlap of protein secretion

Figure 19. URB expression is restricted to adipocytes and muscle.

Pigment Epithelial Derived Factor Contributes in Insulin Resistance in Obesity

Figure 1. PEDF is elevated in obesity and reduced by weight loss.

Figure 2. PEDF expression in mouse tissues.

Figure 3. PEDF expression in mice fed a control (Chow) and high-fat diet (HFD) for 12 weeks.

Figure 4. Acute PEDF administration causes insulin resistance in skeletal muscle and liver

Figure 5. 2-Deoxyglucose uptake experiments in L6 myotubes.

Table 1. Plasma insulin 2 h after PEDF administration and during a glucose tolerance test (GTT).

Figure 6. A direct effect of PEDF on serine/threonine signalling was demonstrated in cultured myotubes.

Figure 7. Prolonged PEDF administration mediates insulin resistance in lean mice.

Figure 8. PEDF causes adipose tissue lipolysis.

Table 2. Body mass and tissue mass following 5 days PEDF neutralization.

Figure 9. PEDF neutralization in obese, insulin-resistant mice improves insulin sensitivity.

Figure 10. Neutralizing PEDF enhances insulin action in myotubes.

Figure 11. Liver diacylglycerol (DG) and ceramide are decreased with PEDF neutralizing antibody treatment.

Figure 12. ATGL does not localise to the plasma membrane or the secretory pathway.

Figure 13. PEDF localises to punctuate structures in adipocytes.

Figure 14. ATGL does not exist at the PM in adipocytes.

Chapter 4 – Depot specific differences in protein secretion from adipose tissue, preadipocytes and adipose tissue derived endothelial cells.

Figure 1. Non-secretory proteins are represented at the lower end of detection range.

Table 1. Comparative secretion of proteins identified from visceral and subcutaneous white adipose tissue explants.

Figure 2. WAT explants secretory proteins are secreted in greater amounts from visceral adipose tissue.

Table 2. Comparative secretion of proteins identified from visceral and subcutaneous adipose tissue derived preadipocytes.

Figure 3. Preadipocyte secreted proteins are secreted at greater amounts from visceral derived preadipocytes.

Table 3. Comparative secretion of proteins identified from visceral and subcutaneous adipose tissue derived endothelial cells.

Figure 4. Endothelial cell secretory proteins are secreted at greater amounts from visceral derived endothelial cells.

Figure 4. Venn diagram showing overlapping proteins detected from samples.

Figure 5. Venn diagram showing overlap of protein secretion from WAT explants, 3T3-L1 adipocytes and isolated rat adipocytes (from Chen et al 2005).

Table 4. Summary of numbers of proteins detected, and relative abundance between visceral and subcutaneous adipose tissue samples.

Chapter 5 – The role of FABP4 in the adipo-insular axis.

Figure 1. Hypoxic adipocyte conditioned media enhances GSIS from islets.

Table 1. MS quantitation of secreted protein abundance during hypoxia.

Figure 2. Alignment and phylogeny of fatty acid binding proteins.

Figure 3. FABP4 is more adipose-specific than FABP5.

Figure 4. FABP4 is released from adipocytes under conditions of hypoxia and mitochondrial stress.

Figure 5. Expression of FABP4 is decreased during hypoxia.

Figure 6. FABP4 is not released via general cell necrosis.

Figure 7. Hypoxia increases cell necrosis.

Figure 8. Fasting levels of FABP4 and insulin are elevated during high fat feeding, despite maintaining normoglycaemia.

Figure 9. Physiological doses of purified recombinant FABP4 enhance glucose-stimulated insulin secretion from islets in the presence of linoleate.

Figure 10. FABP4 is not predicted to have a classical signal peptide, but is predicted to be released via a non-classical route.

Figure 11. FABP4 release occurs via a BFA and Cu^{2+} insensitive pathway.

Figure 12. FABP4 resides primarily in the cytosol, with a substantial pool in the high density membrane fraction.

Figure 13. FABP4 localises to punctuate structures in adipocytes.

Figure 14. Lipid peroxidation leads to 4-hydroxynonenal formation and modification or proteins.

Table 2. Extracellular matrix proteins are downregulated during hypoxia.

Figure 15. Model for hypoxia mediated non-classical secretion of FABP4.

Chapter 6 – General Discussion

Figure 1. Gene expression data illustrating tissue specific expression of TNFα and RBP4.

Abbreviations

2DG	2-deoxyglucose
4-HNE	4-hydroxynonenal
ACN	acetonitrile
AEBP1	adipocyte enhancer binding protein 1
AICAR	aminoimidazole carboxamide ribonucleotide
AMP	adenosine monophosphate
AMPK	adenosine monophosphate activated kinase
ATGL	adipose triglyceride lipase
ATP	adenosine triphosphate
BFA	Brefeldin A
BSA	bovine serum albumin
CILAIR	comparison of isotope-labeled amino acid incorporation rates
CM	conditioned media
CNTF	ciliary neurotrophic factor
ConA	concanavalin a
DG	diglyceride
DMEM	dulbecco's modified eagle medium
DNA	deoxyribonucleic acid
ECM	extracellular matrix
EDTA	ethylene diamine tetraacetic acid
EEA1	early endosome antigen 1
EGTA	ethylene glycol tetraacetic acid
ELISA	enzyme linked immune-sorbent assay
ER	endoplasmic reticulum
ERK1/2	extracellular signal related kinases
EDL	Extensor digitorum longus
FABP3	fatty acid binding protein 3 (heart)
FABP4	fatty acid binding protein 4 (aP2)
FABP5	fatty acid binding protein 5 (Mal1)
FBS	foetal bovine serum
FCS	foetal calf serum
FFA	free fatty acids
FGF	fibroblast growth factor
Flk-1	foetal liver kinase 1 (VEGF receptor 2)
g	unit of gravity
GDR	glucose disposal rate
GIR	glucose infusion rate
GLUT1	glucose transporter 1
GLUT2	glucose transporter 2
GLUT4	glucose transporter 4
GSIS	glucose stimulated insulin secretion

GTT glucose tolerance test
HBSS Hank's balanced salt solution
HCV hepatitis C virus
HEK293 human embryonic kidney 293
HEPES N-[2-hydroxyethyl]piperazine-N'-[2-ethanesolfonic acid]
HFD high fat diet
HGP hepatic glucose production
HOMA-IR homeostatic model assessment of insulin resistance
Huh7 human hepatoma 7
IB immunoblot
IBMX isobutyl-methyl-xanthine
IGF insulin growth factor
IKK Iκ-B kinase complex
IL-1 interleukin 1
IL-6 interleukin 6
IL-8 interleukin 8
IRS-1 insulin receptor substrate 1
ITT insulin tolerance test
iTRAQ isobaric tag for relative and absolute quantitation
JFH1 Japanese patient with fulminant heptatis C infection (HCV strain)
JNK c-Jun N-terminal kinase
KRBH Krebs-Ringer buffer containing HEPES
LAC lectin affinity chromatography
LAC-CILAIR lectin affinity chromatography comparison of isotope-labeled amino acid incorporation rates
LR laminin receptor
MCP1 monocyte chemoattractant protein 1
MMP-1 matrix metalloproteinase 1
MnTBAP manganese tetra (4-benzoic acid) porphyrin
mRNA messenger ribonucleic acid
MS mass spectrometry
MSMS tandem mass spectrometry
mTOR mammalian target of rapamycin
NCBI national centre for biotechnology information
NFκB nuclear factor κ-light-chain enhancer of B-cells
ob/ob homozygous for *obese* gene mutation
p70 S6K 70 kDa protein S6 ribosomal kinase
PAI-1 plasminogen activator inhibitor 1
PBS phosphate buffered saline
PECAM platelet endothelial cell adhesion molecule
PEDF pigment epithelium derived factor
PDGF platelet derived growth factor
PM plasma membrane
PNGase F peptide N-glycosidase F
PPARγ peroxisome proliferator actrivator receptor γ
PRLTS PDGF receptor-like tumour suppressor

PSG	penicillin streptomycin glutamine
QTOF	quadrupole time of flight
RBP4	retinol binding protein 4
RIA	radioimmunoassay
RNA	ribonucleic acid
ROS	reactive oxygen species
RPMI1640	roswell park memorial institute 1640
S100A	protein soluble in 100% ammonium phosphate
SDS	sodium dodecyl sulphate
SDS-PAGE	sodium dodecyl sulphate polyacrylamide gel electrophoresis
Serpin	serine protease inhibitor
SILAC	stable isotope labeling of amino acids in cell culture
SOCS3	suppressor of cytokine signaling 3
sVEGFR2	soluble vascular endothelial growth factor receptor 2
TCA	tricarboxylic acid
TCEP	tris (2-carboxy-ethyl) phosphine
TG	triglycerides
TGF	tumour growth factor
TNFα	tumour necrosis factor α
TTM	tetrathiomolybdate
URB	upregulated in bombesin knockout
VEGF	vascular endothelial growth factor
VEGFR2	vascular endothelial growth factor receptor 2
WAT	white adipose tissue

Chapter 1

General Introduction

Lindsay Wu

The type 2 diabetes epidemic

Though reliable statistics regarding the incidence of diabetes do not exist for earlier time periods, it is generally accepted that the past 60 years of human history have seen a greatly increased incidence of obesity and type 2 diabetes. The post-war years of 1945 onwards in the West witnessed an unprecedented improvement in living conditions, with rising agricultural yields, mechanisation of previously labour-intensive work, increased income, dramatic urbanisation and mass availability of cheap, energy dense foods. This change in lifestyle resulted in decreased physical activity and increased consumption of food (Caballero 2007). This switch in energy consumption and expenditure has been blamed for the rise in, with 32% of adults in the US today considered obese (Ogden, Carroll et al. 2006). Similar rates of obesity have been reported in Australia. The burden of obesity is rising, with the majority of this increase coming from developing nations such as China, India, Mexico and Brazil, where rapidly increasing rates of obesity have been observed. Obesity is accompanied by numerous complications, of which type 2 diabetes and cardiovascular disease inflict the greatest mortality and economic cost burden (Huse, Oster et al. 1989). Projected increases in the number of individuals with type 2 diabetes are shown in Figure 1.

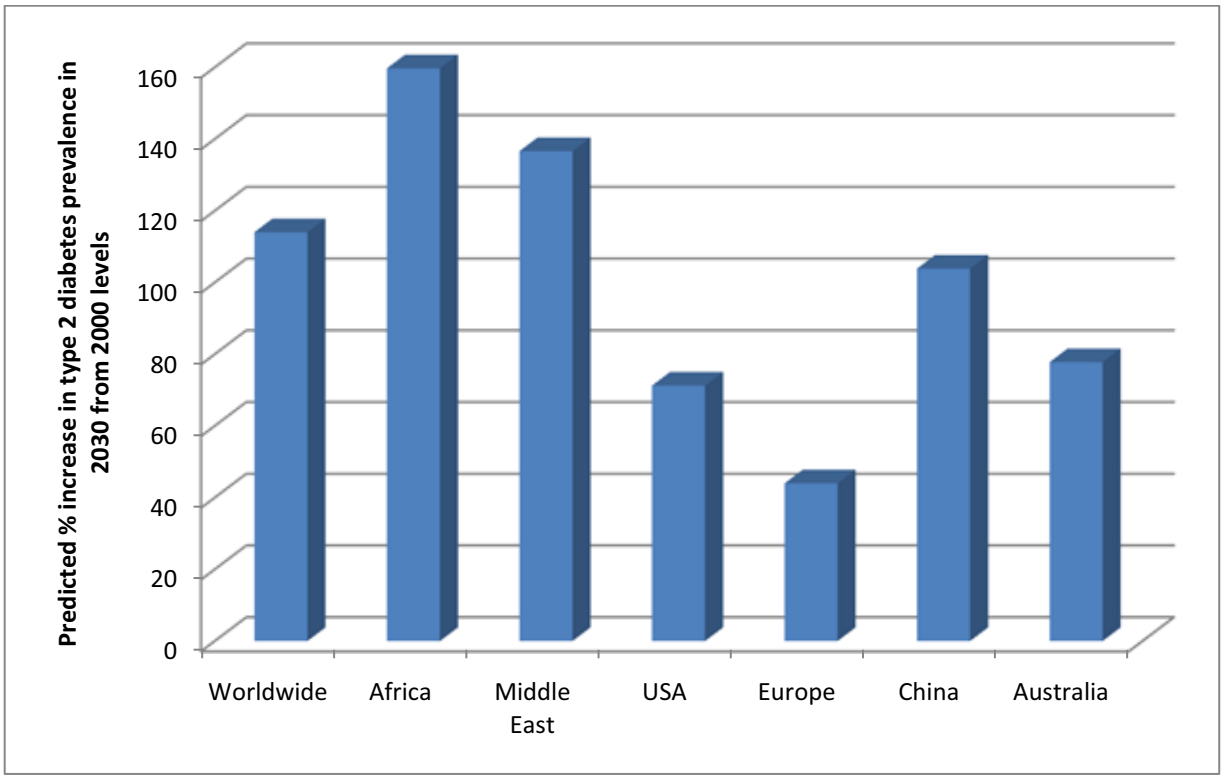

Figure 1. Projected increases in prevalence of type 2 diabetes. Source: World Health Organisation world figures index.

Historical diagnosis of type 2 diabetes

Diabetes mellitus is a chronic disease that has been described in one form or another in history for the past two millennia, beginning with the description of diabetes as a "melting of the flesh into urine" by the ancient Greek physician Arateus (translated by Brown in 1856 (Arateus 1856)). This description refers to two obvious symptoms of untreated diabetes. Diabetes is characterised by an inability to lower blood glucose concentrations by transporting glucose from the bloodstream into the tissues that require it. When tissues receive insufficient glucose supply, tissue wasting and loss of body weight occurs – the so called "melting of the flesh" described by Arateus. The body responds to excessive concentrations of glucose in the bloodstream, which might otherwise cause vascular damage and neurotoxicity, by excreting glucose through urine, and the need for frequent urination is a common symptom of diabetes. This is the second obvious symptom that Arateus refers to. The so called "melting of the flesh into urine" is one of the first attempts to explain the mechanism(s) of diabetes. The next crude diagnostic indicator of diabetes was made in the 17th century with the observation that the urine of diabetics tasted sweet, a reflection of the excretion of glucose into urine. As a consequence of this observation, the word "mellitus" (Latin for "honey") was added to the disease name "diabetes" (Ahmed 2002). Up until the early 20th century, few treatments were available for diabetics, and little was understood of its pathogenesis. The first experiment to shed some light on the mechanism of diabetes was from Joseph von Mering and Oscar Minkowski in 1889. Surgical removal of the pancreas in dogs resulted in diabetes, a reflection of the role of pancreatic β-cells in the maintenance of glucose homeostasis, and the dysregulation of these cells that occurs in diabetes (Luft 1989). In 1922, the duo of Banting and Best repeated this experiment, and showed that the effects of pancreatic

removal could be reversed by administration of pancreatic extracts from healthy dogs (Banting, Best et al. 1991). These extracts were islets of Langerhans, the cells responsible for producing insulin in the body. Further experiments resulted in the identification and purification of insulin from bovine pancreas, allowing injection of exogenous insulin into human diabetic patients, and in doing so alleviating the symptoms of diabetes (Banting 1937). This uncovered the role of insulin in maintaining glucose homeostasis, and resulted in the award of the Nobel Prize for medicine. It was not until 1983 that synthetic insulin could be produced, using newly developed recombinant DNA and bacterial production techniques. Since then, diabetes has been widely treated with purified, sterile, recombinant insulin, and numerous advances have been made in our understanding of energy homeostasis and diabetes.

Type 2 diabetes and insulin resistance

The pioneering work of Banting and Best laid the foundation for the current understanding of glucose homeostasis. Glucose homeostasis is tightly controlled by the liver, pancreas, white adipose tissue and skeletal muscle. During fasting, α-cells in the pancreas secrete the protein hormone glucagon. Glucagon signals to the liver to stimulate gluconeogenesis to produce and release glucose into the bloodstream to supply distal tissues with energy substrates. In addition to its effects on the liver, glucagon stimulates the release of monomeric glucose from glycogen, which is polymeric glucose stored intracellularly. When a meal is consumed however, food is broken down into simple sugars such as glucose. This results in an increase in blood glucose concentrations, which is detected by β cells in the pancreas. These β cells subsequently secrete insulin, which signals to the liver to block glucose release. Insulin also travels throughout the

circulation to interact with peripheral tissues, primarily skeletal muscle and white adipose tissue (Saltiel and Kahn 2001). Upon interaction of insulin with its cognate receptor on these tissues, an intracellular signalling cascade takes place (Taniguchi, Emanuelli et al. 2006). This cascade leads to the eventual translocation of the insulin sensitive glucose transporter GLUT4 to the cell surface, where glucose is transported into the cell, thus lowering concentrations of blood glucose (James, Strube et al. 1989). This system is highlighted in Figure 2. This is a tightly maintained feedback system, and in a healthy situation, blood glucose concentrations are maintained within a range of 4 – 5.5 mmol/L. Lower concentrations may lead to insufficient energy requirements for organs such as the brain, whose function is highly dependent on sufficient blood glucose concentrations. Chronically elevated blood glucose concentrations may result in neuropathy, retinopathy, nephropathy and vascular disease (Nathan 2002). It is these perturbations of glucose homeostasis that give rise to diabetes and its associated pathologies.

Diabetes is now understood to be two very distinct disorders. Type 1 diabetes mellitus is a disease caused by an auto-immune disorder. Pancreatic islets of Langerhans, which contain insulin producing β-cells, are destroyed by the immune system (Barker 2006). This has immediate results for glucose homeostasis, with blood glucose concentrations rapidly increasing, and peripheral tissues unable to access sufficient energy. This results in extreme fatigue, and often, coma. Type 1 diabetes appears with rapid onset, usually during childhood, and is thus often referred “sudden onset” or “juvenile” diabetes (Barker 2006). Type 1 diabetes must be remedied for the rest of the individual’s life by constant injection of insulin in the basal and post-prandial state, and monitoring of blood glucose concentrations for deviations away from ideal physiological concentrations. As far as maintenance of glucose homeostasis in type 1 diabetics is concerned, exogenous insulin administration and monitoring of blood glucose allows for

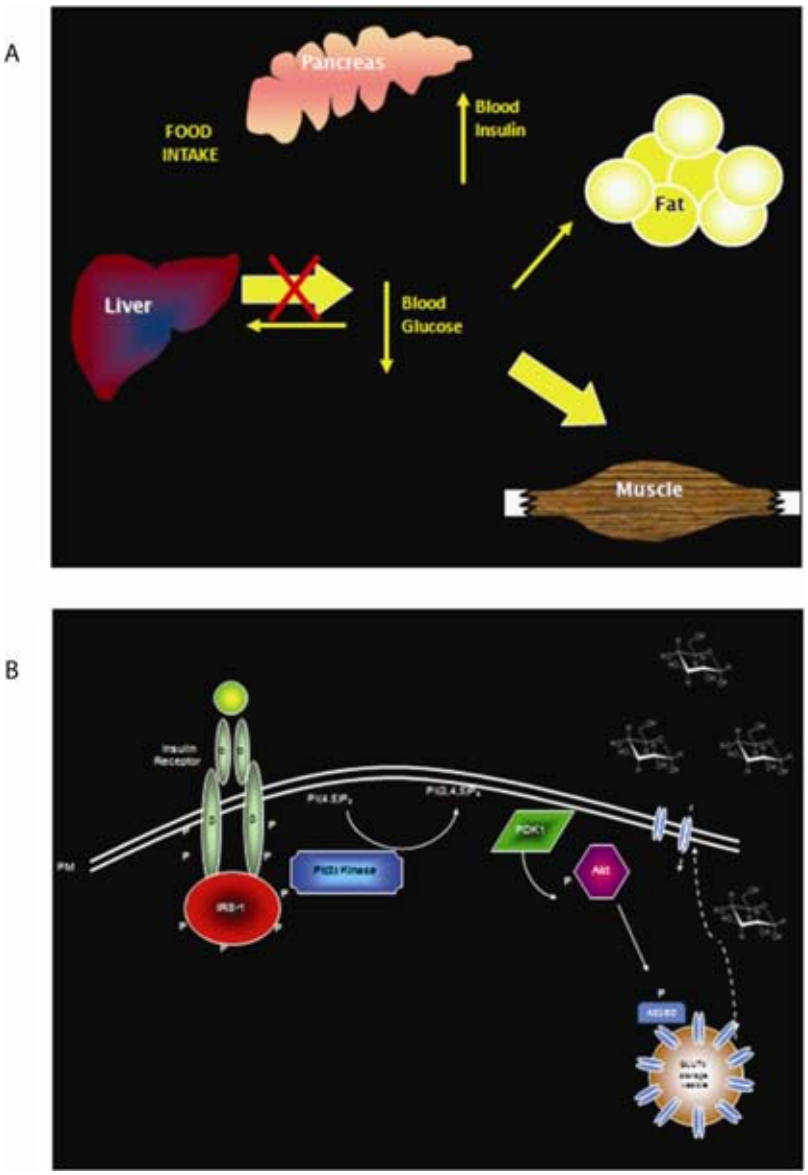

Figure 2. Glucose homeostasis and insulin stimulated glucose transport. A) During fasting the liver is responsible for releasing glucose to maintain glucose output. Upon food intake, blood glucose concentrations rise. This rise is detected by β-cells in the pancreas, which secrete insulin in response to increased glucose concentrations. Insulin travels through the bloodstream to interact with its cognate receptor, causing glucose uptake into muscle and liver and blocking glucose release from the liver, thus lowering blood glucose to normophysiological levels. B) Insulin stimulated glucose uptake into cells. Insulin interacts with its cognate receptor, leading to autophosphorylation and phosphorylation of IRS-1. This in turn leads to the recruitment of PI3 kinase and activation via conformational change. PI3 kinase catalyses the phosphorylation of $PI(4,5)P_2$ into $PI(3,4,5)P_3$, leading to phosphorylation of the central regulator Akt by PDK1. Akt has multiple downstream substrates, including AS160. Phosphorylation of AS160 by Akt leads to its dissociation from GLUT4 storage vesicles, leading to the translocation of these vesicles away from an intracellular storage location the plasma membrane, where the vesicle fuses and GLUT4 enters the membrane. GLUT4 is then able to transport glucose from the intracellular space into the intracellular environment, thus lowering blood glucose concentrations.

relatively simple disease management. By contrast, type 2 diabetes is a much more complicated disorder.

Type 2 diabetes is often referred to as “adult onset” diabetes, and primarily occurs in the later years of life. Of all diabetics, 90% are type 2 diabetics. Whereas in type 1 diabetes, the sole cause of the disorder is the complete destruction of pancreatic β-cells in a relatively short time, type 2 diabetes is a much slower evolving disorder that includes multiple tissue pathologies (Saltiel and Kahn 2001). Type 2 diabetes is often accompanied by obesity, and some debate exists as to whether obesity is a cause of type 2 diabetes or merely correlates with its progression (Haffner 2000). What is clear is that excessive caloric intake leads to a cascade of events, beginning with increased secretion of insulin, which according to the current literature is a response to compensate for increased circulating concentrations of glucose. This is closely followed by insulin resistance (Chisholm, Campbell et al. 1997). During insulin resistance, peripheral tissues such as skeletal muscle, white adipose tissue and the liver exhibit a poorer response to insulin (Saltiel and Kahn 2001). To compensate for this, pancreatic β-cells secrete greater amounts of insulin to achieve a sufficient response in terms of glucose uptake into peripheral tissues, and suppression of hepatic glucose output. It is thought that during this cycle, increased doses of insulin lead to further resistance to insulin in peripheral tissues, even higher amounts of insulin are required from pancreatic β-cells, and a “metabolic arms race” ensues. During this phase termed “insulin resistance”, glucose homeostasis is maintained, and the patient is mostly asymptomatic (Chisholm, Campbell et al. 1997).

Insulin resistance alone is not indicative of frank diabetes. Proper diagnosis of insulin resistance relies on the use of the hyperinsulinaemic euglycaemic clamp technique, which involves infusion of glucose at a rate that results in a constant blood glucose concentration (Kraegen, James et al.

1983). In patients, this technique is time-consuming and invasive. To avoid this, the HOMA-IR calculation, based on fasting glucose and fasting insulin concentrations, was developed to quickly assess insulin sensitivity (Matthews, Hosker et al. 1985). While insulin resistance alone is not indicative of type 2 diabetes, it is a common precursor state to frank diabetes, as defined by the presence of uncontrolled hyperglycaemia (Chisholm, Campbell et al. 1997).

As insulin resistance progresses and higher amounts of insulin are required from pancreatic β-cells, defects in the ability of these cells to secrete insulin may occur (Poitout and Robertson 2002). The inability to secrete sufficient insulin to overcome insulin resistance, often accompanied by β-cell defects, leads to dysregulated glucose homeostasis. An inability to control glucose homeostasis leads to short term and long term symptoms including fatigue, vascular damage, neuropathies, nephropathy, increased thirst, frequent need for urination, atherosclerosis and increased risk of cardiovascular disease (Stratton, Adler et al. 2000; Ayodele, Alebiosu et al. 2004; Said 2007). At the point that hyperglycaemia occurs, frank type 2 diabetes mellitus has occurred. Debate still exists as to whether type 2 diabetes is more a disorder of peripheral insulin resistance or β cell failure, and currently used treatments reflect this.

Oral treatment of type 2 diabetes may target peripheral insulin resistance, or may aim to supplement circulating insulin through increasing insulin secretion from β-cells (Quillen and Kuritzky 2002). Exogenous insulin may also need to be administered when the β-cell is otherwise unable to secrete enough insulin to maintain normoglycaemia. The oldest commonly used drug for treating insulin resistance is metformin, which is a weak metabolic poison that activates the intracellular energy sensor AMP kinase, and decreases hepatic glucose production, while increasing glucose uptake into tissues (Aviles-Santa, Sinding et al. 1999; Zhou, Myers et al. 2001; He, Sabet et al. 2009). While being the drug of choice for treating insulin resistance in

Australia, metformin does not completely alleviate insulin resistance, and often causes gastroenterological side effects (Nisbet, Sturtevant et al. 2004). More recent therapies for treating insulin resistance are thiazolidinediones, used clinically as rosiglitazone, piaglitazone and troglitazone, however troglitazone has been withdrawn from clinical use due to fatal hepatotoxicity (Gale 2001). These compounds are activators of peroxisome proliferator activator receptor γ (PPARγ), a transcription factor that promotes differentiation of adipocytes and upregulates synthesis of insulin sensitive enzymes (Spiegelman 1998). While thiazolidinediones are useful ammunition to enhance insulin sensitivity, they do not completely alleviate insulin resistance, and have been implicated in increased risks of cardiac pathologies (Alter 2007). Metformin and thiazolidinediones are used to treat insulin peripheral insulin resistance, but for adequate treatment of diabetics who have undergone β-cell failure, supplementation of insulin may also be necessary. This may occur through exogenous administration of insulin, or through the use of sulfonylureas to boost endogenous insulin secretion. Sulfonylureas target the ATP sensitive K^+ channel of the β-cell to cause electrical polarisation and secretion of insulin granules (Donath, Ehses et al. 2005). This approach does increase insulin secretion, but does so to the long term detriment of the β-cell. The most recent development in the treatment of type 2 diabetes comes in the form of incretin-based therapies (Drucker and Nauck 2006). Incretins are small peptide hormones secreted from the gut which function to increase insulin secretion, decrease nutrient uptake and decrease appetite in response to food intake (Drucker 2006). Synthetic analogues of incretins are the latest class of therapies for the treatment of metabolic disorders, and one recent compound, Exenatide, is a synthetic analogue of the incretin GLP-1 (Drucker and Nauck 2006). Unfortunately, exenatide has significant off-target effects, and administration is associated with off-target effects including nausea (Bergenstal, Wysham et al.).

Across the medical research community, considerable effort is being devoted to understanding the mechanisms of insulin resistance and subsequent β-cell failure.

Insulin resistance and type 2 diabetes

Insulin resistance occurs when the ability of insulin sensitive tissues to increase glucose uptake in response to insulin is diminished (Chisholm, Campbell et al. 1997). The ability of insulin to stimulate glucose uptake into tissues is mediated by the insulin sensitive glucose transporter GLUT4 (James, Strube et al. 1989), which lies in an intracellular location prior to insulin stimulation, where it translocates to the cell surface to allow glucose uptake. Defects in the ability of GLUT4 to translocate from an intracellular storage compartment to the cell surface in response to insulin broadly defines insulin resistance (Galuska, Ryder et al. 1998). The most commonly studied mechanism to explain this is defective insulin signalling. Insulin-stimulated glucose transport is the result of an intracellular signalling cascade and it has been proposed that defects in this cascade are responsible for insulin resistance (Galuska, Ryder et al. 1998; Leng, Karlsson et al. 2004). Considerable effort has been devoted to defining the signalling defects and their physiological role.

Reduced expression or acitivity of a number of components of key points in the insulin signalling cascade, including IRS-1 and Akt have been reported (Hotamisligil, Peraldi et al. 1996; Kim, Nikoulina et al. 1999). Recent work, however, has cast doubt on the role of signalling defects in insulin resistance (Hoehn, Hohnen-Behrens et al. 2008). While decreased phosphorylation of Akt is observed during insulin resistance, and complete ablation of Akt

blocks insulin-stimulated glucose uptake, activation of less than 5% of the total cellular pool of Akt is sufficient for complete GLUT4 translocation to the cell surface (Ng, Ramm et al. 2008). This means that for defects in Akt phosphorylation to be responsible for insulin resistance, a decrease in Akt activation of at least 95% may be necessary, and this level of decreased activation has not been observed under physiological conditions. Decreased levels and or activation of IRS-1 through activation of the JNK/IKK pathway (Hirosumi, Tuncman et al. 2002) have also been proposed to explain insulin resistance. One recent study, however determined that insulin resistance must lie downstream of IRS-1, as activation of the downstream insulin signalling pathway while bypassing IRS-1 did not ablate insulin resistance (Hoehn, Hohnen-Behrens et al. 2008).

The immune system has also been proposed to play a role in insulin resistance (Xu, Barnes et al. 2003). Obesity, which often accompanies type 2 diabetes, is characterised by a chronic state of low grade inflammation, with elevated serum levels of inflammatory cytokines and macrophage infiltration of adipose tissue (Hotamisligil, Shargill et al. 1993). While insulin resistance is accompanied by inflammation, the interpretation of data showing inflammation in dietary and genetically obese animals is potentially flawed. Closer examination reveals that insulin resistance usually precedes the onset of adipose tissue macrophage infiltration and inflammatory cytokines by several weeks in high fat fed animal models of insulin resistance (Xu, Barnes et al. 2003).

Another mechanism that has been proposed for insulin resistance involves the existence of excess circulating free fatty acids (Boden and Shulman 2002). These free fatty acids may be dietary in origin, or they may be released into the circulation from adipocytes due to increased lipolysis. In the basal situation, adipocytes break down lipids into free fatty acids and glycerol, and this process is inhibited by insulin (Burns, Terry et al. 1979). Insulin resistance in adipocytes

may result in a decrease in insulin-stimulated suppression of lipolysis, leading to excessive lipolysis and serum free fatty acid levels (Reynisdottir, Ellerfeldt et al. 1994). These fatty acids may accumulate in skeletal muscle and liver to decrease insulin sensitivity. However, even superphysiological concentrations of free fatty acids have little effect on adipocyte insulin sensitivity (Hoehn, Hohnen-Behrens et al. 2008). Despite this, decreased insulin sensitivity is also observed in the adipose tissue of insulin resistant animals and humans, meaning that additional mechanisms must be at play.

One possible theory revolves around insulin resistance being a simple response to nutrient oversupply, with reactive oxygen species produced during nutrient oversupply as well as inflammation and exposure to excess free fatty acids linking these mechanisms (Hoehn, Salmon et al. 2009).

Finally, a mechanism linking diet-induced obesity with insulin resistance is that adipose tissue - derived secretory proteins, termed adipokines, are dysregulated in obesity, consequently leading to insulin resistance (Rabe, Lehrke et al. 2008).

Adipokines in insulin resistance

Adipose tissue derived hormones, termed adipokines, may play a key role in insulin resistance (Rabe, Lehrke et al. 2008). Though traditionally viewed as an inanimate storage compartment, adipose tissue has in recent years come to the attention of researchers as an important endocrine organ that is responsible for the secretion of adipokines (Galic, Oakhill et al. 2009). These

proteins regulate a range of systems, including metabolism, the immune system, extracellular enzyme inhibition, redox regulation, and extracellular matrix formation.

The first adipose tissue - derived cytokine (adipokine) to be identified was adipsin (complement factor D), a serine protease inhibitor with a role in the complement pathway (Hyams, Carey et al. 1986; Cook, Min et al. 1987). Though expression of adipsin was perturbed in genetic models of obesity (Flier, Cook et al. 1987), there was little other evidence to suggest that adipsin might mediate an important endocrine role in fat. The importance of this endocrine role first came to attention with the discovery of leptin, a secreted protein that is the product of the ob gene (Halaas, Gajiwala et al. 1995). Mice with double mutations in the ob gene, known as ob/ob mice, have increased appetite and vastly increased body mass. A photo of the ob/ob mouse from the original identification of the strain is shown in Figure 3 (Ingalls, Dickie et al. 1950). This obese phenotype is accompanied by many of the common markers of caloric induced insulin resistance, including low grade inflammation, macrophage infiltration of adipose tissue, elevated circulating free fatty acids, increased β-cell mass, elevated circulating insulin levels and above all, insulin resistance in peripheral tissues (Friedman and Halaas 1998). Despite the existence of the ob/ob mouse strain for 60 years (Ingalls, Dickie et al. 1950), the gene responsible for the phenotype was only identified in 1995 (Halaas, Gajiwala et al. 1995). This gene codes for an adipocyte specific small secreted protein, leptin, which interacts with neurons in the hypothalamus via the leptin receptor to limit food intake (Campfield, Smith et al. 1995). The leptin receptor was found to be encoded for by the *db* gene, which in *db/db* homozygous mice leads to a similar phenotype as *ob/ob* mice (Kobayashi, Forte et al. 2000). The discovery of leptin was the first example of adipose tissue influencing feeding behaviour, and leptin was briefly touted as a panacea for the treatment of obesity.

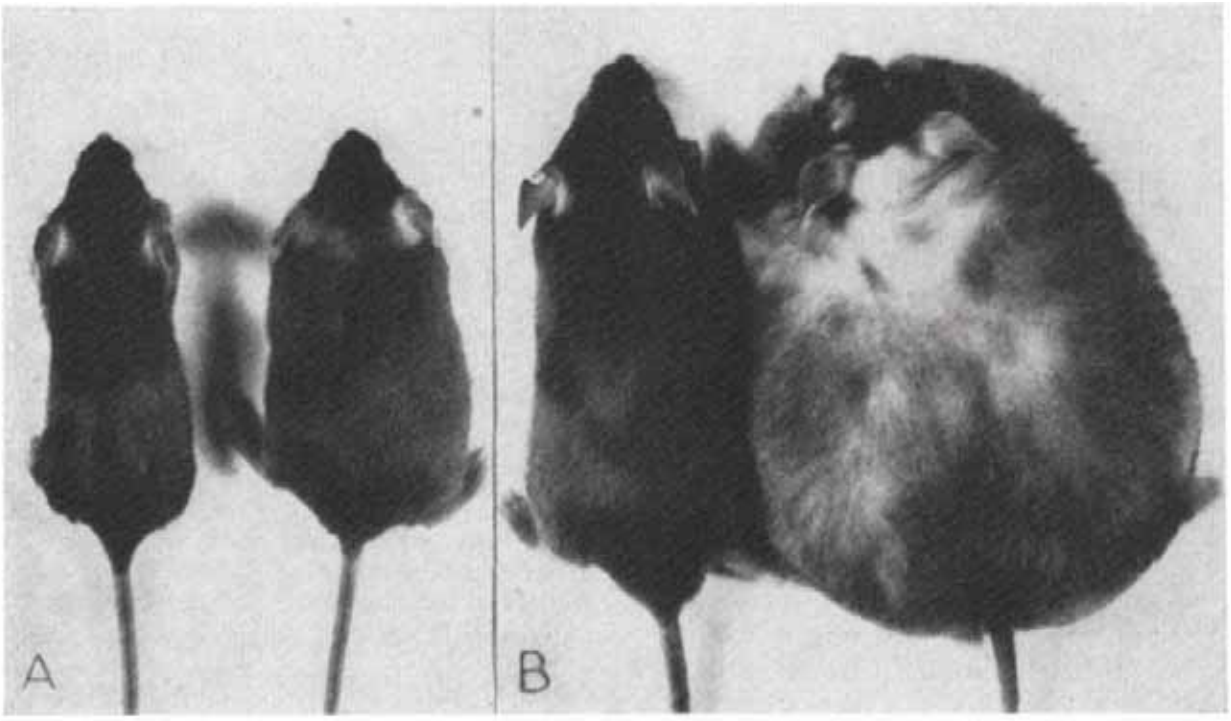

THE FAT MOUSE GROWS UP

Figure 4

A—shows normal control and an obese mouse at 21 days of age. The former weighed 12 grams; the latter 16. *B* shows a normal and obese mouse at ten months of age, when the obese mouse weighed 90 grams and the normal mouse 29 grams.

Figure 3. From the original description of the ob/ob mouse line. The *obese* phenotype was carried by classical mendelian inheritance. The product of the *ob* gene is the adipose secretory protein leptin, which interacts with its cognate receptor in neurons in the hypothalamus to limit appetite. Figure reproduced from Ingalls et al (1950).

Unfortunately, efforts to use leptin as a therapy to treat obesity were hampered by SOCS3-mediated leptin resistance, which occurs even at supraphysiological doses of leptin as observed in obesity (Bjorbaek, El-Haschimi et al. 1999).

While leptin is considered the only adipokine to interact with the brain, conditioned media experiments have pointed towards the existence of additional adipose derived cytokines that interact with the brain to limit appetite (Weigle, Hutson et al. 1998). In the investigation of Weigle and co-workers, adipocyte conditioned media was used to treat the hypothalamus of mice, and suppression of food intake was monitored. At the same time, the concentration of purified leptin needed to achieve a similar reduction in appetite was titrated down to the lowest effective concentration. The concentration of leptin in adipocyte conditioned media was compared to the concentration of purified leptin needed to elicit a similar suppression of appetite. A huge discrepancy was observed, with over 20 times the amount of purified leptin needed to elicit a response similar to adipocyte conditioned media. It is unlikely that post-translational modifications in leptin increase its activity over recombinant leptin, as there are no reported post-translational modifications for this molecule (Cohen, Halaas et al. 1996). This experiment points towards the existence of additional adipocyte secreted factors that act either in concert or in an additive manner with leptin to interact with the brain to suppress appetite. This factor has not yet been identified, and the identification of this unknown adipocyte secretory factor may provide an important therapeutic target in treatment of human obesity.

Unlike leptin, which circulates at low serum concentrations, adiponectin is an adipocyte derived cytokine that is relatively abundant in the serum, being the 10^{th} most abundant serum protein.

Adiponectin has whole body insulin sensitising effects, and acute administration induces glucose uptake into cultured cells via activation of the central energy sensor molecule AMP kinase downstream of the cognate receptor for adiponectin (Yamauchi, Kamon et al. 2002). Although adiponectin is secreted exclusively from adipocytes, serum levels decrease with obesity, during which hypertrophy and hyperplasia of adipocytes occurs (Arita, Kihara et al. 1999). The reasons for hypoadiponectinaemia during obesity are currently unclear; however one recent study implicated the role of adipose tissue hypoxia in suppression of adiponectin secretion during obesity (Hosogai, Fukuhara et al. 2007). In the serum, adiponectin may exist as a trimer, hexamer, or as a 12-18-mer (Pajvani, Du et al. 2003). The existence of adiponectin in multiple forms complicates a clear discussion of its function. There is some evidence that different forms of adiponectin may have different affinities for adiponectin receptors, which are 7-transmembrane proteins that do not bear homology to currently described G-protein coupled receptors (Yamauchi, Kamon et al. 2003). Furthermore, different multimeric forms of adiponectin lead to different metabolic consequences (Lara-Castro, Luo et al. 2006). The identification of adiponectin and its role in mediating insulin sensitivity demonstrates the endocrine importance of adipose tissue for obesity and insulin resistance.

Though leptin and adiponectin are the most well studied adipokines, a plethora of other adipocyte secretory proteins that play a role in metabolism have been identified. These include plasminogen activator inhibitor 1 (PAI-1), lipocalin-2, resistin, chemerin, visfatin, resistin, interleukin-6, tumour necrosis factor (TNFα) and retinol binding protein 4 (RBP4) (Yang, Graham et al. 2005; Alessi, Poggi et al. 2007; Galic, Oakhill et al. 2009). Although adipose tissue secretes these proteins, they are not necessarily secreted from adipocytes *per se*. Adipose tissue contains multiple cell types including adipocytes, preadipocytes, endothelial cells and

macrophages. Non adipocyte cell types in adipose tissue are often referred to as the stromovascular fraction. Cells from the stromovascular fraction secrete a variety of important factors, and indeed one study has suggested that the stromovascular fraction is responsible for secretion of over 90% of the protein species secreted from fat (Fain, Madan et al. 2004). These adipose tissue secretory proteins play varying roles in maintenance of insulin sensitivity, both in a paracrine and in an endocrine manner. Within the literature, this list of adipokines is ever growing.

Despite the long list of adipokines that have been described to date, the adipokines that have been identified to date alone cannot account for the endocrine effects of adipose tissue. As an example, one possible endocrine function of adipose tissue is in regulation of β-cell function. Fasting and fed insulin levels closely correlate with adiposity, but not necessarily with whole body insulin resistance (Bagdade, Bierman et al. 1967). Given that fasting insulin levels are measured after at least 10 hours of fasting, and insulin has a half-life in the serum of 4 – 6 minutes (Duckworth, Bennett et al. 1998), peripheral insulin sensitivity should not affect fasting insulin levels. The observation suggests that fasting insulin varies according to adiposity suggests a possible interaction between adipose tissue and insulin secreting β-cells. This is reinforced by data showing a correlation between adiposity and β-cell mass (Ferrannini, Camastra et al. 2004). Leptin mediates adipocyte – β-cell interactions and so an adipocyte – β-cell axis has been proposed (Huypens 2007). Leptin interacts with the β-cell, however this interaction inhibits insulin secretion and β-cell function (Kieffer and Habener 2000). Little is known about the existence of an adipo – insular axis. Understanding such an interaction would be important to our understanding of glucose homeostasis and insulin resistance, as fasting insulin levels are currently used to determine the extent of insulin resistance. It may be that

fasting insulin levels better reflect adiposity than insulin resistance. If an adipo-insular axis does exist, this would imply the existence of an adipokine or some other adipose secretory factor to mediate the interaction between adipose tissue and β-cells. Identifying this factor may offer an opportunity to intervene in β-cell function and insulin secretion.

Another example of a possible endocrine effect of adipose tissue lies in the deleterious metabolic effects of visceral versus subcutaneous adiposity. Visceral, but not subcutaneous, adiposity leads to an increased risk of insulin resistance, and inherited visceral adiposity has been proposed to mediate genetic influences on insulin resistance (Carey, Jenkins et al. 1996; Carey, Nguyen et al. 1996). Selective removal of visceral adipose tissue can improve whole body insulin sensitivity (Shi, Strader et al. 2007). Visceral and subcutaneous adipose tissues display intrinsically different metabolic characteristics. Visceral adipose tissue displays an increased rate of catecholamine stimulated lipolysis, and a decreased insulin induced suppression of lipolysis (Bolinder, Kager et al. 1983; Wajchenberg 2000). Whereas subcutaneous adipocytes respond to clinically used antidiabetic PPARγ agonists, the response in visceral adipocytes is blunted (Adams, Montague et al. 1997). The ability of visceral adipose tissue removal to improve insulin sensitivity in distal tissues (such as muscle) indicates an endocrine role for visceral adipose tissue that does not exist for subcutaneous adipose tissue. Visfatin is a visceral adipose specific secretory protein that has been proposed to play a role in insulin resistance, however the exact biochemical function of this protein is controversial and is yet to be resolved (Fukuhara, Matsuda et al. 2005; Revollo JR 2007). Identifying factors differentially secreted from visceral and subcutaneous adipose tissue may be important in explaining the deleterious effects of visceral adipose tissue, and may afford an opportunity for either therapeutic intervention or early diagnosis using serum markers.

These data point towards the existence of novel adipokines to mediate the endocrine effects of adipose tissue. Considerable effort has been devoted to identifying novel adipokines, and most of these approaches have utilised mass spectrometry (Kratchmarova, Kalume et al. 2002; Wang, Mariman et al. 2004; Chen, Cushman et al. 2005; Alvarez-Llamas, Szalowska et al. 2007; Zvonic, Lefevre et al. 2007; Roelofsen, Dijkstra et al. 2009). The technique of mass spectrometry and its use in identifying novel adipocyte secretory proteins is herein discussed.

Mass spectrometry and identification of secreted proteins

In light of the discovery of important adipocyte secretory proteins, considerable effort has been devoted to identifying novel members of this important class. Given a list of potential candidates that is largely undefined, an ideal approach for the identification of novel proteins is mass spectrometry based proteomics. Mass spectrometry is a technique that measures the unique molecular weight of amino acids to deduce amino acid sequences of short polypeptides (Aebersold and Mann 2003). The sequences deduced from these polypeptides can be used to identify the protein of origin using protein sequence databases. This technique allows the rapid identification of thousands of polypeptides and corresponding proteins in a relatively short time, making mass spectrometry an ideal way of identifying the protein components of a complex mixture. In a typical mass spectrometry experiment, a protein sample is resolved using gel chromatography, such as SDS-PAGE. Gel lanes are cut into pieces across the molecular weight range, in-gel proteins digested with the proteolytic enzyme trypsin, and peptides are extracted. These peptides are then subjected to liquid chromatography coupled tandem mass spectrometry. Liquid chromatography separates proteins based on their hydrophobicity, and a constant stream

of proteins enter the mass spectrometer as they are eluted from the liquid chromatography column. Depending on the speed and ability of the instrument, only a portion of the peptides that enter the mass spectrometer are actually sequenced. Only one peptide may be sequenced at a time, and other peptides that may elute off liquid chromatography while this is occurring may be lost. Thus, detection of proteins of interest can be diluted by the presence of other peptides, and it is for this reason that sample preparation and removal of contaminating proteins is of critical importance to the reliable detection of low abundance protein species. This issue is of particular relevance to previous studies in the field of identification of secretory proteins. The ability to remove undesired proteins to detect low abundance proteins is addressed in this thesis.

Recent advances in mass spectrometry have made it possible to quantitate differences in protein levels between samples. This has been primarily due to the introduction of isotopic labelling techniques. In these experiments, covalent addition of a stable atomic isotope results in a small shift in peptide molecular weight. While the incorporation or addition of an atomic isotope does not result in any changes to chemical activity, this shift in molecular weight is detectable by mass spectrometry. When two samples labelled with different isotopes are mixed together and subjected to mass spectrometry, peptides from both samples of identical sequence are detected at the same time. The addition of different isotopes and their differing corresponding changes in molecular weight results in a shift the in mass to charge ratio, and two peaks of intensity are detected for each peptide. The relative intensities of each peak are measured as ratios, and this ratio is used as a quantitative guide to ratios of abundance for a particular protein species between the original samples. This technique can allow the relative quantitation of thousands of protein species in a single experiment, and is a powerful tool in biochemistry.

Addition of these atomic isotopes can take several forms. One of the oldest of these techniques involves the trypsin digestion of a protein mixture with trypsin in either normal or ^{18}O labelled water (Miyagi and Rao 2007). Trypsin cleavage of proteins into polypeptides is a hydration reaction, and oxygen from surrounding water is incorporated into cleaved polypeptides. Samples can be mixed together and subjected to mass spectrometry, and the shift in molecular weight caused by incorporation of either a ^{16}O or ^{18}O atom results in a molecular weight shift that allows for relative protein quantitation. While fairly simple in theory, this approach relies heavily upon the scrupulous evaporation of pre-existing water molecules prior to the addition of either ^{16}O or ^{18}O water. Also, given the existence of only two isotopes of oxygen only two samples can be compared.

Rather than using ^{18}O labelled water, there are several commercially available isotope coded chemical tags that can be covalently added to trypsin digested proteins. The most commonly utilised reagents for this sort of experiment are the iTRAQ isotope labelled chemical tags (Ross, Huang et al. 2004). These tags are readily reactive against tryptic peptides and there is no need for prior sample cleanup, as with ^{18}O labelling. In addition, the existence of multiple iTRAQ tags makes simultaneous comparisons of up to 8 different protein samples possible. The main disadvantage to chemical tagging of tryptic peptides is that labelling steps must be performed at the very end of the experimental process, after multiple manipulations have been performed. Performing manipulations of different samples independently of one another is disadvantageous in that experimental error or bias may be selectively introduced into several, but not all, samples, resulting in false reporting of protein changes between samples.

One recently developed method circumvents these problems by labelling proteins prior to experimental intervention. Stable isotope labelling of amino acids in cell culture (SILAC) for

relative quantitation of proteins using mass spectrometry was developed in 2004 by Mann and co-workers, and since then has proved to be a popular experimental approach (Ong, Blagoev et al. 2002). In this type of experiment, cells are cultured in media supplemented with the amino acids arginine and lysine, which contain nuclear isotopes that again result in a shift in molecular weight. As cells divide, they incorporate these isotopic amino acids into newly synthesised proteins. After enough rounds of cell division, cells will eventually be completely composed of proteins containing isotopic arginine and lysine. Cell populations labelled with different isotopes may be treated with the intervention of interest, and proteins obtained through cell lysis or collection of conditioned media. At this early stage of the experiment, different samples are mixed together in equal proportions. Further manipulations such as fractionation or affinity purification may be performed, with the important advantage that all original samples are mixed into one sample, and experimental error or bias will apply equally to all treatments. From here, proteins of interest are subjected to trypsin digestion. Trypsin is a proteolytic enzyme that digests on the N-terminal side of the basic amino acids arginine and lysine. Use of this enzyme ensures that each peptide will only contain one arginine or lysine, and consequently will carry only one set of amino acid isotopes per peptide. Peptides are subjected to mass spectrometry, and shifts in peptide molecular weight are again used to identify changes in relative abundance between samples. Though this technique does rely on extensive labelling of cells in culture with amino acid isotopes prior to an experiment, it does have the advantage of being able to mix samples at an early stage in the experiment, to avoid later experimental bias. SILAC is used in this investigation as a way of interrogating changes in protein secretion during relevant physiological stimuli.

Adipokine identification by mass spectrometry

There have been numerous attempts to identify the complete secretory repertoire of adipocytes and adipose tissue using mass spectrometry (Kratchmarova, Kalume et al. 2002; Celis, Gromov et al. 2004; Wang, Mariman et al. 2004; Chen, Cushman et al. 2005; Alvarez-Llamas, Szalowska et al. 2007; Zvonic, Lefevre et al. 2007; Roelofsen, Dijkstra et al. 2009). These studies encountered varying rates of success. In all studies, cells or tissues were incubated in serum free media, often supplemented with insulin to promote protein synthesis and secretion, and this media after a time period (often 24 hours or less) was collected. This media is most commonly referred to as "conditioned media", and in theory contains the proteins secreted by the cell or tissue of interest. In one case, the interstitial fluid perfusing the breast tumour was collected (Celis, Gromov et al. 2004). Once conditioned media was collected, proteins were indiscriminately precipitated using TCA precipitation or similar means, separated using some form of sized based chromatography (most commonly SDS-PAGE or liquid chromatography), and subjected to mass spectrometry.

The problem with many of these studies is the existence of contaminating proteins in conditioned media samples. While cells or tissue explants are being cultured, a small percentage of cells are necrotic, and may undergo lysis, releasing their intracellular contents into the conditioned media. These intracellular contaminants are far more abundant by dry weight than true secretory proteins, which are released from healthy cells in a regulated manner. Secretory proteins can be distinguished from non-secretory (cytosolic) proteins based on the existence of an N-terminal signal peptide. Here, the presence of a signal peptide is used to retrospectively analyse the success of previous experimental approaches.

Of all published studies, where full datasets were available, it appears that the percentage of detected proteins from conditioned media that contained a signal peptide did not surpass 63% (Wang, Mariman et al. 2004). This particular study was the only one of these investigations that implemented an approach to deal with the problem of intracellular protein contamination. Wang and co-workers (2004) used a strategy to discriminate between secreted and cytosolic proteins in conditioned media prior to mass spectrometry. Proteins were precipitated from the conditioned media of 3T3-L1 adipocytes that had been treated with the secretory inhibitor Brefeldin A (BFA). Alternately adipocytes were incubated at 20°C, a temperature that inhibits protein transport and secretion. Precipitated proteins were resolved by 2-D PAGE and proteins were stained. Those proteins that were sensitive to either BFA treatment or incubation at 20°C were excised from the gel and subjected to mass spectrometry. While this approach succeeded in exclusion of cytosolic proteins during mass spectrometry, the need to run multiple samples, and manually identify BFA or temperature – sensitive protein spots on a gel is not ideal. This process is laborious and not entirely reproducible. It depends on the ability of the experimenter to reliably and reproducibly identify proteins that are temperature or BFA sensitive. It also requires individual protein spots to be excised and subjected to mass spectrometry independently of one another. Furthermore, if a secretory protein exists at the same mass and charge as a cytoplasmic contaminant, it will not be visualised by 2-D PAGE, and will remain undetected.

Prior to the study of Wang and co-workers (2004), Kratchmarova and co-workers (2002) were the first to attempt to survey the adipocyte secretome (Kratchmarova, Kalume et al. 2002). In this very simple study, 3T3-L1 fibroblasts and 3T3-L1 adipocytes were incubated in serum free media, and conditioned media was collected. Proteins were precipitated from conditioned media using TCA precipitation and subjected to SDS-PAGE. A smear of proteins was observed in both

lanes, and those protein species that appeared to be upregulated in adipocytes compared to fibroblasts were excised and subjected to mass spectrometry. Although novel adipocyte secretory proteins were identified, this experiment did little to address the issue of contaminating intracellular proteins.

In a study by Celis and co-workers, the interstitial fluid of breast tumours was obtained in the hope of identifying proteins secreted from mammary carcinomas (Celis, Gromov et al. 2004). Here, raw interstitial fluid obtained from freshly microdissected carcinomas was precipitated, subjected to 2-D PAGE and mass spectrometry. There are several potential problems associated with this approach. Firstly, the presence of a protein species in the interstitial fluid of a carcinoma does not indicate the actual secretion of a protein from that particular carcinoma. Interstitial fluid will be exposed to serum, which as a result of its circulating nature is likely to contain secreted proteins from every tissue in the body. Serum proteins are likely to dilute the detection of carcinoma derived secretory proteins. In addition to the dilution of carcinoma secretory proteins by exogenous serum proteins, the act of dissection most likely led to cell lysis, and release of cytosolic contaminant proteins. These cytosolic proteins again will lead to the dilution of real carcinoma secretory proteins.

One study by Chen and co-workers in 2005 utilised quantitative mass spectrometry to identify changes in protein secretion from adipocytes (Chen, Cushman et al. 2005). Here, primary rat adipocytes were obtained, and incubated in the presence or absence of insulin. Conditioned media was obtained and subjected to extensive separation by liquid chromatography. One sample was dialysed from normal buffer to buffer containing ^{18}O labelled water, and proteins were digested with trypsin. Tryptic cleavage of proteins is a hydration reaction, and involves the conjugation of water to the cleaved peptide. By performing trypsin digests in the presence of ^{18}O

labelled water, a single atom of ^{18}O is added to the peptide, resulting in a small shift in total peptide molecular weight that can be detected only through mass spectrometry. After trypsin digestion of samples in either ^{16}O or ^{18}O water, samples were mixed together and subjected to mass spectrometry. Identical peptides from different samples will be detected simultaneously during mass spectrometry, however the incorporation of either a ^{16}O or ^{18}O atom into the peptide will result in a shift in mass to charge ratio, and the relative signal intensities of these two peptides can be measured as a ratio. This ratio reflects the relative abundance of proteins from different samples, and in this case was used to determine the effect of insulin on protein secretion from adipocytes. Though this study did utilise a novel quantitative approach, the issue of contaminating cytosolic proteins was still not addressed. This problem is exacerbated in primary adipocytes, due to their highly delicate structure. Furthermore, the need to dialyse samples against ^{18}O water is an expensive and time consuming step that may be avoided through other isotopic labelling techniques, such as iTRAQ, or through metabolic labelling techniques such as SILAC or CILAIR.

The first adipose secretome investigation that utilised metabolic labelling was from Alvarez-Llamas and co-workers (2007). The basic premise of this experiment was that human visceral adipose tissue was obtained, washed extensively to remove serum proteins, incubated in media containing SILAC amino acid isotopes, conditioned media was collected, and proteins were subjected to mass spectrometry (Alvarez-Llamas, Szalowska et al. 2007). The advantage of this study was that incorporation of a SILAC amino acid isotope would indicate fresh ex-vivo synthesis of a protein in the tissue of interest. This allowed discrimination between adipose derived secretory proteins and serum proteins that may exist in the tissue explants. To minimise the contribution of serum proteins to conditioned media samples, considerable effort was

devoted in this study to identifying the optimal washing protocol for tissue explants. After various wash protocols, protein concentrations in conditioned media samples were measured, with the assumption that the majority of proteins in conditioned media would be of serum or cytoplasmic origin. The wash protocol that resulted in the lowest protein concentration in conditioned media was chosen, and only after this comprehensive washing protocol were explants incubated in SILAC amino acid isotopes. From extraction of tissues to the end of media conditioning, explants were cultured for between 48 and 114 hours. Tissue explants are not typically viable for these periods of time, and a shorter incubation time is desirable. Though this study did have the advantage of using metabolic labelling to determine whether identified proteins are actually secreted from the tissue of interest, rather than originating from serum, a disadvantage again was the contamination of conditioned media with non-secretory proteins.

A later study similar to that of Kratchmarova and co-workers (2002) was that of Zvonic and co-workers in 2007 (Kratchmarova, Kalume et al. 2002; Zvonic, Lefevre et al. 2007). Rather than comparing the secretome of 3T3-L1 fibroblasts and adipocytes, primary human preadipocytes were isolated, cultured and differentiated into adipocytes. Conditioned media from preadipocytes and differentiated adipocytes were collected, proteins precipitated and resolved by 2-D PAGE. Individual protein spots that changed during adipogenesis were excised and subjected to mass spectrometry for identification. With the exception of the use of human preadipocytes rather than 3T3-L1 cells, and the use of 2-D PAGE rather than 1-D SDS-PAGE, this study was identical to that of Kratchmarova and co-workers (2002). The same disadvantages to that study also applied to the study of Zvonic and co-workers.

The final and most recent study into the proteomics of adipokine secretion was from Roelofsen and co-workers (2009). This study was an adaptation of the experimental approach used earlier

by this same group (Alvarez-Llamas, Szalowska et al. 2007). Rather than simply using amino acid isotope incorporation as an indicator of protein synthesis in explants, comparative rates of isotope incorporation were measured under unstimulated and insulin stimulated conditions. This approach was given the name CILAIR (comparison of isotope-labelled amino acid incorporation rates) (Roelofsen, Dijkstra et al. 2009). This approach suffered the same disadvantages (described above) as their earlier study (Alvarez-Llamas, Szalowska et al. 2007), with long ex-vivo incubation times, a complicated wash protocol, and dilution of secreted protein detection during mass spectrometry by cytosolic contaminants. While the concept of measuring rates of amino acid isotope incorporation was novel, this study was still limited in several respects. For example, it would have been far more efficient if different isotopes were used for each treatment, so that samples could be mixed together and subjected to mass spectrometry at the same time, avoiding bias from different mass spectrometry runs. An adapted CILAIR workflow was used in chapter 4 of this study, and is shown in Figure 4.

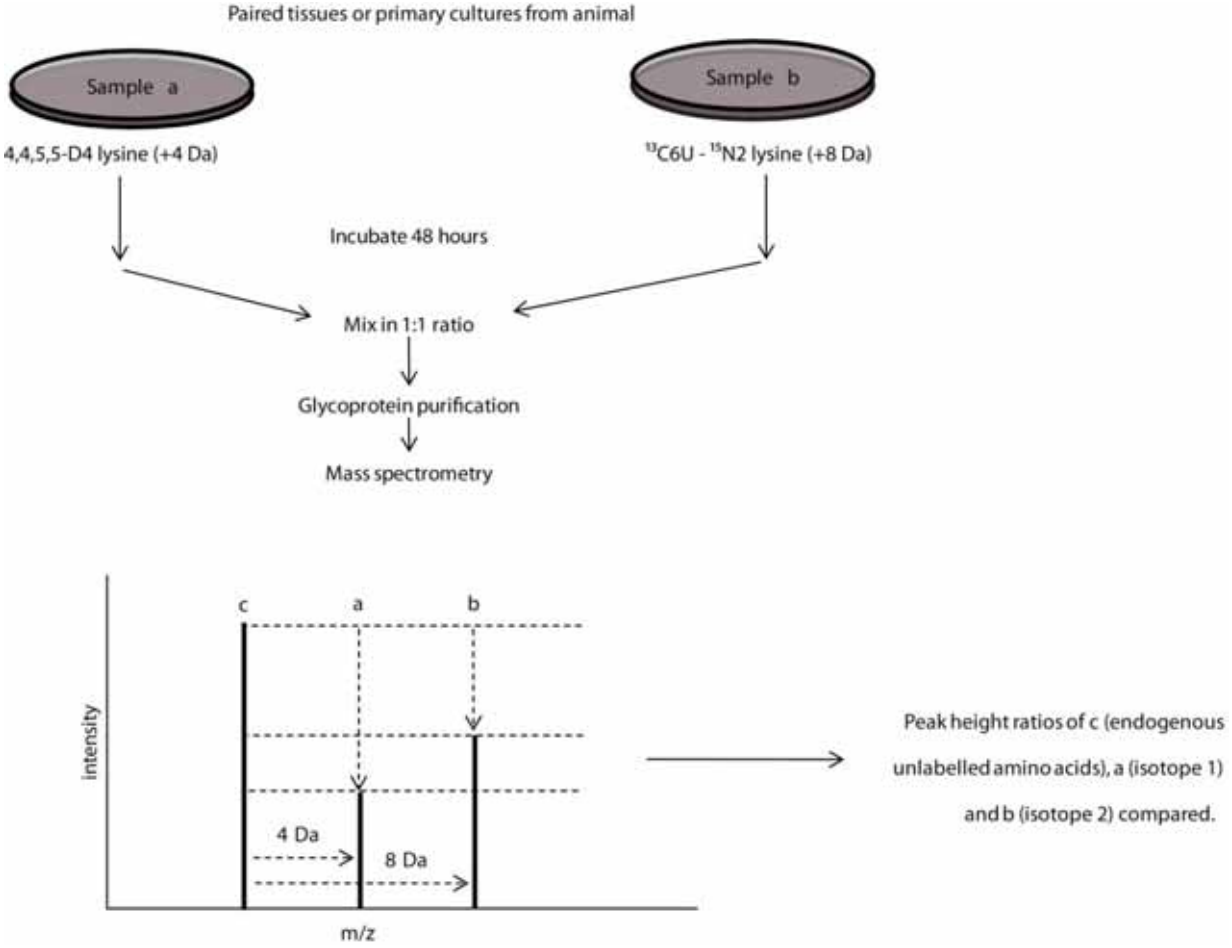

Figure 4. Modified CILAIR workflow for comparing protein synthesis and secretion from two different samples. Paired cell cultures or tissues are obtained from an animal and incubated in media containing different isotopes of lysine, which is incorporated into newly synthesised and secreted proteins. Samples are mixed in equal proportions, and proteins subjected to mass spectrometry. Incorporation of amino acid isotopes results in a shift in molecular weight and m/z ratio. Peak heights are measured, and ratios used to determine relative abundance of proteins from samples *y* and *z*.

Improvement on previous studies

All previously described studies suffer from the same problem: the contamination of conditioned media samples with cytoplasmic proteins from necrotic cells, leading to dilution of secretory protein detection by mass spectrometry. An ideal way to circumvent this problem would be to exploit the existence of some common characteristic unique to secretory proteins. Secretory proteins differ from cytosolic proteins in their synthesis. Unlike cytosolic proteins, secretory proteins are targeted by the existence of an N-terminal hydrophobic signal peptide to ribosomes on the surface of the ER (Blobel and Dobberstein 1975; Blobel and Dobberstein 1975; Scheele, Dobberstein et al. 1978). Here, the growing polypeptide chain is fed into the lumen of the endoplasmic reticulum through the Sec61 containing protein translocon complex. During this process, carbohydrate side chains are conjugated to asparagine residues that lie within the Asn – X – (Ser/Thr) motif (Helenius and Aebi 2004). The addition of these carbohydrates is termed N-glycosylation, and this post-translational modification is thought to add stability to secretory proteins in the extracellular space (Lis and Sharon 1993; Helenius and Aebi 2004; Shental-Bechor and Levy 2008). N-glycosylation is a characteristic common to secretory proteins, largely absent from cytosolic proteins, and so can be exploited.

One ideal way of exploiting the differences between secretory and cytosolic proteins would be to purify N-glycosylated proteins. Lectins are a class of proteins that have high affinity for glycosylated proteins (Freeze 2001). By using immobilised lectins, N-glycosylated secretory proteins can be purified from conditioned media samples to the exclusion of cytosolic proteins. This enrichment step may allow for a more pure sample, with less dilution of secretory protein detection by abundant cytosolic proteins. This should allow for identification of secretory

proteins of low abundance that may have been missed in previous studies. Indeed, lectin affinity chromatography has recently been used with some success to identify secreted proteins from serum (Jung, Cho et al. 2009). One disadvantage of this approach is that the highly heterogeneous nature of protein glycosylation will lead to varying binding affinities between proteins. As a consequence, comparison of abundance between protein species may not be feasible.

There are other possible ways of purifying glycoproteins. One method might be to oxidise carbohydrate moieties to form reactive aldehydes. These aldehydes covalently react with hydrazine, which may be coupled to an immobilised substrate. Non glycoproteins can then be removed using high salt washes, and glycoproteins eluted by low *p*H and heat. This technique has successfully been used in the past to identify glycosylation sites in proteins (Zhang, Li et al. 2003). The advantage of this technique is that a simple covalent reaction can be performed to isolate glycoproteins. The main disadvantage is that all glycoproteins are purified with equal affinity, including O-glycosylated proteins. In contrast, lectins have varying specificity for different carbohydrates. A lectin that prefers binding to mannose residues of the type found in N-linked secretory glycoproteins (such as concanavalin A) can be used over a lectin that preferentially binds O-linked carbohydrate residues.

Another method that has been used to purify glycoproteins and identify glycosylation sites has been isotope labelling of glycosylated peptides (Kaji, Saito et al. 2003). In a study by Kaji and co-workers, glycoproteins were purified by lectin chromatography as in this study, trypsin digested, and carbohydrate moieties removed by digestion with peptide N-glycosidase (PNGase F) in the presence of ^{18}O labelled water (Kaji, Saito et al. 2003). This labelling technique is much like the isotopic labelling of peptides with ^{18}O water during trypsin digestion. PNGase F

digestion results in the hydration of the peptide, and consequent isotope labelling with an ^{18}O atom when performed in ^{18}O water. Peptides are consequently subjected to mass spectrometry, and identification of peptides labelled with an ^{18}O isotope allows identification of glycosylation sites. Although this technique allows for identification glycoproteins and their glycosylation sites, trypsin digestion of proteins at an early stage in the process means that SDS-PAGE separation of proteins cannot be performed, lowering the resolution of separation by liquid chromatography. The most ideal technique that was chosen in this investigation was simple lectin affinity chromatography using the lectin Concanavalin A.

Aims of investigation

The aim of this investigation was to develop a method for purifying secreted proteins from the conditioned media of cultured cells and ex-vivo tissues. Upon establishment of this technique, the secretome of insulin sensitive tissues would be surveyed, providing the first comprehensive study into the endocrine contributions of insulin sensitive tissues. Any proteins of interest that were identified would be pursued with further experiments to gain an understanding of their role in metabolic disease. This technique would further be developed in combination with SILAC labelling to probe the dynamics of protein synthesis and secretion of adipocyte secretory proteins. To gain physiologically useful information out of these data, semi-quantitative and quantitative mass spectrometry approaches would be used to compare the secretomes of cells and tissues under physiologically relevant models relevant to insulin resistance and type 2 diabetes. The effect of *in vitro* insulin resistance models on protein secretion from 3T3-L1 adipocytes would be studied, as adipokines have been described to play a strong role in insulin sensitivity.

The role of hepatocyte secretory proteins in disease progression is largely unknown. Another aim of this study was to use quantitative proteomics techniques to identify changes in hepatocyte protein secretion firstly under conditions mimicking fatty liver disease, and secondly under infection with hepatitis C virus. Both of these conditions are liver diseases that are strongly associated with insulin resistance and type 2 diabetes, and the data gained from these experiments would enhance our understanding of these pathologies.

Once established, the ability to purify secreted proteins would be used in combination with partial metabolic labelling to survey the secretome of animal white adipose tissue explants and stromovascular fraction primary cultures. This would be used to compare the secretory profiles of white adipose tissue and its constituent cell types from visceral and subcutaneous adipose tissue depots, with the aim of identifying the factor(s) responsible for the increased metabolic risk associated with visceral but not subcutaneous adipose tissue.

Lastly, this study aimed to investigate the possible existence of an adipo-insular axis, by looking at the effects of adipocyte conditioned media on glucose stimulated insulin release from pancreatic β-cells, and to use mass spectrometry to identify the factor(s) that may be involved in this. In all, the aim of this investigation was to provide a wealth of data concerning the secretory ability of various insulin sensitive tissues under various physiologically relevant stimuli, as well as to provide preliminary data concerning the metabolic contribution of these secreted proteins. It was hoped that these investigations would lay the foundation for future investigations into the metabolic role of individual secretory proteins and whole tissue types.

Chapter 2

Measuring Protein Secretion from Insulin Sensitive Tissues

Lindsay Wu

Data from this chapter were published in an equal first author manuscript (reproduced in chapter 3), "Pigment Epithelial Derived Factor Contributes to Insulin Resistance in Obesity" Crowe S, Wu LE, Economou C, Turpin SM, Matzaris M, Hoehn KL, Hevener AL, James DE, Duh EJ, Watt MJ Cell Metabolism 10:1 40-47, 2009. Data from this chapter were also presented as a poster at the 69th Scientific Sessions of the American Diabetes Society (2009), "Proteomic survey of adipokine secretion during insulin resistance" Wu LE, Larance ML, Raftery M, Guilhaus M, James DE. Data from this chapter were also presented as a poster at the 2009 Australian Diabetes Society meeting in Adelaide, "Proteomic Survey of Myokines Secreted from L6 myotubes" Wu LE, Raftery M, Guilhaus M, James DE. Supplementary mass spectrometry data from this data are provided in the attached DVD-ROM. Conditioned media from JFH1 infected hepatocytes was obtained from Dr. Enoch Tay, Westmead Millenium Institute. Primary hepatocytes were isolated by Dr. Bronwyn Hegarty, Garvan Institute of Medical Research. Microarray data were from experiments performed by Dr. Kyle Hoehn, Garvan Institue of Medical Research and Genentech, USA.

Abstract

Secreted proteins are ideal targets for diagnosis and therapy of disease states. Numerous studies have attempted to survey the complete secretory profile of cultured cells and tissues, primarily in adipocytes due to the importance of adipocyte secretory proteins in insulin resistance. These studies have frequently encountered the problem of conditioned media contamination by cytosolic proteins released from necrotic cells. To circumvent this problem, a glycoprotein affinity purification approach was adopted to selectively enrich for secretory proteins from conditioned media, followed by mass spectrometry for protein identification. This resulted in enrichment of secretory proteins, as indicated by the presence of N terminal signal peptides within a high percentage of these proteins. Protein secretion was measured from major insulin sensitive cells, including adipocytes, myotubes and hepatocytes. Primary hepatocytes secreted a greater number of proteins than adipocytes, challenging the undue attention adipose tissue receives as an endocrine organ, to the detriment of the role of other tissues. Protein secretion from adipocytes under physiologically relevant conditions of insulin resistance yielded the identification of the PDGF receptor like tumour suppressor (PRLTS) as a novel adipocyte secretory protein. Quantitative mass spectrometry was used both to measure rates of secretory protein synthesis, and to compare protein secretion under models of disease. Treatment of hepatocytes with palmitate to simulate non-alcoholic fatty liver disease resulted in a lower rate of protein secretion than control treatment. Infection of hepatocytes with hepatitis C virus altered the secretion of a number of proteins including α-fetoprotein. The experimental strategy described here forms a template for the study of protein secretion during disease.

Introduction

Secretomics is concerned with the secreted portion of the proteome. This group of proteins mediates the many endocrine effects distal to the cell or tissue of origin. While the level of many proteins is known to change prior to the onset of disease, it is the change in secreted proteins that occur with disease that afford the most realistic opportunity to detect and intervene in disease progression. Detection of secreted proteins in plasma is a very powerful way of measuring disease susceptibility or progression, as surgically invasive biopsy procedures are expensive, may lead to complications, and may not always be possible in a tissue of interest. Bioinformatic analysis has identified all genes coding for proteins possessing an N-terminal hydrophobic signal peptide sequence, however a gap in our knowledge exists in data pertaining to tissue distribution and regulated secretion. Identifying secretion patterns of tissues under normal and perturbed physiological conditions is of interest, as this knowledge will more realistically point towards novel diagnostics and therapies.

Identifying secreted proteins released from cells or tissues into conditioned media is technically challenging, primarily due to the presence of cytoplasmic factors released from necrotic cells. In fact, close inspection of the proto-constituents of many different conditioned media experiments reveals an abundance of cytoplasmic proteins. Where complete data are available, it appears that of all published studies (Kratchmarova, Kalume et al. 2002; Celis, Gromov et al. 2004; Wang, Mariman et al. 2004; Chen, Cushman et al. 2005; Alvarez-Llamas, Szalowska et al. 2007; Zvonic, Lefevre et al. 2007; Roelofsen, Dijkstra et al. 2009), the proportion of proteins detected by mass spectrometry that are true classically secreted proteins (as determined by the presence of an N-terminal signal peptide) does not exceed 63% (Wang, Mariman et al. 2004) and in some

cases is as low as 19% (Zvonic, Lefevre et al. 2007). This proportion decreases even further when the source of secreted proteins is derived from ex-vivo tissues from an animal or human patients (Alvarez-Llamas, Szalowska et al. 2007). This is due to the presence of serum proteins still present in microvasculature, despite extensive washing prior to collection of the conditioned media. This high proportion of contaminant proteins from necrotic cells and from serum is to be avoided, as contaminating proteins dilute the ability to detect truly secreted proteins by mass spectrometry, which has a finite limit for the number of peptides that can be sequenced at any one time.

Most classically secreted proteins are synthesized in the ER and as such are often characterised by the presence of an N-terminal hydrophobic signal peptide which targets the growing polypeptide to the translocon complex in the endoplasmic reticulum membrane. The growing polypeptide chain is inserted into the lumen of the ER, where folding is assisted by chaperones, and post-translational modifications such as N-glycosylation occur (Helenius and Aebi 2004). While not all secreted proteins undergo post-translational modifications such as glycosylation, many do, and there is considerable evidence that N-glycosylation contributes to the stability of proteins in the extracellular space (Shental-Bechor and Levy 2008). Conversely, cytoplasmic proteins that are not targeted to the endoplasmic reticulum for processing largely lack N-glycosylation.

This study has exploited this post-translational modification for purification of secreted proteins, to the exclusion of cytoplasmic proteins. Concanavalin A is a plant lectin derived from the fruit of the jack bean *Canavalia ensiformis*, and binds mannose residues of the type found in N-glycosyl conjugated proteins, with high affinity. In the current study commercially available concanavalin A bound to Sepharose was used to purify N-glycosylated proteins from conditioned

media. This method vastly improved the proportion of proteins present in conditioned media that fulfilled the criteria of secretory proteins.

This technique was validated in 3T3-L1 adipocytes, where a high number of secretory proteins were identified with minimal cytosolic contamination. Adipocytes play an important endocrine role. Despite numerous attempts (Kratchmarova, Kalume et al. 2002; Wang, Mariman et al. 2004; Alvarez-Llamas, Szalowska et al. 2007; Zvonic, Lefevre et al. 2007; Roelofsen, Dijkstra et al. 2009), the repertoire of adipocyte secretory proteins has not been sufficiently characterised to explain the endocrine effects of adipose tissue. This technique was also applied to skeletal muscle cells, the secretory profile of which is poorly described, despite the existence of data pointing towards an endocrine role for skeletal muscle (Febbraio and Pedersen 2002; Steensberg, Keller et al. 2002). Additional studies examined the secretory profile of primary hepatocytes, as there is again little information regarding the secretory repertoire of these cells. When combined with quantitative mass spectrometry, the secretion of proteins under various physiologically relevant stimuli was measured. These data indicate that this is a robust method for measuring protein secretion from cultured cells, which may be used to reveal novel aspects concerning protein secretion during disease states.

Methods

Cell culture

3T3-L1 fibroblasts were maintained in DMEM containing 10% NCS and PSG at a maximum confluence of 50% for subculturing. For differentiation of fibroblasts into adipocytes, 50% confluent fibroblasts were detached using trypsin/EDTA and seeded into new dishes at a ratio of 1:2. Four days later (day zero of differentiation), post-confluent fibroblasts were treated with a differentiation cocktail containing 350 nM insulin, 500 µM IBMX, biotin and dexamethasone in DMEM supplemented with 10% FCS and PSG. At day 3 post differentiation, cells took on a retracted, spindle-like morphology, and were fed media containing 350 nM insulin in DMEM supplemented with 10% FCS and PSG. On day 6 of differentiation, intracellular lipid droplets could clearly be observed and media was replaced with DMEM containing 10% FCS supplemented with PSG. Mature adipocytes were usually used for experiments at day 8 post-differentiation.

L6 myoblasts were maintained in α-MEM supplemented with 10% FCS and PSG at a maximum confluence of 50% for subculturing. For differentiation, myoblasts were grown to a confluence of around 80%, and media was replaced with α-MEM supplemented with 2% horse serum. After 4 days, cells had begun fusing to form polarised multinucleated myotubes. Myotubes were used at day 4 post-differentiation for experiments.

Hepatocytes were obtained as primary cultures from C57BL6 mice in accordance with appropriate animal ethics guidelines. Mice were anaesthetised by intraperitoneal injection of ketamine/xylazine mix. Once anaesthesia had taken effect, the abdominal cavity was opened, the

inferior vena cava cannulated, and the hepatic portal vein was cut open. Liver was perfused via inferior vena cava with warmed perfusion buffer (138 mM NaCl, 50 mM HEPES, 5.6 mM glucose, 5.4 mM KCl, 0.34 mM Na_2HPO_4, 0.44 mM KH_2PO_4, 4.17 mM $NaHCO_3$, 0.5 mM EGTA, pH 7.4) at a rate of 4 ml per min for 15 min. Perfusion buffer was replaced with collagenase digestion buffer (138 mM NaCl, 50 mM HEPES, 5.6 mM glucose, 5.4 mM KCl, 0.34 mM Na_2HPO_4, 0.44 mM KH_2PO_4, 4.17 mM $NaHCO_3$, 1 mM $CaCl_2$, 1 mg/ml collagenase H from Roche, pH 7.4). After perfusion of ~45 ml of collagenase digest buffer, liver was carefully dissected away from surrounding tissue, gall bladder was carefully removed, and liver sac torn open to release hepatocytes into ice-cold collagenase buffer. The mixture was passed through a mesh filter, and cells were centrifuged at 50 *g* for 3 min. Cells were washed three times in ice-cold Ca^{2+} buffer, with filtering steps after each wash. Cells were resuspended in cold M199 buffer (Gibco), counted and diluted in seeding solution (2% FCS, 100 nM insulin, 100 nM dexamethasone, 1x PSG in M199 media). Hepatocytes were seeded at a concentration of 1.55 x 10^7 cells per 10 cm dish, and allowed to adhere overnight prior to incubation in DMEM and conditioned media experiments. For palmitate treatment of hepatocytes, equal numbers of hepatocytes were divided into different culture dishes and cells were grown for 24 h in normal primary hepatocyte media with isotopic arginine and lysine. Different isotopes were used for different treatments. After 24 h, cells were treated either with 2% BSA alone (control), or with 400 µM palmitic acid conjugated to 2% BSA. Treatment was conducted for a further 24 h after which, media was replaced with serum free media containing amino acid isotopes and supplemented with 100 nM insulin. Cells were incubated for a further 18 h, conditioned media was collected, aliquots were taken, mixed together in equal proportions.

Conditioned media experiments

In all experiments, cells were washed at least four times in PBS at room temperature, and incubated with serum free media supplemented with insulin (100 nM) to stimulate protein synthesis and secretion. Serum free media for adipocytes experiments was DMEM, for hepatocytes it was DMEM containing dexamethasone (100 nM), and for myotubes it was α-MEM. Cells were maintained in the appropriate serum free media for 18 h. Conditioned media was collected and centrifuged at 2,000 *g* for 10 min to remove cell debris. Conditioned media was used for either glycoprotein purification or application to fresh cells for glucose uptake experiments.

Glycoprotein purification

The plant lectin Concanavalin A (ConA), derived from the jackbean *Canavalia ensiformis*, was used to enrich for secreted glycoproteins. ConA bound sepharose beads were added to conditioned media samples, followed by 1 mM $MnCl_2$, which is needed for the glycoprotein binding activity of ConA. Samples were rotated overnight at 4°C. Sepharose beads were washed extensively with ConA binding buffer (0.5 M NaCl, 0.1 M Tris, 1 mM $MnCl_2$ and 1 mM $CaCl_2$, adjusted to *p*H 7.4). Glycoproteins were eluted using ConA elution buffer (0.3 M methyl-α-D-mannopyranoside, 0.5 M NaCl, 0.1 M Tris, 10 mM EDTA and 10 mM EGTA adjusted to *p*H 7.4). ConA sepharose beads were incubated with ConA elution buffer (100 µL) for at least 2 h at room temperature. Eluted proteins were precipitated using the chloroform:methanol method (Wessel and Flugge 1984) and resolved by SDS-PAGE using 10% acrylamide gels. Proteins in gels were visualised by through either silver staining or SYPRO ruby staining.

Protein visualisation

For SYPRO ruby staining, gels were fixed in a fresh solution of 50% methanol and 10% acetic acid twice for 40 min, during which gels turned visibly white in colour and shrunk in size. Gels were incubated overnight at room temperature in SYPRO ruby stain in the dark. Following staining, gels were washed once for 40 min in a solution of 10% methanol and 7% acetic acid. Gels were stored in distilled water for subsequent visualisation using a Fuji gel scanner. For silver staining, gels were again fixed in 50% methanol with 10% acetic acid for at least 30 min, followed by three 5 min washes in 5% methanol, followed by three one min washes in distilled water. Gels were then sensitised to silver by incubation in sodium thiosulphate (0.2 g/L) for 3 min. Gels were washed three times for 30 s in distilled water, and incubated in $AgCl_2$ (2 g/L) for 30 min. Gels were again washed three times for 30 s, and gels incubated in developing solution of sodium thiosulphate (0.004 g/L), formaldehyde (0.02% v/v) and sodium carbonate (30 g/L) until bands appeared on gel, at which point development was stopped by incubation of gel with EDTA (14 g/L).

Amino acid isotopes

All isotopes were from Cambridge laboratories. The "medium" isotope of arginine was U-13C6 arginine (catalogue number CLM-2265), "heavy" arginine was U-^{13}C6 U-^{15}N4 arginine (catalogue number CNLM-539), "medium" lysine was 4,4,5,5-D4 lysine (catalogue number CNLM-2640), heavy lysine was U-^{13}C6 U-^{15}N2 lysine (catalogue number CNLM-291). Growth media was low glucose Dulbecco's modified eagle media (DMEM) deficient in leucine, arginine, lysine and phenol red from Sigma (catalogue number D9443). Glucose was adjusted to 4.5 g/L,

leucine was added to a concentration of 0.105 g/L, and phenol red was added to 0.0159 g/L. Arginine and lysine were added at 25% of normal concentration in DMEM to avoid conversion of excess isotopes into proline (O'Quinn, Knabe et al. 2002; Ong, Kratchmarova et al. 2003). Arginine isotopes were added back at a concentration of 0.021 g/L, lysine isotopes were added back at a concentration of 0.0365 g/L. After addition of all ingredients, media was passed through a 0.20 µm filter.

Mass spectrometry

Peptide extraction and mass spectrometry was performed as previously described (Larance, Ramm et al. 2005; Crowe, Wu et al. 2009). Proteins were resuspended in Laemmli buffer containing 50 mM Tris (2-carboxy-ethyl) phosphine (TCEP) (Bond-Breaker, Pierce), and loaded onto a 10% acrylamide gel. Lanes were sliced into 12 equal sized portions, and diced into ~1 mm^3 cubes. Gel cubes were incubated in 50% acetonitrile, 250 mM NH_4HCO_3 with shaking at room temperature for 30 min, followed by 100% acetonitrile with shaking at room temperature for 10 min. Trypsin (12.5 ng/µl in 100 mM NH_4HCO_3) was added to submerged gel pieces (~ 40 µL), and incubated for 12 h at 37°C. Tryptic peptides were extracted by addition of 100 µL of 5% formic acid for one h at 37°C, followed by 100 µL of 100% acetonitrile for two h, followed finally by an additional 500 µL of acetonitrile until gel slices turned completely white (usually <10 min). The resulting solution was removed and dried under vacuum. Peptides were resuspended in 20 µL of 5% formic acid. These samples were loaded onto a Waters Ultima tandem mass spectrometer. Peak picking and database searching was performed using the Mascot distiller software package, version 2.3.1.0. MDRO 2.3.1.0 (Matrix Sciences). The SwissProt database on Mascot server 2.2 was used for protein identification, with taxonomy

restricted to Mus musculus, MS tolerance set at 0.5 Da and MSMS tolerance set at 0.05 Da. Variable modifications were set to carbamidomethyl, propionamide and oxidation (M). No fixed modifications were used. Trypsin was set as cleavage enzyme after arginine or lysine and a maximum of 2 missed cleavages were permitted. Quantitation method was as follows. Method: constrain search – yes, protein ratio type – weighted, protein score type – standard, report detail – yes, minimum peptides – 1. Protocol: precursor, allow mass time match – yes, allow elution shift – no, all charge states – no. Component "light" was mode – exclusive, unmodified site – K, position – anywhere, unmodified site – R, position – anywhere. Component "medium" was mode – exclusive, modification – Label: 2(H)4 (K), modification – Label: 13C(6) (R). Component "heavy" was mode – exclusive, modification – Label: 13C(6)15N(2) (K), modification – Label: 13(6)15N(4) (R). For all ratios measured, numerators and denominators were set to 1.0. Integration – trapezium, integration source – survey, precursor range – envelope. Quality: minimum precursor charge – 1, isolated precursor – No, Minimum a(1) – 0.0, peptide threshold type – minimum score. Outlier – auto. The presence of a signal peptide in detected proteins was determined using SignalP 3.0 (Bendtsen, Nielsen et al. 2004). "Medium" and "heavy" isotopes are expressed here in relation to "light" (endogenous amino acid) isotopes. Ratios of isotope to "light" below 0.05 were discounted as "no label incorporation". Keratin peptides were in all cases ignored. The presence of a signal peptide in detected proteins was determined using SignalP 3.0 (Bendtsen, Nielsen et al. 2004).

Antibodies

Adiponectin antibody (A6354) was from Sigma (Australia). Complement C3 antibody (ICN55444) was from Aurora, Ohio, USA. PRLTS antibody (ABVAP67LQ1) was from Abnova, Taiwan, ROC. Flk-1 (sc-6251), PDGFR-β (sc-339), PDGF (sc-7879) and VEGF (sc-152) antibodies were from Santa Cruz, CA, USA. Cytochrome C antibody (4272) was from Cell Signalling Technologies, MA, USA. EEA1 antibody was a gift from Dr. Marvin Fritzler, University of Calgary. GM130 (1837-1) antibody was from Epitomics, CA, USA. Tubulin (DM1A) antibody was from Sigma (Australia).

Glucose uptake assay

3T3-L1 adipocytes were cultured in 24-well plates, and at day 8 post-differentiation, cells were treated for 24 hours with 10 kDa filtered and three times concentrated conditioned media from a separate batch of adipocytes treated with insulin resistance models as described previously (Hoehn, Hohnen-Behrens et al. 2008). Cells were then incubated in KRP with 0.2% BSA at 37°C for 2 h. Cells were then incubated in KRP with 0.2% BSA, 1mM DOG and 10.5 µCi ^{3}H-DOG per well. Insulin was used to stimulate cells at a concentration of 100 nM. 2-DOG uptake was stopped after 5 min by washing of cells in ice-cold PBS. Cells were lysed with 500 µL 1% Triton X-100, and 400 µL of lysates were mixed with 3 ml scintillation fluid. Radiation was measured using a β-counter.

Insulin resistance models

Two insulin resistance models were used in this study: chronic insulin exposure and chronic TNFα exposure. Both have been described previously (Hoehn et al, Cell Metab 2008). Chronic insulin: mature adipocytes are treated with serum free DMEM supplemented with 10 nM insulin at 1200 hr, media was then replaced at 1600, and 2000 and 0800 hr. At 1200 hr, media was replaced with DMEM supplemented with 100 nM insulin. After 18 hr, this media was collected and subjected to glycoprotein purification. Chronic TNFα: mature adipocytes were treated with 2 ng/ml recombinant TNFα (Calbiochem) in DMEM and 10% FCS. Media was replaced every day at 1200 hr for four days. After four days, at 1200 hr media was replaced with serum free DMEM supplmented with 2 ng/ml TNF and 100 nM insulin. After 18 hr, this media was collected and subjected to glycoprotein purification. For control cells, adipocytes were left untreated, and media was replaced with serum free DMEM supplemented with 100 nM insulin. After 18 hr, this media was collected and subjected to glycoprotein purification.

Results

Glycoprotein purification reduces cytoplasmic contamination in conditioned media samples.

A number of approaches were tested for optimisation of glycoprotein purification, which was performed using the lectin concanavalin A. Typical adipocyte culture protocols frequently include the use of bovine serum albumin (BSA), which binds free fatty acids that are present in reasonably high concentrations in adipocyte cultures. Free fatty acids can be problematic because they can cause cell lysis and subsequent lipid release. However, the effect of exogenously added

BSA on adipokine secretion is not known. It was also not known whether BSA (which is one of the few non-glycosylated serum proteins) would interfere with glycoprotein purification. To optimise this and other variables a screening strategy examining adiponectin secretion, a known adipokine, was established. Another issue that needed addressing was the most efficient buffer needed to purify secreted proteins from conditioned media. Concanavalin A is a lectin that is dependent on Ca^{2+} and Mn^{2+} for its glycoprotein binding activities. It also displays most specific binding in a high salt environment. Furthermore, as a lectin, concanavalin A has an affinity for carbohydrates including glucose, which is present in culture media at high (25 mM) concentrations. To optimise the method in the presence of the above mentioned confounding factors, a simple experiment was designed, using the ability to enrich for the well studied adipocyte secretory factor adiponectin (Kadowaki, Yamauchi et al. 2006) as a read-out for the success of the approach (Fig. 1). 3T3-L1 adipocytes were cultured in serum free media with or without 2% BSA. Conditioned media was collected, and BSA added back into one BSA free sample at a concentration of 2%. A variety of methods for providing the most efficient environment for ConA were trialled. Dialysis against ideal ConA binding buffer (0.5 M NaCl, 1 mM $MnCl_2$, 1 mM $CaCl_2$, 100 mM Tris, pH 7.4) using a 10 kDa molecular weight cut-off filter was trialled, as was dilution of sample in ConA binding buffer, addition of 1 mM $MnCl_2$ to conditioned media and no alteration of conditioned media. Dilution and no treatment of conditioned media samples did not result in any detectable enrichment of adiponectin. Dialysis allowed enrichment of adiponectin, irrespective of BSA addition during or after media conditioning. Addition of $MnCl_2$ resulted in the highest enrichment of adiponectin, however this was intriguingly ablated in samples containing BSA. It is possible that the fatty acids that BSA carries may interfere with Concanavalin A, as dialysis of samples, which would allow the

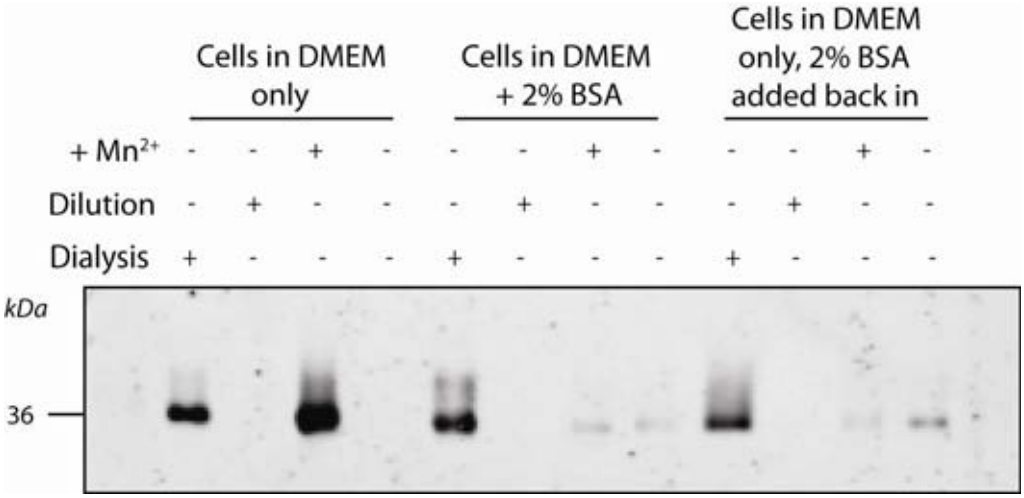

Figure 1. Optimisation of ConA pulldown. Conditioned media was collected from 3T3-L1 adipocytes left in DMEM with or without 2% BSA. BSA was subsequently added back to one lot of DMEM only samples after adipocyte conditioning. Samples were divided and prepared as described. For dialysis samples, conditioned media was dialysed extensively against ConA binding buffer using a 10 kDa molecular weight cut-off dialysis tubing. For dilution samples, conditioned media was diluted 10-fold into ConA binding buffer. For Mn^{2+} samples, $MnCl_2$ was added back to conditioned media at a concentration of 1 mM. Concanavalin A sepharose beads were added to all samples and incubated for 16 hours at 4°C. Beads were washed with ConA binding buffer, proteins eluted using methyl-α-D-mannopyranoside and subsequently precipitated using the chloroform : methanol method. Proteins were immunoblotted for the known adipocyte secretory protein adiponectin.

removal of free fatty acids, restored the ability of ConA to enrich for adiponectin in the presence of Mn^{2+}. As a result of this experiment, it was decided that BSA was not necessary during conditioned media experiments, and that the most efficient method of providing an ideal environment for ConA to enrich for glycoproteins was for simple addition of 1 mM $MnCl_2$ to conditioned media samples.

During conditioned media experiments, it is important that cells are incubated in serum free media, as serum contains a high concentration of exogenous secreted proteins that may confound the detection of adipocyte derived secretory proteins. In the absence of the mitogenic growth factors contained in serum, there is no activation of mTOR and p70 S6 kinase, which in theory would result in poor protein synthesis. To determine the importance of maintaining protein synthesis for protein secretion, the effect of insulin on protein secretion was investigated (Fig. 2). Insulin stimulated the appearance of most protein species in conditioned media after glycoprotein enrichment, and so in all future experiments insulin was added to media. As a determinant of specificity of this method for measuring protein secretion, experiments were performed in the presence of the antibiotic Brefeldin A, a drug that blocks retrograde transport from the Golgi to the ER and also protein secretion (Dinter and Berger 1998). This occurs via inhibition of Arf-GAP proteins that regulates the budding of vesicles from the Golgi (Dinter and Berger 1998). Inhibition of this process by BFA potently inhibits the secretion of proteins via the classical secretory pathway. As shown in Fig. 3 the majority of proteins detected by the ConA enrichment method were not present following incubation with BFA, indicating that the majority of proteins in this sample are secreted proteins. In contrast, TCA protein precipitation, which examines total proteins in conditioned media, yielded a sample containing BFA insensitive proteins, emphasising the degree of contamination by cytosolic proteins in conditioned media.

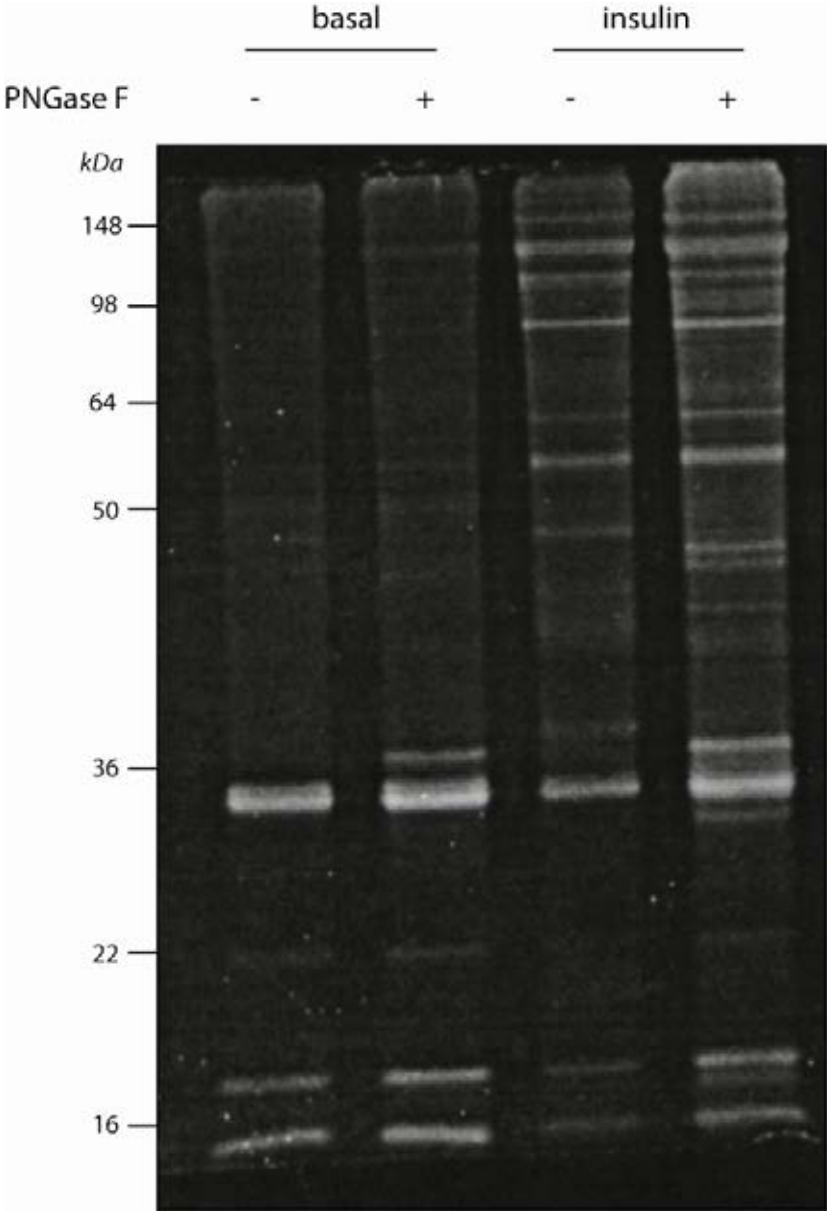

Figure 2. Secretion of a majority of protein species is insulin sensitive. 3T3-L1 adipocytes were incubated in serum free DMEM for 16 hours in the presence or absence of 1 nM insulin. Glycoproteins were purified as described in methods section, and treated with the de-glycosylating enzyme, peptide N-glycosidase F (PNGase F). Proteins were resolved by SDS-PAGE and total protein visualised using SYPRO ruby stain. Proteins species that undergo a noticeable shift in electrophoretic mobility with PNGase F treatment are secretory proteins.

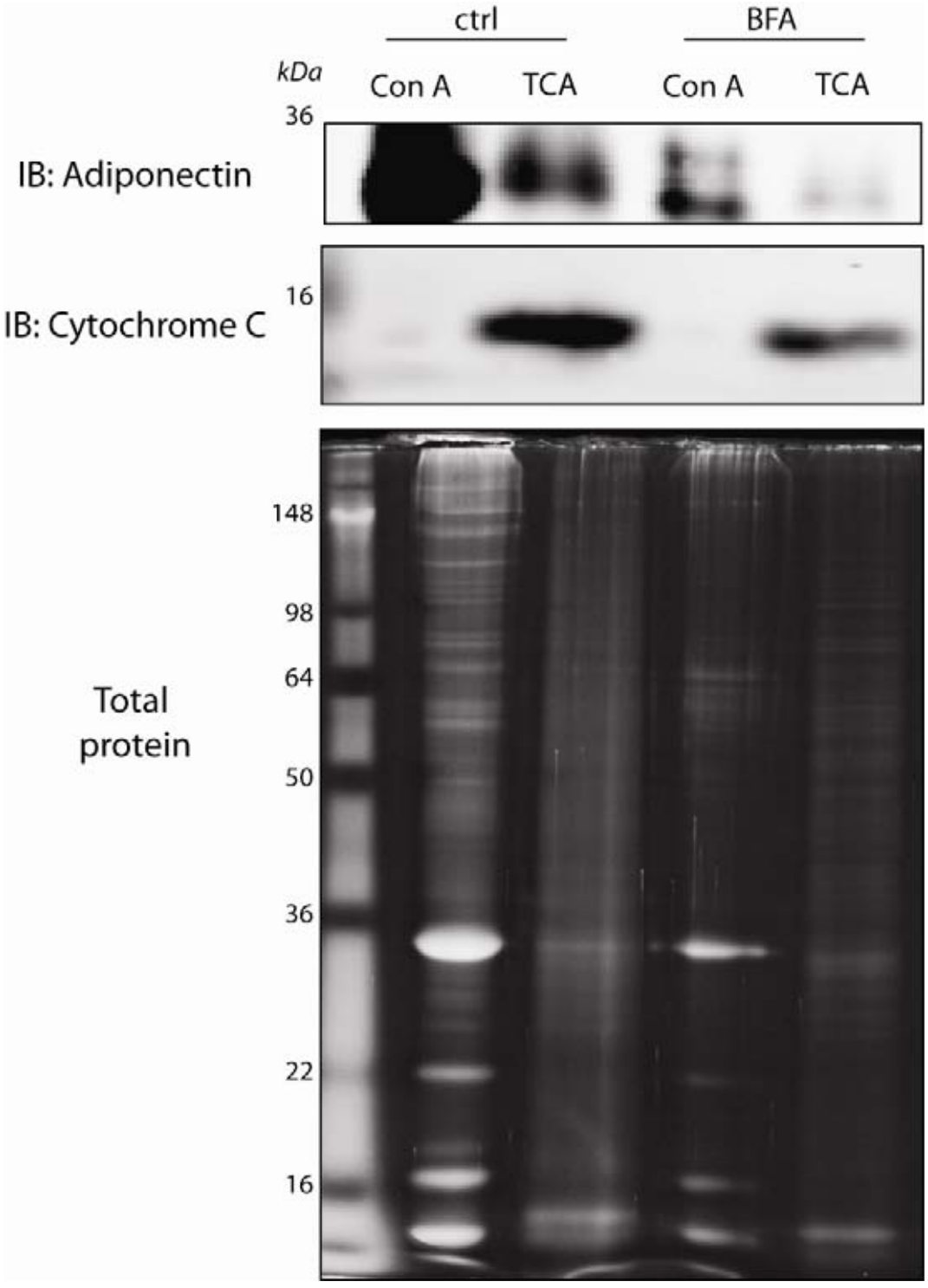

Figure 3. Con A affinity purification enriches for BFA sensitive secretory proteins from conditioned media to the exclusion of cytosolic proteins. Conditioned media samples from control or Brefeldin A (BFA) treated adipocytes was subjected to Con A affinity purification or TCA protein precipitation. Samples were immunoblotted for the adipocyte secretory protein adiponectin, and cytosolic protein cytochrome C, or stained for total protein.

To underline this, samples were immunoblotted with antibodies raised against secretory and non-secretory proteins. Glycoprotein purification enriched for secreted proteins when compared with TCA protein precipitation. Cytoplasmic proteins were present in total TCA precipitations, and largely absent from glycoprotein enrichments.

Secretome of insulin sensitive tissues

Survey of the adipocyte secretome

Adipocytes are non-dividing cells that are formed as a result of a complex differentiation process (termed adipogenesis) from fibroblast precursor cells. During adipogenesis, cells undergo significant morphological changes with formation of lipid droplets, accompanied by altered gene expression and protein levels. To mimic this process *in vitro*, the 3T3-L1 cell line (Green and Meuth 1974) was used. These cells are propagated as fibroblasts, and treated with a cocktail of isobutylmethylxanthine, insulin, biotin and dexamethasone to induce differentiation. Three previous studies have attempted to identify changes in protein secretion during the course of adipogenesis. However, in the two cases where full data are available, the experiments were dominated by intracellular cytosolic proteins (Kratchmarova, Kalume et al. 2002; Wang, Mariman et al. 2004; Molina, Yang et al. 2009). Furthermore, changes in protein secretion could not be fully visualised in these studies. To address this, conditioned media from 3T3-L1 fibroblasts and differentiated 3T3-L1 adipocytes were collected, subjected to glycoprotein purification and proteins were separated by SDS-PAGE (Fig. 4). A vastly different polypeptide profile was observed in the two samples, highlighting the changes in secretion profiles that occur

during adipogenesis, and the ability of glycoprotein purification to remove cytosolic contaminants, allowing differences in protein secretion to be clearly seen.

To identify the secreted proteins present in adipocyte conditioned media samples, proteins were trypsin digested and subjected to mass spectrometry. A total of 129 proteins were detected (Table 1). The presence of an N-terminal signal peptide in each detected protein was determined using the SignalP algorithm (Bendtsen, Nielsen et al. 2004). Of these 129 proteins, 114 displayed an N-terminal signal peptide. The proportion of proteins with a predicted signal peptide in this study was 86% of proteins detected, or 99% of all peptides detected. This compares favourably with previous studies, for which the success rate does not exceed 63% (Wang, Mariman et al. 2004). The protein stain shown in Fig. 4 indicates that the majority of proteins are of above 26 kDa in size. An analysis of the detected proteins shows that only 25 of 129 detected proteins have a theoretical molecular weight below 36 kDa, however post-translational modifications including N-glycosylation are likely to add a considerable amount the the actual molecular weight. A comparative analysis showing the success of previous approaches in detecting secreted proteins from adipocytes is shown in Fig. 5.

Several proteins previously known to be abundantly secreted from adipocytes including adiponectin and complement C3 were identified in this screen, validating the integrity of the approach used here. The proteins identified in this study were from a number of classes, including acute phase reactant proteins, extracellular matrix proteins, signalling proteins and serine protease inhibitors. The most abundant protein detected in the screen was the acute phase reactant complement C3, which plays a key role in the innate immune system complement pathway. The serum levels of complement C3 rise during bacterial infection, where it undergoes proteolytic cleavage and interacts with other members of the complement pathway to form the

membrane attack complex. This complex is able to puncture the outer membrane of bacterial pathogens. Complement C3 serum levels are increased in insulin resistance and obesity (Engstrom, Hedblad et al. 2005), possibly contributing to the chronic inflammation that is known to occur in these syndromes. Other abundant proteins in the screen were extracellular matrix proteins of the collagen family. These proteins are required to maintain adipose tissue structure possibly by forming a tight net around the existing tissue, limiting its further expansion. This argument is supported by studies in mice in which the gene collagen (VI) has been deleted. These mice display abnormal adipose tissue expansion on a high fat diet, accompanied by protection against diet-induced insulin resistance (Khan, Muise et al. 2009). In view of the ubiquitous tissue distribution of collagen VI this is not a strong target for therapy. Other proteins identified in this experiment include the antioxidant extracellular superoxide dismutase (SOD3), the haem-binding acute phase reactant haptoglobin, the anti-angiogenic cytokine thrombospondin, insulin-like growth factor binding protein 7, and numerous members of the serine protease inhibitor family, which included the non-catalytically active serine protease inhibitor pigment epithelial derived factor (PEDF). Of the 114 adipocyte-secreted proteins identified in this screen, 42 were not found in previous studies (Kratchmarova, Kalume et al. 2002; Wang, Mariman et al. 2004; Chen, Cushman et al. 2005; Alvarez-Llamas, Szalowska et al. 2007; Zvonic, Lefevre et al. 2007; Roelofsen, Dijkstra et al. 2009), demonstrating the advance made from the glycoprotein enrichment method. The 42 novel proteins were from a variety of functional classes, and are highlighted in grey in Table 1. These proteins included the acute phase reactant orosmucoid, growth arrest specific 6 (GAS6), the biotin processing enzyme biotinidase, and the serine protease inhibitor contrapsin.

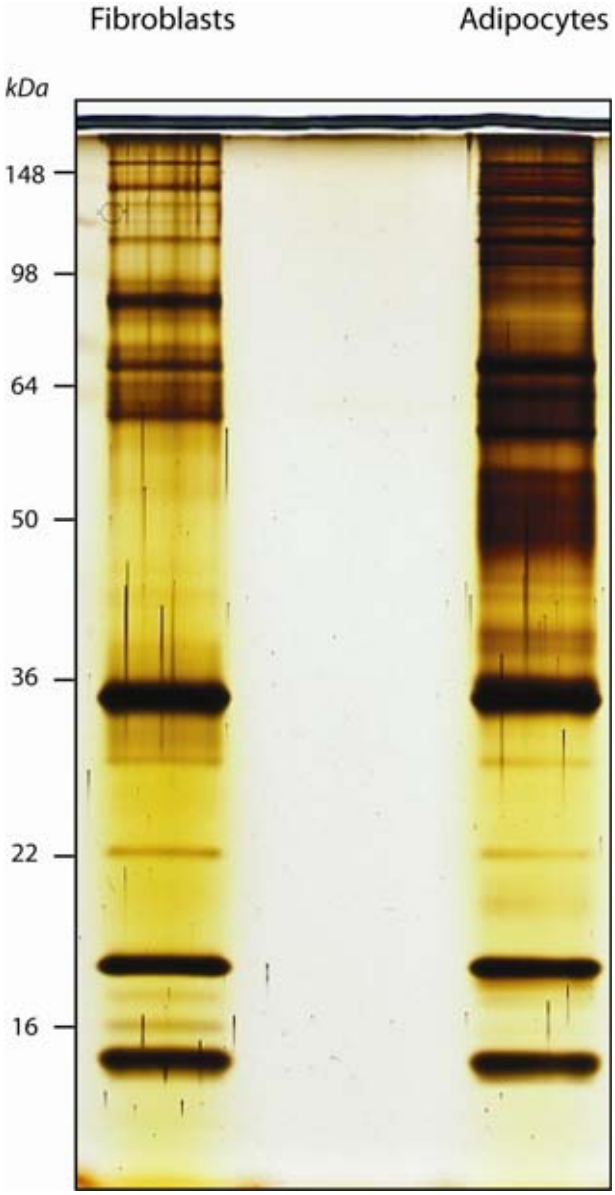

Figure 4. Secretory profile of 3T3-L1 fibroblasts and differentiated adipocytes. Fully confluent fibroblasts or differentiated adipocytes were left in serum free media supplemented with 1 nM insulin for 16 hours. Conditioned media was collected, subjected to glycoprotein purification as described in methods, proteins resolved by SDS-PAGE, and visualised by silver staining.

Accession	Name	No. peptides identified	MW	Signal peptide?
gi|1352102	Complement C3	357	186365	Y
gi|50489	collagen alpha-2(I)	302	129524	Y
gi|34328108	collagen, type I, alpha 1	123	137948	Y
gi|94363816	collagen, type VI, alpha 3, isoform 2	97	354997	Y
gi|36031080	collagen, type IV, alpha 2	83	167287	Y
gi|5921190	Collagen alpha-1(III) chain precursor	63	138858	Y
gi|148708135	mCG12867, isoform CRA_a	58	286510	Y
gi|31791061	collagen, type VI, alpha 3	51	286706	Y
gi|22203747	collagen, type VI, alpha 2	46	110266	Y
gi|2493790	Adiponectin	40	26824	Y
gi|125490382	procollagen C-proteinase enhancer protein	40	50136	Y
gi|6753484	procollagen, type VI, alpha 1	39	108422	Y
gi|6681143	decorin	36	39784	Y
gi|198862	lipoprotein lipase	33	53107	Y
gi|8850219	Haptoglobin	32	38727	Y
gi|3320907	extracellular superoxide dismutase	30	27376	Y
gi|470674	collagen pro-alpha-1 type I chain	29	137859	Y
gi|8393173	collagen, type V, alpha 3	29	171864	Y
gi|49809	alpha-2 collagen	26	109743	Y
gi|7304867	adipsin	24	28039	Y
gi|113881	Angiotensinogen precursor (Serpin A8)	24	51958	Y
gi|6678077	secreted acidic cysteine rich glycoprotein (osteonectin)	24	34428	Y
gi|179433	biglycan	19	44254	Y
gi|192281	complement 3	16	24176	Y
gi|8132999	voltage-gated potassium channel KCNQ5	15	96971	Y
gi|6755891	protease, serine, 3	14		Y
gi|126302535	Collagen alpha-1(IV) chain precursor	13	160579	Y
gi|23396610	IGF-binding protein 7 (IGF BP-7) (follistatin)	13	29005	Y
gi|6755106	procollagen-lysine, 2-oxoglutarate 5-dioxygenase 1	11	83542	Y
gi|22203763	carboxypeptidase 3	10	53222	Y
gi|7657429	periostin, osteoblast specific factor	10	90198	Y
gi|695629	superoxide dismutase	10	27392	Y
gi|201995	thrombospondin	10	95972	Y
gi|18958361	URB	10	107573	Y
gi|88193016	Chain E, Crystal Structure Of A Bpti Variant (Cys14->ser) In Complex With Trypsin	9	23287	N
gi|3808221	pigment epithelium-derived factor	9	46229	Y
gi|303678	47-kDa heat shock protein	7	46504	Y
gi|17390745	Complement component 1, s subcomponent	7	77365	Y
gi|2498391	Follistatin-related protein 1 precursor (Follistatin-like 1) (TGF-beta-inducible protein TSC-36)	7	34516	Y
gi|6753556	cathespin D	6	44925	Y
gi|192912	cystatin C	6	15541	Y
gi|1181242	fibronectin	6	160848	Y

gi|459877	lysyl oxidase	6	46657	Y
gi|113205063	tissue inhibitor of metalloproteinase 1	6	22613	Y
gi|9055252	inter alpha-trypsin inhibitor, heavy chain 4	5	104643	Y
gi|34328049	lipocalin-2	5	22860	Y
gi|6678740	lumican	5	38327	Y
gi|6679373	serine (or cysteine) proteinase inhibitor, clade E, member 1	5	45141	Y
gi|62990160	complement component 1, r subcomponent	4	80054	Y
gi|224360	concanavalin A	4	25624	N
gi|6679182	orosomucoid 1	4	23880	Y
gi|119893035	PREDICTED: similar to alpha-2-macroglobulin isoform 1 [Bos taurus]	4	164239	Y
gi|67972647	arylsulfatase A	3	53714	Y
gi|13384648	biotinidase	3	59240	Y
gi|6680840	calumenin	3	27041	Y
gi|22203763	carboxypeptidase E	3	53222	Y
gi|3560547	chloride channel CaCC	3	99976	Y
gi|3169729	hematopoietic lineage switch 2	3	47829	Y
gi|293691	laminin B2	3	176939	Y
gi|19527008	lysophospholipase 3	3	47277	Y
gi|6678902	matrix metalloproteinase 2	3	74055	Y
gi|6754854	nidogen 1	3	136439	Y
gi|129729	Protein disulfide-isomerase precursor (PDI) (Prolyl 4-hydroxylase subunit beta) (Cellular thyroid hormone-binding protein) (p55) (Erp59)	3	57108	Y
gi|387401	adipocyte lipid binding protein	2	14683	N
gi|122065132	Arylsulfatase B precursor (ASB) (N-acetylgalactosamine-4-sulfatase) (G4S)	2	59609	Y
gi|42734447	Bone morphogenetic protein 1 precursor (BMP-1) (Procollagen C-proteinase) (PCP)	2	111595	N
gi|117553604	carboxylesterase 3	2	61749	Y
gi|81915013	Cell surface glycoprotein MUC18 precursor (Melanoma-associated antigen MUC18) (Melanoma cell adhesion molecule) (Gicerin) (CD146 antigen)	2	71500	Y
gi|57956	collagen alpha 1 chain type VI	2	61844	Y
gi|1498641	extracellular matrix associated protein	2	72272	Y
gi|4103925	extracellular matrix protein	2	62794	Y
gi|6806909	FK506 binding protein 7	2	24897	Y
gi|29144947	FK506 binding protein 9	2	62928	Y
gi|220434	heparin binding protein 44	2	42058	Y
gi|88909565	Macrophage mannose receptor 2 precursor (Lectin lambda) (CD280 antigen)	2	166988	Y
gi|809337	Pngase F	2	34759	N
gi|309181	procollagen type V alpha 2	2	144877	Y

gi|18087743	protocadherin gamma subfamily B, 7	2	100825	Y
gi|12963609	quiescin Q6 sulfhydryl oxidase 1 isoform b	2	63296	Y
gi|15929248	Sbf2 protein	2	93764	N
gi|116961	Serine protease inhibitor A3K precursor (Serpin A3K) (Contrapsin) (SPI-2)	2	46850	Y
gi|2145149	treacle	2		ambiguous
gi|12852628	unnamed protein product	2	50315	Y
gi|202351	vascular endothelial growth factor	2	22524	Y
gi|11967947	abhydrolase domain containing 8	1	48258	N
gi|1587060	alpha dystroglycan	1	70537	Y
gi|6679891	alpha glucosidase 2 alpha neutral subunit	1	109335	Y
gi|1478074	alpha-D-mannosidase	1	112352	Y
gi|191765	alpha-fetoprotein	1	47195	Y
gi|2623222	ATP synthase beta-subunit	1	56344	ambiguous
gi|124486622	calcium channel, voltage-dependent, L type, alpha 1S subunit	1	210184	Y
gi|469422	calmodulin	1	16884	N
gi|227293	cathepsin B	1	37370	Y
gi|4886998	cathepsin L	1	37505	Y
gi|11066226	cathepsin Z	1	34153	Y
gi|27923753	cingulin	1	136635	N
gi|397800	cyclophilin C-associated protein	1	64014	Y
gi|13626390	Dipeptidyl-peptidase 2 precursor	1	56234	Y
gi|6754450	fatty acid binding protein 5, epidermal	1	15127	N
gi|145301603	growth arrest specific 6	1	74561	Y
gi|60687514	guanine nucleotide exchange factor for Rap1	1	93623	N
gi|817939	Histone H2A	1	14737	N
gi|85701562	hypothetical protein LOC546166	1	15937	N
gi|21312106	hypothetical protein LOC73481	1	28387	Y
gi|99876778	immunoglobulin heavy chain complementarity determining region 3	1	2727	Y
gi|31982258	insulin-like growth factor binding protein, acid labile subunit	1	66948	Y
gi|126369	Laminin subunit gamma-1 precursor (Laminin B2 chain)	1	177492	Y
gi|6678682	lectin, galactose binding, soluble 1	1	14856	N
gi|16418335	leucine-rich alpha-2-glycoprotein	1	37408	Y
gi|13878586	Lysyl oxidase homolog 3 precursor (Lysyl oxidase-like protein 3) (Lysyl oxidase-related protein 2)	1	83627	Y
gi|10946772	matrix metallopeptidase 19	1	59085	Y
gi|6754698	multiple inositol polyphosphate histidine phosphatase 1	1	54503	Y

gi|7527462	N-acetylgalactosamine-6-sulfate sulfatase	1	57636	Y
gi|33238890	olfactory receptor 693	1	35129	Y
gi|10179944	phosphoglycerate mutase 1	1	28919	N
gi|82902957	PREDICTED: similar to Putative uncharacterized serine/threonine-protein kinase SgK110 (Sugen kinase 110)	1	36914	N
gi|91160	procollagen I C-proteinase enhancer protein precursor	1	42495	Y
gi|33859526	procollagen, type III, alpha 1	1	64134	Y
gi|1381582	prosaposin	1	61365	Y
gi|112293264	protein disulfide isomerase associated 3 (ERp61)	1	56643	Y
gi|18087735	protocadherin gamma subfamily B, 2	1	100831	Y
gi|6755702	suppressor of variegation 3-9 homolog 1	1	47724	N
gi|12004583	unknown	1	66220	Y
gi|12849539	unnamed protein product	1		
gi|26346817	unnamed protein product	1	26068	N
gi|26348945	unnamed protein product	1	147969	N
gi|124487135	uracil phosphoribosyltransferase (FUR1) homolog	1	34256	N
gi|202349	vascular cell adhesion molecule phosphatidylinositol-form precursor	1	38347	Y
gi|7715928	immunoglobulin heavy chain variable region			Y

Table 1. Adipocyte secretory factors identified. Fully differentiated 3T3-L1 adipocytes were incubated in serum free media supplemented with 100 nM insulin for 18 hours. Conditioned media was collected, glycoprotein purification (methods), SDS-PAGE (figure 4). Proteins were digested and subjected to mass spectrometry, identification results shown. Presence of N-terminal signal peptides were detected using SignalP 3.0.

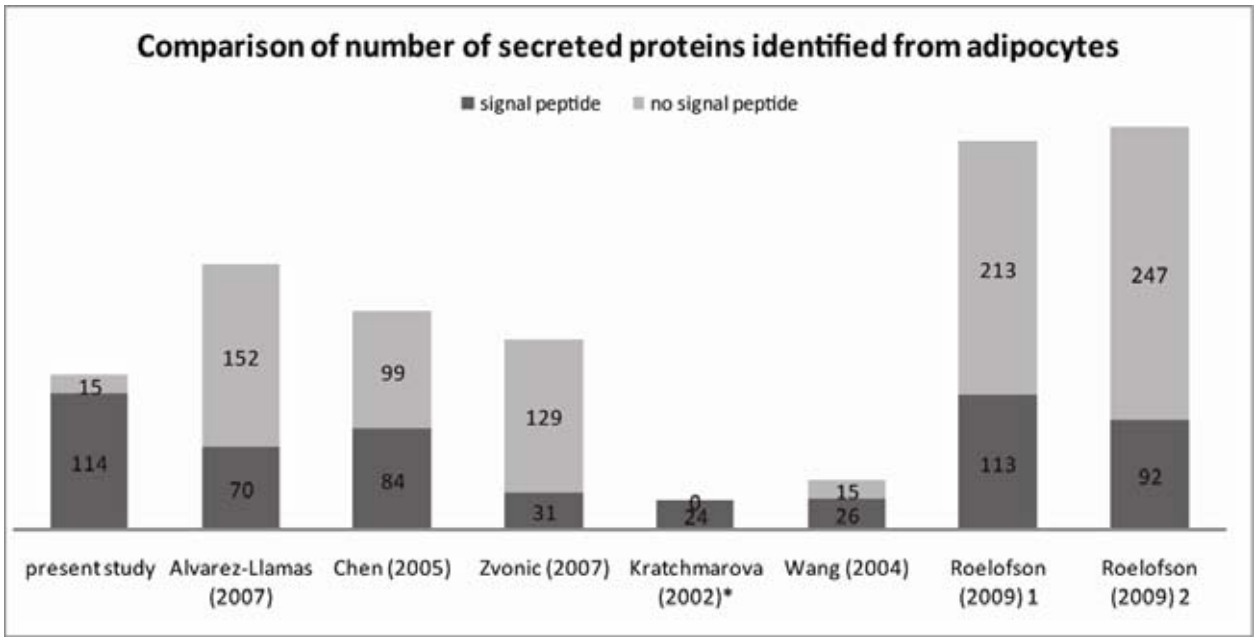

Figure 5. Comparative success of published studies for identifying secreted proteins in conditioned media using mass spectrometry. The present study, which utilised glycoprotein purification for excluding non-secretory proteins from samples, yielded the highest number of secreted proteins, with the lowest number of contaminating cytosolic proteins.

A number of known adipocyte secretory proteins were identified, however these were not identified in earlier proteomics studies and include lipocalin-2 and URB. While correlations between serum levels of some adipocyte secretory proteins and obesity or insulin resistance have been described, further work is needed to identify their receptors and mechanisms of action. To identify which of these proteins may be involved in insulin resistance or type 2 diabetes, it is necessary to identify which secretory proteins are dysregulated under relevant perturbed conditions. This is addressed later in this chapter. Interrogation of the adipocyte secretome revealed the identification of a number of proteins with related functions – in particular; angiogenesis, serine proteases and extracellular matrix remodelling. This gives rise to the notion that in general the secretory profile of the cell is geared towards a concerted effort at achieving a few key biological endpoints such as angiogenesis. This is to be compared to true *bona fide* secretory cells, which control one key function via the secretion of an individual endocrine factor, as is the case for leptin or insulin.

Survey of hepatocyte secretome

While numerous studies have focused on the secretory ability of adipocytes, the metabolic contributions of secretory proteins from other insulin sensitive tissue, such as the liver, which is a major secretory organ, have been largely ignored. The liver is responsible for secretion of the single most abundant serum protein, albumin. This single protein species accounts for over 90% of serum protein, and is present in the serum at concentrations of 45-55 g per litre. A number of other highly abundant serum proteins are secreted exclusively from the

liver, including fetuin, hemopexin and c-reactive protein. Despite this, there have been no systematic studies into the secretome of hepatocyte.

To approach this problem, primary hepatocytes from C57BL6 mice were used rather than cell lines, as cultured hepatocyte lines do not display characteristic features of the liver such as insulin sensitivity. Primary hepatocytes are sometimes cultured in the presence of dexamethasone, which increases expression of the insulin receptor and consequently enhances insulin sensitivity (Yamada S 1979). In this experiment, hepatocytes were cultured in the presence or absence of dexamethasone. Hepatocytes were incubated in serum free media supplemented with 100 nM insulin for 18 h. Conditioned media was collected, subjected to glycoprotein affinity purification, resolved by SDS-PAGE and proteins visualised using SYPRO ruby staining (Fig. 6). No difference in secretory profile was observed in hepatocytes treated with or without dexamethasone. The dexamethasone treated lane was sliced, trypsin digested, peptides extracted and subjected to mass spectrometry. The results of this experiment are shown in Table 2. A total of 130 proteins with a score above 60 were identified. Of these, 101 contained an N-terminal signal peptide. By far the most abundantly detected class of proteins from hepatocytes were the serine protease inhibitors, which made up 9 of the top 12 hits. Caution must be taken when making comparisons between different protein species. The purification step used here relied on glycosylation, a highly heterogeneous modification. In addition, peptides display a highly variable ability to ionise during mass spectrometry in a manner that makes detection possible. This makes comparisons between different protein species difficult. A number of proteins identified from 3T3-L1 adipocytes were also present in hepatocyte-conditioned media.

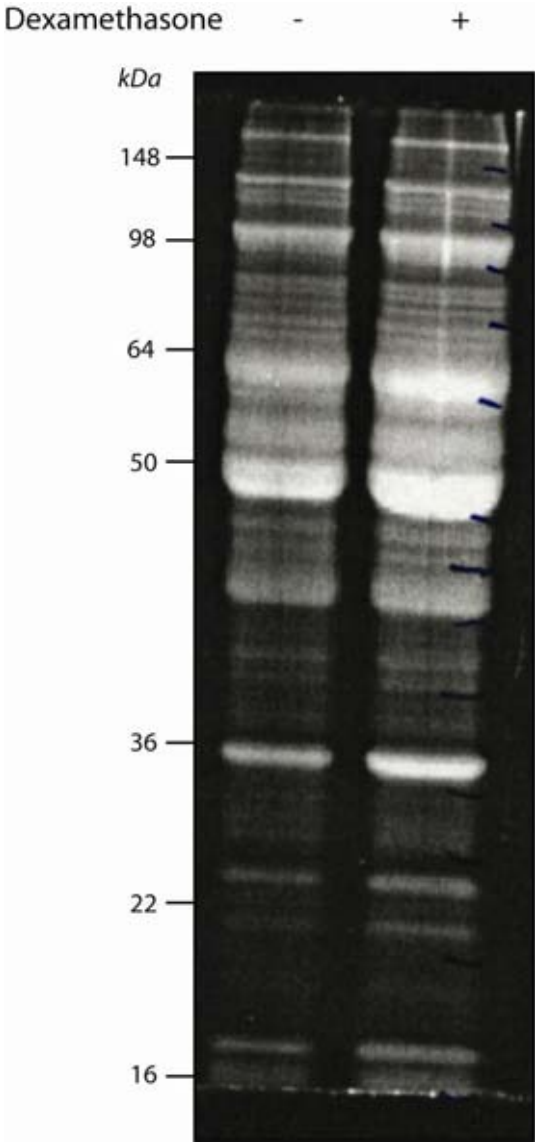

Figure 6. Secretory profile of primary hepatocytes. Hepatocytes were isolated from C57BL6 mice and incubated in media with or without the common hepatocyte supplement dexamethasone (100 nM). Conditioned media was collected, subjected to glycoprotein purification, SDS-PAGE, SYPRO ruby protein staining and visualisation. The dexamethasone treated lane was excised and proteins subjected to mass spectrometry (Table 2).

accession	score	peptides	name	signal peptide
SPA3K	3349	113	Serine protease inhibitor A3K	1
CO3	1949	108	Complement C3	1
A1AT1	1617	89	Alpha-1-antitrypsin 1-1	1
SPA3M	1603	66	Serine protease A3M	1
A1AT3	1559	89	Alpha-1-antitrypsin 1-3 (Serine protease inhibitor 1-3)	1
HEMO	1553	81	Hemopexin	1
A1AT6	1452	79	Alpha-1-antitrypsin 1-6 (serine protease inhibitor 1-6)	1
A1AT5	1431	59	Alpha-1-antitrypsin 1-5 (Serine protease inhibitor 1-5)	1
A1AT2	1367	71	Alpha-1-antitrypsin 1-2 (Serine protease inhibitor 1-2)	1
SPA3N	1290	47	Serine protease inhibitor A3N	1
A1AT4	1276	68	Alpha-1-antitrypsin 1-4 (serine protease inhibitor 1-4)	1
ANGT	1045	33	Angiotensinogen	1
CLUS	985	53	Clusterin (sulfated glycoprotein)	1
HPT	912	69	Haptoglobin	1
ITIH1	827	41	Inter-alpha-trypsin inhibitor heavy chain H1	1
ESTN	713	26	Liver carboxylesterase N	1
MUG1	700	54	Murinoglobulin-1	1
K2C1B	698	22	Keratin, type II cytoskeletal 1b	0
KNG1	639	47	Kininogen-1	1
CFAB	595	33	Complement factor B	1
A2M	582	39	Alpha-2-macroglobulin (pregnancy zone protein)	1
ITIH2	553	37	Inter-alpha-trypsin inhibitor heavy chain H2	1
QSCN6	551	23	Sulfyhdrl oxidase 1 (Quiescin Q6)	1
CERU	545	27	Ceruloplasmin (Ferroxidase)	1
CO5	455	23	Complement C5	1
CO6A1	438	17	Collagen alpha-1 (VI)	1
A1AG1	431	26	Alpha-1-acid glycoprotein 1 (Orosmucoid-1)	1
MUG4	416	31	Murinoglobulin-4	1
FETUA	396	33	Alpha-2-HS-glycoprotein (Fetuin A) (Countertrypsin)	1
CO1A2	394	16	Collagen alpha-2 (I)	1
ANT3	380	28	Antithrombin-III	1
CO8A	361	14	Complement component C8 alpha chain	1
CO4A2	345	15	Collagen alpha-2 (IV) chain	1
MBL2	334	7	Mannose binding protein C	1
TSP1	322	13	Thrombospondin-1	1
LIPL	321	13	Lipoprotein lipase	1
A2AP	315	20	Alpha-2-antiplasmin	1
CO4B	315	16	Complement C4-B	1
CO9	315	16	Complement component C9	1
CO8B	276	8	Complement component C8 beta	1

ADIPO	274	10	Adiponectin	1
PAI1	272	14	Plasminogen activator inhibitor 1	1
IC1	262	17	Plasma protease C1 inhibitor	1
SODE	261	13	Extracellular superoxide dismutase [Cu-Zn]	1
APOH	253	13	Beta-2-glycoprotein 1	1
SAMP	249	9	Serum amyloid P-component (SAP)	1
TRFE	247	15	Serotransferrin (transferrin) (siderophilin)	1
PROC	244	7	Vitamin K-dependent protein C (autoprothrombin IIA)	1
HA10	228	11	H-2 class I histocompatibility antigen, Q10 alpha chain	1
PTX3	226	8	Pentraxin-related protein PTX3	1
ADH1	211	16	Alcohol dehydrogenase 1	0
FAS	201	8	Fatty acid synthase	0
TSP2	197	6	Thrombospondin-2	1
NRP1	194	5	Neuropilin-1 (A5 protein)	1
RSSA	180	4	40S ribosomal protein SA	0
CATB	172	5	Cathepsin B	1
IBP7	171	8	Insulin-like growth factor-binding protein 7	1
THRB	170	13	Prothrombin	1
GPDA	166	9	Glycerol-3-phosphate dehydrogenase [NAD+], cytoplasmic	0
ACTB	163	16	Actin, cytoplasmic 1	0
CES3	160	7	Carboxylesterase 3	0
HA11	160	5	H-2 class I histocompatibility antigen, D-B alpha chain	0
SPARC	155	8	SPARC (secreted protein rich in cysteine) (osteonectin)	1
FINC	154	4	Fibronectin	1
EST1	154	7	Liver carboxylesterase 1	1
LIFR	149	7	Leukaemia inhibitory factor receptor (LIF receptor)	1
CBG	139	4	Corticosteroid-binding globulin (Transcortin) (SerpinA6)	1
APOE	136	10	Apolipoprotein E	1
MBL1	135	7	Mannose binding protein A	1
SUMF2	130	3	Sulfatase-modifying factor 2	1
HA1L	130	4	H-2 class I histocompatibility antigen, L-D alpha chain	1
GSTP1	129	3	Glutathione S-transferase P 1	0
APOA1	129	5	Apolipoprotein A-I	1
ACTA	127	14	Actin, aortic smooth muscle	0
CO6A2	122	12	Collagen alpha-2 (VI) chain	1
FTHFD	121	14	10-formyltetrahydrofolate dehydrogenase	0
FSTL1	121	5	Follistatin-related protein 1	1
ZPI	121	5	Protein Z-dependent protease inhibitor (Serpina10)	1
HEP2	119	7	Heparin cofactor 2	1
PCOC1	118	4	Procollagen C-endopeptidase enhancer 1	1
ALBU	114	5	Serum albumin	1

CO1A1	114	5	Collagen alpha-1(I) chain	1
A1AG2	113	13	Alpha-1-acid glycoprotein 2 (Orosmucoid-2)	1
CFAD	113	5	Complement factor D	1
CFAH	112	11	Complement factor H	1
GFAP	108	6	Glial fibrillary acidic protein, astrocyte	0
AFAM	107	2	Afamin (alpha-albumin)	1
CO4A1	104	4	Collagen alpha-1 (IV)	1
ZA2G	103	8	Zinc-alpha-2-glycoprotein	1
CS1A	103	7	Complement C1s-A subcomponent	1
GDN	99	2	Glia-derived nexin (protease nexin I) (Serine protease inhibitor 4)	1
EF1A1	97	4	Elongation factor 1-alpha 1	0
ENPL	97	6	Endoplasmin (Heat shock protein 90 kDa member 1)	1
MAAI	96	7	Maleylacetoacetate isomerase (glutathione transferase zeta)	0
SAHH	96	4	Adenosoylhomocysteine	0
HGFA	93	3	Hepatocyte growth factor activator	1
HS90A	93	2	Heat shock protein HSP90-alpha	0
VTNC	88	3	Vitronectin (serum spreading factor)	1
AMRP	88	4	Alpha-2-macroglobulin receptor-associated protein	1
ALDOB	87	6	Fructose-bisphosphate aldolase B (liver type aldolase)	0
SPRE	87	1	Sepiaterin reductase	0
PGS1	87	4	Biglycan	1
CATZ	85	4	Cathepsin Z	1
CBPB2	83	5	Carboxypeptidase B2	1
CO8G	83	3	Complement C8 gamma chain	1
ANGL3	81	4	Angiopoietin-related protein 3 precursor (Angiopoietin-like 3)	1
HA1B	81	3	H-2 class I histocompatibility antigen, K-B alpha chain precursor (H-2K(B))	1
CO3A1	79	2	Collagen alpha-1(III) chain	1
TIMP1	79	3	Metalloproteinase inhibitor 1 precursor (TIMP-1)	1
DPP4	78	2	Dipeptidyl peptidase 4	0
CPSM	78	4	Carbamoyl-phosphate synthase [ammonia], mitochondrial	0
KLKB1	75	2	Plasma kallikrein	1
AMBP	74	3	AMBP protein	1
G3P	73	5	Glyceraldehyde-3-phosphate dehydrogenase	0
DAG1	73	2	Dystroglycan	1
CAH2	71	3	Carbonic anhydrase 2	0
ALDOA	71	4	Fructose-bisphosphate aldolase A	0
EF2	71	2	Elongation factor 2 (EF-2)	0
PGS2	70	8	Decorin	1
MDHM	68	1	Malate dehydrogenase, mitochondrial	0
RGMA	68	1	Repulsive guidance molecule A	1

TBBC	68	2	Tubulin beta-2C chain	0
ASSY	66	8	Argininosuccinate synthase	0
MASP1	66	1	Complement-activating component of Ra-reactive factor	1
A2MP	66	2	Alpha-2-macroglobulin-P	1
CISY	65	2	Citrate synthase, mitochondrial	0
GNMT	64	1	Glycine N-methyltransferase	0
EGFR	62	3	Epidermal growth factor receptor precursor	1

Table 2. Hepatocyte secretory proteins. Primary hepatocytes were isolated, seeded into 10 cm plates, incubated in serum free DMEM supplemented with 100 nM insulin for 18 hours. Conditioned media was collected, subjected to glycoprotein purification, and SDS-PAGE (Fig. 6). Proteins were digested and subjected to mass spectrometry, results shown.

These include serine protease inhibitors, acute phase reactants such as haptoglobin, and extracellular matrix proteins such as collagen. Interestingly, while multiple members of the complement pathway were secreted from liver, only one of these, complement C3, was secreted from adipocytes, which itself was found to secrete multiple members of the complement pathway. It is possible that this lack of redundancy in complement protein secretion between adipocytes and hepatocytes represents multi-tissue co-ordination of the complement pathway. The sheer number of proteins detected from hepatocytes highlights the secretory nature of this organ, which exceeds the secretory ability of adipose tissue. In contrast to the liver, adipose tissue receives extensive focus in the literature as an important endocrine organ, and in light of these data this is perhaps unjustified.

Survey of skeletal muscle secretome

So far in this investigation, the secretome of two of the primary insulin responsive tissues, fat and liver, have been investigated both under control conditions and conditions of metabolic insult. The other primary insulin responsive tissue in the body is skeletal muscle. This tissue alone accounts for the vast majority (80%) of insulin-stimulated glucose clearance. Skeletal muscle reportedly secretes molecules that can regulate glucose metabolism including interleukin-6 and TNFα (Steensberg, Keller et al. 2002). Despite the discovery of these so-called "myokines", there have been no studies that have attempted to survey the skeletal muscle secretome. To address this issue, the L6 myocyte cell line was utilised. These cells are rat-derived myoblasts that under conditions of confluency and serum deprivation undergo intercellular fusion to differentiate into multinucleated myotubes, or muscle fibres. To survey the

secretome of these cells, differentiated myotubes were incubated in serum free media supplemented with 100 nM insulin for 18 h. Conditioned media was collected, subjected to glycoprotein purification, SDS-PAGE and visualised using SYPRO ruby protein stain (Fig. 7). Gels were cut into equal sized pieces, trypsin digested, peptides extracted and subjected to mass spectrometry. The proteins identified in this experiment are shown in Table 3. A total of 78 proteins were identified, of which 60 proteins (77%) contained an N-terminal signal peptide. One interesting protein that was identified was macrophage colony stimulating factor, a secreted protein involved in regulation of differentiation of macrophages from progenitor cell types (Takahashi, Miyakawa et al. 1998). The remaining proteins fall broadly into the category of extracellular matrix proteins, which fulfil a paracrine, not an endocrine, role. In contrast with previous studies, neither IL-6 nor TNFα were detected from myotubes. It is possible that these proteins are in fact not muscle derived proteins *per se*, but secreted from other cell types such as macrophages in response to stimuli normally associated with muscle, such as exercise. Indeed, in many cases IL-6 expression is undetectable in resting muscle, it is only after intense exercise (42 km marathon race) that IL-6 becomes detectable (Ostrowski, Rohde et al. 1998). This sort of exercise is associated with muscle damage and consequent macrophage infiltration (Tiidus 2008), which may account for the increased gene expression observed post-exercise. If myotubes are indeed a source of IL-6, sustained contraction is required for expression to become apparent. Resting, not contracting L6 myotubes were used in this study, and this may account for the absence of IL-6 from this screen.

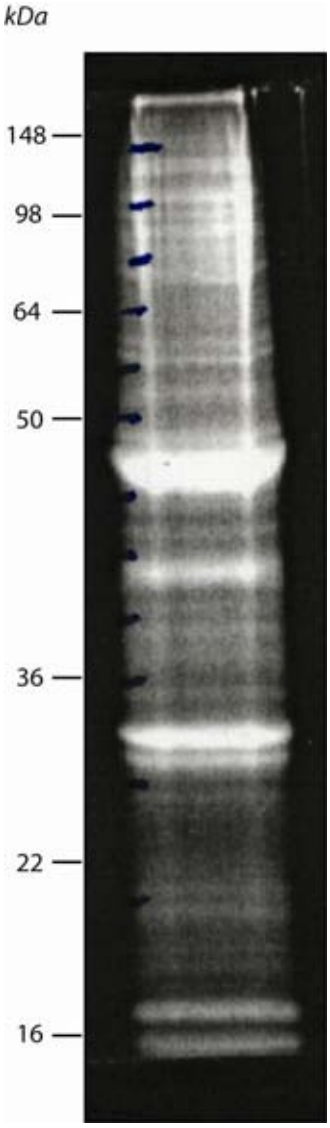

Figure 7. Secretory profile of L6 myotubes. Fully differentiated L6 myotubes were incubated in serum free DMEM supplemented with 100 nM insulin for 18 hours. Conditioned media was collected, subjected to glycoprotein affinity purification, proteins resolved by SDS-PAGE and visualised by SYPRO ruby protein stain. Lane was excised and subjected to mass spectrometry (Table 3).

accession	score	name	no. peptides	signal sequence?
gi|506417	2951	glypican	86	Y
gi|149015979	2879	fibronectin 1, isoform CRA_b	55	Y
gi|16758080	1821	procollagen, type I, alpha 2	85	Y
gi|2181948	1757	cell adhesion molecule (AA 1 - 681) (2262 is 1st base in codon)	41	N
gi|348962	1744	biglycan	44	Y
gi|9506703	1720	fibronectin 1	36	Y
gi|155369293	1249	AE (adipocyte enhancer) binding protein 1	22	Y
gi|149015980	1216	fibronectin 1, isoform CRA_c	23	Y
gi|149062421	1196	rCG47487, isoform CRA_b	20	Y
gi|109483719	1161	Collagen alpha-1(XII) chain precursor	19	N
gi|58865966	1145	tumor rejection antigen gp96 (predicted)	22	Y
gi|109509326	1093	Collagen alpha-1(VI) chain precursor	23	Y
gi|134047725	740	Chordin precursor	17	Y
gi|109505096	733	Nidogen-1 precursor (Entactin)	12	Y
gi|83301554	730	Collagen alpha-1(I) chain precursor	16	Y
gi|7710028	692	glypican 1	20	Y
gi|28461161	671	low-density lipoprotein receptor	28	Y
gi|13540699	649	neuropilin 2	12	Y
gi|6753418	630	chordin	15	Y
gi|600381	196	osteonectin	5	Y
gi|58865670	140	biotinidase	2	Y
gi|28201782	98	Macrophage colony-stimulating factor 1 precursor (CSF-1) (MCSF)	5	Y
gi|7021449	62	steroid sensitive gene-1 protein (URB)	6	Y

Table 3. Myotube secretory proteins. Fully differentiated L6 myotubes were incubated in serum free DMEM supplemented with 100 nM insulin for 18 hours. Conditioned media was collected, subjected to glycoprotein purification, SDS-PAGE (figure 13). Proteins were digested and subjected to mass spectrometry, results shown.

Use of SILAC to probe rates of protein synthesis and secretion

Previously in this investigation, a method to identify secretory proteins from conditioned media was developed. This was used to survey protein secretion from multiple insulin sensitive tissues. Whilst the ability to measure changes in protein secretion is useful, this method was next adapted to provide data regarding the temporal kinetics of protein synthesis and secretion. This was performed using stable isotopic labelling of amino acids in cell culture (SILAC) (Ong, Blagoev et al. 2002). SILAC relies on the substitution of normal amino acids for non-radioactive isotope labelled amino acids, usually ^{3}H, ^{13}C and ^{15}N into arginine and lysine, in cell culture media. These isotopic amino acids do not display altered biophysical activity, and are incorporated into newly synthesised proteins. The incorporation of amino acids containing these isotopes results in a small shift in molecular weight that is only discernable by mass spectrometry. Multiple samples that are composed of multiple isotopes of arginine and lysine can be mixed and treated as a single sample during all subsequent manipulations to avoid inter-sample handling variability. The use of the enzyme trypsin is important as it cleaves on the N-terminal side of the basic amino acids arginine and lysine, ensuring that every peptide contains only one arginine or lysine. When peptides are separated by mass / charge ratio, peptides of the same amino acid sequence will appear together, however they will be separated by the molecular weight difference of the single isotopic amino acid present in each tryptic peptide, which is in this case 4 to 10 Da. The signal intensity of the peaks corresponding to various isotopic species is directly related to the abundance of proteins, and the ratio of peak intensities between isotopes can be used as a fairly accurate guide to relative abundances of proteins from different samples in a mixture. This technique typically relies on complete labelling of cells with isotopic amino acids prior to experimentation. Often cells are divided for a minimum of 12 rounds of division before

they can be used for an experiment. In the present study, SILAC labelling was not used to compare between different treatments, but was used as a sophisticated modification of the classical "pulse chase" type experiment to identify rates of protein synthesis. In the classical "pulse chase" type of experiment, cells are incubated in the presence of radioactive amino acids such as ^{35}S-methionine or ^{14}C-leucine, followed by a "chase" period where radioactivity is removed for varying times. Specific proteins are isolated, usually by immunoprecipitation, and radioactivity measured. The time points at which radioactive labelling of the protein of interest does not increase is counted as steady state labelling, half of the minimum steady state time point is deemed to be the half-life of the protein. There are numerous problems with this approach that make it time consuming. This technique is suited for identifying the half-life of a single protein, but when a family of proteins is targeted, the amount of work required increases greatly as each specific protein species must be immunoprecipitated separately. This relies on the existence of antibodies that have sufficient immunoprecipitation efficiency. Antibodies can be expensive to purchase, particularly when their reliability is questionable. A large number of samples are needed to establish a sufficiently detailed time course of radioactivity, increasing the workload. In particular, a point of steady state radioactivity must be established, as the point at which further incubation does not increase radioactivity is assumed to be the point of complete protein labelling. A solution to this problem that was investigated in this study is to use SILAC amino acid incorporation into proteins from non-dividing cells as a means of simultaneously tracking the half-lives of a number of proteins. There are several advantages to this approach. Numerous proteins can be detected at once, as in this case where the entire secretome of 3T3-L1 adipocytes (~100 different protein species) was targeted. SILAC provides an exact quantitative ratio of protein abundance, so there is no need to establish a steady state of incorporation to ascertain

when complete labelling has occurred. These data are available through the ratio of un-labelled to labelled protein that is detected. This overcomes the need for antibodies and the technical limitations associated with them. The SILAC approach is also safer, as it avoids the need to work with radioactive isotopes such as ^{35}S.

In the present study, mature 3T3-L1 adipocytes were incubated with non-radioactive isotopes of arginine and lysine for 24, 48 or 96 h. After each period of incubation with isotopic amino acids, cells were incubated in serum free media supplemented with 1 nM insulin for 16 h. Conditioned media was collected, subjected to glycoprotein affinity purification, SDS-PAGE and protein visualisation. Visualisation of SDS-PAGE gels by SYPRO ruby protein staining did not show any effect of introduction of isotopic amino acids. Trypsin digestion, peptide extraction and mass spectrometry were subsequently performed, and the ratios of isotopic to non-labelled arginine and lysine were determined (Table 4). Interestingly, the degree of amino acid incorporation and the rate of incorporation varied with different protein species. This may reflect the rate of protein secretion, with some proteins constitutively released from the secretory pathway, whilst other proteins are stored at points along the secretory pathway, and released at a slower rate. For example, adiponectin is stored in the lumen of the endoplasmic reticulum, where it is slowly released (Wang, Schraw et al. 2007). Label incorporation rates of adiponectin are low compared to other species, and this may reflect the release of exiting pools of adiponectin rather than newly synthesised adiponectin. In contrast, collagen α-1(III) had the highest rate of label incorporation, indicating high levels of synthesis and secretion for this protein. It is hoped that this powerful technique may be used as a standard way of measuring protein synthesis and secretion, rather than traditional radioactive pulse-chase type experiments.

		ISOTOPE / NON-LABELLED RATIO		
		24 hr	48 hr	96 hr
CO3A1_MOUSE	Collagen alpha-1(III) chain	1.164	7.624	
ADIPO_MOUSE	Adiponectin	0.1698		
ANGT_MOUSE	Angiotensinogen	0.5855	0.7903	
CO1A1_MOUSE	Collagen alpha-1(I) chain	0.6674	0.8143	0.9519
CO6A1_MOUSE	Collagen alpha-1(VI) chain	0.2477	0.7248	
CO3_MOUSE	complement C3	0.5976	0.8902	
CO4B_MOUSE	complement C4-B	1.079	1.758	
CFAD_MOUSE	Complement factor D (adipsin)	0.5099	0.9523	
ENPP2_MOUSE	Ectonucleotide pyrophosphatase/phosphodiesterase family member 2 (Autotaxin)	0.3307		
HPT_MOUSE	haptoglobin	0.2155	0.9659	
LAMB1_MOUSE	Laminin subunit beta 1	0.1891	1.097	
LIPL_MOUSE	Lipoprotein lipase	0.3544		
POSTN_MOUSE	Periostin	0.3631		
SPRL1_MOUSE	SPARC-like protein 1	0.5861		

Table 4. Use of stable isotopes and mass spectrometry for determining rates of protein synthesis. Differentiated 3T3-L1 adipocytes were incubated in normal growth media containing isotopes of arginine and lysine for indicated periods. Cells were then incubated in serum free media supplemented with 100 nM insulin for 24 hours. Conditioned media was collected, subjected to glycoprotein affinity purification and mass spectrometry. The ratio of labelled to un-labelled peptide is used as a guide to the degree of protein incorporation.

Protein secretion during perturbed states

A major goal of proteomic studies of the kind used here is to firstly identify the complete set of proteins and then break this down into functionally relevant information. To do this it is necessary to use screens that can pinpoint potentially relevant proteins from the entire proteome list that are specially involved in particular functions. One way of doing this is to compare the proteomes of normal and perturbed cells or tissues. In the next set of studies, the secretomes of healthy (control) cells were compared to cells under conditions relevant to insulin resistance and type 2 diabetes. In the first part of the study, changes in the secretory repertoire of adipocytes under conditions of insulin resistance were examined. In the second part of the study, changes in protein secretion from hepatocytes under conditions mimicking fatty liver disease were measured. In the third part of the study, changes in protein secretion from hepatocytes infected with hepatitis C virus were measured, with the intention of identifying secreted proteins that might explain the insulin resistance that occurs in peripheral tissues that occurs during hepatitis C infection.

Adipokine secretion during insulin resistance

As shown earlier, the adipocyte secretome is vast, comprising >100 proteins. To simplify this list and identify secretory molecules that are relevant to insulin resistance, the purification and identification of adipocyte secretory proteins was performed using physiologically relevant models of insulin resistance. To recapitulate insulin resistance, adipocytes were incubated with 10 nM insulin for 24 h or with the inflammatory cytokine TNFα

at a concentration of 2 ng/ml for 96 h. Both of these insults have been shown to cause insulin resistance in cultured models (Hoehn, Hohnen-Behrens et al. 2008).

Conditioned media was collected from either control or insulin resistant cells, subjected to glycoprotein purification and samples were resolved by SDS-PAGE and visualised using silver staining (Fig. 8). Strikingly, the overall polypeptide composition of the adipocyte secretome was significantly different in insulin resistant cells compared to control cells. Most notably, the total amount of protein secreted by IR cells was much higher than observed in control cells, particularly in the high molecular weight range. There were clear differences in protein secretion between the two different IR models (marked with asterisks Fig. 8). As indicated in Fig.8, there was a protein of Mr 36 that was very abundant in the chronic insulin treated samples when compared to the other samples. There were numerous species in the higher molecular weight range that were more abundant in both insulin resistance models when compared to the control. There were also secreted proteins at Mr 90, 55 and 22 kDa that were more abundant in samples from TNFα treated adipocytes compared to other treatments. To identify these proteins, gel slices were excised from regions where there were obvious differences in polypeptide, digested with trypsin and analysed by mass spectrometry. The number of peptides detected for each protein was used as a semi-quantitative tool to measure protein abundance. A total of 48 proteins containing a signal peptide were identified (Table 5). Among these, 34 proteins were >2 fold more abundant in insulin resistant samples compared to controls and 14 less abundant. The most abundant proteins whose secretion was modified during insulin resistance were members of the complement pathway. The secretion of these proteins was increased during treatment with the inflammatory cytokine TNFα. Given the role of TNFα and complement C3 in inflammation, this result is not surprising. The secretion of lipocalin-2 was increased during both chronic insulin

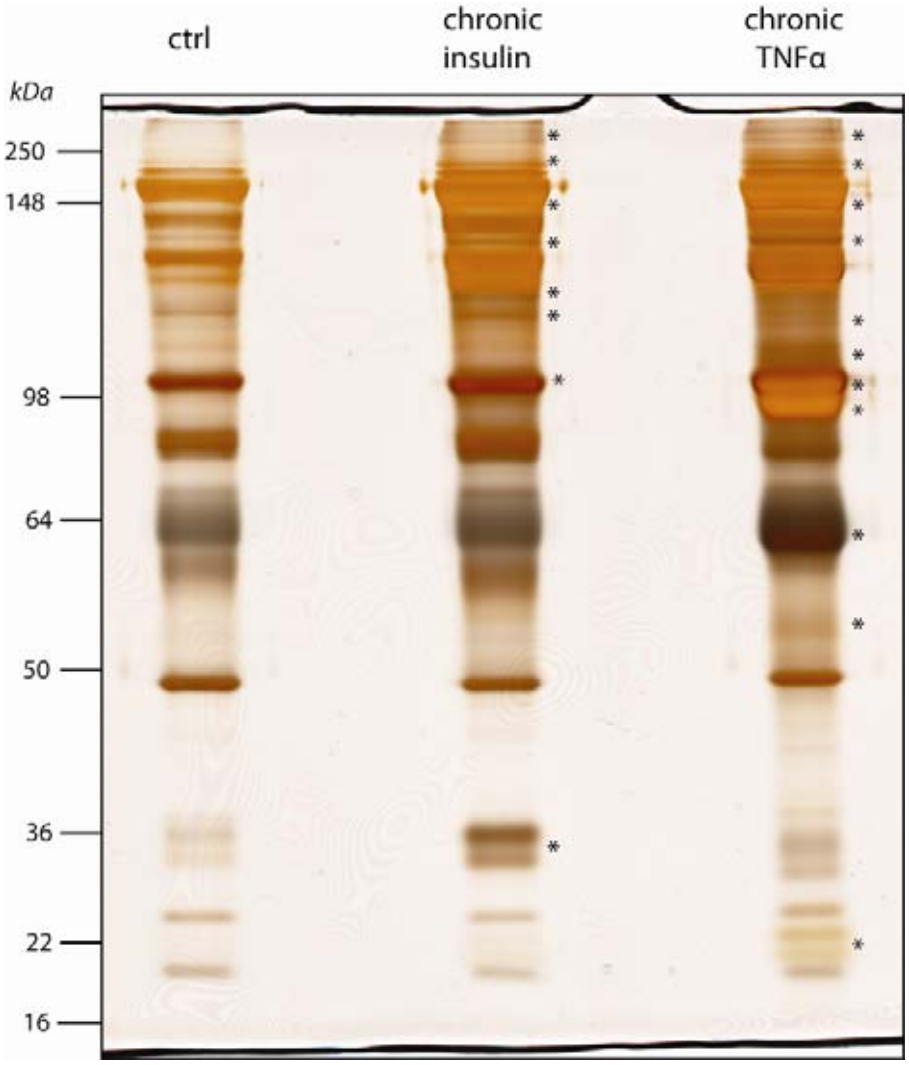

Figure 8. Insulin resistance models alter secretion profile of 3T3-L1 adipocytes. 3T3-L1 adipocytes were treated with insulin resistance models as described previously (Hoehn, Hohnen-Behrens et al. 2008) and in methods. Insulin resistant or control adipocytes were incubated in serum free media supplemented with 100 nM for 18 hours. Conditioned media was collected and subjected to glycoprotein purification. Proteins were specifically eluted, separated by SDS-PAGE on a 10% acrylamide gel and subjected to silver staining.

accession	name	basal peptides	chronic insulin peptides	TNFα peptides
ADIPO_MOUSE	adiponectin precursor	20	22	11
A1AG1_MOUSE	Alpha-1-acid glycoprotein 1 (Orosomucoid-1)	16	15	6
ENPP2_MOUSE	Autotaxin; Ectonucleotide pyrophosphatase/phosphodiesterase 2	0	18	5
CERU_MOUSE	Ceruloplasmin precursor	4	17	38
CH3L1_MOUSE	Chitinase-3-like protein 1 (Cartilage glycoprotein 39)	0	0	8
CLUS_MOUSE	Clusterin precursor (Sulfated glycoprotein 2)	4	2	8
C1RA_MOUSE	Complement C1r-A subcomponent	7	0	18
C1RB_MOUSE	Complement C1r-B subcomponent	0	0	9
CS1A_MOUSE	Complement C1s-A subcomponent	8	6	20
CO3_MOUSE	complement C3	157	223	409
CO4B_MOUSE	Complement C4-B	1	0	4
CFAB_MOUSE	Complement factor B precursor (C3/C5 convertase)	21	13	85
CFAD_MOUSE	Complement factor D precursor	18	12	5
FBLN4_MOUSE	EGF-containing fibulin-like extracellular matrix protein 2 (Fibulin-4)	5	5	0
HA13_MOUSE	H-2 class I histocompatibility antigen, D-K alpha chain	0	0	4
HPT_MOUSE	Haptoglobin	38	53	99
LBP_MOUSE	Lipopolysaccharide-binding protein precursor (LBP)	0	0	8
LIPL_MOUSE	Lipoprotein lipase precursor	41	44	18
LUM_MOUSE	Lumican	9	8	0
TIMP1_MOUSE	Metalloproteinase inhibitor 1 precursor (TIMP-1)	0	3	6
NGAL_MOUSE	Neutrophil gelatinase-associated lipocalin (Lipocalin-2)	2	7	10
NID1_MOUSE	Nidogen-1 precursor (Entactin)	10	26	15
OLFL3_MOUSE	Olfactomedin-like protein 3	2	7	0
PTX3_MOUSE	Pentraxin-related protein PTX3	3	0	17
PAI1_MOUSE	Plasminogen activator inhibitor 1 precursor (PAI-1)	0	9	6
PGFRL_MOUSE	Platelet-derived growth factor receptor-like protein	1	2	11
PCOC1_MOUSE	Procollagen C-endopeptidase enhancer 1	0	1	9
PRELP_MOUSE	Prolargin precursor (Proline-arginine-rich end leucine-rich repeat protein)	0	5	0
SPA3C_MOUSE	Serine protease inhibitor A3C (Kallikrein-binding protein)	6	0	0
QSCN6_MOUSE	Sulfhydryl oxidase 1 (Quiescin Q6)	11	20	0
TSP1_MOUSE	Thrombospondin-1	10	9	17
TSP2_MOUSE	Thrombospondin-2	0	0	5
VEGFA_MOUSE	Vascular endothelial growth factor A	3	2	0

Table 5. Insulin resistance models alter adipokine secretion. 3T3-L1 adipocytes were untreated or treated with chronic insulin or chronic TNFα models of insulin resistance. Conditioned media was collected, subjected to glycoprotein purification, resolved by SDS-PAGE (figure 7) and bands corresponding to changes in intensity were excised at the same molecular weight range for all samples. Proteins were digested, extracted and subjected to mass spectrometry, and total peptide counts were used as a semi-quantitative guide to protein abundance under the various conditions.

treatment and chronic TNFα treatment. This is consistent with data showing elevation of this protein in the serum of high fat fed rodents and in the serum of insulin resistant humans (Wang, Lam et al. 2007; Yan, Yang et al. 2007). Another protein identified was autotaxin. Autotaxin is an enzyme that catalyses the formation of lysophosphatidic acid in the extracellular space, and is elevated in the serum of insulin resistant humans and high fat fed rodents (Ferry, Tellier et al. 2003). In one study, autotaxin was found to be secreted in greater amounts from 3T3-L1 adipocytes made insulin resistant through chronic insulin or chronic TNFα treatments, a finding that was almost exactly recapitulated in the present study (Boucher, Quilliot et al. 2005). Chitinase 3-like protein 1 is known to be released from cells treated with inflammatory cytokines (Recklies, Ling et al. 2005), and has appeared in one previous proteomic study in a list of proteins that were secreted from human visceral fat (Alvarez-Llamas, Szalowska et al. 2007).

To investigate the importance of secretory proteins in adipocyte biology, conditioned media from insulin resistant adipocytes were obtained and dialysed against a 10 kDa molecular weight cut off filter, thus removing small and presumably non-protein molecules, and replacing the environment of secreted proteins with fresh DMEM. These conditioned media were applied to fresh adipocytes for 24 h, after which insulin sensitivity was measured by ^{3}H 2-deoxyglucose uptake (Fig. 9). When compared to adipocytes treated with control-conditioned media, TNFα-conditioned media resulted in a significant ($p = 0.03$) reduction in insulin-stimulated glucose uptake. At the same time, treatment with any of the conditioned media samples resulted in a significant ($p<0.0001$) increase in basal glucose uptake. These data point towards paracrine effects of adipocyte secretory proteins and it is possible that some of the endocrine effects attributed to adipokines are more localised, than mediated distally to adipose tissue. Further

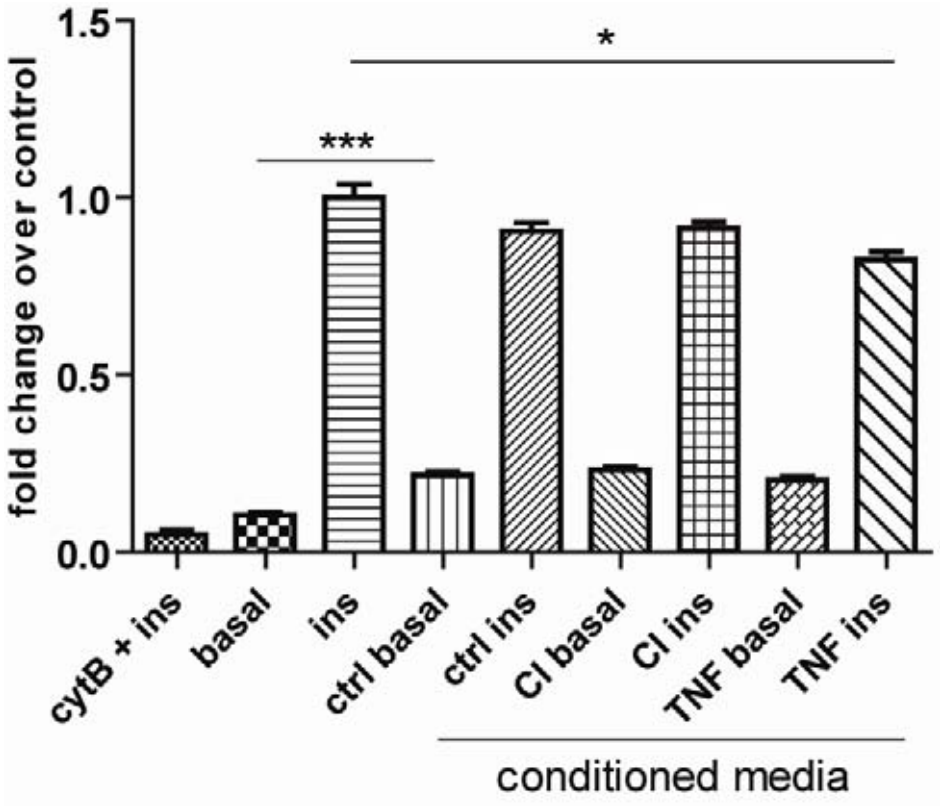

Figure 9. Adipocyte conditioned media displays paracrine effects towards insulin sensitivity. 10cm dishes of 3T3-L1 adipocytes were treated with insulin resistance models, chronic insulin (CI) or TNFα. Insulin resistant and control adipocytes were incubated in serum free media supplemented with 100 nM insulin for 18 hours. Conditioned media were collected and dialysed extensively against serum free DMEM through a 10 kDa molecular weight cut-off filter using an amicon centrifugal filtration device, to separate small molecule metabolites from larger molecular species, presumably proteins. FCS was added to conditioned media samples, and these samples were used to treat fresh adipocytes in 24-well plates for 24 hours prior to insulin stimulated glucose uptake assay using ^{3}H 2-deoxyglucose. Adipocyte conditioned media re-applied to fresh adipocytes enhanced basal glucose uptake for all treatments, whereas treatment with TNFα induced insulin resistant conditioned media resulted in a significant decrease in insulin stimulated glucose uptake. *$p<0.05$, ***$p<0.001$ two tailed t-test.

experiments will be needed to identify which protein(s) from the identified list mediate the effect on insulin sensitivity that was observed.

Identification of PRLTS as an adipocyte secretory factor

Of particular interest in this experiment was the identification of PDGF receptor like tumour suppressor (PRLTS) as an adipocyte secretory protein. Little is known of PRLTS, which was first cloned in 1995, when it was identified as a gene sporadically mutated in hepatocellular carcinomas, colorectal cancers and non-small cell lung from a cohort of patients in Japan (Fujiwara, Ohata et al. 1995). Since the initial discovery of PRLTS, there has only been one additional study performed on this protein, which identified mutations in this gene in 42% of a cohort of prostate cancer patients (Komiya, Suzuki et al. 1997). PRLTS bears significant identity to the extracellular domain of the PDGF receptor. Since the last study on PRLTS, performed in 1997, the ligand binding domains of the PDGF receptor have been characterised. Alignment of PRLTS with PDGF receptor β shows 27% identity (Fig. 10). The region of identity between PRLTS and PDGF receptor β lies within the third extracellular IgG like domain, which is the area responsible for binding to its ligand, PDGF (Lokker, O'Hare et al. 1997). After the PDGF receptor, PRLTS also bears identity with the ligand binding domain of the VEGF receptor, Flk-1. Both PDGF and VEGF signal to enhance angiogenesis (Brakenhielm and Cao 2008). PRLTS is predicted to display an N-terminal signal peptide necessary for secretion (predicted cleavage point amino acids 21-22) (Fig. 11). If the identity of PRLTS with the ligand binding domain of PDGF receptor and Flk-1 translates into functional similarities, PRLTS can possibly be thought of as a soluble form of the PDGF receptor, chelating free PDGF, thereby inhibiting angiogenesis.

A

B

```
Score = 73.9 bits (180),  Expect = 2e-17, Method: Compositional matrix adjust.
Identities = 69/235 (29%), Positives = 105/235 (44%), Gaps = 29/235 (12%)

PRLTS       LTLVNSTAADTGEFSCWEQLCNGYICRRDEAKTGSTYIFFTEKGELFVPSPSYFDVVYLN  187
            LTL N T  DTGE+ C      G     + ++    YIF  +    F+P  S    +++
PDGFRB      LTLTNVTGGDTGEYFCVYNNSLG----PELSERKRIYIFVPDPTMGFLPMDSEDLFIFVT  139

PRLTS       PDRQAVVPCRVTAPSAKVTLHREFPAKEIPANGTDIVYDMKRGFVYLQPHSDHQGVVYCK  247
               +  +PCRVT P  +VTLH +    +IP +   + YD +RGF      +       CK
PDGFRB      DVTETTIPCRVTDPQLEVTLHEK--KVDIPLH---VPYDHQRGFT----GTFEDKTYICK  190

PRLTS       AEAGGKSQISVKYQLLYVEVPSGPPSTTILASSNKVRGGDDISVLCTVLGEPDVEVEFRW  307
               G +   S  Y +  ++V S   + ++ A    VR G+ I++ C V+G  DV V F+W
PDGFRB      TTIGDREVDSDTYYVYSLQVSSI--NVSVNAVQTVVRQGESITIRCIVMGN-DV-VNFQW  246

PRLTS       LFPGQKDER---PVTIQDTWRLIHRGLGHTTRISQSVIIVEDFETIDAGYYICTA  359
             +P  K  R   PVT          G  +RI  S++ +   E  D+G Y C
PDGFRB      TYPRMKSGRLVEPVT--------DYLFGVPSRIG-SILHIPTAELSDSGTYTCNV  292
```

Figure 10. PRLTS sequence shares identity with ligand binding domain of PDGF receptor β subunit. The sequence of PRLTS is known to share significant similarities with the sequence of the β subunit of the PDGF receptor. To identify regions of similarity, the sequences of PDGFRL_MOUSE and PGFRB_MOUSE in the SwissProt database were aligned using ClustalW. A graphical representation of the alignment is shown in A). Details of the alignment are shown in B). The region of the PDGF receptor responsible for ligand binding is highlighted in red, this lies within the region of identity with PRLTS.

A

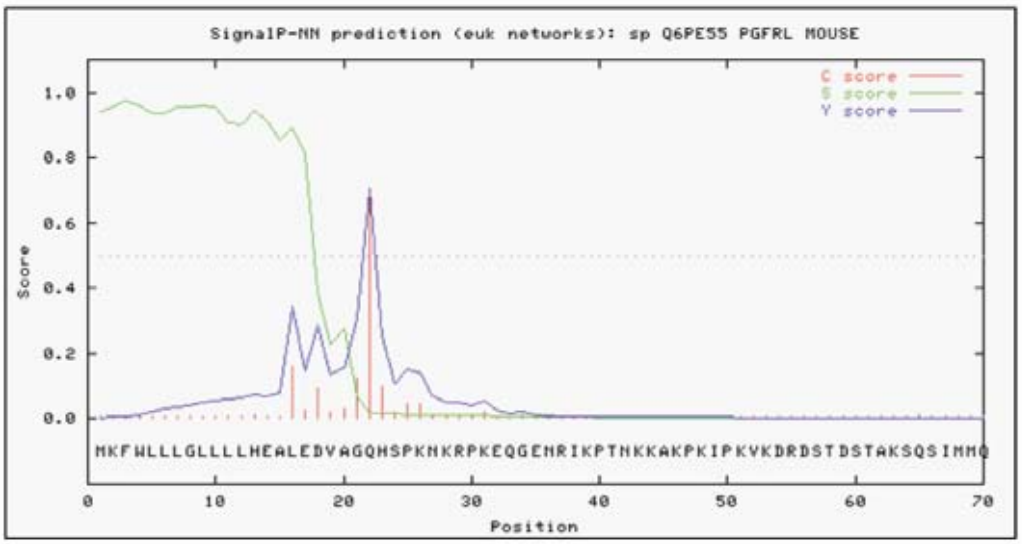


```
# Measure  Position  Value  Cutoff  signal peptide?
  max. C     22       0.703   0.32   YES
  max. Y     22       0.705   0.33   YES
  max. S      3       0.975   0.87   YES
  mean S     1-21     0.796   0.48   YES
       D     1-21     0.750   0.43   YES
# Most likely cleavage site between pos. 21 and 22: VAG-QH
```

B

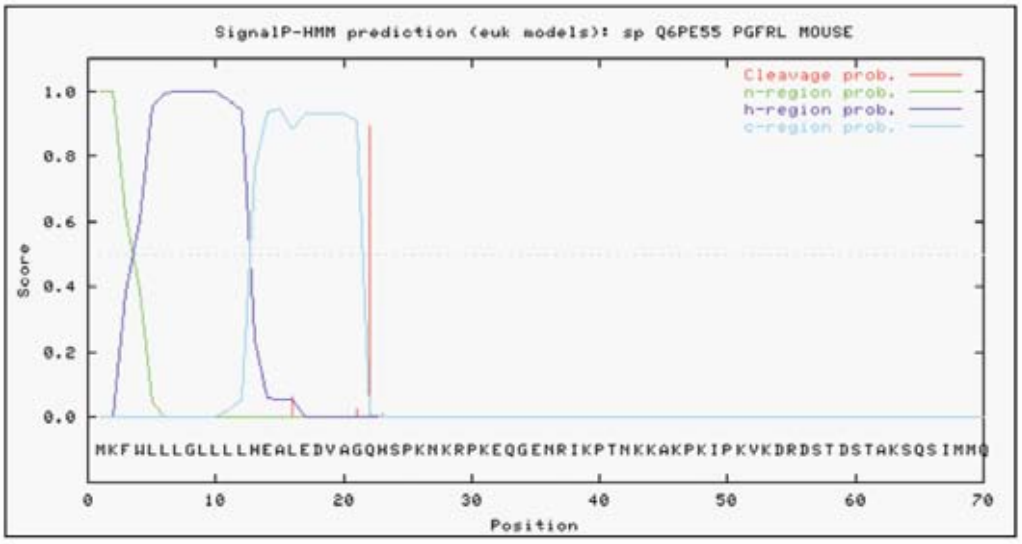


```
>sp_Q6PE55_PGFRL_MOUSE
Prediction: Signal peptide
Signal peptide probability: 1.000
Signal anchor probability: 0.000
Max cleavage site probability: 0.893 between pos. 21 and 22
```

Figure 11. PRLTS is predicted to have a signal peptide with peptide cleavage between residues 21 and 22. The sequence of PGFRL_MOUSE was submitted to the SignalP signal peptide prediction server, which predicts a signal peptide from amino acids 1-21 using A) neural networking algorithm and B) hidden markov modelling.

During differentiation of preadipocytes into adipocytes, expression of the PDGF receptor decreases (Huppertz, Schwartz et al. 1996; Vaziri and Faller 1996). This finding was recapitulated in Fig. 12 by immunoblotting 3T3-L1 cell lysates at different times during adipogenesis. 3T3-L1 cells are also known to express the pro-angiogenic cytokines PDGF, which is the ligand for the PDGF receptor, and VEGF, which is the ligand for Flk-1 (also known as VEGF receptor 2). Immunoblotting of a differentiation time course showed decreased expression of PDGF and VEGF during adipogenesis. An antibody specific to the VEGF receptor Flk-1 was not able to detect a protein of the correct predicted molecular weight (152 kDa). However, a single protein at approximately 30 kDa that increased in expression during adipogenesis was recognised by the Flk-1 specific antibody (Fig. 13). This is potentially interesting as smaller, soluble splice truncations of Flk-1 have been reported (Kou, Li et al. 2004). These splice truncations act as extracellular ligands for free VEGF, and inhibit the action of VEGF. A similar role for PRLTS is theorised. Interestingly, PRLTS expression also increases with adipogenesis, which is in contrast with the expression of pro-angiogenic molecules including PDGF, VEGF, and PDGF receptor (Fig. 12). Further experiments will be needed to identify this species. In all, these data highlight the anti-angiogenic nature of differentiated adipocytes. It may be that preadipocytes display pro-angiogenic signals to increase vasculature and blood flow to developing adipose tissue, which when mature, does not require further angiogenesis. This concept is explored further in relation to the anti-angiogenic protein PEDF in Chapter 3.

In the present study, PRLTS was identified as an adipocyte derived secretory product. This protein has never been detected in adipose tissue. Publicly available gene expression data shows significant expression of PRLTS in adipocytes (Fig. 14). To confirm these data, tissues from C57BL6 mice were immunoblotted for PRLTS, and immunoreactive bands were observed

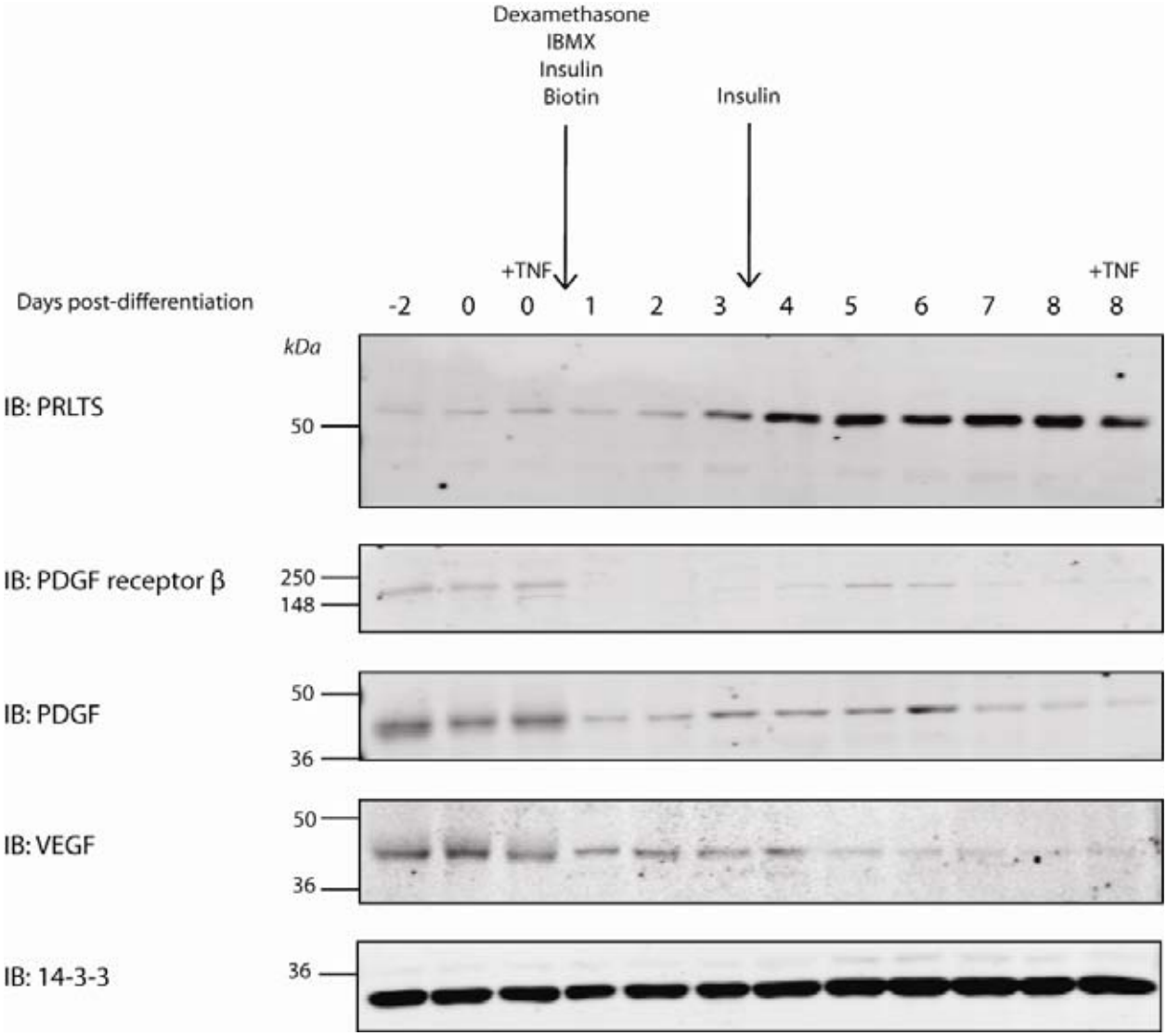

Figure 12. PRLTS expression increases during adipogenesis, whilst expression of pro-angiogenic proteins decreases. 3T3-L1 fibroblasts were differentiated into adipocytes as per standard protocol in methods. Each day of differentiation, cells were lysed for that particular timepoint. When cells were 100% confluent fibroblasts as well as fully differentiated adipocytes, TNFα was added for 24 hours prior to cell lysis to look for possible effects of TNFα on PRLTS expression. 10 μg of protein for each sample were loaded onto gels and immunoblotted as indicated.

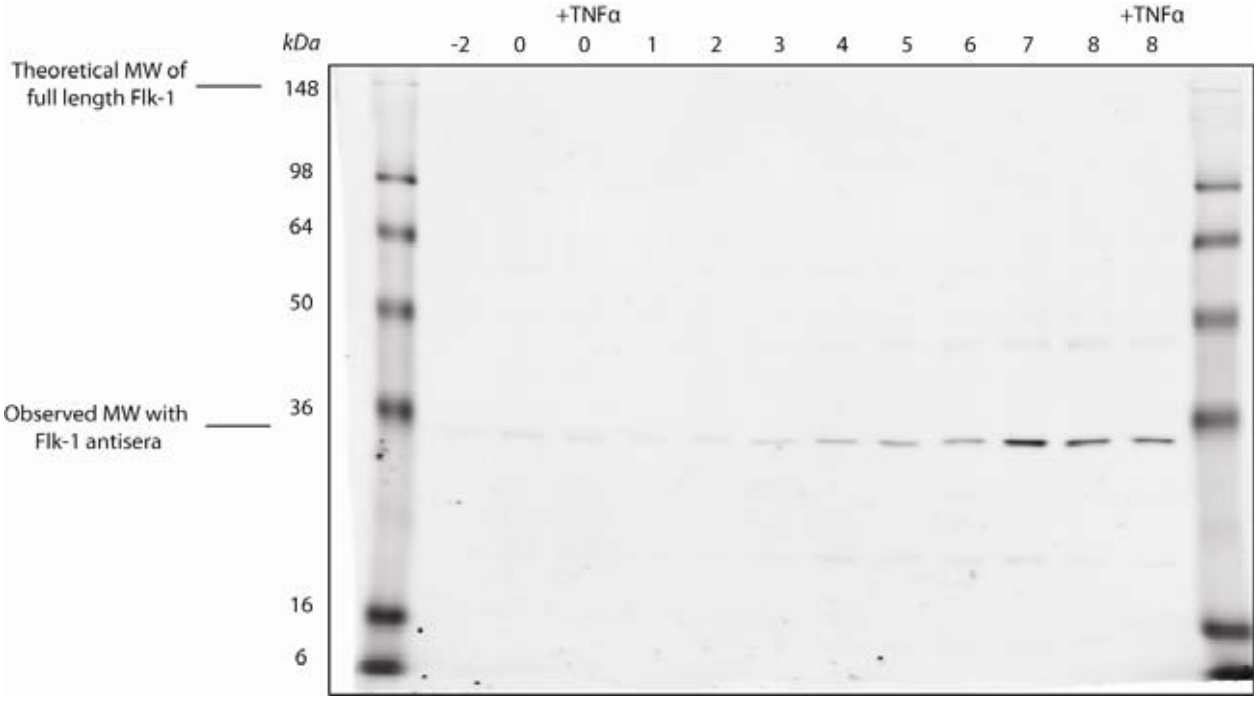

Figure 13. Flk-1 (VEFGR2) antisera recognise a protein species of 30 kDa that increases with adipogenesis. 3T3-L1 fibroblasts were differentiated into adipocytes as per standard protocol in methods. Each day of differentiation, cells were lysed for that particular timepoint. When cells were 100% confluent fibroblasts as well as fully differentiated adipocytes, TNFα was added for 24 hours prior to cell lysis to look for possible effects of TNFα on PRLTS expression. 10 µg of protein for each sample were loaded onto gels and immunoblotted with Flk-1 antisera. The theoretical molecular weight of Flk-1 is indicated. Soluble truncations of VEGFR2 are known, however none of these are of the molecular weight observed here.

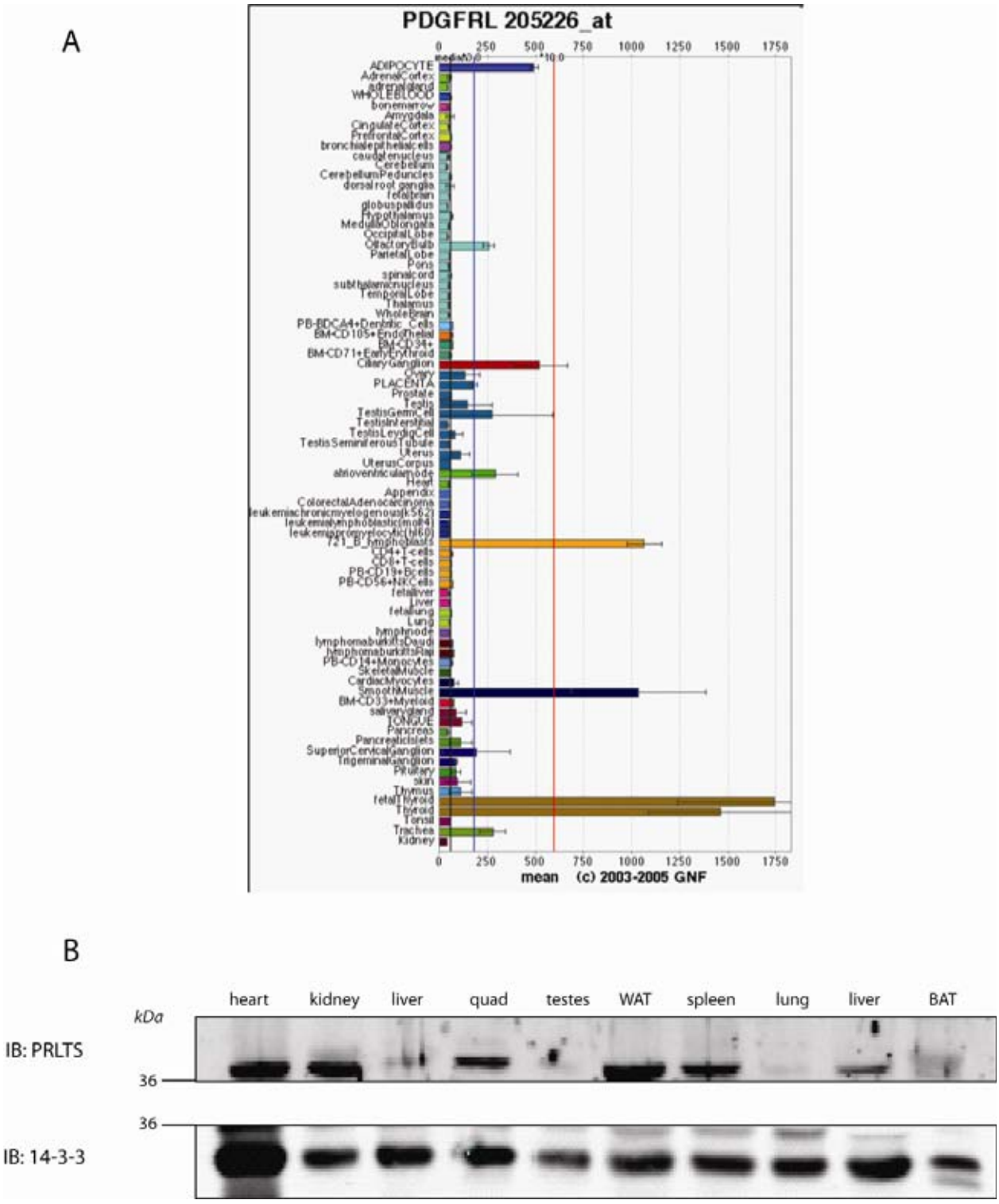

Figure 14. Tissue distribution of PRLTS reveals expression in WAT. A) Publicly available gene expression data for PRLTS shows expression ~9 times mean tissue expression in adipocytes. B) PRLTS immunoblot for tissues from C57BL6 mice shows PRLTS expression in WAT. Care must be taken in interpreting this last result, as secretory proteins may accumulate distal to their tissue of origin.

in a number of tissues, including white adipose tissue, supporting the initial identification of PRLTS from adipocytes. To identify the sub-cellular localisation of PRLTS, adipocytes were stained using a PRLTS specific antibody (Fig. 15). Staining showed partial overlap with the Golgi marker GM130, indicating the presence of PRLTS in the classical secretory pathway. In this mass spectrometry experiment, PRLTS was not uniformly secreted across treatments. Very little PRLTS (1-2 peptides) was detected in control or chronic insulin treated samples, and chronic TNFα treatment resulted in a greater abundance of PRLTS (11 peptides). To confirm these findings, conditioned media samples from control, chronic insulin and chronic TNFα treated 3T3-L1 adipocytes were immunoblotted for PRLTS. While an immunoreactive TNFα responsive species near the predicted molecular weight for PRLTS was initially observed in conditioned media, the detection of PRTLS in conditioned media was not highly reproducible in subsequent experiments. Affymetrix gene expression arrays of control, chronic insulin or chronic TNFα treated 3T3-L1 adipocytes shows increased expression of PRLTS under TNFα treatment (Table 6). TNFα is an inflammatory cytokine that is known to activate the NFκB signalling pathway, which results in transcription of an array of genes that have an upstream NFκB response element. There is one such site for NFκB upstream of the genomic location of PRLTS on human chromosome 8p21.3. These data further support the initial identification of PRLTS as a TNFα responsive adipocyte secretory protein. Further experiments will be needed to fully elucidate the physiological role of this poorly studied protein.

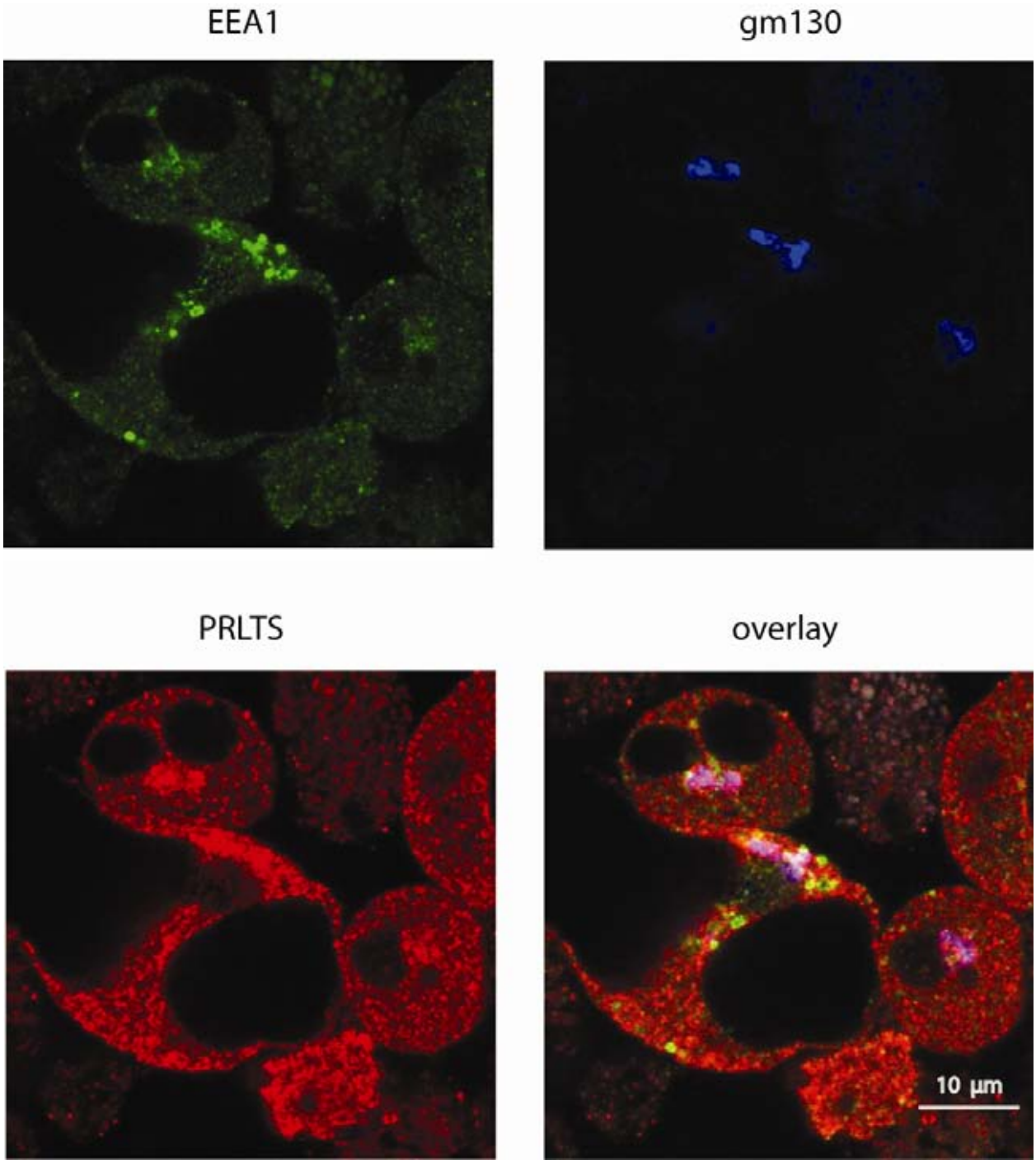

Figure 15. PRLTS staining in adipocytes. Differentiated 3T3-L1 adipocytes were stained for the early endosome marker EEA1 (green), the golgi marker gm130 (blue), and PRLTS (red). Partial overlap of PRLTS with the golgi is observed.

insulin resistance model	PRLTS expression
ctrl	898.164
chronic insulin	520.593
TNFα	1768.313
dexamethasone	614.944
glucose oxidase	687.1

Table 6. PRLTS is upregulated during TNFα treatment. 3T3-L1 adipocytes were treated with multiple insulin resistance models. RNA was extracted and hybridised with affymetrix DNA microarrays. Expression levels of PRLTS are shown.

Partial SILAC labelling for measuring effects of palmitate on hepatocyte protein secretion

Earlier in the investigation, the use of SILAC isotopes was explored in relation to tracking the synthesis and secretion of adipocyte secretory proteins. It was next decided to apply the SILAC technique to understand the effects of the fatty acid palmitate on protein secretion from hepatocytes. Excess availability of hepatic intracellular fatty acids is correlated with non-alcoholic fatty liver disease, a condition that has important physiological implications for whole body glucose homeostasis (Brunt). Treatment of hepatocytes with saturated fatty acids such as palmitate has previously been described as a model for lipid induced hepatic damage (Li, Berk et al. 2009). To investigate secretory changes in hepatocytes treated with excess fat, a partial SILAC labelling technique was applied. In a normal SILAC experiment, cells undergo at least 12 rounds of division in the presence of isotopic amino acid culture media to achieve complete protein labelling. Complete labelling of cells with isotopic amino acids is not always possible, particularly in primary (non-immortalised) cultures such as primary hepatocytes. To overcome this, a partial labelling approach was adopted. There are currently available two different unnatural isotopes of arginine and lysine, in addition to the naturally occurring non-isotopic versions of arginine and lysine. This means that by using the two unnatural isotopes as well as the naturally occurring isotopes, three different samples may be compared. In this case, by applying the two different unnatural isotopes to only two different treatments, the degree of amino acid incorporation can be measured as a guide to the relative rate or abundance of synthesis and secretion. Since this investigation, partial labelling has been used as CILAIR (comparison of isotope labelled amino acid incorporation rates) (Roelofsen, Dijkstra et al. 2009).

To quantitatively measure the effect of palmitate on protein secretion from hepatocytes, primary cultures were isolated from the livers of C57BL6 mice as before, cultured in isotopes of arginine and lysine, and treated with palmitate as described in methods. Aliquots of samples were taken, and the remaining samples mixed in equal proportions. Glycoprotein purification was performed on aliquots as well as the mixed sample, proteins resolved by SDS-PAGE and visualised by SYPRO ruby protein staining (Fig. 16). Strikingly, the secretion profile of hepatocytes varied markedly with palmitate treatment. The mixed sample was then subjected to mass spectrometry. Isotopic peak ratios for individual protein species were quantified, and are shown in Table 7. In general, the data showed an overall trend towards reduced protein secretion with palmitate treatment. This trend did not appear to be specific for individual proteins or for any particular category or biological pathway. The overall reduction in protein secretion observed during palmitate treatment could possibly be explained by effects of palmitate on the intracellular protein secretory pathway. Palmitate has previously been shown to induce endoplasmic reticulum (ER) stress at low concentrations (Wei, Wang et al. 2006). The integrity of the ER for proper protein secretion is of paramount importance, and this result perhaps highlights one effect of excess fatty acid availability on liver function.

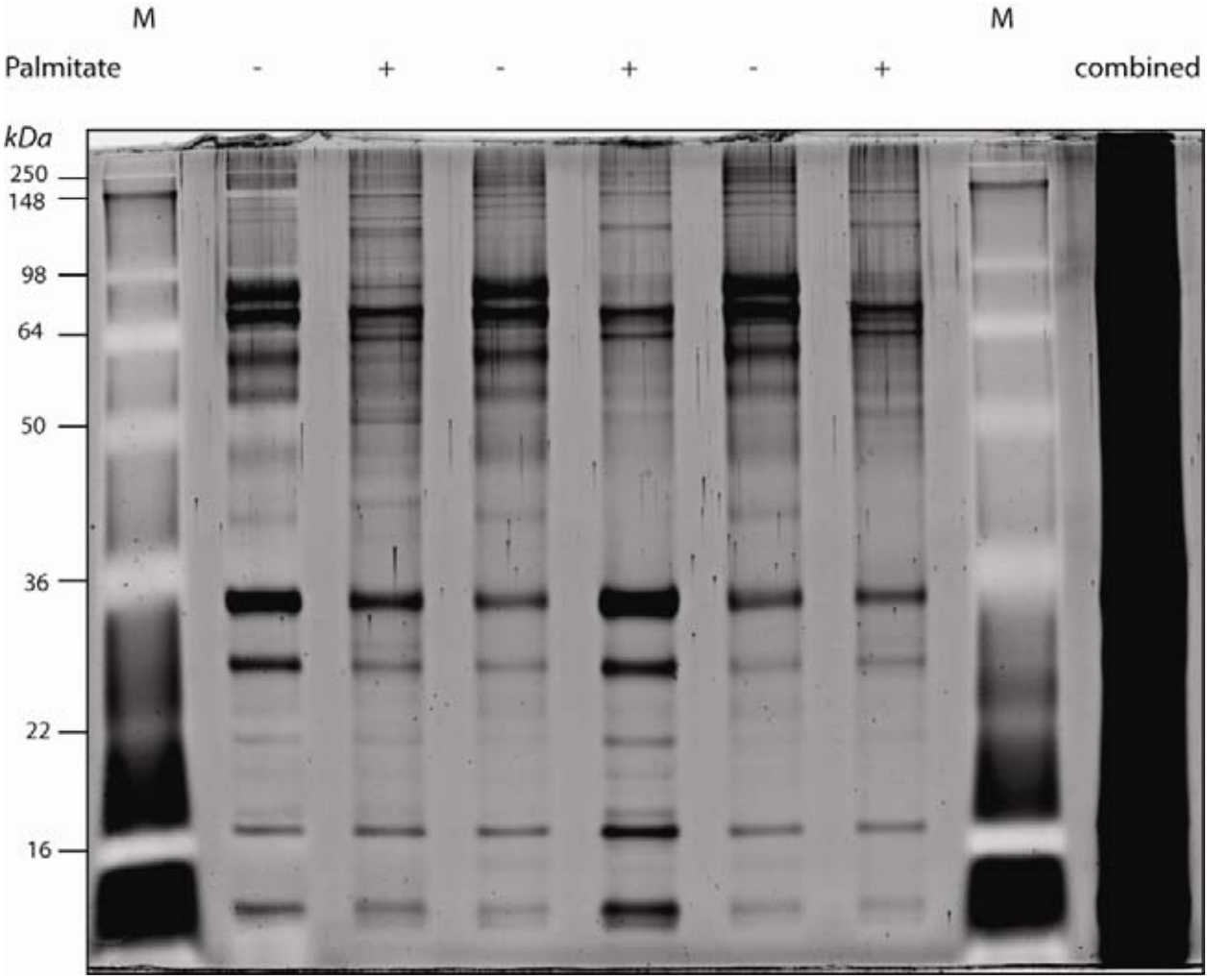

Figure 16. Palmitate treatment alters secretion of proteins from hepatocytes. Primary hepatocytes were isolated from C57BL6 mice, cultured in serum-free DMEM containing two different isotopes of lysine and arginine and either 400 µM palmitate coupled to 1% BSA or BSA alone. After 18 hours of treatment, hepatocytes were incubated in amino acid isotope containing serum free media supplemented with 100 nM insulin. Conditioned media were obtained, aliquots of each were taken, and remaining samples mixed in equal proportions. Conditioned media subjected to glycoprotein purification, proteins subjected SDS PAGE and visualised using SYPRO ruby protein stain. Combined sample was excised, proteins extracted and subjected to quantitative mass spectrometry (Table 7).

ion score	name	ctrl / palmitate	palmitate / ctrl	signal peptide?
3595	fibronectin-1	18.22618	0.054866	1
1715	hemopexin	18.09209	0.055273	1
1257	Es31 protein	3.917704	0.255252	1
1094	triacylglycerol hydrolase	5.770412	0.173298	0
908	Aminopeptidase N	5	0.2	1
902	serine (or cysteine) proteinase inhibitor, clade A, member 3K	7.664589	0.13047	1
888	EG13909 protein	1.901042	0.526027	1
857	haptoglobin	18.65972	0.053591	1
673	pregnancy zone protein	2.940105	0.340124	1
650	hypothetical protein LOC234564	0.359398	2.782429	0
650	mCG9581	6.003458	0.166571	1
616	esterase 31-like	0.946429	1.056604	1
550	serine (or cysteine) proteinase inhibitor, clade A, member 1a	6.531264	0.15311	1
537	alpha-1 protease inhibitor 2	18.85361	0.05304	1
523	hematopoetic lineage switch 2	0.577273	1.732283	0
499	dipeptidylpeptidase 4	1.784669	0.560328	1
484	ATP synthase beta subunit	2.958333	0.338028	0
451	murinoglobulin	4.451693	0.224634	1
404	EGF receptor	3.934066	0.25419	1
385	apolipoprotein A-IV	4.255165	0.235009	1
368	fructose-bisphosphate aldolase B	1.608108	0.621849	0
347	hypothetical protein LOC433182	0.801619	1.247475	0
339	carboxylesterase	10.25774	0.097487	1
335	carboxylesterase 6	1.062147	0.941489	1
319	arginase 1, liver			0
311	inter alpha-trypsin inhibitor	6.820289	0.146621	1
305	albumin			1
293	ceruloplasmin isoform b	2.441624	0.409563	1
284	serine (or cysteine) proteinase inhibitor, clade A, member 3N	20.44231	0.048918	1
281	transferrin	9.718206	0.1029	1
274	similar to carboxylesterase 2	1.175	0.851064	1
247	acetyl-CoA acyltransferase 2	0.808498	1.236861	0
238	C1 inhibitor	7.476923	0.133745	1
231	complement C3	6.788298	0.147312	1
226	Hsp60; chaperonin groEL	0.847458	1.18	0
223	orosmucoid 1	3.924448	0.254813	1
220	C4 complement protein	2.645217	0.378041	1
220	unnamed filament protein	0.835733	1.196555	1
214	clusterin	4.04388	0.247287	1
213	glutathione-s-trasferase	0.910256	1.098592	0

203	cathepsin Z	11.6299	0.085985	1
194	Anpep protein	1.325373	0.754505	1
193	clustrin	12.69868	0.078748	1
193	endoplasmic reticulum aminopeptidase 1	3.15544	0.316913	1
180	esterase 1	2.013378	0.496678	1
179	triosephosphate isomerase	1.281081	0.780591	0
178	sorbitol dehydrogenase precursor	0		0
177	Hsp8	4.253589	0.235096	0
176	laminin, gamma 1	14.30387	0.069911	1
175	laminin, subunit gamma 1	24.04902	0.041582	1
173	Adenosylhomocysteinase	1.553763	0.643599	0
170	sulfated glycoprotein-2 isoform 2	9.849558	0.101527	1
169	P2B/LAMP-1	1.670209	0.598728	0
168	orthinine transcarbamylase	0.45515	2.19708	0
166	serine protease inhibitor A3M	17.72131	0.056429	1
147	lipocalin-2	40.45161	0.024721	1
137	cathepsin D	3.472	0.288018	1
132	cathepsin L			1
131	alpha-2-macroglobulin	3.617117	0.276463	1
130	hypothetical protein LOC244595			0
129	serine (or cysteine) proteinase inhibitor, clade A, member 1c	10.47938	0.095425	1
123	zinc-alpha-2-glycoprotein	2.593792	0.385536	1
115	H-2 class I histocompatability antigen, Q8 alpha chian	23.73913	0.042125	1
108	apolipoprotein A1	2.830357	0.353312	1
102	cellular repressor of E1A-stimulated genes 1	4.067797	0.245833	0
102	H-2D cell surface glycoprotein	13.76923	0.072626	1
102	peroxisomal acyl-CoA oxidase	0		0
100	serine (or cysteine) proteinase inhibitor, clade C (antithrombin), member 1	1.307692	0.764706	1
97	C1 inhibitor			1
96	leucine-rich alpha-2-glycoprotein	8.016949	0.124736	1
95	F12 protein	13.57741	0.073652	1
94	carboxypeptidase B2			1
93	serpina1d protein			1
92	alanyl (membrane) aminopeptidase			0
92	glutathione-s-trasferase A2	1.768456	0.565465	0
86	dipeptidylpeptidase 2	0.910891	1.097826	1
85	lysosomal membrane glycoprotein-type B			0
85	mCG134629, isoform CRA_c	31.30435	0.031944	1
81	H6pd protein	0		1
80	Q10	7.577143	0.131976	1
79	aldolase A, fructose bisphosphate	4.065844	0.245951	0
75	MHC H-2Dr	38.43478	0.026018	1

75	mouse preprocathepsin			1
74	betaine-homocysteine methyltransferase	6.782609	0.147436	0
74	serine (or cysteine) proteinase inhibitor, clade A, member 1e			1
70	alpha-D-mannosidase			1
69	fibrinogen-like protein 1			1
68	alpha-1 antitrypsin	9.795349	0.102089	1
68	antigen H-2Dq,histocompatability	13.84615	0.072222	1
66	Kininogen-1			1
65	hypothetical protein LOC72361	0.121951	8.2	0
59	coagulation factor II			1
59	mCG132226, isoform CRA_a			1
57	thiolase	2.827466	0.353674	0
54	H-2D4(q)	31.30435	0.031944	1
53	transglutaminase			
51	dystroglycan			1
51	vitronectin			1
50	unknown			0
48	beta-2 glycoprotein I	2.920988	0.34235	1
48	contrapsin			1
47	polymeric immunoglobulin receptor	1.912959	0.52275	1
45	serpina10 protein			1

Table 7. Quantitative proteomic comparison of protein secretion from primary hepatocytes during chronic palmitate treatment. Primary hepatocytes were isolated from C57BL6 mice, cultured in serum-free DMEM containing two different isotopes of lysine and arginine and either 400 µM palmitate coupled to 1% BSA or BSA alone. After 18 hours of treatment, hepatocytes were incubated in amino acid isotope containing serum free media supplemented with 100 nM insulin. Conditioned media were collected, mixed in equal proportions, subjected to glycoprotein purification and mass spectrometry. Ratios of isotopic peptides were measured to obtain relative abundance.

Protein secretion from hepatocytes during infection with hepatitis C virus

Another example of the importance of liver function on whole body energy homeostasis is highlighted by the recent discovery that infection of individuals with the liver specific hepatitis virus greatly increases the risk of developing insulin resistance (Yoneda, Saito et al. 2007; Milner, van der Poorten et al. 2009). This insulin resistance does not occur in the liver, and instead occurs in peripheral tissues such as muscle and to a lesser extent white adipose tissue. Perhaps the most intriguing part of this discovery was the observation that subcutaneous adiposity, and not visceral adiposity, was a predictor of insulin resistance, whereas in the uninfected situation, the inverse is true. The existence of insulin resistance distal to the point of primary infection (the liver) raises the possibility that viral infection may modulate the secretion of factors from the liver that induce insulin resistance in peripheral tissues.

An experiment was designed to investigate potential alterations in protein secretion from hepatitis C virus infected hepatocytes. To achieve this, it was necessary to use a human hepatocyte cell line, as hepatitis C is a human specific virus. The Huh7 human hepatoma cell line was consequently chosen as a model (Nakabayashi, Taketa et al. 1982). Up until recently, hepatitis C virus could not be maintained outside a human and could not be cultured *in vitro*. Recently, a strain of hepatitis C virus that can be maintained outside of a human body *in vitro* has been isolated (Lindenbach, Evans et al. 2005; Wakita, Pietschmann et al. 2005; Zhong, Gastaminza et al. 2005; Scheel, Gottwein et al. 2008). The JFH1 (Japanese patient with Fulminant Hepatitis) strain can infect and multiply within cultured human hepatocytes, and causes infection when re-introduced into simians (Wakita, Pietschmann et al. 2005). This study aimed to investigate the effects of hepatitis C infection on the secretome of hepatocytes using the JFH1 strain of hepatitis C to infect Huh7 hepatocytes. There is a possibility that hepatitis C

infection causes necrosis of hepatocytes, and it may be the release of intracellular factors that causes distal insulin resistance, possibly through an inflammatory response. To address this possibility and survey all proteins released from hepatocytes, enrichment for secreted proteins using glycoprotein affinity purification was not performed, and instead, total protein was precipitated using tricarboxylic acid (TCA) protein precipitation. Since only two samples were being compared, partial isotopic labelling as previously described in this investigation was used. Huh7 cells infected or uninfected with JFH1 were incubated in DMEM containing isotopes of arginine and lysine for 24 h. Following this, cells were incubated in serum free DMEM with isotopic amino acids supplemented with 100 nM insulin for 18 h. Conditioned media was collected, mixed in equal proportions, subjected to TCA protein precipitation, SDS-PAGE, trypsin digestion and mass spectrometry. After protein identification, isotopic ratios of peptides were measured and used to identify ratios of abundance between uninfected and infected samples (Table 8).

A total of 163 proteins were identified, of which 101 proteins incorporated the isotopic label. A total of 49 of 101 proteins (49%) identified displayed an N-terminal signal peptide. Out of the 101 proteins that incorporated the label, 45 proteins differed in abundance by more than 2-fold between control and JFH1 infected adipocytes (Table 8). The 45 proteins that did differ in abundance included 17 proteins (38%) with signal peptides. Of the 45 proteins with a greater than 2-fold change, 21 of these were increased in uninfected cells, whilst 24 were increased in infected cells. Of the 21 proteins increased in uninfected cells, 7 proteins (33%) had a signal peptide, whilst of the 24 proteins increased in infected cells, 10 proteins (42%) had a signal peptide. When these percentages are compared with the overall ratio of proteins containing signal peptides, there is little cause to believe that hepatitis C infection increases cell necrosis

Accession	Score	uninfected / 12C	infected / 12C	uninfected / infected	infected / uninfected	Description	signal peptide
ALBU_HUMAN	2796	**3.928**	3.279	1.198	0.835	Serum albumin	Y
A2MG_HUMAN	2141	4.387	5.375	0.816	1.225	Alpha-2-macroglobulin	Y
FIBA_HUMAN	1608	2.337	**4.217**	0.554	1.804	Fibrinogen alpha chain	Y
FINC_HUMAN	1388	5.876	3.706	1.586	0.631	Fibronectin	Y
TRFE_HUMAN	1126	4.434	5.229	0.848	1.179	Serotransferrin	Y
A1AT_HUMAN	1093	**7.922**	**4.142**	1.913	0.523	Alpha-1-antitrypsin	Y
CLUS_HUMAN	1087	**8.515**	**5.305**	1.605	0.623	Clusterin	Y
APOE_HUMAN	920	**2.725**	3.917	0.696	1.437	Apolipoprotein E	Y
APOA1_HUMAN	851	7.721	2.986	2.586	0.387	Apolipoprotein A-I	Y
FETA_HUMAN	847	4.937	3.37	1.465	0.683	Alpha-fetoprotein	Y
ITIH2_HUMAN	829	**4.236**	2.368	1.789	0.559	Inter-alpha-trypsin inhibitor heavy chain H2	Y
FIBG_HUMAN	827	**5.605**	13.45	0.417	2.400	Fibrinogen gamma chain	Y
FIBB_HUMAN	813	**4.501**	**8.647**	0.521	1.921	Fibrinogen beta chain	Y
APOB_HUMAN	596	4.477	2.461	1.819	0.550	Apolipoprotein B-100	Y
GRP78_HUMAN	592	**0.2785**	0.3678	0.757	1.321	78 kDa glucose-regulated protein	Y
CO3_HUMAN	483	3.582	**6.211**	0.577	1.734	Complement C3	Y
AMBP_HUMAN	479	**4.192**	3.801	1.103	0.907	Protein AMBP	Y
PAI1_HUMAN	461	2.815	2.614	1.077	0.929	Plasminogen activator inhibitor 1	Y
RET4_HUMAN	458	7.853	9.221	0.852	1.174	Retinol-binding protein 4	Y
ENOA_HUMAN	431	0.225	0.8791	0.256	3.907	Alpha-enolase	Y
PPIB_HUMAN	381	0.5714	0.5981	0.955	1.047	Peptidyl-prolyl cis-trans isomerase B	Y
PRDX1_HUMAN	381	**0.07734**	**0.224**	0.345	2.900	Peroxiredoxin-1	Y
APOA2_HUMAN	326	3.529	**9.032**	0.391	2.559	Apolipoprotein A-II	Y
TTHY_HUMAN	297	1.315	2.07	0.635	1.574	Transthyretin	Y
PEDF_HUMAN	294	**16.38**	**15.22**	1.076	0.929	Pigment epithelium-derived factor	Y
GELS_HUMAN	277	0.8657	0.902	0.960	1.042	Gelsolin	Y
VTNC_HUMAN	259	**7.218**	**3.253**	2.219	0.451	Vitronectin	Y
FETUA_HUMAN	234	1.67	3.628	0.460	2.172	Alpha-2-HS-glycoprotein	Y
TSP1_HUMAN	230	2.85	3.244	0.879	1.138	Thrombospondin-1	Y
GDF15_HUMAN	221	0.07547	0.6262	0.121	8.297	Growth/differentiation factor 15	Y
CATD_HUMAN	214	1.499	2.492	0.602	1.662	Cathepsin D	Y
NID1_HUMAN	194	1.47	2.554	0.576	1.737	Nidogen-1	Y
MATN3_HUMAN	174	0.1991	0.4548	0.438	2.284	Matrilin-3	Y
ENPL_HUMAN	164	0.3951	**0.288**	1.371	0.729	Endoplasmin	Y
ANGT_HUMAN	161	**15.29**	13.01	1.175	0.851	Angiotensinogen	Y

BGH3_HUMAN	142	9.942	21.57	0.461	2.170	Transforming growth factor-beta-induced protein ig-h3	Y
IPSP_HUMAN	142	**4.495**	3.079	1.460	0.685	Plasma serine protease inhibitor	Y
CSTN1_HUMAN	122	2.506	109.1	0.023	43.536	Calsyntenin-1	Y
HEP2_HUMAN	121	2.189	3.285	0.666	1.501	Heparin cofactor 2	Y
OSTP_HUMAN	118	2.89	2.634	1.097	0.911	Osteopontin	Y
SAP_HUMAN	111	0.3813	0.009	42.156	0.024	Proactivator polypeptide	Y
PDIA3_HUMAN	103	0.4078	0.4191	0.973	1.028	Protein disulfide-isomerase A3	Y
TSP4_HUMAN	93	2.986	1.102	2.710	0.369	Thrombospondin-4	Y
THRB_HUMAN	92	0.09134	0.0004	255.783	0.004	Prothrombin	Y
FUCO2_HUMAN	76	0.8971	0.2173	4.128	0.242	Plasma alpha-L-fucosidase	Y
MEP1A_HUMAN	76	9.611	5.909	1.627	0.615	Meprin A subunit alpha	Y
CO5A2_HUMAN	75	4.513	1.5	3.009	0.332	Collagen alpha-2(V) chain	Y
CO5_HUMAN	74	0.3663	0.8742	0.419	2.387	Complement C5	Y
COCH_HUMAN	73	7.913	14.66	0.540	1.853	Cochlin	Y
ACTG_HUMAN	1143	**0.3128**	**0.242**	1.291	0.775	Actin, cytoplasmic 2	N
ACTC_HUMAN	835	**0.2623**	**0.234**	1.123	0.890	Actin, alpha cardiac muscle 1	N
HS90A_HUMAN	817	0.1396	**0.209**	0.668	1.496	Heat shock protein HSP 90-alpha	N
HS90B_HUMAN	750	0.1434	**0.209**	0.686	1.457	Heat shock protein HSP 90-beta	N
HSP7C_HUMAN	693	**0.2619**	**0.254**	1.031	0.970	Heat shock cognate 71 kDa protein	N
A26CA_HUMAN	528	0.2729	**0.242**	1.126	0.888	ANKRD26-like family C member 1A	N
ACTBL_HUMAN	395	0.6934	0.3543	1.957	0.511	Beta-actin-like protein 2	N
HSP72_HUMAN	360	**0.2826**	**0.254**	1.113	0.899	Heat shock-related 70 kDa protein 2	N
TBB5_HUMAN	339	**0.216**	0.2259	0.956	1.046	Tubulin beta chain	N
ACTK_HUMAN	329	1.758	0.2423	7.255	0.138	Kappa-actin	N
EF1A3_HUMAN	321	0.1791	**0.272**	0.658	1.520	Putative elongation factor 1-alpha-like 3	N
GSTP1_HUMAN	295	**0.06802**	**0.103**	0.664	1.507	Glutathione S-transferase P	N
KPYM_HUMAN	292	0.0331	**0.17**	0.195	5.127	Pyruvate kinase isozymes M1/M2	N
TPIS_HUMAN	274	0.1322	**0.241**	0.548	1.825	Triosephosphate isomerase	N
HS71L_HUMAN	258	0.1119	**0.206**	0.543	1.841	Heat shock 70 kDa protein 1L	N
AL1A1_HUMAN	254	0.3741	0.1518	2.464	0.406	Retinal dehydrogenase 1	N
HSP76_HUMAN	237	**0.1119**	**0.211**	0.530	1.886	Heat shock 70 kDa protein 6	N

UBIQ_HUMAN	235	0.3321	0.8781	0.378	2.644	Ubiquitin	N
ALDOA_HUMAN	226	0.7072	0.2711	2.609	0.383	Fructose-bisphosphate aldolase A	N
EF2_HUMAN	215	0.3625	0.5002	0.725	1.380	Elongation factor 2	N
VIME_HUMAN	203	0.3677	0.227	1.620	0.617	Vimentin	N
TBA1C_HUMAN	200	1.112	0.5985	1.858	0.538	Tubulin alpha-1C chain	N
PPIA_HUMAN	180	**0.2131**	**0.177**	1.203	0.832	Peptidyl-prolyl cis-trans isomerase A	N
PEBP1_HUMAN	178	1.117	0.1102	10.136	0.099	Phosphatidylethanolamine-binding protein 1	N
G3P_HUMAN	169	0.08448	0.2288	0.369	2.708	Glyceraldehyde-3-phosphate dehydrogenase	N
NDKA_HUMAN	169	**0.2103**	0.1093	1.924	0.520	Nucleoside diphosphate kinase A	N
TERA_HUMAN	168	0.8966	0.4459	2.011	0.497	Transitional endoplasmic reticulum ATPase	N
H90B3_HUMAN	167	0.9921	0.4612	2.151	0.465	Putative heat shock protein HSP 90-beta-3	N
RSSA_HUMAN	142	0.8106	0.2208	3.671	0.272	40S ribosomal protein SA	N
STMN1_HUMAN	132	**0.229**	2.052	0.112	8.961	Stathmin	N
ROA2_HUMAN	128	1.991	1.697	1.173	0.852	Heterogeneous nuclear ribonucleoproteins A2/B1	N
NPM_HUMAN	121	0.1632	0.4092	0.399	2.507	Nucleophosmin	N
1433Z_HUMAN	121	**0.07292**	0.1819	0.401	2.495	14-3-3 protein zeta/delta	N
CH60_HUMAN	119	0.7432	1.347	0.552	1.812	60 kDa heat shock protein, mitochondrial	N
COF1_HUMAN	116	**0.3273**	0.8902	0.368	2.720	Cofilin-1	N
1433B_HUMAN	101	1.914	0.5333	3.589	0.279	14-3-3 protein beta/alpha	N
SET_HUMAN	81	0.2311	0.6491	0.356	2.809	Protein SET	N
IDHC_HUMAN	80	1.772	**0.161**	11.040	0.091	Isocitrate dehydrogenase [NADP] cytoplasmic	N
GOLM1_HUMAN	74	0.4274	**0.43**	0.994	1.006	Golgi membrane protein 1	N
CLIC1_HUMAN	72	0.6793	**0.224**	3.031	0.330	Chloride intracellular channel protein 1	N
STMN2_HUMAN	71	**0.229**	2.052	0.112	8.961	Stathmin-2	N
CYTC_HUMAN	70	38.14	38.1	1.001	0.999	Cystatin-C	N

Table 8. Quantitative proteomic comparison of protein secretion from Huh7 hepatomas during hepatitis C infection. Huh7 hepatoma cells infected with or without the hepatitis C strain JFH1 were subcultured into media containing isotopes of arginine and lysine. One day later, cells were incubated in serum free isotope containing media supplemented with 100 nM insulin for 24 hours. Conditioned media was collected, mixed in equal proportions, and proteins precipitated using TCA. Precipitated proteins were resolved by SDS-PAGE, trypsin digested and subjected to mass spectrometry. Ratios of isotopic peptides were measured to obtain relative abundance.

and the release of cytoplasmic proteins. Of the proteins that did alter with hepatitis C infection, α-2-HS-glycoprotein emerges as a candidate for investigation. Levels of this protein in serum correlate with insulin resistance (Stefan, Hennige et al. 2006), and exogenous administration with α-2-HS-glycoprotein suppresses adiponectin production (Hennige, Staiger et al. 2008). Investigation of this and other proteins identified in the current study may form the basis of future experiments.

Discussion

This investigation began with the aim of developing an approach for enriching secretory proteins from conditioned media to the exclusion of cytoplasmic proteins while maintaining sufficient sensitivity to detect low abundance secretory proteins. During mass spectrometry, only a finite number of peptides can be detected at any one time, and if the amount of protein introduced into the mass spectrometer exceeds the limits of detection, not all peptides will be detected and some protein identifications could be missed. The existence of contaminating proteins in a mixture would typically lead to dilution of target protein identification, and it was for this reason that purification of secretory proteins from conditioned media samples was necessary. To purify secretory proteins from conditioned media samples, a lectin based glycoprotein affinity purification strategy was developed. This strategy exploited N-glycosylation of secretory proteins, a post-translational modification common to secretory proteins but largely absent from cytoplasmic proteins. This approach afforded a rapid and cost-effective enrichment step for secretory proteins. By enriching for secreted proteins from conditioned media, the secretome of adipocytes could be sequenced at a greater depth than previous studies, with the identification of

a higher number of secretory proteins. The non-secretory proteins that were detected were at the lower end of detection, as shown by a scatter plot of protein ion scores in Fig. 17. This approach was applied to the primary insulin sensitive cell types, including adipocytes, hepatocytes and myotubes. This study was the first to survey the secretome of hepatocytes and myotubes, and provided a powerful comparative analysis, summarised in Fig. 18 and detailed in Table 9.

During this investigation, 101 secretory proteins were identified from adipocytes, 53 from myotubes, and 227 from hepatocytes. The secretory profile of each of these cell types was not unique, with some overlap in protein identifications between cell types. Adipose tissue secreted serine protease inhibitors, acute phase reactants, members of the complement pathway, extracellular matrix proteins, cathepsins, regulatory proteins such as adiponectin, enzymes such as biotinidase, and a number of other proteins whose physiological role remains unclear, such as URB. Skeletal muscle had a distinctly less diverse secretome, with the vast majority of secretory proteins involved in the regulation of the extracellular matrix with the possible exception of macrophage colony stimulating factor. Liver had the largest and most diverse secretome, and released serine protease inhibitors, acute phase reactants, members of the complement pathway, and extracellular matrix proteins. The majority of conserved secretory protein species across multiple cell types were extracellular matrix proteins. There were only 7 protein species that were consistently identified across adipocytes, myotubes and hepatocytes. All of these were widely expressed extracellular matrix proteins, indicating the likely generic function of these proteins for general cell function and growth. There were 15 secretory proteins identified from both muscle and liver. The majority of these were extracellular matrix proteins, with the notable exception of the protein URB (up-regulated in bombesin receptor knockout mice; also known as steroid-sensitive gene 1). Publicly available gene expression databases show expression of URB

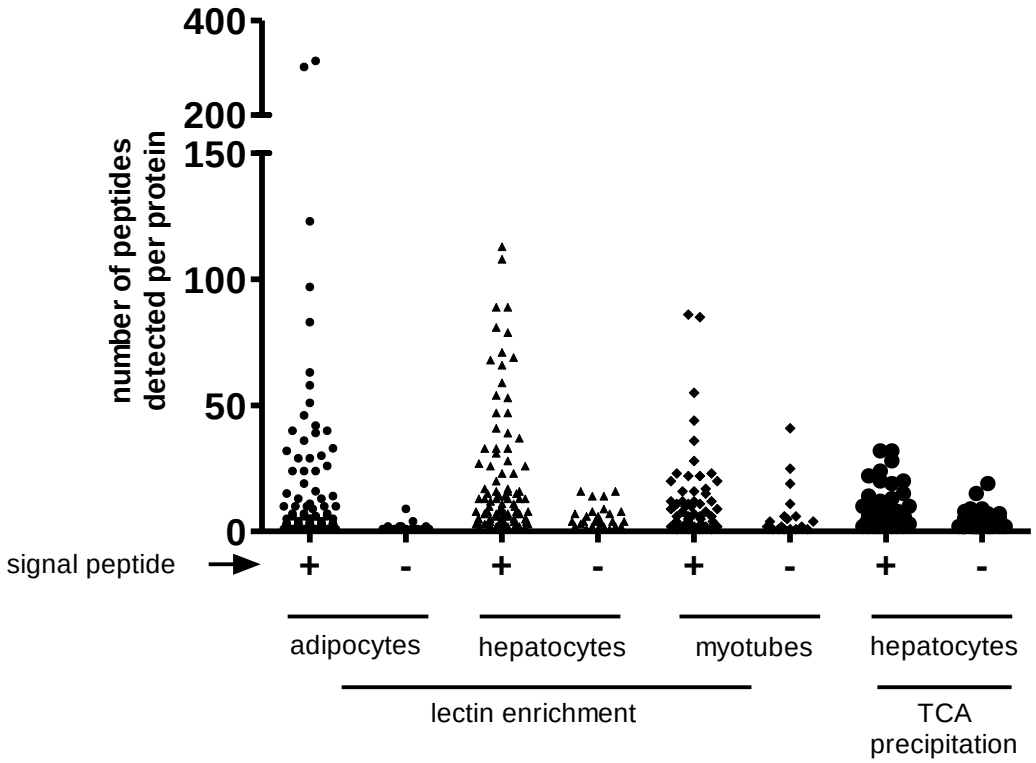

Figure 17. Glycoprotein enrichment increases the detection of secretory proteins. For each experiment, all detected proteins were divided into those with and without a signal peptide. The number of peptides detected for each protein identification (a semiquantitative method for measuring relative protein abundance) is used to plot the distribution of protein identifications.

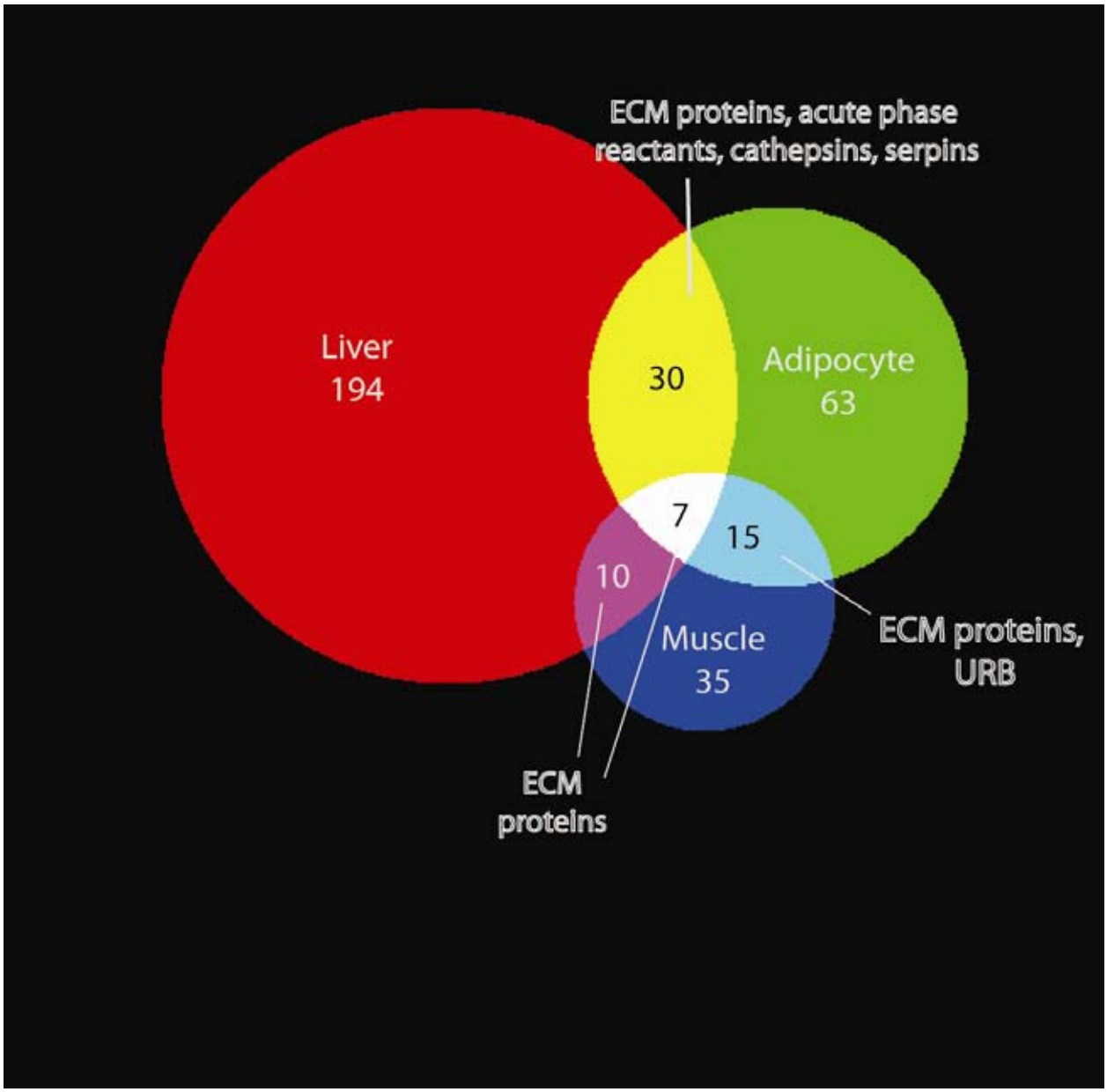

Figure 18. Overlap of protein secretion. Secretory proteins identified from 3T3-L1 adipocytes, L6 myotubes, primary hepatocytes and hepatoma cells were combined and the existence of a protein species across multiple cell types was noted. The majority of cell overlap was due to extracellular matrix (ECM) proteins.

limited to adipocytes and skeletal muscle only (Fig. 19), confirming the findings of this study. At the outset of this investigation adipose tissue was not known to express URB, however data were published during the course of this investigation confirming the secretion of URB from white adipose tissue (Okada, Nishizawa et al. 2008). URB expression levels were found to be dysregulated during *in vitro* insulin resistance models, as well as in the adipose tissue of obese mice.

The greatest similarities in protein secretion occurred between adipocytes and hepatocytes, with 30 secretory proteins identified from both of these cell types. These 30 proteins included not only the widely expressed generic extracellular matrix proteins (of which there were 10), but serine protease inhibitors (3 proteins), acute phase reactants (4 proteins), cathepsins (2 proteins) and enzymes including extracellular superoxide dismutase and lipoprotein lipase. This indicates that in terms of secretion, adipose tissue is most similar to the liver. Interestingly, between adipocytes and hepatocytes a total of 14 members of the complement pathway were detected, however only one of these, complement C3, was conserved in both. This indicates a lack of redundancy in secretion of members of the complement pathway, with different tissues responsible for secretion of different parts of the pathway.

Liver and muscle were dissimilar in their secretion, with only 10 proteins secreted from both myotubes and hepatocytes. All of these proteins were extracellular matrix proteins, with the exception of procollagen C-endopeptidase enhancer protein and calsyntenin. Whilst not actually forming the extracellular matrix, procollagen-C-endopeptidase enhancer protein is involved in regulation and remodelling of the extracellular matrix. The lack of similarities in protein secretion between hepatocytes and myotubes is evidence of the differing endocrine roles of these tissues, if an endocrine role for skeletal muscle exists at all.

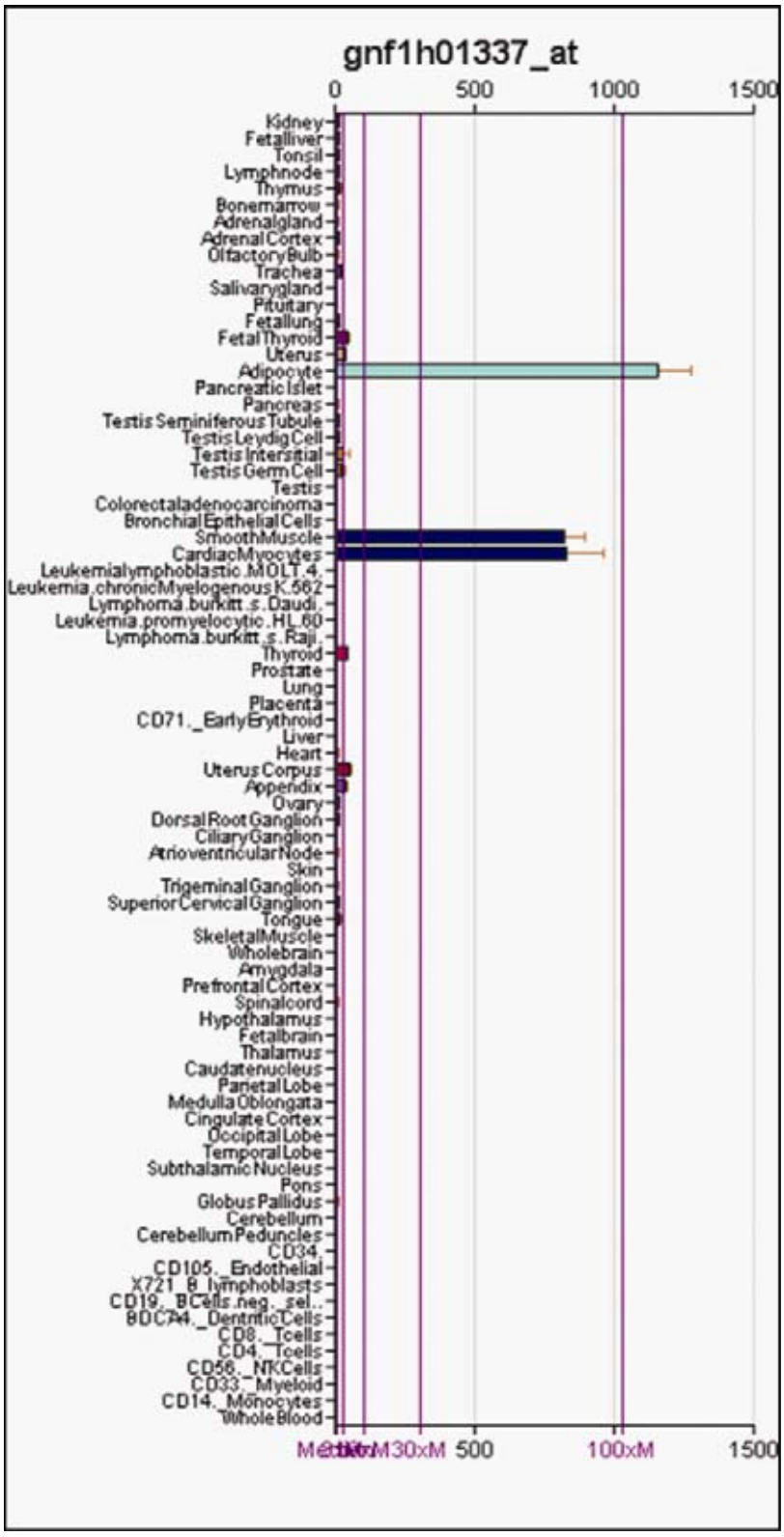

Figure 19. URB expression is restricted to adipocytes and muscle. Publicly available tissue distribution data from BioGPS (biogps.gnf.org) for URB, also known as steroid sensitive gene 1.

Although a large number of secretory proteins were identified in this study, the existence of a signal peptide necessary for secretion does not necessarily reflect an endocrine role for these proteins *per se*. It must be noted that for a secretory protein to play an endocrine role, it must interact with targets distal to the tissue of origin to effect a physiological change. Most of the proteins identified are more likely to act in a paracrine manner. This especially includes extracellular matrix proteins, which were the most abundantly detected class of proteins. This is not to detract from the importance of paracrine acting secretory proteins, as data from this investigation showed a paracrine effect of adipocyte secretory proteins on insulin sensitivity (Fig. 8).

n the field of metabolic research, much attention has been devoted to the endocrine capability of adipose tissue (Maury and Brichard ; Fruhbeck, Gomez-Ambrosi et al. 2001; Trujillo and Scherer 2006; Gualillo, Gonzalez-Juanatey et al. 2007; Lago, Dieguez et al. 2007; Rabe, Lehrke et al. 2008; Galic, Oakhill et al. 2009). In contrast, the possible endocrine contributions of organs such as liver and skeletal muscle are largely ignored, with the exception of muscle derived interleukin-6 (Febbraio and Pedersen 2002). In this study, 115 secretory proteins were identified from adipocytes, 67 were identified from myotubes, and 241 were identified from primary hepatocytes. Although the possible metabolic roles of all these proteins have not yet been elucidated, the identification of this number of proteins from other tissues suggest that white adipose tissue is by no means unique or extraordinary in its secretory ability. Traditionally, endocrine organs are highly dynamic in their secretion of proteins or small molecule hormones, with changes in protein secretion co-ordinated in a matter of seconds. Professional secretory cells such as β-cells that make up traditional endocrine organs have a very distinct morphology, with an extensive ER – Golgi network that occupies most of the cytoplasm. In addition, they contain

ready releasable secretory granules that contribute to the highly dynamic temporal secretion of proteins. In contrast, changes in protein secretion from adipocytes occur slowly, and are regulated at the transcriptional level. Although adipose tissue certainly is responsible for the secretion of important proteins such as leptin and adiponectin, adipocytes do not display the hallmarks of professional secretory cells. In contrast to adipose tissue, the liver displays a far greater secretory capacity. Despite this, comparatively little attention is devoted to the endocrine role of the liver in metabolic dysfunction.

Chapter 3

Pigment Epithelial Derived Factor Contributes to Insulin Resistance in Obesity

Lindsay Wu

This work was performed as a collaboration between LE Wu and researchers at the Department of Physiology at Monash University, Melbourne, Australia. Cell biochemistry experiments were performed by LE Wu, animal physiology experiments were performed at Monash University. This chapter was published as an equal first author manuscript "Pigment Epithelial Derived Factor Contributes to Insulin Resistance in Obesity" Crowe S, Wu LE, Economou C, Turpin SM, Matzaris M, Hoehn KL, Hevener AL, James DE, Duh EJ, Watt MJ Cell Metabolism 10:1 40-47, 2009.

Summary

Obesity is a major risk factor for insulin resistance; however, the factors linking these disorders are not well defined. Here, it is shown that the non-inhibitory serine protease inhibitor, pigment epithelium derived factor (PEDF), plays a causal role in insulin resistance. Adipocyte PEDF expression and serum levels are elevated in several rodent models of obesity and reduced upon weight loss and insulin sensitization. Lean mice injected with recombinant PEDF exhibited reduced insulin sensitivity during hyperinsulinemic-euglycemic clamps. Acute PEDF administration activated the pro-inflammatory serine/threonine kinases c-Jun terminal kinase and extracellular regulated kinase in both muscle and liver, which corresponded with reduced insulin signal transduction. Prolonged PEDF administration stimulated adipose tissue lipolysis, resulted in ectopic lipid deposition and reduced insulin sensitivity, while neutralizing PEDF in obese mice enhanced insulin sensitivity. Overall, these results identify a causal role for PEDF in obesity-induced insulin resistance.

Introduction

The increased prevalence of obesity in industrialized countries is closely associated with the development of chronic diseases including atherosclerosis, non-alcoholic fatty liver disease, dyslipidemia and type 2 diabetes (Wellen and Hotamisligil 2005). Insulin resistance is a central feature of the pathophysiology of most obesity-related disorders including type 2 diabetes, and is defined as a subnormal response of tissues to the actions of insulin. Several possible mediators of insulin resistance in obesity, including dysregulation of lipid metabolism (Savage, Petersen et al. 2007) and low grade inflammation (Wellen and Hotamisligil 2005), have been identified. However, the mechanistic link between these parameters is not understood.

Adipocytes are known to regulate whole body metabolism, at least in part via the release of secretory or endocrine factors such as leptin (Halaas, Gajiwala et al. 1995) and adiponectin (Maeda, Shimomura et al. 2002). Modifications in the secretion of several adipocyte secreted factors contributes to dysregulation of metabolism either via central or peripheral effects (Rosen and Spiegelman 2006). This has led to major investigation of adipose secretory factors in the hope of identifying other regulatory molecules that might play other, as yet unidentified roles, in whole body metabolism. One of the limitations with many studies in this area is that the contribution of adipose tissue secretion to circulating levels of such factors is not clear and in some cases it remains controversial if adipocytes *per se* are the source of the secretory factor, as opposed to non-parenchymal cells such as endothelial cells.

In the present studies the serine protease inhibitor (serpin), pigment epithelium-derived factor (PEDF, SerpinF1) was identified as a *bona fide* adipocyte secretory factor. This is an exciting observation as circulating PEDF was recently found to be upregulated in individuals with the metabolic syndrome (Yamagishi, Adachi et al. 2006) and patients with type 2 diabetes mellitus (Ogata, Matsuoka et al. 2007; Jenkins, Zhang et al. 2008). PEDF is a multifunctional protein that promotes neuronal survival and differentiation and possesses anti-angiogenic activities (Tombran-Tink and Barnstable 2003). It is a unique serpin because its c-reactive loop is inactive and is thereby non-inhibitory, meaning that it does not directly inhibit serine proteases or other serpin targets such as caspases. In this way, PEDF may provide a link between obesity and insulin resistance. Using a range of physiological methods strong evidence is provided in favour of this claim.

Methods

Animal maintenance and experimental protocols

Experimental procedures were approved by the St. Vincent's Hospital Animal Experimentation Ethics Committee, the School of Biomedical Sciences Animal Ethics Committee (Monash University) and the Committee on Animal Research at the University of California, Los Angeles. Eight-week old male C57Bl/6J mice (Monash Animal Services, Victoria, Australia) were fed a standard chow diet for 4 weeks or a high-fat diet (60% calories from fat) for 16 weeks. Mice were fasted for 4 h prior to all experiments. Metabolic monitoring was performed in a Comprehensive Lab Animal Monitoring System (Columbus Instruments, OH, USA). For *ex vivo* experiments, mice were anaesthetized by intraperitoneal injection of sodium pentobarbital (60 mg/kg body mass). Either the soleus and extensor digitorum longus (EDL) muscles were dissected and placed in oxygenated Krebs buffer. Epidydimal fat was removed, rinsed in 0.9% saline, dissected into 30 mg pieces and transferred to oxygenated Krebs buffer for lipolysis experiments. Animals were sacrificed by lethal injection of sodium pentobarbital. For insulin tolerance tests (ITT), mice were injected IP with 50 µg PEDF or 0.9% saline and 2 h later with insulin (0.5 units/kg; Actrapid, Novo Nordisk, Bagsværd, Denmark). Tail blood was collected at 15 min intervals for 90 min and blood glucose was determined using a glucometer (Accu-Chek, Roche). For glucose tolerance tests, mice were injected with 1 g D-glucose / kg body mass and blood glucose assessed. For neutralization experiments, a micro-osmotic pump (Alzet, Cupertino, CA) filled with PEDF antibody or heat-inactivated antibody was inserted subcutaneously between the scapula of anaesthetized mice. Pumps were left for 5 days before experiments. For prolonged PEDF administration studies, PEDF was loaded into mini-osmotic

pumps and infused for 5 days as described (Apte, Barreiro et al. 2004). The CNTF and calorie restriction studies are described elsewhere (Crowe, Turpin et al. 2008).

Hyperinsulinemic-euglycemic clamps

Glucose clamp studies were performed in chronically cannulated mice 3 days after surgery as previously described (Hevener, He et al. 2003). A basal blood sample was taken at –90 minutes and measured for glucose. Following this, a primed constant infusion of 5.0 μCi/h, 0.12 ml/h of [3-^{3}H]d-glucose (NEN Life Science Products) was initiated. At time 0, a basal blood sample was drawn for determination of glucose-specific activity. Following basal sampling, glucose (50% dextrose; Abbott) and insulin (10 mU/kg/min; Novo Nordisk) plus tracer (5.0 μCi/h) infusions were initiated simultaneously, and glucose levels clamped at euglycemia using a variable glucose infusion rate (GIR). Steady state was achieved when blood glucose was successfully clamped and the GIR fixed for a minimum of 30 minutes. At the end of the clamp, a blood sample was taken at 100 and 120 minutes for the determination of tracer-specific activity. At steady state, the rate of glucose disappearance or the total GDR is equal to the sum of the rate of endogenous HGP plus the exogenous (cold) GIR. The IS-GDR is equal to the total GDR minus the basal glucose turnover rate.

Glucose uptake

Myotubes or isolated EDL muscles were pre-treated with 100 nM PEDF or an equal volume of PBS for 2 h. 2-Deoxy-D-glucose (2DG) uptake was measured by adding 2-Deoxy-D-[1,^{3}H] glucose (1 mM, 0.5 μCi /ml) and D-[1-^{14}C]mannitol (8 mM, 0.2 μCi /ml) (Amersham

Biosciences) to Krebs buffer containing 0.1% BSA. Cells were treated with PBS (basal) or 10 nM insulin and 2DG uptake was measured over 20 min for cells and 10 min for isolated muscles. Cells or muscles were washed three times in ice-cold PBS and lysed. Radioactivity in the supernatant was measured using liquid scintillation counting and 2DG uptake was normalised to protein content (BCA kit, Pierce, Progen Industries, Darra, QLD, Australia)

Cell Culture

L6 myoblasts were maintained at 37°C (90% O_2 / 10% CO_2) in low glucose Dulbecco's modified Eagle's medium (DMEM) containing 10% fetal bovine serum (FBS) culture media and 1% penicillin/ streptomycin. Differentiation was induced by switching to media containing 2% FBS when the myoblasts were ~90% confluent. Experimental treatments were started after 6 days. 3T3-L1 adipocytes were generated by growing preadipocytes until 90% confluent in DMEM supplemented with 10% FBS, 1% penicillin/ streptomycin. Cells were differentiated as described (Watt, Holmes et al. 2006). All cells were serum starved for 16 h prior to experiments.

Conditioned Media experiments

Conditioned media was collected from adipocytes, sterile filtered (0.45 µm) and transferred to plates containing L6 myotubes. PEDF-neutralizing antibody was added to conditioned media at 2.0 µg/ml. Cells were incubated for 24 h prior to 2DG determination.

Production of recombinant PEDF

Recombinant PEDF was purified from a HEK293 cell line stably transfected with human PEDF (Duh, Yang et al. 2002) and bioactivity was assessed by proliferation assay of SaOS-2 osteosarcoma cells.

Lipolysis

3T3-L1 adipocytes or isolated epididymal fat (30 mg) were incubated in Krebs buffer, 4% BSA, 8 mM glucose for 2 h. PEDF (100 nM) or isoproterenol (1 μM) were added as indicated.

ConA affinity chromatography

In each experiment, a minimum of six 10 cm dishes of mature 3T3-L1 adipocytes were washed three times in PBS, once in serum free DMEM, and left overnight in 8 ml serum free DMEM supplemented with 100 nM insulin for maintenance of protein synthesis and secretion. Conditioned medium was collected, pooled, and dialysed overnight with a 3,000 MW cut-off membrane against ConA binding buffer (0.5 M NaCl, 0.1 M Tris HCl, 1 mM MnCl2, 1 mM CaCl2, pH 7.4) at 4^{o}C. Concanavalin A sepharose 4B (GE Healthcare 17-0440-03) was added and left to mix overnight at 4^{o}C for batch format affinity chromatography. Sepharose beads were washed five times by centrifugation and addition of 50 mL Con A binding buffer. Glycoproteins were specifically eluted by addition of elution buffer (0.5 M NaCl, 0.1 M Tris HCl, 10 mM EDTA, 10 mM EGTA, 0.3M methyl α-D-mannopyranoside), and mixing overnight at 4^{o} C. Proteins were precipitated by chloroform methanol precipitation, resuspended in Laemmle buffer, and separated out onto a 10% SDS-PAGE gel.

Mass spectrometry

Following ConA affinity purification, SDS-PAGE and staining of samples, lanes were excised, and cut into equal sized slices (10-16 per lane). Gel slices were diced into 1 mM cubes and dehydrated by addition of 1 mL acetonitrile for 20 min. Acetonitrile was removed, 30-50 µL 12.5 ng/µL sequencing grade trypsin (Promega) in 100 mM NH_4CO_3 added, and left to incubate at 37^{o}C overnight. To remove digested peptides from gel, 100 µL 5% formic acid was added, incubated for 2 h, 100 µL acetonitrile added, incubated for two hours, and 400 µL acetonitrile added for 10 min. The combined solution was collected and evaporated to yield peptides, which were resuspended in 5% formic acid. Peptides were separated by liquid chromatography, and subjected to tandem mass spectrometry on a Waters Ultima quadrupole time of flight (QTOF) mass spectrometer, as described previously (Larance, Ramm et al. 2005). Mascot Daemon was used to search spectra using the NCBI protein database, with taxonomy restricted to proteins from *Mus musculus*.

Cell fractionation

Four ten centimetre dishes of mature 3T3-L1 adipocytes were washed three times in HES buffer (250 mM sucrose, 20 mM HEPES, 1 mM EDTA, pH 7.4), and scraped down in 1 ml HES buffer with protease inhibitor (Complete Protease Inhibitor, Roche) and phosphatase inhibitors (2 mM sodium orthovanadate, 1mM ammonium molybdate, 1 mM sodium pyrophosphate and 10 mM sodium fluoride.) Cells were passed ten times through a 22G syringe, and then ten times through a 27 ½ G syringe. Lysates were centrifuged at 2500 g for 10 minutes to pellet unbroken cells. Supernatant was then centrifuged at 12,000 g for 12 minutes to pellet plasma membrane, nuclei

and mitochondria. Supernatant was retained as whole cells minus plasma membrane, and pellet was resuspended in 1 ml HES plus inhibitors. Resuspended pellets were layered onto 9 ml sucrose in HES with inhibitors. Samples were centrifuged at 50,000 g for 1 hr, and the upper layer was collected as plasma membrane. Plasma membrane was washed of high sucrose buffer by resuspension in 5ml HES buffer with inhibitors and centrifugation at 12,000 for 12 minutes. Pellet was resuspended in 1 ml HES. Plasma membrane and whole cell minus plasma membrane were assayed for protein using the BCA method, and equal amounts of protein loaded.

Immunofluorescent analysis

3T3-L1 adipocytes were fixed for 30 minutes with 3% paraformaldehyde in PBS, and quenched with 50 mM glycine in PBS for 20 min. Cells were blocked and permeabilised in blocking buffer (2% BSA, 0.1% saponin in PBS), and incubated for one hour in primary antibodies. These were EEA1 human polyclonal antibody (gift from Marvin Fritzler), gm130 mouse monoclonal antibody (BD Transduction Laboratories 610823) and ATGL rabbit polyclonal human antibody, all diluted 1:100. Cells were washed and incubated in secondary antibodies for one hour. Secondary antibodies were Cy3 conjugated donkey anti-rabbit, Cy5 conjugated donkey anti-mouse, and Cy2 conjugated donkey anti-human. Microscopy was performed using a Leica DMR confocal. Images were overlaid using MacBiophotonics ImageJ version 1.41.

Muscle lipids

Muscle lipids were extracted in chloroform : methanol. TG was assessed by measuring glycerol after saponification and DG and ceramide were measured by a radiometric method as described (Watt, Holmes et al. 2006).

qRT-PCR

Total RNA was extracted, reverse transcribed and quantitative PCR was performed as described (Steinberg, Kemp et al. 2007). PEDF and 18S primers were purchased from Applied Biosystems.

Plasma hormone and metabolite analysis

PEDF was analyzed by ELISA for mouse PEDF (Chemicon, Temecula, CA). Plasma glucose was assessed by a glucose oxidase method (Sigma), FFA by an enzymatic colorimetric method (Wako) and insulin by RIA.

Statistical analysis

Statistical analysis was performed using unpaired Student's t-test. A two-way ANOVA with repeated measures was applied where appropriate and a Student Newman-Keuls post hoc analysis performed. Statistical significance was set at $P<0.05$.

Immunoblot analysis

Immunoblotting was performed antibodies against IRS1, IRS-1 Y20, Akt, Akt S473, Akt T308, phosphor- and total ERK1/2, JNK1/2 and IKK-β from Cell Signaling (Danvers, MA, USA), α-actin (Sigma), tubulin (Sigma T9026), IRS1 Y612 (Biosource, Carlsbad, CA, USA) and PEDF (Duh, Yang et al. 2002). Cells lysates normalized for protein concentration (bicinchoninic acid method, Pierce Kit, Progen Industries, Darra, QLD, Australia) were solubilised in Laemmeli sample buffer and boiled for 5 min, resolved by SDS-PAGE on 8-14% polyacrylamide gels, transferred to a PVDF membrane, blocked with 5% milk for 1 h and probed with the appropriate polyclonal primary antibody overnight at $4^{o}C$. After washing and incubation with horseradish peroxidase-conjugated secondary antibody (Amersham Biosciences, Castle Hill, NSW, Australia), the immunoreactive proteins were detected with enhanced chemiluminescence and quantified by densitometry (Scion Image, Frederick, Maryland). For secreted PEDF analysis, 15 ul of Krebs was solubilized and loaded for SDS.

Results

Identification of the adipocyte secretome by mass spectrometry

Previous efforts to identify the secretome of adipocytes have included the use of a signal sequence trap cloning procedure and proteomics. In the case of proteomics, media is usually collected from cells grown in culture; proteins are concentrated and then sequenced using mass spectrometry. A major limitation is the presence of contaminants in the media due to cell surface shedding or cellular lysis and release of intracellular content. To circumvent these limitations, a lectin affinity chromatography step to enrich for glycoproteins prior to mass spectrometry was implemented on the assumption that many, but not all, secretory proteins undergo complex N-linked glycosylation prior to release. Using this method conditioned media from 3T3-L1 adipocytes was screened. One of the most abundant proteins identified in this screen based upon peptide coverage in the mass spectrum (20.6% of the full length protein detected) was PEDF. While PEDF has been implicated as an important metabolic regulatory secretory factor little is known of its mechanism of action.

Adipose tissue and plasma PEDF levels are elevated in obesity

Initially, plasma PEDF levels in obesity were examined. Mice were fed a low-fat (Chow: 4% fat) or high-fat (HFD: 60% fat) diet for 12 wks. The high fat diet resulted in elevated body mass (Chow: 28.9 ± 0.6 g vs. HFD: 35.8 ± 1.2 g) and adipose tissue mass (epididymal fat pad, Chow: 335 ± 29 mg vs. HFD 1439 ± 192 mg). Mice fed a HFD were mildly hyperglycaemic (blood glucose: Chow, 8.8 ± 0.4 mM vs. HFD, 10.2 ± 0.9 mM) and hyperinsulinemic (plasma insulin:

Chow, 49 ± 6 pM vs. HFD, 107 ± 21 pM), suggestive of insulin resistance. The plasma PEDF concentration averaged 4.9 ± 1.6 ng/ml for Chow and was increased 3.2-fold by HFD (Fig. 1A). A similar increase in the PEDF mRNA (Fig. 1B) and protein expression levels (Fig. 1C) in adipose tissue was also observed in HFD mice. PEDF expression was increased in both the adipocyte and stromal vascular fraction of adipose tissue (Fig 1B), and most of the whole tissue increase was attributable to enhanced adipocyte expression. *Ex vivo* analysis revealed that adipose tissue PEDF secretion was greater in obese versus lean mice (Fig. 1D), supporting a link between adipose tissue PEDF production and plasma levels. While PEDF was readily detected as an adipose secretory factor, only modest PEDF secretion was detected in cultured hepatocytes and myocytes and in whole mouse liver and skeletal muscle incubated *ex vivo* for 5 h in oxygenated Krebs buffer (data not shown). This is intriguing because this pattern does not correspond to the relative tissue specific expression profile of PEDF (Fig. 2). This suggests that adipocytes likely make an important contribution to circulating levels of this factor. The level of the PEDF mRNA and protein was also increased in the adipose tissue of obese, leptin deficient *ob/ob* mice compared with lean littermate controls (Fig. 1E and 1F). There was no striking effect of obesity on skeletal muscle or liver PEDF expression (Fig. 3). The effects of weight loss on adipose PEDF expression in obese mice using either caloric restriction or ciliary neurotrophic factor administration were assessed as described previously (Crowe, Turpin et al. 2008). PEDF mRNA expression was decreased by 2.1 and 5.4-fold, respectively, compared with mice fed a HFD (Fig. 1G). Together, these data show that circulating levels of PEDF as well as its expression in adipose tissue correlates very well with whole body adiposity and insulin sensitivity.

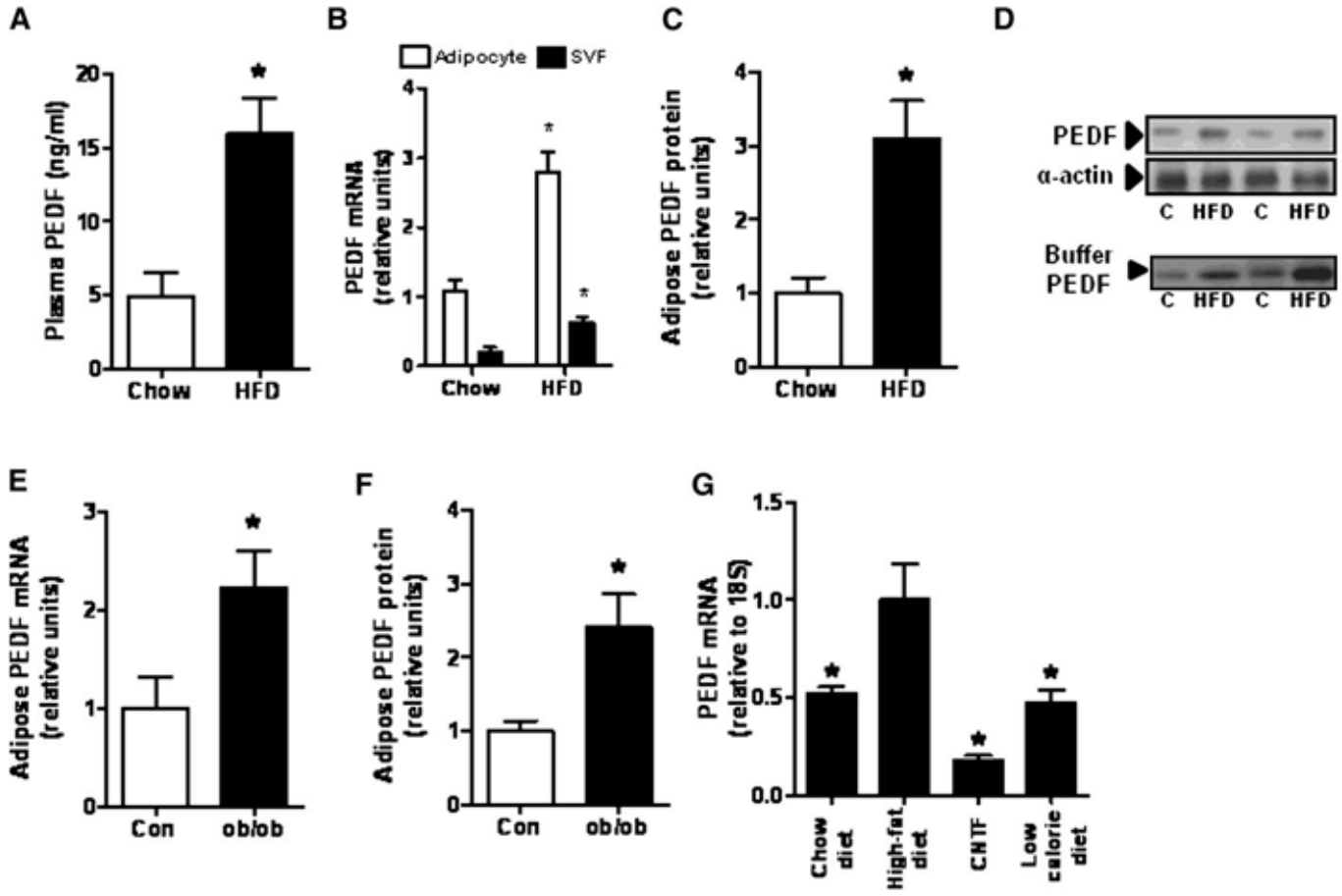

Figure 1. PEDF is elevated in obesity and reduced by weight loss. (A) Plasma PEDF concentrations in mice fed a control (chow) and high-fat diet (HFD) for 12 weeks. (B–D) PEDF mRNA in the adipocyte and stomal vascular fraction (SVF), (C) PEDF protein expression, and (D) PEDF release from epididymal adipose tissue of mice after chow and HFD. (E and F) PEDF mRNA and (F) protein in obese *ob/ob* mice and lean littermates. (G) PEDF mRNA content in mice fed a HFD or mice that lost ~15% of their body mass by 7 day ciliary neurotrophic factor (CNTF) administration or caloric restriction (low-calorie diet). n = 8 mice for all groups; error bars are ± SEM; $^{*}p < 0.05$ versus group with open bars.

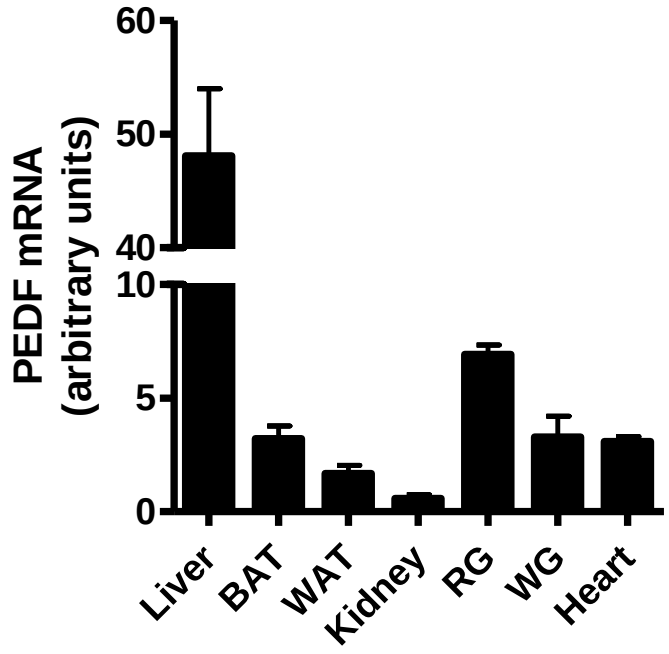

Figure 2. PEDF expression in mouse tissues. Tissues were excised from 16 week old mice fed a chow diet after a 4 h fast. Tissues were dissected and analysed from PEDF mRNA (D) (n=5 animals per group).

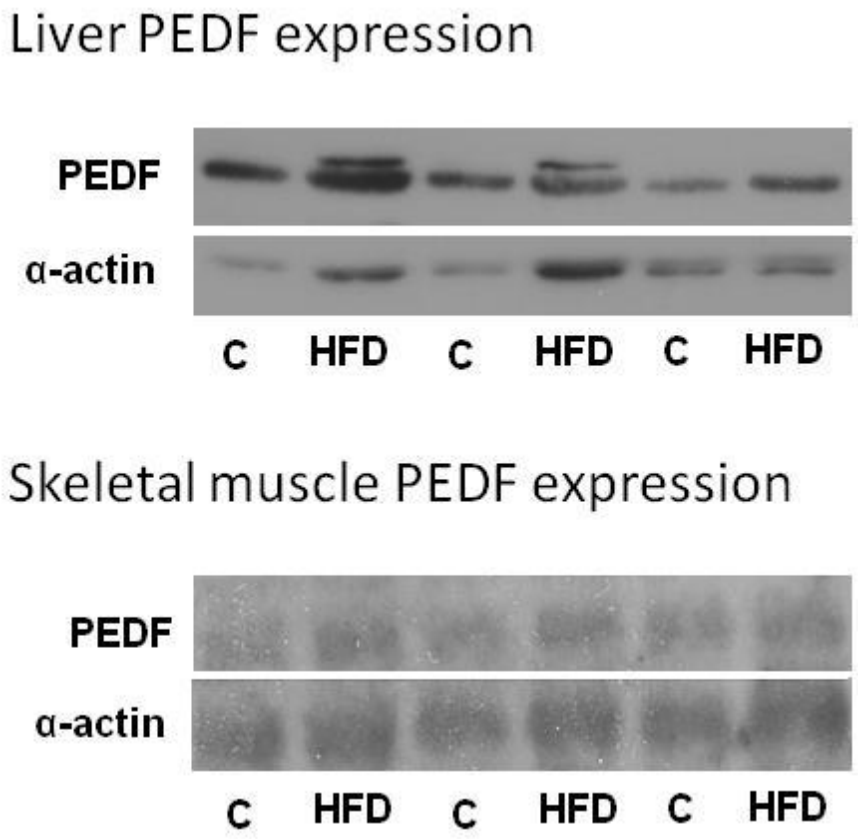

Figure 3. PEDF expression in mice fed a control (Chow) and high-fat diet (HFD) for 12 weeks. There was no striking effect of obesity on skeletal muscle or liver PEDF expression in lysates.

PEDF regulates glucose metabolism in skeletal muscle and liver

To determine whether PEDF directly regulates skeletal muscle insulin sensitivity, isolated EDL muscles from lean mice were treated with recombinant PEDF for 2 h and assessed 2-Deoxy-glucose (2DG) uptake. PEDF did not affect basal 2DG uptake but reduced insulin-stimulated 2DG disposal by ~30% (Fig. 4A). The specific effect of PEDF on skeletal muscle glucose uptake was also verified in L6 myotubes (Fig. 5) and was maintained for 24 h (data not shown). To test whether these effects could be recapitulated *in vivo*, lean mice were injected with 50 µg PEDF for 2 h prior to an insulin tolerance test (ITT), resulting in an increase in circulating PEDF levels from 3.8 ± 1.2 ng/ml to 12.4 ± 3.1 ng/ml (Fig. 4B). These levels are similar to those observed in lean and obese mice, respectively (Fig. 1A). There was no change in basal plasma glucose concentration following PEDF injection (Saline: 6.9 ± 0.7 mM, PEDF: 7.6 ± 0.5 mM, P=0.45) whereas whole body insulin sensitivity was decreased (Fig. 4C). Mice pre-treated with PEDF also displayed impaired glucose tolerance (Fig. 4D), independent of changes in plasma insulin levels (Table 1). These effects of PEDF raise the possibility that obesity-associated elevations in PEDF might play a role in insulin resistance.

To investigate this further and quantitatively examine the contribution of liver and skeletal muscle to PEDF-induced insulin resistance, lean mice were injected with PEDF 2.5 h prior to hyperinsulinemic-euglycemic clamps. There were no differences in basal glucose turnover between vehicle (24 ± 1.6 mg/kg/min) or PEDF (23 ± 0.8 mg/kg/min) treated mice; however, the amount of exogenous glucose required to maintain euglycemia during insulin stimulation was significantly diminished with prior PEDF administration, indicating whole body insulin resistance (Fig. 2E). The insulin-stimulated glucose disposal rate, primarily reflecting skeletal

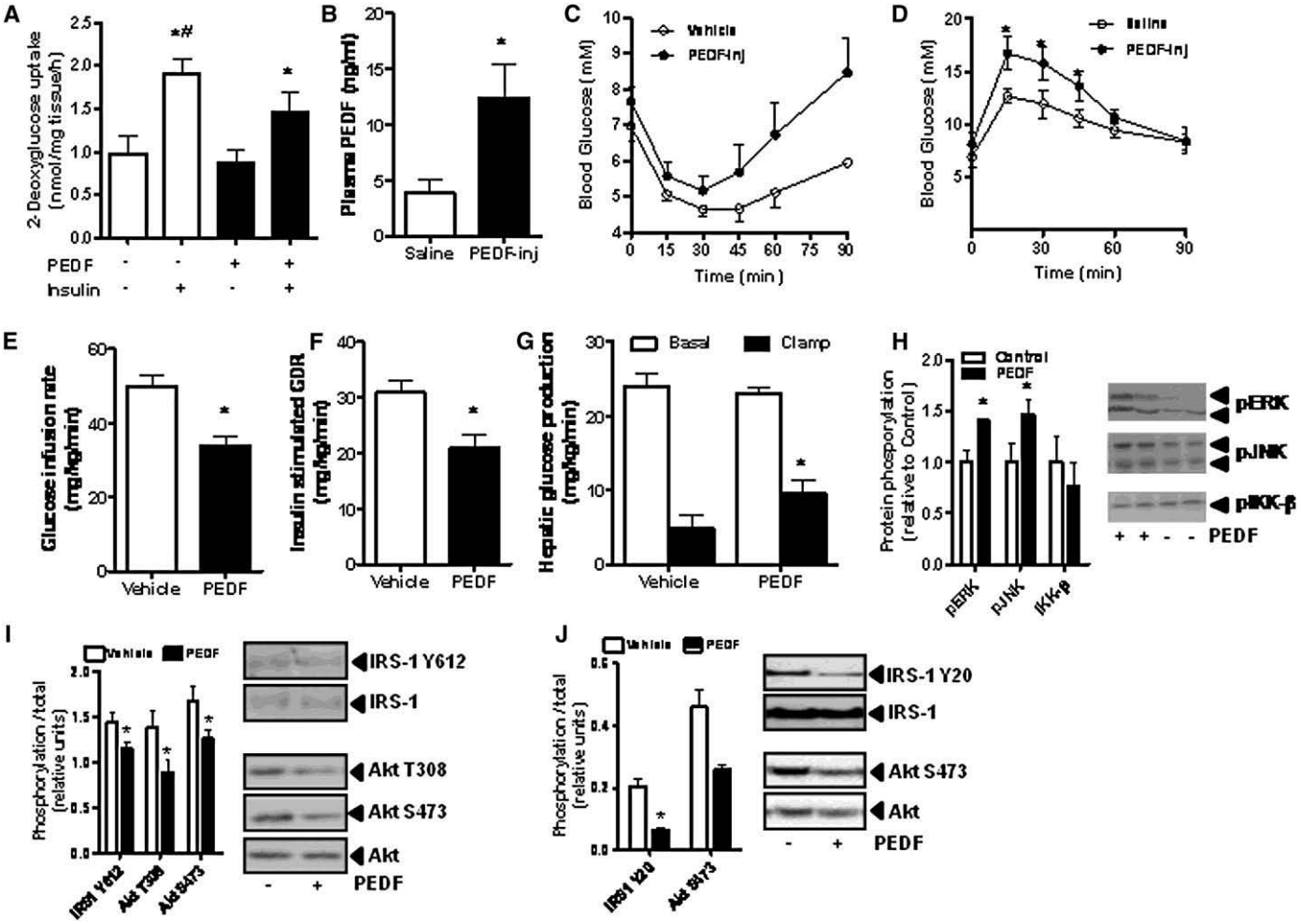

Figure 4. Acute PEDF administration causes insulin resistance in skeletal muscle and liver (A) 2-deoxyglucose uptake experiments in EDL muscles isolated from C57Bl/6 mice. Muscles were pretreated without (open bars) or with (closed bars) 100 nM PEDF for 2 hr. The media was removed and basal and insulin stimulated 2DG uptake determined. n = 8 EDL muscles from independent mice for each group. $^{*}p < 0.05$ versus basal within the same treatment; #$p < 0.05$ versus PEDF insulin treatment. Values are means ± SEM. (B) Plasma PEDF concentrations 2 hr after C57Bl/6 mice were injected with saline (open bars) or PEDF (closed bars) in the intraperotineal cavity. $^{*}p < 0.05$ versus saline; n = 8 mice for each group. (C and D) Insulin tolerance tests and (D) glucose tolerance tests 2 hr after C57Bl/6 mice were injected with saline (open bars) or PEDF (closed bars) in the intraperotineal cavity. n = 6 mice for each group; $^{*}p < 0.05$ versus saline. (E–G) Direct measures of insulin sensitivity by hyperinsulinemic-euglycemic clamp after PEDF injection. Lean C57Bl/6 mice aged 10 weeks were injected with PEDF 2.5 h prior to clamps where whole-body glucose infusion rate (E), glucose disposal rate (F), and hepatic glucose production (G) were determined. $^{*}p < 0.05$ versus vehicle; n = 8 mice for each group. (H) Phosphorylation of the serine/threonine kinases ERK, JNK, and IKK-β in skeletal muscle at the end of the hyperinsulinemic-euglycemic clamp. (n = 8 per group); $^{*}p < 0.05$ versus vehicle. (I and J) Insulin signaling in muscle (I) and liver (J) at the end of the hyperinsulinemic-euglycemic clamp. n = 8 per group; $^{*}p < 0.05$ versus vehicle; error bars are ± SEM.

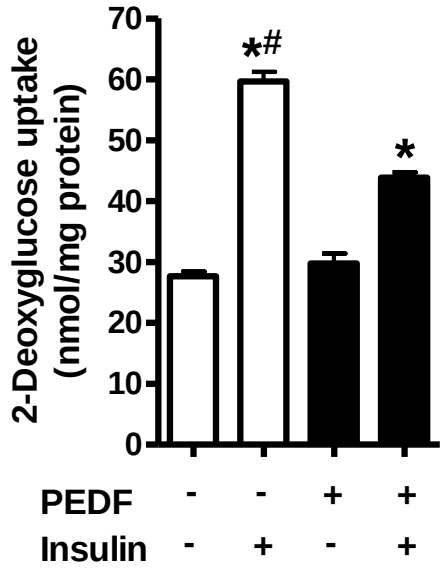

Figure 5. 2-Deoxyglucose uptake experiments in L6 myotubes. Cells were pre-treated without (open bars) or with (closed bars) 100 nM PEDF for 2 h. The media was removed and basal and insulin stimulated 2DG uptake determined. *n*=12 for each group where each experiment was performed in triplicate on 4 occasions. *p<0.05 vs. basal within the same treatment, #p<0.05 vs. PEDF insulin treatment.

	Vehicle	**PEDF**
Basal	0.51 ± 0.13	0.77 ± 0.10
GTT insulin- 15 min	1.12 ± 0.13	1.13 ± 0.05

Table 1. Plasma insulin 2 h after PEDF administration and during a glucose tolerance test (GTT). Units are ng/ml. Values are mean ± SEM (n=4 mice per group).

muscle glucose disposal, was decreased with PEDF (Fig. 4F). In addition, suppression of hepatic glucose production was blunted in PEDF treated animals (Fig. 4G), as indicated by the increased rate of glucose production by the liver during the clamp. It is unlikely that these effects are due to changes in insulin secretion as plasma insulin levels were identical between PEDF treated and control mice during the hyperinsulinemic clamps. Moreover, basal plasma insulin levels were not different 2 h after PEDF injection or following a glucose load (Table 1).

PEDF induces proinflammatory signaling and impairs insulin signalling

The next stage of this investigation was to identify the mechanism for PEDF-induced insulin resistance. PEDF induces proinflammatory signaling in several cell types (Tombran-Tink and Barnstable 2003), which is of interest in view of the possible role of inflammation in insulin resistance (Aguirre, Uchida et al. 2000; Gao, Hwang et al. 2002; Bost, Aouadi et al. 2005). PEDF was associated with an increase in phospho ERK and phospho JNK in skeletal muscle (Fig. 4H) and liver (Fig. 4I), concomitant with a reduction in the insulin-dependent activation of insulin receptor substrate-1 and Akt, as indicated by reduced phosphorylation at their activating sites (Fig. 4J and 4K) during the hyperinsulinemic-euglycemic clamp studies. Similar effects were observed in cultured myotubes (Fig. 6).

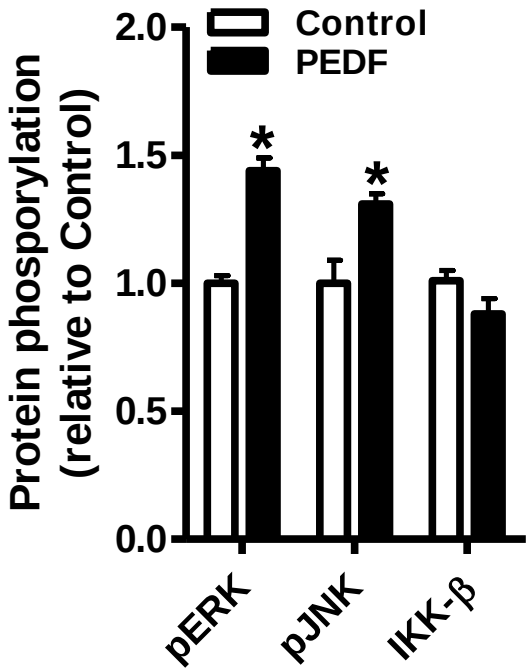

Figure 6. A direct effect of PEDF on serine/threonine signalling was demonstrated in cultured myotubes. PEDF administration to L6 myotubes causes phosphorylation of ERK1/2 and JNK1/2 on their activating sites. IKK-β phosphorylation was unaffected (n=6 per group). *$p<0.05$ vs. control.

Prolonged PEDF administration in lean mice causes ectopic lipid deposition and insulin resistance

To explore the effect of prolonged PEDF administration *in vivo*, mini-osmotic pumps were surgically implanted into lean C57Bl/6 mice. PEDF was continuously infused for 5 days as validated and described previously (Apte, Barreiro et al. 2004). Fasting plasma glucose and insulin were unaffected by PEDF (Fig. 7A and 7B), whereas whole body insulin sensitivity (Fig. 7C) and insulin-stimulated glucose uptake into skeletal muscle were reduced (Fig. 7D). Obesity is characterized by excessive basal adipose tissue lipolysis and increased post-absorptive circulating fatty acid levels (Wolfe, Peters et al. 1987; Horowitz, Coppack et al. 1999), that in turn contribute to the development of ectopic lipid deposition and insulin resistance (Boden and Chen 1995; Boden, Chen et al. 1995). The role of PEDF in lipid metabolism was explored by examining its effects on adipose tissue lipolysis. As shown in Fig. 8A, PEDF acutely increased lipolysis in cultured 3T3-L1 adipocytes and in mice *in vivo* as assessed by plasma glycerol and FFA levels (by-products of triglyceride lipolysis) (Fig. 6b). Plasma FFA levels were increased following prolonged *in vivo* PEDF administration (15%, P=0.13, Fig. 7E) coupled with an increase in muscle lipid storage (Fig. 7F and 7G). Liver TG was elevated by 66% in animals treated with PEDF (Fig 7H). Together, these data support two possible mechanisms for PEDF-induced insulin resistance, via stress signalling events in the short-term (Fig.s 4A-J) and via lipid deposition in skeletal muscle and liver in the longer-term.

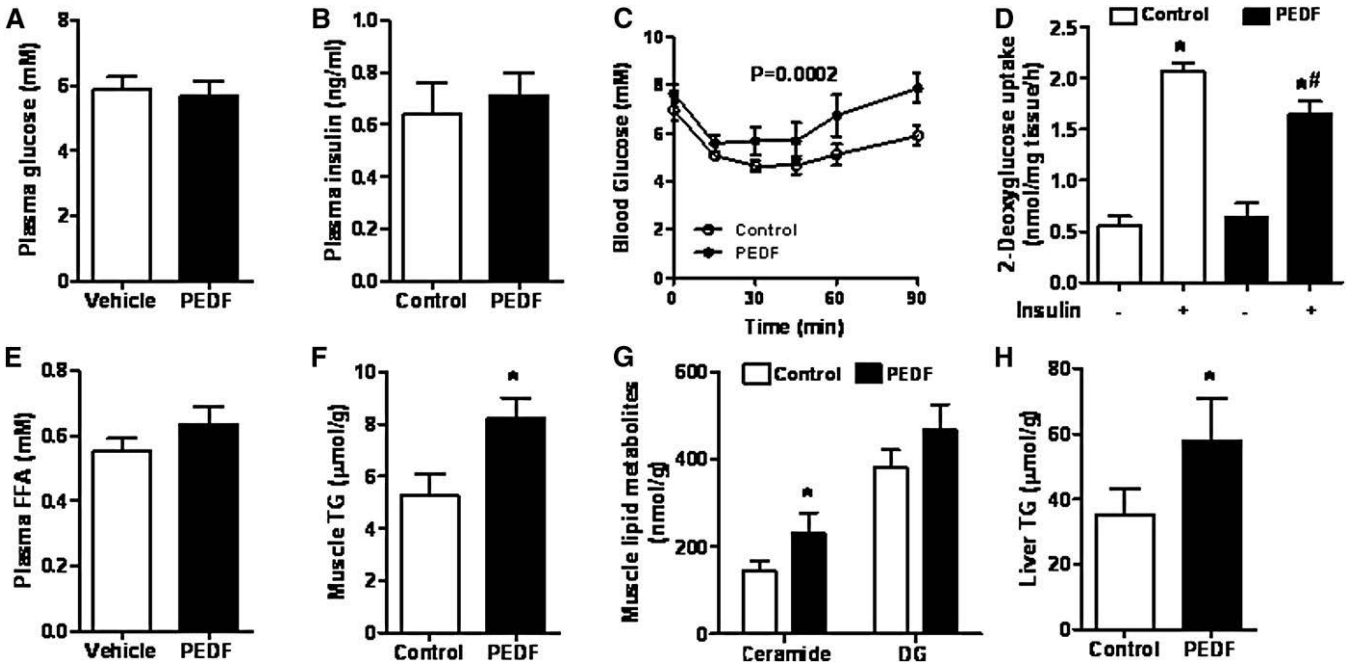

Figure 7. Prolonged PEDF administration mediates insulin resistance in lean mice. (A and B) Lean C57bl/6 mice were continuous infused with recombinant PEDF (closed bars) or sterile saline (open bars) for 5 days. Plasma glucose (A) and insulin (B) were assessed in 4 hr fasted mice. (C) Whole-body insulin sensitivity was assessed by ITT. (D) Skeletal muscle 2DG uptake was assessed in EDL muscle ex vivo with or without the addition of 10 nM insulin. $^{*}p < 0.05$ versus basal; #p < 0.05 versus control insulin. (E) Plasma FFA were assessed in 4 hr fasted mice. (F and G) Skeletal muscle was removed and triglyceride (TG), diglyceride (DG) and ceramide assessed. (H) Liver TG. $^{*}p < 0.05$ versus control. For all experiments, n = 6 mice per group. Error bars are ± SEM.

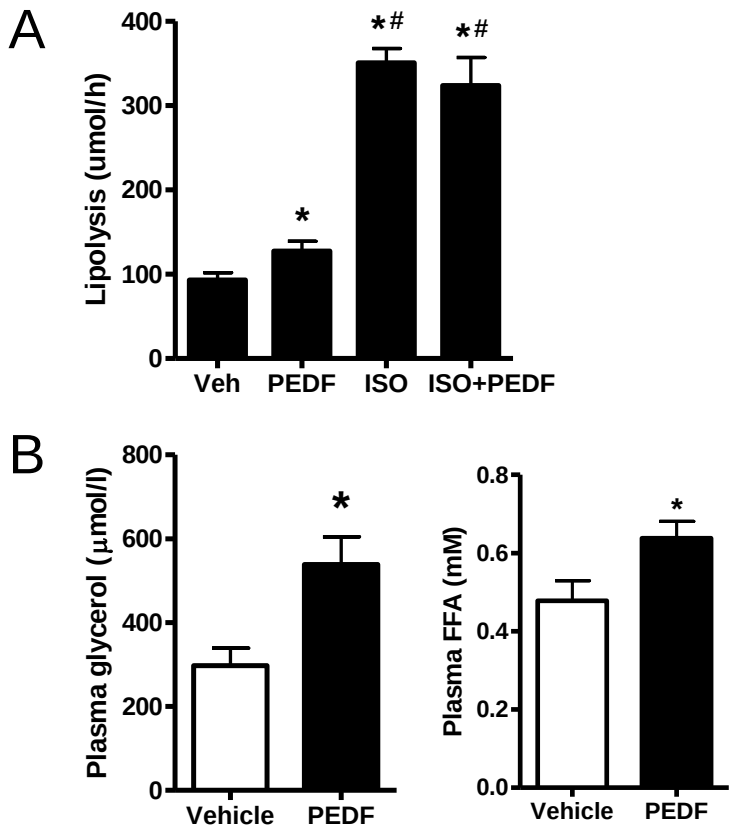

Figure 8. PEDF causes adipose tissue lipolysis. (A) Lipolysis was assessed as glycerol release in 3T3-L1 adipocytes. Cells were incubated without (Veh) or with PEDF (100 nM). Isoproterenol (ISO, 1 µM) was used for maximal lipolytic stimulation. (n=8 per group where experiments were performed on 3 independent occasions, * P<0.05 vs. Vehicle, # P<0.05 vs. PEDF). (B) *In vivo* lipolysis is increased by PEDF. Lean C57Bl/6 mice were injected with PEDF IP and blood was obtained after 30 min. Glycerol and FFA was assessed in the plasma. (*n=6* individual mice per group, * P<0.05 vs. Vehicle).

PEDF neutralization in obese, insulin resistant mice improves insulin sensitivity

It was next tested whether blocking PEDF action could restore insulin sensitivity in obese mice. Mini-osmotic pumps were implanted into obese C57Bl/6 mice (mass: 36.1 ± 0.5 g) and neutralizing PEDF antibody or control solution was continuously infused for 5 d (Apte, Barreiro et al. 2004). The PEDF neutralizing antibody did not affect fasting blood glucose (Fig. 9A) and insulin levels (Fig. 9B) but did improve whole-body insulin sensitivity in these obese mice (Fig. 9C), independent of changes in body mass and adiposity (Table 2). Consistent with this notion, parallel studies in cultured myotubes showed that adipocyte conditioned media containing PEDF caused insulin resistance, whereas co-incubation with the PEDF neutralizing antibody largely restored insulin action (Fig. 10). Sequestering fatty acids in adipocytes and/or reducing adipose tissue lipolysis reduces fatty acid delivery to non-adipose tissues such as skeletal muscle and liver, thereby limiting the progression of insulin resistance (Unger 2003; Bajaj, Suraamornkul et al. 2005). It is believed that this effect is mediated, in part, by minimizing the accumulation of bioactive lipid metabolites known to cause insulin resistance (Yu, Chen et al. 2002; Holland, Brozinick et al. 2007). Plasma FFA was reduced with PEDF antibody administration (Fig. 9D), suggesting an inhibition of adipose tissue lipolysis. Skeletal muscle triacylglycerol and diacylglycerol contents were reduced with PEDF antibody administration (Fig. 9E and 9F). Furthermore, liver triacylglycerol (Fig. 9I), diacylglycerol and ceramide (Fig. 11) levels were also reduced with PEDF neutralizing antibody treatment. These data demonstrate that reducing PEDF action *in vivo* restores insulin action in the context of obesity. The reduction in circulating FFA, and muscle and liver lipid accumulation may have been one mechanism underlying this insulin sensitizing effect of PEDF neutralization obesity.

	Vehicle	**PEDF-Ab**
Body (g)	36.0 ± 0.5	36.2 ± 0.5
Epididymal fat (mg)	732 ± 121	656 ± 84
Retroperitoneal fat (mg)	215 ± 56	226 ± 31
Liver (g)	1.32 ± 0.12	1.25 ± 0.11

Table 2. Body mass and tissue mass following 5 days PEDF neutralization. Values are mean ± SEM (n=6 mice per group)

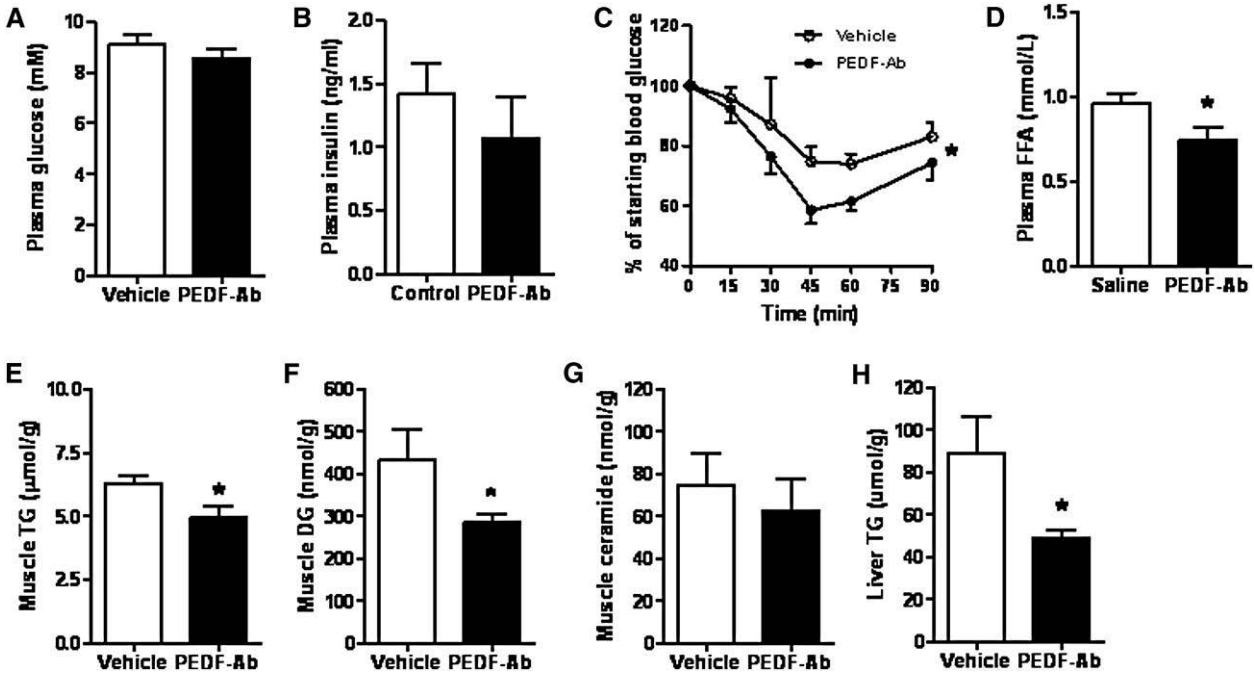

Figure 9. PEDF neutralization in obese, insulin-resistant mice improves insulin sensitivity. (A–D) Miniosmotic pumps were placed in obese mice and saline or PEDF-neutralizing antibody was infused for 5 days. Plasma glucose (A), insulin (B), and FFA (D) were assessed in 4 hr fasted mice. In (C), mice were fasted for 4 hr and insulin tolerance tests were performed. n = 6 mice per group; $^{*}p < 0.05$ main effect for treatment. (E–H) Skeletal muscle and liver lipids are decreased with PEDF neutralizing antibody treatment. Skeletal muscle triglyceride (E; TG), diglyceride (F; DG), and ceramide (G), and liver TG (H) were assessed. n = 5 mice per group; $p < 0.05$ versus vehicle; error bars are ± SEM.

A

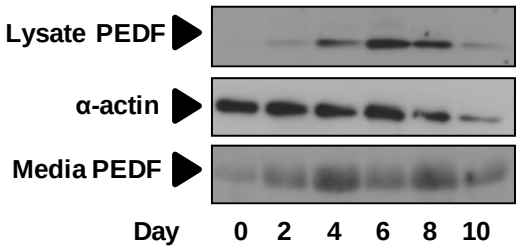

B

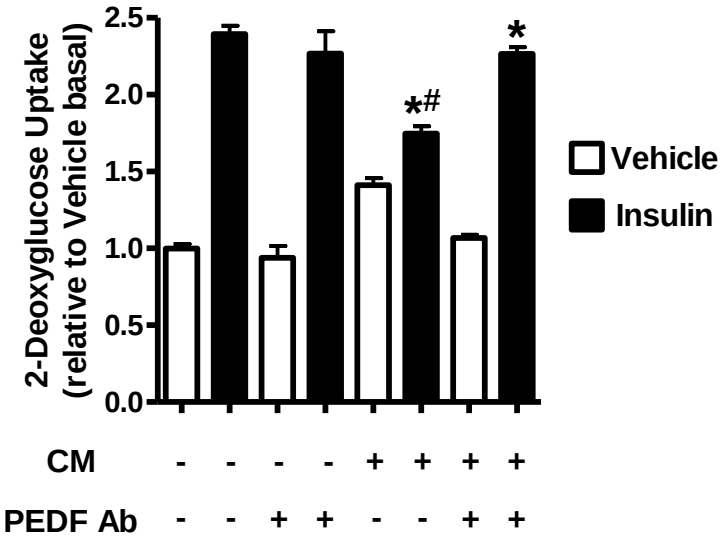

Figure 10. Neutralizing PEDF enhances insulin action in myotubes. (A) PEDF protein expression and PEDF secretion were assessed in 3T3-L1 pre-adipocytes and during differentiation into mature adipocytes (n= 5 per group for mRNA). A representative blot of 3 independent experiments is shown. (B) L6 myotubes were treated without (open bars) or with (black bars) PEDF-containing conditioned media (CM) from 3T3-L1 adipocytes for 24 h. PEDF neutralizing antibody was also added where indicated. The media was removed and basal and insulin stimulated 2DG uptake determined. The experiment was repeated on 2 occasions giving an *n*=8 for each group. *p<0.05 vs. control cells (open bars) insulin treatment, #p<0.05 vs. conditioned media plus PEDF antibody cells with insulin treatment.

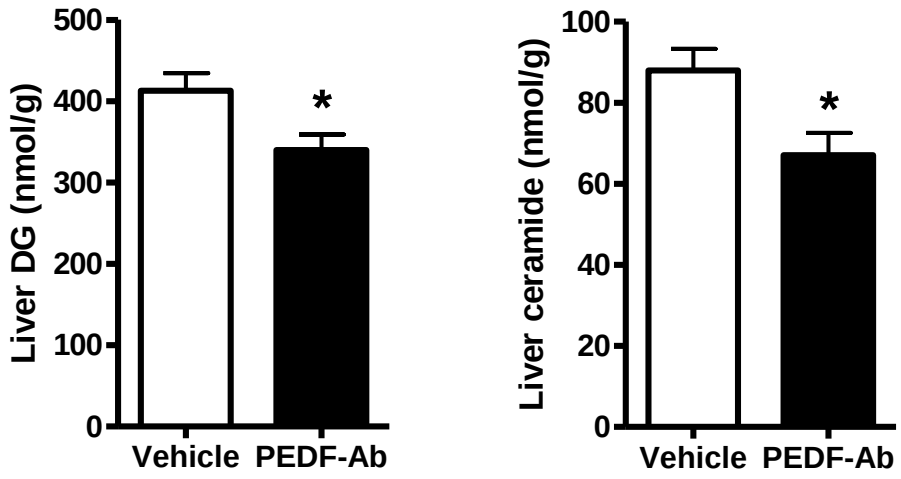

Figure 11. Liver diacylglycerol (DG) and ceramide are decreased with PEDF neutralizing antibody treatment. Obese C57Bl/6 mice were treated with PEDF neutralizing antibodies for 5 days via mini-osmotic pump then sacrificed (n=5 mice per group, $P<0.05$ vs. Vehicle). For all Figures data are presented as means ± SEM.

Identity of the PEDF receptor

One question posed by this study is what is the identity of the receptor by which PEDF exerts its effects? The literature on the identity of the PEDF receptor is variable. One early paper describes the saturatable binding of PEDF to human retinal blastoma cells and cerebellar granule neuron cells (Alberdi, Aymerich et al. 1999). This study used co-immunoprecipitation to identify an unidentified protein species of 80 kDa that interacted with PEDF. In 2006, adipose triglyceride lipase (ATGL) was identified through yeast-2-hybrid screening as a binding partner for PEDF (Notari, Baladron et al. 2006). Yeast-2-hybrid is a non-physiological method for identifying protein binding partners, and the identification of ATGL in this screen is a possible reflection of this. ATGL is a cytosolic protein that is involved in lipid synthesis from fatty acids. It is enriched at the surface of lipid droplets, where it catalyses the formation of lipids for the lipid droplet. ATGL is not predicted to contain any transmembrane domains and does not contain an N-terminal signal peptide for entry into the ER – Golgi mediated insertion into the PM. It seems unlikely that a lipid droplet protein is inserted into the plasma membrane. The surface of the lipid droplet is a vastly different biophysical environment to the plasma membrane. The lipid droplet is surrounded by a lipid monolayer, unlike the lipid bilayer that forms the plasma membrane. While the plasma membrane is surrounded by an aqueous environment on both sides, the lipid droplet membrane is aqueous on one side, and hydrophobic on the other side. There is little evidence for localisation of ATGL to the plasma membrane, and it seems unlikely that a protein could stably exist in both the plasma membrane and the lipid droplet membrane unless it has an unusual membrane anchor that spans only one layer of the bilayer. To address this, 3T3-L1 adipocytes were subjected to immunofluorescence microscopy using ATGL specific antibodies (Fig. 12). Strong ATGL staining was observed around the rim of the lipid droplet. However, no

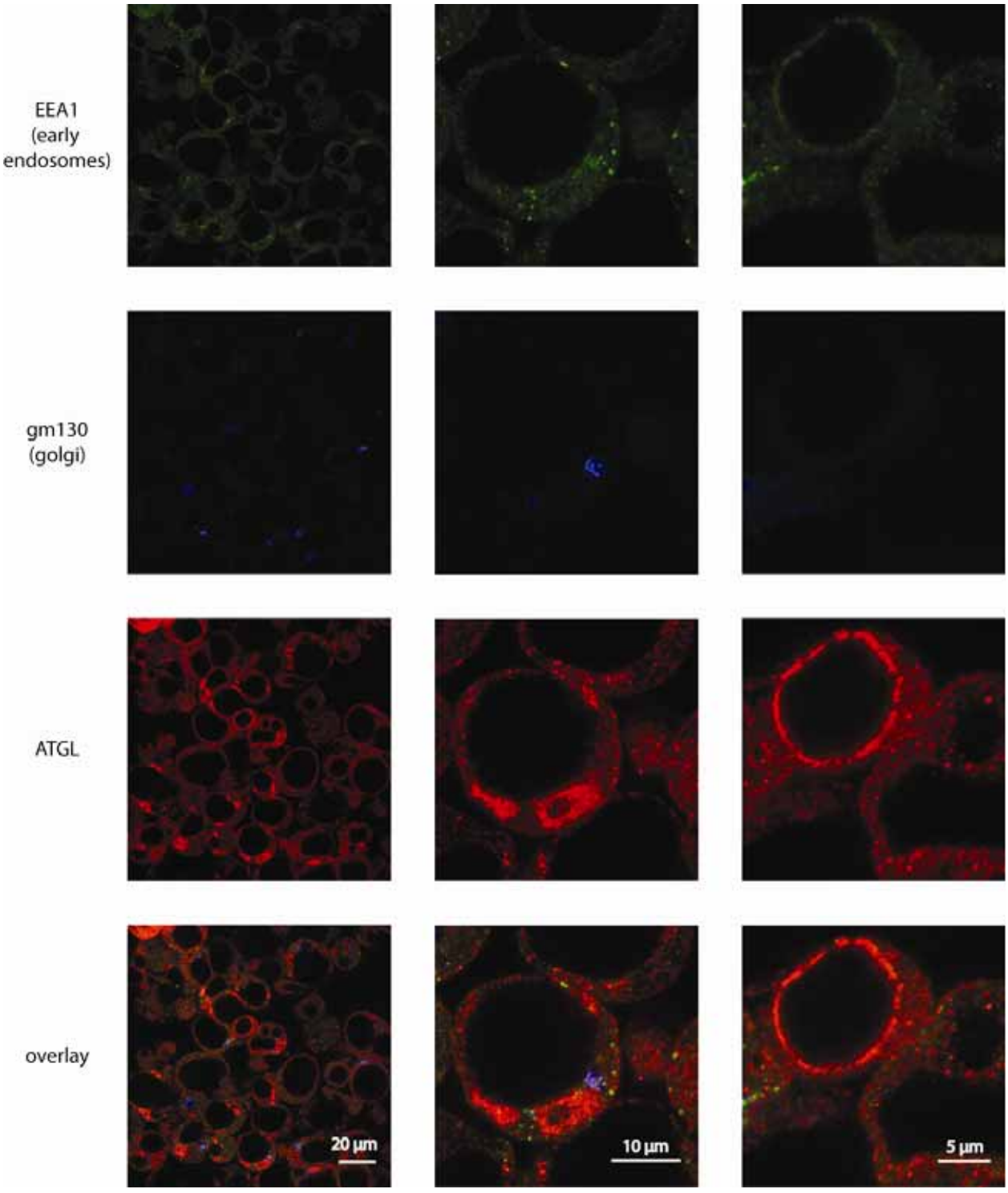

Figure 12. ATGL does not localise to the plasma membrane or the secretory pathway. 3T3-L1 adipocytes were immunostained for early endosome marker EEA1, *trans*-golgi network marker gm130 and ATGL. Staining is observed in the cytosol and the periphery of lipid droplets, consistent with the known role of ATGL as a lipid droplet protein.

staining was observed at the plasma membrane. In this study, PEDF influenced glucose uptake and lipolysis in 3T3-L1 adipocytes. If this was to occur via an interaction with ATGL, some localisation of PEDF to the cytosol and lipid droplets might be expected. 3T3-L1 adipocytes were immunostained with an antibody specific for PEDF (Fig. 13). PEDF localised to punctuate structures, that had no resemblance to the ATGL –positive structures. This does not support a role for ATGL as the PEDF receptor. To further localise ATGL in adipocytes, 3T3-L1 adipocytes were separated into PM and non-PM containing fractions using differential centrifugation (Fig. 14). ATGL was localised exclsuively to the non-PM containing fraction and no ATGL was present in the plasma membrane fraction. This study showed acute effects of PEDF in skeletal muscle. However, very little ATGL was expressed in skeletal muscle, whereas abundant expression exists in adipose tissue. Western blotting and immunofluorescence microscopy of L6 myotubes with an ATGL specific antibody could not detect ATGL (data not shown). This again makes it unlikely that ATGL is the cell surface receptor for PEDF. In a more recent study, again performed using a yeast-2-hybrid system, the 67 kDa laminin receptor (LR) was identified as a receptor for PEDF (Bernard, Gao-Li et al. 2009). Though LR was shown to interact with PEDF, it again seems unlikely that LR is the cell surface receptor for PEDF. Like ATGL, LR is not predicted to contain any transmembrane domains, and does not contain a signal peptide needed for localisation and insertion into the plasma membrane. Despite its name, the laminin receptor was originally identified as a ribosome binding protein, and was named 40S ribosomal protein SA (Auth and Brawerman 1992). The identification of this protein as a receptor occurred during a search for laminin-interacting proteins from the plasma membrane. To purify plasma membranes for identification of laminin binding proteins, cells were mechanically lysed and subjected to strong (40,000 *g*) centrifugation (Barsky, Rao et al. 1984).

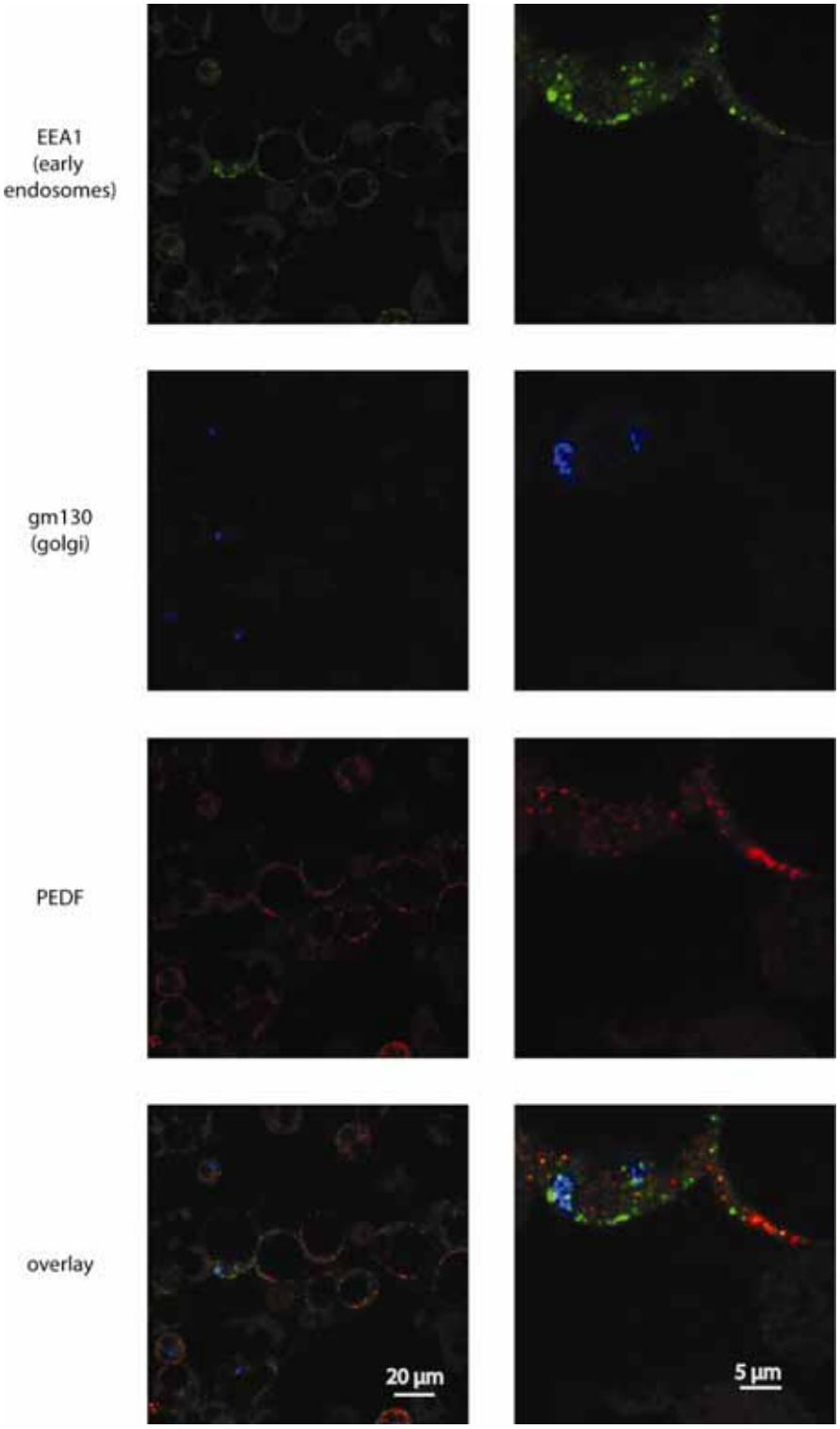

Figure 13. PEDF localises to punctuate structures in adipocytes. 3T3-L1 adipocytes were immunostained for early endosome marker EEA1, *trans*-golgi network marker gm130 and PEDF. Punctate staining of PEDF is observed in a different location to golgi and early endosomes. These punctuate structures might represent secretory granules. PEDF localisation is to be contrasted with that of ATGL (Fig. 5).

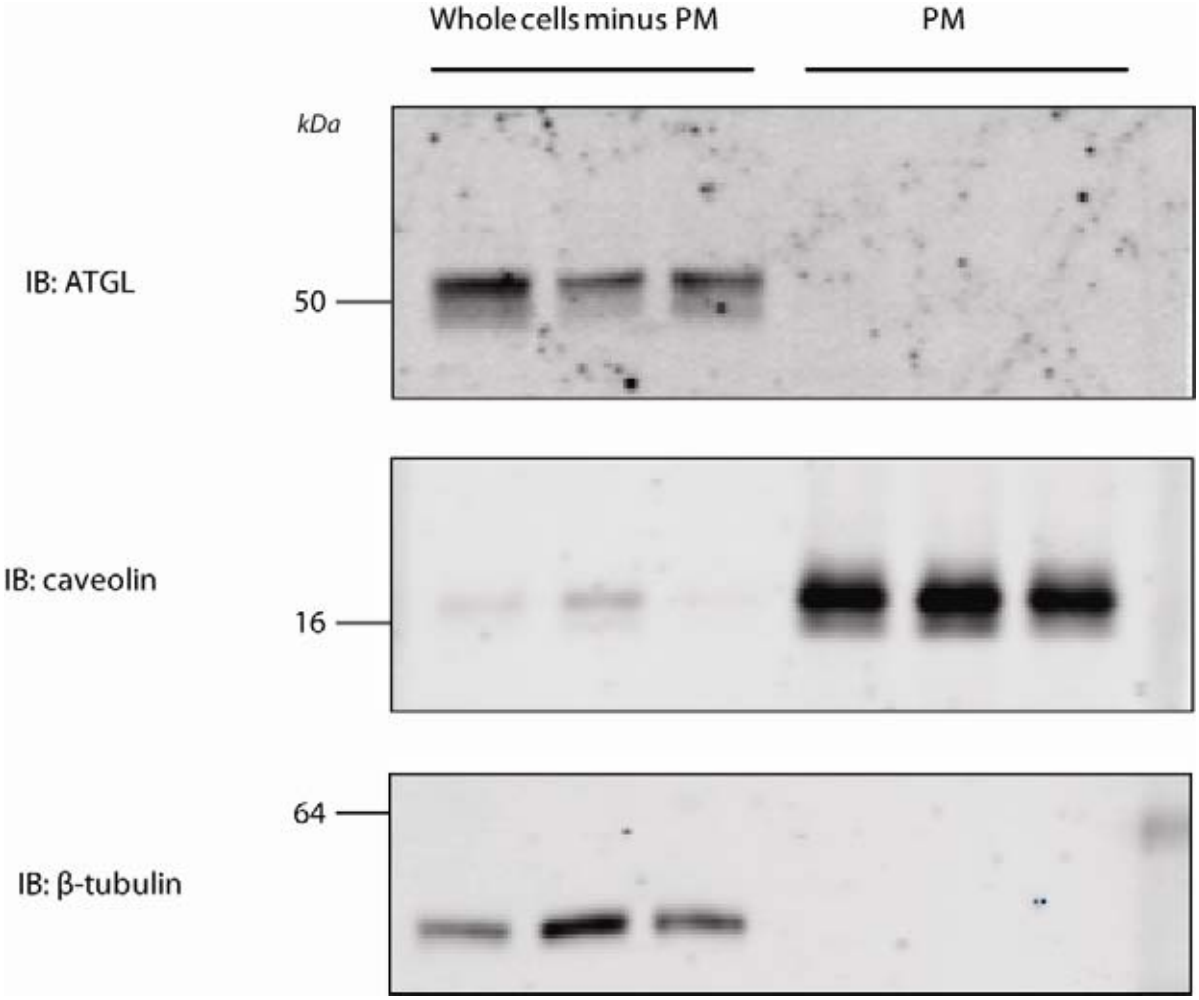

Figure 14. ATGL does not exist at the PM in adipocytes. Mechanically lysed 3T3-L1 adipocytes were fractionated using differential centrifugation to obtain PM and non-PM fractions. Equal amounts of protein from each fraction were immunoblotted for the PM marker caveolin, the cytosolic marker β-tubulin, and the putative PEDF receptor ATGL. No ATGL is observed at the plasma membrane.

The pelleted fraction was considered to be a plasma membrane enriched fraction. However, a single high speed centrifugation will contain a mixture of many membranous organelles including the endoplasmic reticulum, which will be studded with ribosomes and presumably, 40S ribosomal binding protein SA. Thus, there is insufficient evidence to conclude that laminin receptor / 40S ribosomal binding protein SA functions as a cell surface receptor for PEDF. Further work will be needed to identify the real cell surface receptor of PEDF, if such a protein exists at all.

Discussion

Changes in fat cell size are accompanied by reprogramming of the fat cell secretory profile and this is thought to play an important role in the link between obesity and insulin resistance (Tilg and Moschen 2006; Guilherme, Virbasius et al. 2008). In this study a role is described for a novel adipokine, PEDF, in whole body metabolism. Expression of PEDF in adipose tissue and plasma levels of PEDF positively correlate with obesity and insulin resistance. This is consistent with studies reporting a significant correlation between plasma PEDF and adiposity in humans (Yamagishi, Adachi et al. 2006; Jenkins, Zhang et al. 2008). To test the relationship between circulating PEDF and insulin resistance mice were administered with either PEDF or PEDF neutralizing antibodies, and this was accompanied by reduced or enhanced whole body insulin sensitivity, respectively. These studies therefore provide novel insights into yet another factor secreted from adipose tissue that appears to play a key role in regulating whole body metabolism.

The mechanism by which PEDF induces insulin resistance is not fully resolved. In addition to its role in neurogenesis and angiogenesis, PEDF induces inflammatory signaling and gene expression in several cell types (Filleur, Nelius et al. 2009) and circulating PEDF levels correlate with inflammation in individuals with Type 1 diabetes (Jenkins, Zhang et al. 2007). Obesity triggers a low-grade inflammatory state that results from the excessive release of pro-inflammatory cytokines and chemokines from adipocytes and activated macrophages that surround dead adipocytes (Cinti, Mitchell et al. 2005; Lumeng, Deyoung et al. 2007). This inflammatory stress activates several serine/threonine signaling molecules including IKKβ, JNK and ERK that in turn inhibit downstream insulin signal transduction by inhibitory phosphorylation (Hirosumi, Tuncman et al. 2002; Arkan, Hevener et al. 2005). Consistent with this notion, it is shown that PEDF directly activates several pro-inflammatory signaling proteins in skeletal muscle and liver *in vivo*, which is associated with reduced insulin signal transduction. These effects occur within 30 min of PEDF administration and prior to the upregulation of other known mediators of insulin resistance including lipid metabolite accumulation and ER stress induction.

The "lipocentric" view of insulin resistance development suggests that obesity is characterized by elevated basal adipose tissue lipolysis (Langin, Dicker et al. 2005) and greater systemic FFA availability (Horowitz, Coppack et al. 1999), that in turn contribute to excessive ectopic lipid deposition and the development of insulin resistance (Schmitz-Peiffer, Craig et al. 1999; Yu, Chen et al. 2002; Holland, Brozinick et al. 2007). A striking observation in this study was that several of these metabolic events were recapitulated with PEDF treatment in lean mice. It was shown here that PEDF can cause diabetogenic effects indirectly through stimulation of adipocyte

lipolysis and subsequent ectopic diacylglycerol and ceramide deposition in insulin sensitive tissues. These events were reversed with PEDF neutralization in obese, insulin resistant mice. Taken together, these studies indicate that PEDF can induce insulin resistance through several mechanisms including acute activation of serine/threonine kinases known to impair insulin signal transduction and by altering systemic lipid metabolism that results in ectopic tissue lipid deposition. This dual effect is reminiscent of other adipokines known to cause insulin resistance. For example, tumor necrosis factor (TNF) α, resistin and interleukin-6 are all capable of inducing serine/threonine kinase activation and lipolysis (Ort, Arjona et al. 2005; Ryden and Arner 2007). Interestingly, PEDF appears to rapidly induce lipolytic stimulation by interacting directly with the key lipolytic protein adipose triglyceride lipase (Chung, Doll et al. 2008), while other adipokines such as TNFα act more slowly (Plomgaard, Fischer et al. 2008), presumably by modifying translational control of lipid droplet associated proteins such as perilipin A (Ryden and Arner 2007). Evidently, other factors are likely to contribute to PEDF-induced insulin resistance and will require further detailed analysis. More definitive elucidation of PEDF interactions with its putative receptors and high affinity ligands (Filleur, Nelius et al. 2009) will further assist in deciphering the biological roles of PEDF.

An important question raised by these experiments is why it is that adipocytes secrete PEDF in obesity. In light of PEDFs powerful anti-angiogenic function, there is good reason to assume that PEDF is secreted to act as a brake on excessive vascularisation during adipocyte expansion. Adipocytes and stromal vascular cells produce multiple angiogenic factors including leptin, platelet derived growth factor (PDGF), vascular endothelial growth factor (VEGF), fibroblast growth factor (FGF)-2, transforming growth factor (TGF)-β, insulin-like growth factor (IGF) and

TNFα that contribute to adipose neovascularisation, which is undoubtedly an essential process for adipose tissue development (Cao 2007). Precursor fibroblasts, which exist to expand adipose tissue depots, produce these pro-angiogenic factors, and their production is down-regulated during adipogenesis (chapter 2 Fig. 12). Meanwhile PEDF, which is known to inhibit angiogenesis, is upregulated during adipogenesis, and is mostly produced by mature adipocytes. It is likely then that other anti-angiogenic factors are secreted by mature adipocytes to restrict excessive vascularisation and maintain homeostasis during adipose tissue growth. Indeed, a number of angiogenesis inhibitors including thrombospondin 1, soluble VEGFR2 and endostatin are produced in overweight or obese humans (Silha, Krsek et al. 2005; Voros, Maquoi et al. 2005). Both the observations reported here and previously (Yamagishi, Adachi et al. 2006) suggest that PEDF can be added to this list and supports the premise that an homeostatic balance between pro-angiogenic factors secreted from fibroblasts and anti-angiogenic factors secreted from mature adipocytes is important for appropriate vascularisation during the development of white adipose tissue depots (Cao 2007). These pro-angiogenic factors are produced by fibroblasts in the stromovascular fraction. As fibroblasts undergo differentiation into mature adipocytes, production of pro-angiogenic factors such as PDGF and VEGF is down-regulated, whilst production of anti-angiogenic PEDF is increased. This may act as a sort of negative feedback loop for vascularisation during the formation of adipose tissue.

In conclusion, this study has identified a novel role for PEDF as a negative regulator of insulin action in obesity. Given the observation that PEDF is increased in obese type 2 diabetic humans (Yamagishi, Adachi et al. 2006; Jenkins, Zhang et al. 2008), therapeutic strategies to inhibit

PEDF action in muscle and liver, or prevent adipocyte PEDF release, may prove a viable approach to ameliorate obesity-induced insulin resistance and its associated pathologies.

Chapter 4

Depot – specific differences in protein secretion from white adipose tissue

Lindsay Wu

This work was performed in collaboration with Dr. Samantha Hocking, Garvan Insitute of Medical Research. Data from this chapter were presented as an oral presentation in the Pincus Taft Young Investigator Award finalist session at the 2009 meeting of the Australian Diabetes Society meeting in Adelaide, South Australia. At the time of submission, this chapter was under preparation for submission to the journal *Diabetes*. Supplementary mass spectrometry data for this chapter is provided in the attached DVD-ROM.

Abstract

Visceral adiposity is more closely linked to insulin resistance and type 2 diabetes than subcutaneous adiposity. Visceral and subcutaneous adipocytes display key differences in cell size, lipolytic response to insulin and catecholamines, insulin responsiveness and secretion of adipokines. It is postulated that these differences in adipokine secretion account for the adverse metabolic consequences of visceral adiposity. In this study, the technique of lectin affinity chromatography followed by comparison of isotope-labeled amino acid incorporation rates (LAC-CILAIR) was developed to selectively enrich for secreted proteins and quantitate relative differences in the secretome of visceral and subcutaneous adipose tissue explants. A total of 86 secretory proteins were identified, of which 45% were secreted in greater abundance from visceral compared with subcutaneous adipose tissue explants. Adipose tissue is comprised of both mature adipocytes and a stromovascular fraction containing preadipocytes, microvascular endothelial cells, neurons and immune cells. To determine which cell type was responsible for the observed differences in the adipose secretome between the two depots, preadipocytes and microvascular endothelial cells were isolated and LAC-CILAIR was performed. The majority of proteins were secreted in greater abundance from visceral compared to subcutaneous preadipocytes and microvascular endothelial cells. These findings indicate that the secretory capacity of both parenchymal and non parenchymal cell types is significantly greater in visceral than subcutaneous adipose tissue offering a potential explanation for depot specific differences in insulin resistance and type 2 diabetes.

Introduction

It is well known that obesity increases the risk of developing type 2 diabetes, however the distribution of body fat may be more important than obesity *per se*. The accumulation of central or visceral adiposity is associated with an increased risk of insulin resistance, dyslipidaemia, hypertension and type 2 diabetes. (Vague 1956; Kissebah, Vydelingum et al. 1982; Bjorntorp 1990)). This relationship between increased abdominal fat and insulin resistance persists even in non-obese individuals (Carey, Jenkins et al. 1996). In contrast, the accumulation of subcutaneous or peripheral adiposity (in the gluteofemoral regions) is associated with a decreased risk of developing type 2 diabetes (Snijder, Dekker et al. 2003; Snijder, Dekker et al. 2003). Consistent with this, the improvement in insulin sensitivity that occurs with exercise is predicted by reduction in visceral but not peripheral fat mass (Gan, Kriketos et al. 2003). Conversely, thiazolidinedione therapy which increases total adiposity improves insulin sensitivity as it selectively increases subcutaneous adipose tissue depots (Mori, Murakawa et al. 1999). Further evidence that visceral adiposity has a stronger detrimental metabolic impact than subcutaneous adiposity is provided by surgical studies in which the removal of omental (visceral fat) results in improved insulin sensitivity (Thorne, Lonnqvist et al. 2002) whereas liposuction (removal of subcutaneous fat alone) does not result in any improvement (Klein, Fontana et al. 2004). At a cellular level, visceral adipocyte cell size is a strong predictor of insulin resistance but no such correlation exists for subcutaneous adipocyte cell size (Kissebah, Vydelingum et al. 1982).

There are a number of distinct physiological differences between visceral and subcutaneous adipose tissue depots that could account for the link between visceral fat and insulin resistance,

the most obvious being anatomical location. The venous drainage of visceral adipose tissue is via the portal vein directly into the liver. Visceral adipose tissue is particularly sensitive to lipolytic stimuli, being more lipolytic in response catecholamines and insensitive to the antilipolytic effects of insulin. Therefore an enlarged visceral adipose tissue depot will result in an increased flux of free-fatty acids in the portal circulation. This in turn results in increased hepatic gluconeogenesis and hepatic insulin resistance (Bjorntorp 1990; Nielsen, Guo et al. 2004). Although important, the anatomical location of visceral adipose tissue cannot be the sole mechanism whereby visceral adiposity causes insulin resistance. Studies in obese mice have shown that removal of gonadal adipose tissue results in improved glucose tolerance and insulin sensitivity, in a manner similar to omentectomy studies in humans (Gabriely, Ma et al. 2002). Unlike other visceral fat depots in mice and in humans, gonadal fat pads are not drained by the portal vein, and so this data argues against the portal hypothesis. Thus, the role of anatomical location in mediating the deleterious effects of visceral adipose tissue *per se* remains unresolved.

The divergent metabolic effects associated with visceral and subcutaneous adipose tissue may be due to intrinsic cell-autonomous differences between visceral and subcutaneous adipose tissue. Visceral adipose tissue displays higher rates of fatty acid uptake and release (Engfeldt and Arner 1988); reduced antilipolytic response to insulin (Engfeldt and Arner 1988); increased lipolytic response to catecholamines (Wajchenberg 2000); higher glucocorticoid receptor levels (Rebuffe-Scrive, Bronnegard et al. 1990) and increased response to glucocorticoids with increased lipoprotein lipase activation (Fried, Russell et al. 1993). The increased rate of lipolysis in visceral adipose tissue may result in higher circulating free fatty acids concomitant with insulin desensitisation in tissues such as liver and skeletal muscle. Visceral and subcutaneous adipose

tissue depots respond differently in response to a high fat diet. Visceral adipocytes display a greater degree of hypertrophy, whilst subcutaneous adipocytes display a greater degree of hyperplasia (DiGirolamo, Fine et al. 1998). Visceral and subcutaneous adipose tissues vary in their susceptibility to the lipodystrophy that occurs during treatment with antiretroviral drugs, which appears to be selective for subcutaneous, but not visceral, adipose tissue, an effect that can be recapitulated in adipocytes differentiated from preadipocytes derived from these different adipose tissue depots (Kovsan, Osnis et al. 2009). Studies of gene expression have found major differences in expression of patterning and developmental genes in whole fat tissue as well as adipocytes and preadipocytes from visceral and subcutaneous adipose tissue depots supporting the hypothesis that cells from each location display intrinsic differences at a very early stage of cell differentiation (Gesta, Bluher et al. 2006). Taken as a whole, these data point to the existence of intrinsic differences between the cells that make up visceral and subcutaneous adipose tissue.

Adipose tissue is now recognised as an important endocrine organ secreting numerous proteins, collectively termed adipokines, with potent effects on the metabolism of distant tissues and also on the adipose tissue itself via a paracrine effect (Galic, Oakhill et al. 2009). The discovery of leptin, an adipocyte-derived hormone which has a profound effect on whole-body metabolism by stimulating energy expenditure and inhibiting food intake firmly established adipose tissue as an important endocrine organ (Halaas, Gajiwala et al. 1995). Leptin is differentially expressed between subcutaneous and visceral adipose tissue, with lower mRNA expression in omental adipose tissue (Van Harmelen, Reynisdottir et al. 1998). Other adipocyte-derived factors were subsequently discovered including adiponectin, resistin and retinal-binding protein-4 (RBP4). Adiponectin is secreted exclusively from adipose tissue and increases whole body insulin

sensitivity by increasing energy expenditure and fatty-acid oxidation. Adiponectin is secreted in higher amounts from subcutaneous adipose tissue and circulating adiponectin levels decrease with obesity (Lihn, Bruun et al. 2004; Kadowaki, Yamauchi et al. 2006). While adipose tissue secretes adipokines with beneficial metabolic effects, it also secretes factors such as resistin, which circulate at higher concentrations in the serum of obese, insulin resistant animals. Resistin is expressed by adipocytes in mice but by macrophages in humans (Curat, Wegner et al. 2006). Injection of rodents with exogenous resistin reduces insulin sensitivity, and neutralisation of endogenous resistin with neutralising antibodies improves insulin sensitivity (Steppan, Bailey et al. 2001). Its role however in human insulin resistance remains unclear. Similarly, RBP4 causes insulin resistance when overexpressed or injected into mice (Yang, Graham et al. 2005) however the relationship between RBP4 and insulin sensitivity in humans has been inconsistent. RBP4 is more highly expressed in visceral than in subcutaneous adipose tissue (Kloting, Graham et al. 2007). Concurrent with the discovery of leptin, adipose tissue was identified as a source of pro-inflammatory cytokines with the discovery of TNF-α expression in the adipose tissue of obese humans (Hotamisligil, Shargill et al. 1993). This was the first adipose tissue derived factor thought to be the link between inflammation, obesity and type 2 diabetes. Originally TNF-α was thought to be derived from adipocytes but it has now been recognised that adipose tissue macrophages from the stromovascular fraction are the primary source and that macrophage infiltration is increased in obesity (Weisberg, McCann et al. 2003). Furthermore visceral adipose tissue exhibits increased macrophage infiltration compared with subcutaneous adipose tissue in both the lean and obese state (Harman-Boehm, Bluher et al. 2007). Subsequently other pro-inflammatory macrophage-derived cytokines including MCP-1, IL-8 and IL-6 were discovered to be expressed in higher amounts from visceral adipose tissue (Bruun, Lihn et al. 2004; Bruun,

Lihn et al. 2005; Fain and Madan 2005). Therefore, the differential secretion of beneficial and detrimental adipokines from the subcutaneous and visceral adipose tissue depots respectively may account for the differing metabolic consequences of visceral and subcutaneous adiposity. It is possible that other as yet unknown adipokines are differentially secreted from subcutaneous and visceral adipose tissue depots that could further explain the detrimental metabolic consequences of visceral adiposity or conversely the protective effects of subcutaneous adiposity.

This study aimed to fully characterise the secretion profile of visceral and subcutaneous adipose tissue using a proteomics approach. Previous studies have used mass spectrometry to identify adipocyte secretory factors. In every case the basis of these experiments was to concentrate proteins from adipocyte conditioned media samples, and subject these proteins to mass spectrometry (Kratchmarova, Kalume et al. 2002; Wang, Mariman et al. 2004; Chen, Cushman et al. 2005; Zvonic, Lefevre et al. 2007). These studies have been successful in identifying novel adipocyte secretory proteins, however they have all been limited to using cultured 3T3-L1 adipocyte cell-lines (Kratchmarova, Kalume et al. 2002; Wang, Mariman et al. 2004) or collagenase digested primary adipocytes (Chen, Cushman et al. 2005; Zvonic, Lefevre et al. 2007). Immortalized cell-lines such as 3T3-L1 adipocytes provide a useful experimental tool but are unable to fully replicate the physiology of adipocytes or provide depot-specificity. Isolated adipocytes differ from whole adipose tissue samples in that they lack the complex three dimensional architecture of adipose tissue and the interplay between adipocyte and non-adipocyte cell types which may have profound influence on the adipocyte secretion profile. Furthermore, the standard procedure for isolating primary adipose cells from adipose tissue

triggers induction of many genes encoding inflammatory mediators. Therefore, disturbing adipocytes from their environment may be problematic as it induces changes in gene expression, (Ruan, Zarnowski et al. 2003). Using whole adipose tissue explants introduces the presence of non-adipose derived serum factors, which are difficult to eradicate prior to media conditioning. These can be lessened by performing multiple washing steps however this prolongs tissue handling and may induce the expression of inflammatory genes as for adipocyte isolation. As a consequence, it is not possible to differentiate between adipose secretory proteins and contaminating serum proteins. One way of circumventing this approach is to use partial labelling of tissues with isotopic amino acids (Alvarez-Llamas, Szalowska et al. 2007; Roelofsen, Dijkstra et al. 2009), as based on the SILAC technique developed by Matthias Mann and co-workers (Ong, Blagoev et al. 2002). One recent adaptation of these experiments is comparison of isotope labelled amino acid incorporation rates (CILAIR) (Roelofsen, Dijkstra et al. 2009). In these experiments, cells or tissues are incubated with isotopically labelled amino acids, which become incorporated into newly synthesised proteins. The incorporation of ^{13}C and ^{15}N isotopes results in a small shift in molecular weight, which can be resolved by mass spectrometry. The difference in peak intensity between different isotope labelled peptides reflects relative differences in the rate of incorporation of isotope labelled amino acids into newly synthesized proteins. This implies that a protein with a higher incorporation of labelled isotope is synthesised at a greater rate or in greater abundance. This technique may be used to survey differences in the relative abundance of thousands of proteins within a single combined protein sample.

When collecting cell or tissue conditioned media, contamination of samples with intracellular, non-secretory proteins often occurs. This problem is exacerbated in cells or tissues with delicate

structure, such as primary adipocytes. Where full datasets are available, previous attempts to survey the secretome of adipose tissue using mass spectrometry have encountered the problem of a high degree of sample contamination with cytosolic, non-secretory proteins (Celis, Gromov et al. 2004; Wang, Mariman et al. 2004; Alvarez-Llamas, Szalowska et al. 2007; Zvonic, Lefevre et al. 2007; Roelofsen, Dijkstra et al. 2009). Contamination of samples with non-target proteins results in a significant dilution of target proteins rendering them harder to detect. To circumvent this problem lectin affinity chromatography was utilised as a way of enriching for secreted proteins, whilst avoiding intracellular contaminants (Crowe, Wu et al. 2009). Secreted proteins commonly undergo N-glycosylation as they are synthesized by ribosomes at the endoplasmic reticulum and pass through the secretory pathway, whereas cytosolic proteins, synthesized at cytosolic ribosomes, do not undergo N-glycosylation. Lectin affinity chromatography exploits this differential N-glycosylation to selectively enrich for proteins targeted for secretion. This approach greatly improved the purity of samples as compared to similar previous studies.

This study sought to accurately compare differences in adipokine secretion that exist between visceral and subcutaneous adipose tissue. To do this, lectin affinity chromatography was combined with partial isotopic amino acid labelling (CILAIR) to quantify relative changes in protein secretion from two different adipose tissue depots, to the exclusion of cytosolic proteins. This method was termed “LAC-CILAIR” (lectin affinity chromatography – comparative isotope labelled amino acid incorporation rate). This technique was firstly used to measure protein secretion from whole adipose tissue. The bulk of cell mass in adipose tissue is mature adipocytes, accounting for between 25 and 70% of total tissue mass. Despite accounting for the majority of tissue mass, the large size of adipocytes means they only account for around 25% of

the total number of cells in adipose tissue (Fruhbeck 2008). The remaining cells comprise a stromovascular fraction consisting of preadipocytes and microvascular endothelial cells. Cells from the stromovascular fraction are a rich source of adipokines. In fact, one study found that 90% of the adipokines released from adipose tissue were released from non-adipocyte cell types (Fain, Madan et al. 2004). To detect proteins secreted from these stromovascular cells, isolated preadipocytes and endothelial cells were isolated from whole adipose tissue, cultured *ex vivo*, and LAC-CILAIR was performed as for whole adipose tissue. These results show that there are a large number of proteins differentially secreted from both the adipocyte and non-adipocyte components of visceral adipose tissue compared with subcutaneous adipose tissue which could contribute to the adverse metabolic sequelae of visceral adiposity. These data are an important addition to our understanding of adipose tissue biology.

Methods

Materials and buffers

All tissue culture reagents were obtained from Gibco unless otherwise stated.

Transfer medium: Dulbecco's modified eagle medium / Ham's F-12 (DMEM/Ham's F-12) 1:1 containing 1% BSA and supplemented with 100 units/mL penicillin, 0.1 mg/mL streptomycin and 0.25 µg/mL amphotericin B (Antibiotic-Antimycotic, Invitrogen).

SILAC medium: Low glucose Dulbecco's modified eagle media (DMEM) without leucine, lysine and arginine (Sigma Aldrich) supplemented with 0.105 g/L leucine, 100 units/mL penicillin, 0.1 mg/mL streptomycin, 0.0159 g/L phenol red and 100 nM insulin. Glucose was added to a final concentration of 4.5 g/L. 'Heavy' or 'medium' isotopes of both arginine (0.021

g/L) and lysine (0.0365 g/L) were added to produce ‘heavy’ and ‘medium’ SILAC medium respectively,

Endothelial cell growth medium: Low-glucose DMEM supplemented with 100 units/mL penicillin, 0.1 mg/mL streptomycin, 20mM HEPES, 1% non-essential amino acids, 50 mM 2-mercaptoethanol, 20% heat-inactivated foetal calf serum, 12 U/mL heparin and 150 ug/mL endothelial cell growth supplement (Sigma Aldrich).

Endothelial cell SILAC medium: Low glucose Dulbecco’s modified eagle media (DMEM) without leucine, lysine and arginine (Sigma Aldrich) supplemented with 0.105 g/L leucine, 100 units/mL penicillin, 0.1 mg/mL streptomycin, 0.0159 g/L phenol red, 20mM HEPES, 1% non-essential amino acids, 50 mM 2-mercaptoethanol and 100 nM insulin. ‘Heavy’ or ‘medium’ isotopes of both arginine (0.021 g/L) and lysine (0.0365 g/L) were added to produce ‘heavy’ and ‘medium’ SILAC medium respectively,

Preadipocyte growth medium: DMEM/Ham’s F-12 1:1 supplemented with 100 units/mL penicillin, 0.1 mg/mL streptomycin and 10% FCS.

Animals

Male C57BL/6J mice were purchased from the animal resources centre (Perth, Australia). Animals were kept in a temperature-controlled room (22 ± 1°C), 80% relative humidity on a 12-h light/dark cycle with free access to food and water. Experiments were carried out with the approval of the Garvan Institute/St. Vincent's Hospital Animal Experimentation Ethics Committee, following guidelines issued by the National Health and Medical Research Council of Australia. For each experiment, 2 – 5 mice were used as tissue donors.

Preparation of Anti-CD31 antibody-coated magnetic beads

Sheep anti-rat IgG Dynabeads (Invitrogen) were pre-coated with rat anti-mouse monoclonal antibody to CD31 (BD Pharmingen) according to the manufacturer's instructions at a concentration of 1 μg rat anti-mouse CD31 antibody per 1 x 10^7 Dynabeads. Dynabeads were stored in phosphate-buffered saline with 0.1% BSA at 4^0C at a concentration of 4 x 10^8 beads/mL.

Adipose tissue explants

Paired visceral (epididymal) and subcutaneous (inguinal) adipose tissue depots were obtained from 6 week old C57BL/6J mice. Fat pads were surgically removed under sterile conditions and placed immediately into warm transfer medium. Subsequent handling of adipose tissue occurred in a sterile tissue culture hood. Adipose tissue biopsies were placed in fresh transfer medium and finely minced using scissors into ~1 mm^3 pieces. The minced explants were rinsed in sterile pre-warmed PBS and centrifuged at 250 *g* to remove cell debris and red blood cells. Adipose tissue explants (200 μL) were incubated in 1 mL SILAC medium. After 48 h incubation at 37°C in 5%CO_2, conditioned media was collected and centrifuged at 2,000 *g* to pellet cell debris. Lectin affinity chromatography and subsequent mass spectrometry was performed (below).

Preadipocyte and endothelial cell isolation and culture

Preadipocytes and microvascular endothelial cells were isolated from the same biopsies. Paired visceral (epididymal) and subcutaneous (inguinal) adipose tissue depots were obtained from six wk old C57BL/6J mice. Fat pads were surgically removed under sterile conditions and placed immediately into warm transfer medium. Subsequent handling of adipose tissue occurred in a sterile tissue culture hood. Adipose tissue biopsies were placed in fresh transfer medium and finely minced using scissors into ~1 mm^3 pieces. Media was removed and replaced with fresh transfer medium containing 1 mg/mL collagenase type I and incubated with gentle shaking at 37^0C for one hour. The ratio of adipose tissue to digest solution was 4:1. The resulting material was filtered through a 250 µm mesh and the adipocytes and free oil separated from the stromovascular components by centrifugation at 250 *g* for 5 minutes at room temperature. The stromovascular pellet was resuspended and washed in PBS and centrifuged at 250 *g* for 5 minutes at room temperature. This washing step was repeated twice. The stromovascular pellet was resuspended and plated in 2% gelatin-coated 10cm dishes in endothelial cell growth medium. This mixed cell population was cultured for 5 – 6 days at 37°C in 5% CO_2. After this short culture period, cells were detached using 0.25% trypsin containing 3.42 mM EDTA and the trypsin subsequently neutralised by addition of Hank's balanced salt solution containing 5% foetal calf serum (HBSS-FCS). The cell solution was then centrifuged at 600 *g* for 5 minutes at room temperature. The cell pellet was resuspended in 0.5 mL HBSS-FCS and incubated with 25 µl of anti-PECAM-1 coated dynabeads for 15 min at 4 ^{0}C under constant rotation. The cell/bead suspension was brought to a total volume of 10 mL with HBSS-FCS and endothelial cells selected using a magnet. Non-selected cells in the wash were transferred to a fresh tube. This wash and selection procedure was repeated 5 times. Selected cells were resuspended in endothelial cell growth medium and transferred to 2% gelatin coated culture dishes. After 3 – 5

days cells, were routinely passaged and plated at equal density in endothelial cell growth medium. Non-selected cells in the wash medium were centrifuged at 600 *g* for 5 min at room temperature. The resultant pellet was resuspended in preadipocyte growth medium and plated at equal density in 10 cm culture dishes. Endothelial cells and preadipocytes were grown until confluent. At confluence, media was replaced with endothelial cell SILAC media and SILAC media, respectively. After 48 h, conditioned media was collected and centrifuged at 2,000 *g* to pellet cell debris. Lectin affinity chromatography and subsequent mass spectrometry was performed.

Lectin affinity chromatography

Paired visceral and subcutaneous samples were mixed in equal proportions, and glycoprotein purification was performed as previously described (Crowe, Wu et al. 2009). Briefly, $MnCl_2$ was added to conditioned media at a concentration of 1 mM, and 50 µL of 50% slurry of Concanavalin A sepharose (GE Healthcare) was added per 1 ml of conditioned media. Samples were rotated overnight at 4°C. Sepharose beads were washed extensively with ConA binding buffer (0.5 M NaCl, 0.1 M Tris, 1 mM $MnCl_2$ and 1 mM $CaCl_2$, pH 7.4). Proteins were eluted with buffer containing 0.3 M methyl-α-D-mannopyranoside, 0.5 M NaCl, 0.1 M Tris, 10 mM EDTA and 10 mM EGTA, pH 7.4. Eluted proteins were precipitated using chloroform : methanol as described (Wessel and Flugge 1984).

Amino acid isotopes

All isotopes were from Cambridge laboratories. The “medium” isotope of arginine was U-13C6 arginine (catalog number CLM-2265), “heavy” arginine was U-^{13}C6 U-^{15}N4 arginine (catalog number CNLM-539), “medium” lysine was 4,4,5,5-D4 lysine (catalog number CNLM-2640), heavy lysine was U-^{13}C6 U-^{15}N2 lysine (catalog number CNLM-291). Growth media was low glucose Dulbecco’s modified eagle media (DMEM) deficient in leucine, arginine, lysine and phenol red from Sigma (catalog number D9443). Glucose was adjusted to 4.5 g/L, leucine was added to a concentration of 0.105 g/L, and phenol red was added to 0.0159 g/L. Arginine and lysine were added at 25% of normal concentration in DMEM to avoid conversion of excess isotopes into proline (O'Quinn, Knabe et al. 2002; Ong, Kratchmarova et al. 2003). Arginine isotopes were added back at a concentration of 0.021 g/L, lysine isotopes were added back at a concentration of 0.0365 g/L. After addition of all ingredients, media was passed through a 0.20 μm filter.

Mass spectrometry

Peptide extraction and mass spectrometry was as previously described using a Waters Ultima mass spectrometer (Larance, Ramm et al. 2005; Crowe, Wu et al. 2009). Peak picking and CILAIR quantitation was performed using the mascot distiller software package (Matrix Sciences). The SwissProt database was used for protein identification, with taxonomy restricted to Mus musculus, MS tolerance set at 0.5 Da and MSMS tolerance set at 0.05 Da. Ratios of isotope to “light” below 0.05 were discounted as “no label incorporation”. “Heavy and “medium” isotope ratios were used to determine relative abundance of proteins from visceral or

subcutaneous samples. Peak picking and database searching was performed using the Mascot distiller software package, version 2.3.1.0. MDRO 2.3.1.0 (Matrix Sciences). The SwissProt database on Mascot server 2.2 was used for protein identification, with taxonomy restricted to Mus musculus, MS tolerance set at 0.5 Da and MSMS tolerance set at 0.05 Da. Variable modifications were set to carbamidomethyl, propionamide and oxidation (M). No fixed modifications were used. Trypsin was set as cleavage enzyme after arginine or lysine and a maximum of 2 missed cleavages were permitted. Quantitation method was as follows. Method: constrain search – yes, protein ratio type – weighted, protein score type – standard, report detail – yes, minimum peptides – 1. Protocol: precursor, allow mass time match – yes, allow elution shift – no, all charge states – no. Component "light" was mode – exclusive, unmodified site – K, position – anywhere, unmodified site – R, position – anywhere. Component "medium" was mode – exclusive, modification – Label: 2(H)4 (K), modification – Label: 13C(6) (R). Component "heavy" was mode – exclusive, modification – Label: 13C(6)15N(2) (K), modification – Label: 13(6)15N(4) (R). For all ratios measured, numerators and denominators were set to 1.0. Integration – trapezium, integration source – survey, precursor range – envelope. Quality: minimum precursor charge – 1, isolated precursor – No, Minimum a(1) – 0.0, peptide threshold type – minimum score. Outlier – auto. The presence of a signal peptide in detected proteins was determined using SignalP 3.0 (Bendtsen, Nielsen et al. 2004). "Medium" and "heavy" isotopes are expressed here in relation to "light" (endogenous amino acid) isotopes. Ratios of isotope to "light" below 0.05 were discounted as "no label incorporation". Keratin peptides were in all cases ignored. The presence of a signal peptide in detected proteins was determined using SignalP 3.0 (Bendtsen, Nielsen et al. 2004).

Results

It was hypothesised that there would be significant differences in protein secretion from visceral and subcutaneous adipose tissue. Adipose tissue explants were obtained from young, lean mice from the epididymal (visceral) and inguinal (subcutaneous) fat depots. Equal amounts of minced adipose tissue from visceral and subcutaneous depots were incubated for 48 hours in the presence of "heavy" and "medium" isotopes of arginine and lysine, respectively. After incubation for 48 hours, media was collected, mixed in an equal ratio, and subjected to lectin affinity chromatography. Lectin affinity chromatography utilises the N-glycosylation of secretory proteins to purify secretory proteins from conditioned media to the exclusion of cytosolic proteins released from mechanically damaged or necrotic cells. By removing contaminating cytosolic proteins, which can be present in large amounts, less abundant secretory proteins can be sequenced at a greater sensitivity than would otherwise be possible. After lectin affinity chromatography, proteins were resolved by SDS-PAGE and stained with SYPRO ruby. Lanes were cut into 16 equal sized pieces, and subjected to quantitative mass spectrometry (Table 1 and supplementary data). A minimum ion score of 60 and a minimum isotope to "light" ratio of 0.05 were chosen as criteria for positive identification. For reference, an ion score over 40 indicates identification with 95% confidence. A total of 145 proteins were identified, of which 86 (60%) were predicted to contain an N-terminal signal peptide using SignalP. Proteins that did not contain a signal peptide had lower ion scores, indicating that these proteins were detected with lower confidence – that is only small amounts of these contaminating non-secretory proteins were present (Fig.1) When the ion score of all detected proteins was summated, 88% of this total was from secretory proteins, indicating the majority of protein detection during mass

spectrometry was devoted to sequencing true secretory proteins. This demonstrates the utility of lectin affinity chromatography for isolating true secretory proteins. Of the 145 proteins that incorporated the label, 74 were found to be present at >2 fold higher abundance in conditioned media from visceral adipose tissue than subcutaneous adipose tissue. Conversely, 40 proteins were found to be present at >2 fold higher abundance in conditioned media from subcutaneous adipose tissue than visceral adipose tissue. Once non-secretory proteins were excluded, 51 proteins (59%) were found to be present at >2 fold higher abundance in conditioned media from visceral adipose tissue than subcutaneous adipose tissue, whereas only 18 proteins (21%) were found to be present at >2 fold higher abundance in conditioned media from subcutaneous adipose tissue than visceral adipose tissue. The frequency distribution of the visceral to subcutaneous ratio for detected proteins is shown in Fig. 2. The frequency distribution for proteins with no signal peptide resembles a normal distribution whereas the frequency distribution for proteins with a signal peptide is skewed to the right. This indicates that release of true secretory proteins into conditioned media is increased from the visceral relative to the subcutaneous adipose tissue depot. The secreted proteins identified were from a number of families. The serine protease inhibitor family was particularly well represented, with 8 members of this family detected. Members of the acute phase response were up-regulated from the visceral adipose depot. These proteins included multiple members of the complement pathway, as well as haptoglobin, ceruloplasmin and fibrinogen. Clustering analysis of proteins was performed using the database for annotation, visualisation and integrated discovery (DAVID) (Dennis, Sherman et al. 2003; Huang da, Sherman et al. 2009).

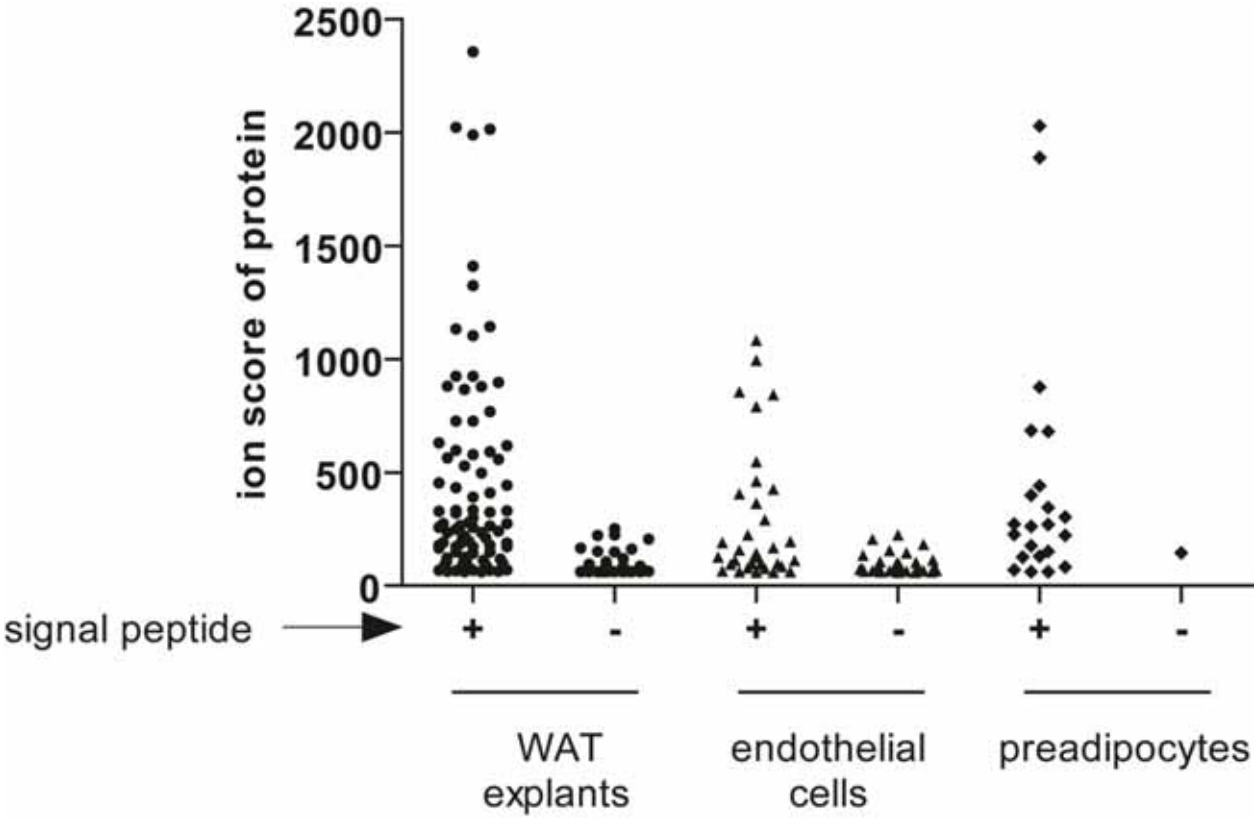

Figure 1. Non-secretory proteins are represented at the lower end of detection range. Proteins identified from each sample are split into those with and without a signal peptide, and plotted according to ion score, which is a function of the number of peptides detected and confidence associated with peptide sequencing.

Accession	Score	subcut. / ^{12}C	visceral / ^{12}C	visceral / subcut	subcut / visceral	Name	signal peptide?
CO3_MOUSE	2356	0.2345	1.4037	3.8962	0.2568	Complement C3	1
A2M_MOUSE	2021	0.0027	0.1973	1.0462	0.5873	Alpha-2-macroglobulin	1
LAMB1_MOUSE	2013	147.856	0.0131	0.0465	14.0493	Laminin subunit beta 1	1
LAMC1_MOUSE	1988	0.0116	0.0924	5.3939	0.1574	Laminin subunit gamma-1	1
LAMA2_MOUSE	1409	0.2347	79.6618	5.8369	0.079	Laminin subunit alpha-2	1
COEA1_MOUSE	1323	0.1049	0.0068	0.2932	3.3802	Collagen alpha-1(XIV) chain	1
FINC_MOUSE	1142	0.0947	0.0889	3.4279	0.1466	Fibronectin	1
CES3_MOUSE	1132	0	0.2224	7.7748	0.1269	Carboxylesterase 3	1
HPT_MOUSE	1103	0.6071	1.4466	2.5003	0.3962	Haptoglobin	1
CO1A2_MOUSE	925	0.8646	2.4478	1.0944	0.37	Collagen alpha-2(I) chain	1
TRFE_MOUSE	924	0.1393	0.3349	1.3117	0.3748	Serotransferrin	1
LAMB2_MOUSE	896	2.5529	2.9645	0.5017	0.0465	Laminin subunit beta-2	1
CFAB_MOUSE	880	1.2984	0.9025	2.2097	0.4522	Complement factor B	1
CERU_MOUSE	879	0.2978	0.09174	4.2408	0.2357	Ceruloplasmin	1
SPA3N_MOUSE	865	0.3548	0.0785	4.1321	0.236	Serine protease inhibitor A3N	1
SPA3K_MOUSE	767	0.0921	0.2829	3.1605	0.3164	Serine protease inhibitor A3K	1
ESTN_MOUSE	726	0	410.334	21.8136	0.0438	Liver carboxylesterase N	1
GELS_MOUSE	725	2.1874	1.8006	1.0615	1.1021	Gelsolin	1
CO4B_MOUSE	630	4.7321	0.1162	13.7332	0.0729	Complement C4-B	1
NID2_MOUSE	618	0.1335	0.0743	3.4691	0.288	Nidogen-2	1
CATB_MOUSE	596	0.9457	2.8716	6.2497	0.16	Cathepsin B	1
ANT3_MOUSE	591	0.9917	0.0275	0.1622	0.4252	Antithrombin-III	1
PGS2_MOUSE	579	0.003	0.0878	4.737	0.1735	Decorin	1

Table 1. Comparative secretion of proteins identified from visceral and subcutaneous white adipose tissue explants. Visceral or subcutaneous WAT explants were incubated in media containing different isotopes of arginine and lysine. Conditioned media were mixed, subjected to lectin affinity chromatography and subjected to quantitative mass spectrometry. Peak height ratios of isotope to endogenous (^{12}C) amino acids and ratios between isotopes are shown. Complete dataset available in supplementary data.

Analysis of proteins increased from visceral adipose tissue revealed an enrichment of proteins involved in endopeptidase inhibition, including members of the Serpin family, and proteins involved in innate immune system regulation, including members of the complement pathway. Cluster analysis of proteins increased from subcutaneous adipose tissue failed to provide any functional similarities.

Adipose tissue is comprised of a complex array of different cell types in addition to adipocytes, most notably preadipocytes, endothelial cells and macrophages, collectively referred to as the stromovascular fraction. While adipocytes make up the greatest mass of white adipose tissue, the stromovascular cells may make a significant contribution to the secretory capacity of white adipose tissue, perhaps even exceeding the secretory contribution of adipocytes (Fain, Madan et al. 2004). The interplay between cells of the stromovascular fraction and adipocytes may also be important in dictating the secretion profile of whole adipose tissue. To investigate this complex inter-relationship further, the secretion of proteins from preadipocytes and microvascular endothelial cells isolated from the stromovascular fraction were measured. This study sought to determine the relative contribution of mature adipocytes, preadipocytes and micro-vascular endothelial cells to the whole adipose tissue secretome and in addition to determine whether the depot-specific differences in protein secretion that were observed from whole adipose tissue explants persisted in cells from the stromovascular fraction.

First preadipocytes were isolated from paired visceral and subcutaneous adipose tissue biopsies. Visceral and subcutaneous preadipocytes were cultured *in vitro* for at least one week before incubation in media containing “heavy” and “medium” isotopes of arginine and lysine

respectively, in the presence of insulin. Conditioned media was collected, mixed in equal ratio and subjected to lectin affinity chromatography and quantitative mass spectrometry (Table 2 and supplementary data). Preadipocytes secreted a more limited set of proteins than minced adipose tissue, with only 23 proteins that incorporated the label detected. Strikingly, 22 of these 23 proteins were predicted to contain an N-terminal signal peptide, demonstrating the effectiveness of lectin affinity chromatography in enriching for secretory proteins. Of the 22 preadipocyte secretory proteins, 15 were upregulated more than 2-fold from visceral compared to subcutaneous derived preadipocytes. Not one protein was upregulated more than two-fold from subcutaneous as compared to visceral derived preadipocytes. The frequency distribution of the visceral to subcutaneous ratio for detected proteins is shown in Fig. 3. Again, the frequency distribution for proteins with a signal peptide is skewed to the right, indicating that release of secretory proteins into conditioned media is increased from visceral relative to subcutaneous preadipocytes. Cluster analysis of the proteins upregulated from visceral derived preadipocytes showed an enrichment of extracellular matrix proteins. Next, microvascular endothelial cells isolated from paired visceral and subcutaneous adipose tissue depots were examined. Although endothelial cells are known to secrete proteins, including thrombospondin, fibronectin and collagen, to date there has been no survey to determine the secretome of endothelial cells. In addition, it is unknown whether microvascular endothelial cells display depot-specific differences in the profile of secreted proteins in a similar manner to mature adipocytes and preadipocytes. Endothelial cells were isolated using CD31 magnetic bead separation, and subsequently cultured *in vitro*.

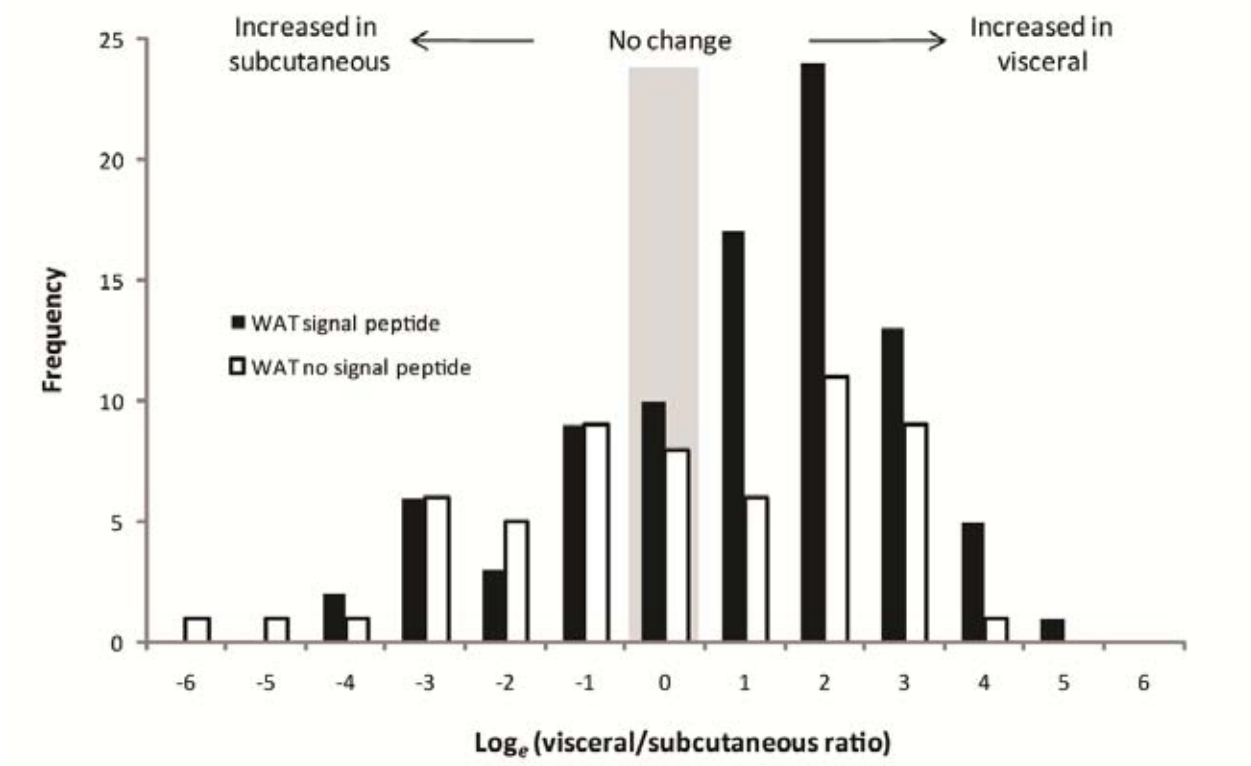

Figure 2. WAT explants secretory proteins are secreted in greater amounts from visceral adipose tissue. WAT explants from visceral and subcutaneous depots were cultured in media containing two different isotopes of arginine and lysine. LAC-CILAIR mass spectrometry was performed, and isotopic ratios calculated. Histogram shows distribution of visceral to subcutaneous ratios for proteins detected. Note use of natural log scale.

Accession	Score	visceral / ^{12}C	subcut / ^{12}C	visceral / subcut	subcut / visceral	Description	signal peptide?
CO1A1_MOUSE	2029	1.205	0.118	0.5169	1.061	Collagen alpha-1(I) chain	1
CO1A2_MOUSE	1889	0.3381	0.9631	4.006	0.2345	Collagen alpha-2(I) chain	1
CO3A1_MOUSE	876	0.2252	**1.807**	**4.702**	**0.191**	Collagen alpha-1(III) chain	**1**
CO5A2_MOUSE	684	1.307	14.64	**19.26**	**0.052**	Collagen alpha-2(V) chain	**1**
FINC_MOUSE	680	0.261	0.6717	**1.579**	**0.319**	Fibronectin	**1**
FBLN2_MOUSE	440	0.1604	0.7822	5.163	0.1936	Fibulin-2	**1**
SPRC_MOUSE	399	0.02	0.07566	**3.36**	**0.284**	SPARC	**1**
PEDF_MOUSE	344	0.3005	**1.884**	**7.085**	**0.133**	Pigment epithelium-derived factor	**1**
CO5A1_MOUSE	304	0.9905	0.03282	0.06207	1.111	Collagen alpha-1(V) chain	**1**
HPT_MOUSE	271	**0.0522**	0.01015	**23.01**	**0.039**	Haptoglobin	**1**
CATB_MOUSE	269	**0.0635**	0.4512	0.8618	1.168	Cathepsin B	**1**
IC1_MOUSE	262	0.1031	1.05	2.591	0.3861	Plasma protease C1 inhibitor	**1**
PAI1_MOUSE	227	0.1255	0.4702	6.119	0.1634	Plasminogen activator inhibitor 1	**1**
CO2A1_MOUSE	222	**0.1194**	4.4E-05	3.991	0.0861	Collagen alpha-1(II) chain	**1**
TIMP1_MOUSE	175	0.3783	1.539	4.046	0.2473	Metalloproteinase inhibitor 1	**1**
CO4A1_MOUSE	150	3.269	8.87	1.003	0.9969	Collagen alpha-1(IV) chain	**1**
TITIN_MOUSE	145	**0.0015**	0.1432	**15.4**	**0.058**	Titin	**0**
PGS1_MOUSE	131	0.8874	1.82	4.14	0.2419	Biglycan	**1**
CATL1_MOUSE	126	0.1189	0.6414	17.19	0.0582	Cathepsin L1	**1**
EGFR_MOUSE	82	0.3773	0.5286	4.062	0.2462	Epidermal growth factor receptor	**1**
COBA2_MOUSE	70	0.00097	0.4203	1.566	0.6379	Collagen alpha-2(XI) chain	**1**
FSTL1_MOUSE	61	0.5309	19.07	8.844	0.113	Follistatin-related protein 1	**1**
ATS7_MOUSE	61	2.07	0.09041	0.3296	0.3974	A disintegrin and metalloproteinase with thrombospondin motifs 7	**1**

Table 2. Comparative secretion of proteins identified from visceral and subcutaneous adipose tissue derived preadipocytes. Visceral or subcutaneous WAT derived preadipocytes were incubated in media containing different isotopes of arginine and lysine. Conditioned media were mixed, subjected to lectin affinity chromatography and subjected to quantitative mass spectrometry. Peak height ratios of isotope to endogenous (^{12}C) amino acids and ratios between isotopes are shown. Complete dataset available in supplementary data.

As for preadipocytes, visceral and subcutaneous microvascular endothelial cells were incubated in media containing “heavy” and “medium” isotopes of arginine and lysine, respectively. Conditioned media was collected, mixed in equal ratio and subjected to lectin affinity chromatography and quantitative mass spectrometry (Table 3 and supplementary data). A total of 66 proteins that incorporated the label were detected. Of these 66 proteins, 34 proteins (52%) displayed an N-terminal signal peptide indicative of secretion. When total ion scores were summated, 76% of this total was derived from signal peptide containing proteins, indicating 76% of detection ability was devoted to sequencing secretory proteins. Of the 66 proteins that incorporated the SILAC label, 31 proteins were increased by at least 2-fold from visceral derived microvascular endothelial cells, whereas only 19 proteins were increased by at least 2-fold from subcutaneous derived microvascular endothelial cells. Once proteins lacking an N-terminal signal were excluded, 21 of 34 secreted proteins (62%) were increased more than 2- fold from visceral derived microvascular endothelial cells, and only 5 secreted proteins were increased more than 2-fold from subcutaneous derived microvascular endothelial cells. The frequency distribution of the visceral to subcutaneous ratio for detected proteins is shown in Fig. 4. Once again, these data are skewed towards increased protein secretion from visceral derived endothelial cells (Fig. 4). This is consistent with the enhanced secretory capacity of visceral adipose tissue that was observed in both minced whole adipose tissue and isolated preadipocytes. The proteins identified include a number of proteins known to be secreted from endothelial cells, including thrombospondin-1 and thrombospondin-2, and extracellular matrix proteins such as fibronectin and collagens. In addition, several proteins not previously known to be secreted from adipose tissue derived microvascular endothelial cells were identified.

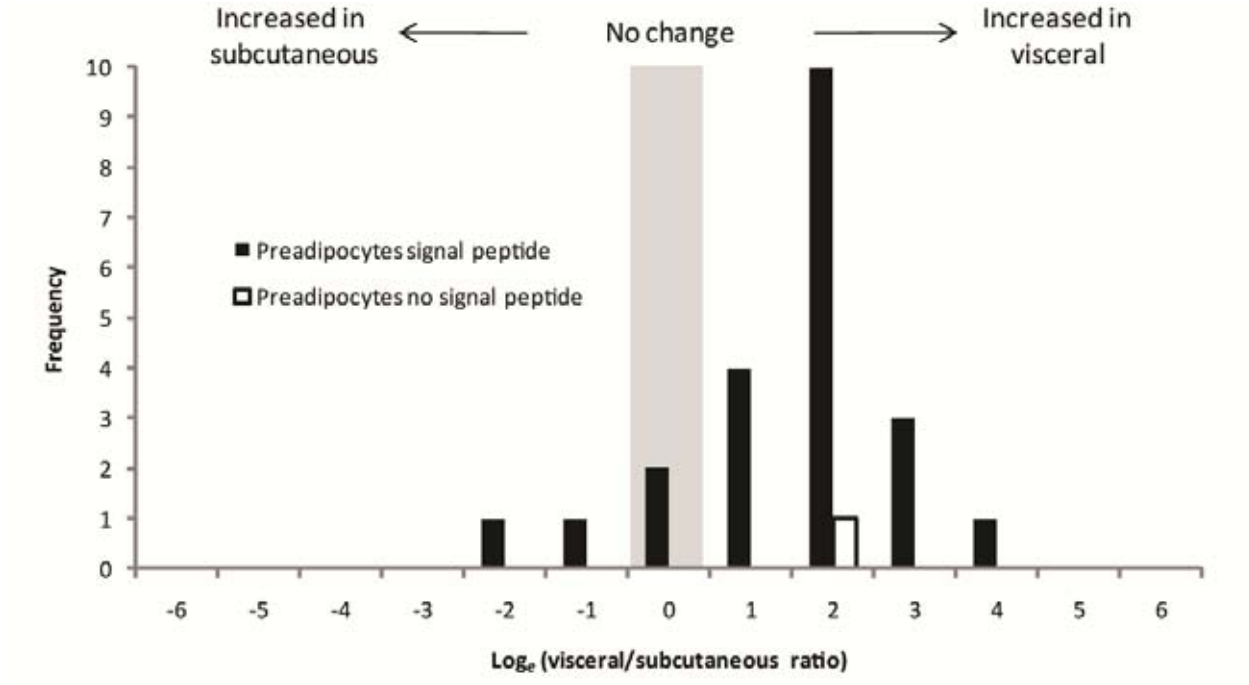

Figure 3. Preadipocyte secreted proteins are secreted at greater amounts from visceral derived preadipocytes. Preadipocytes isolated from visceral and subcutaneous WAT depots were cultured in media containing two different isotopes of arginine and lysine. LAC-CILAIR mass spectrometry was performed, and isotopic ratios calculated. Histogram shows distribution of visceral to subcutaneous ratios for proteins detected. Note use of natural log scale.

Accession	Score	visceral / ^{12}C	subcut / ^{12}C	visceral / subcut	subcut / visceral	Description	signal peptide?
TENA_MOUSE	1082	1.2607	0.159	0.1746	0.9585	Tenascin	1
AEBP1_MOUSE	994	0.202	0.3621	14.616	0.0512	Adipocyte enhancer-binding protein 1	1
COL1A2_MOUSE	855	2.904	0.0436	0.1228	3.9031	Collagen alpha-2(I) chain	1
TSP1_MOUSE	842	0.0012	0.2726	1.4505	0.5318	Thrombospondin-1	1
IC1_MOUSE	791	0.0343	0.8245	4.7622	0.104	Plasma protease C1 inhibitor	1
EMIL1_MOUSE	546	582.837	0.0041	0.0258	25.0008	EMILIN-1	1
PGS1_MOUSE	462	0.0657	0.5655	7.9442	0.1298	Biglycan	1
CO1A1_MOUSE	426	0.136	0.165	2.9346	0.0947	Collagen alpha-1(I) chain	1
PGBM_MOUSE	405	0.8171	0.0019	0.7816	1.2762	Basement membrane-specific heparan sulfate proteoglycan core protein	1
PGS2_MOUSE	363	0.0702	0.2934	3.5699	0.2713	Decorin	1
CO3A1_MOUSE	290	0.0092	0.1544	3.9785	0.4259	Collagen alpha-1(III) chain	1
PAI1_MOUSE	225	0.0191	0.1778	2.0433	0.4845	Plasminogen activator inhibitor 1	1
TITIN_MOUSE	225	0.1867	0.0217	0.3374	10.6359	Titin	0
1433Z_MOUSE	205	0.034	0.0954	0.4732	2.0953	14-3-3 protein zeta/delta	0
A2M_MOUSE	194	0.0002	4.288	9.6076	0.0042	Alpha-2-macroglobulin	1
LIPL_MOUSE	191	2.2195	0.8978	1.695	0.2307	Lipoprotein lipase	1
ACTBL_MOUSE	182	0.0002	160.23	0.1492	5.2137	Beta-actin-like protein 2	0
APOE_MOUSE	167	0.5233	1.1052	3.1261	0.3198	Apolipoprotein E	1
ITIH3_MOUSE	157	0.1795	0.0519	0.2654	3.7673	Inter-alpha-trypsin inhibitor heavy chain H3	1
H2B1C_MOUSE	155	0.7296	1.0693	1.7378	0.058	Histone H2B type 1-C/E/G	0

Table 3. Comparative secretion of proteins identified from visceral and subcutaneous adipose tissue derived endothelial cells. Visceral or subcutaneous WAT derived endothelial cells were incubated in media containing different isotopes of arginine and lysine. Conditioned media were mixed, subjected to lectin affinity chromatography and subjected to quantitative mass spectrometry. Peak height ratios of isotope to endogenous (^{12}C) amino acids and ratios between isotopes are shown. Complete dataset available in supplementary data.

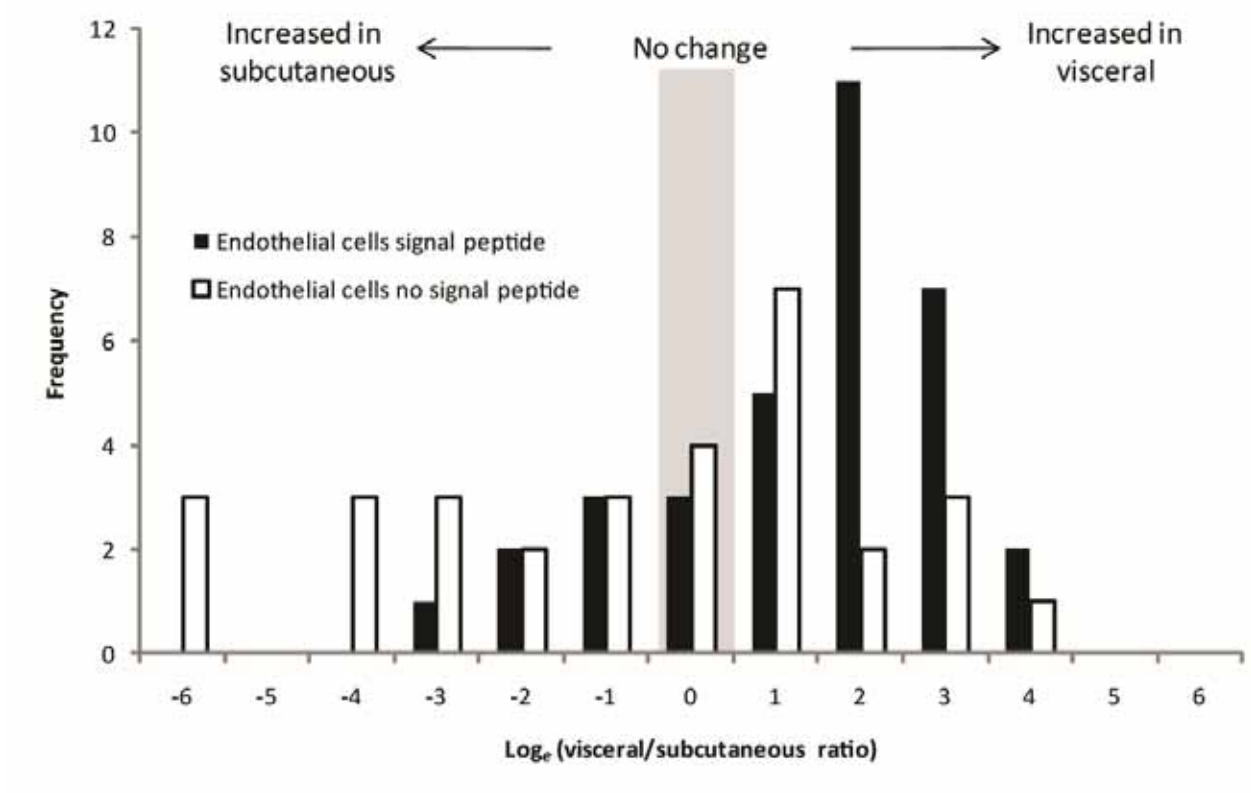

Figure 4. Endothelial cell secretory proteins are secreted at greater amounts from visceral derived endothelial cells. Endothelial cells from visceral and subcutaneous WAT depots were cultured in media containing two different isotopes of arginine and lysine. LAC-CILAIR mass spectrometry was performed, and isotopic ratios calculated. Histogram shows distribution of visceral to subcutaneous ratios for proteins detected. Note use of natural log scale.

These include the most abundantly detected protein that incorporated label, adipocyte enhancer binding protein 1 (AEBP1). This secretory protein has been proposed to influence adipocyte differentiation via a direct interaction with the aP2 promoter sequence in the nucleus. It has also been shown to influence inflammation in macrophages via a direct interaction with LXR and PPARγ sites. Multiple members of the complement pathway were also identified. Cluster analysis showed proteins more abundantly secreted from visceral endothelial cells were involved in extracellular matrix formation, including collagen and fibronectins, and endopeptidase inhibition, including members of the Serpin family. There were no defined clusters for the five secretory proteins that were more abundantly secreted from subcutaneous compared to visceral endothelial cells.

When the secretome of whole adipose tissue explants, preadipocytes and microvascular endothelial cells was compared, eight common secreted proteins were identified (Fig. 5). Seven secreted proteins were shared between the whole adipose tissue and microvascular endothelial cell secretomes and four between the whole adipose tissue and preadipocyte secretomes. These shared proteins included proteins involved in extracellular matrix formation, such as collagen and fibronectin and other proteins known to be produced by adipocytes such as osteonectin. Interestingly these data suggest that the majority of proteins identified in the whole adipose tissue secretome are secreted either by adipocytes themselves or by other cells in the stromovascular fraction such as macrophages and neurons. To interrogate this further the secretome of whole adipose tissue explants was compared to the secretome of differentiated 3T3-L1 adipocytes (previously published by (Crowe, Wu et al. 2009) and in Chapter 2).

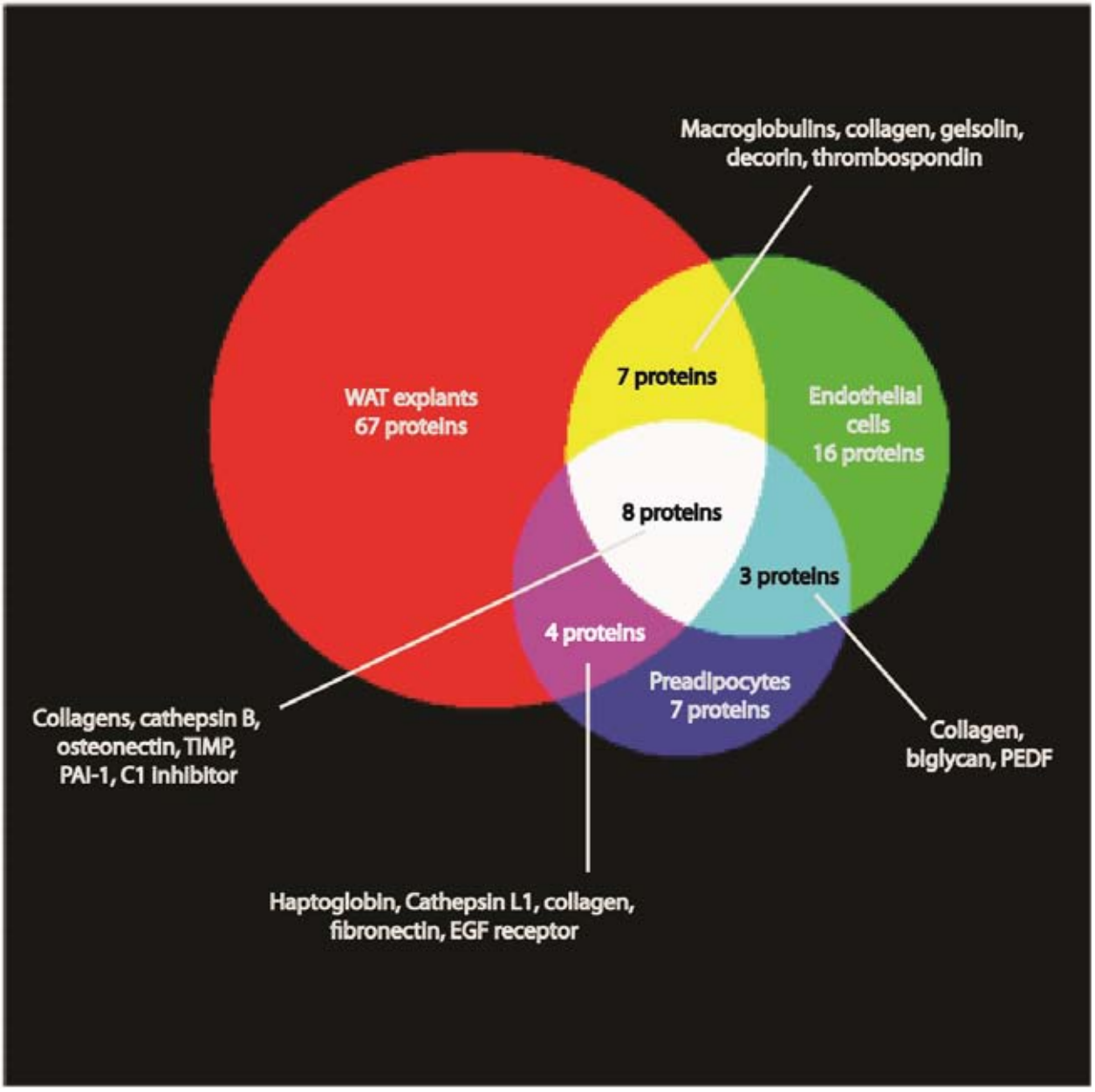

Figure 5. Venn diagram showing overlapping proteins detected from samples. A total of 116 secretory proteins were detected across all samples. PEDF – pigment epithelial derived factor, PAI-1 – plasminogen activator inhibitor 1, TIMP – tissue inhibitor of metalloproteinase 1. Diagram composed using 3-Venn applet (Chow and Rodgers 2005).

Of the 86 proteins identified in the whole adipose tissue secretome, 26 were shared with 3T3-L1 adipocyte secretome (Figure 6). These data suggest that adipocytes are not the principal source of proteins in the whole adipose tissue secretome. As 3T3-L1 adipocytes are an immortalised cell-line and may display differences to primary adipocytes, the secretome of whole adipose tissue explants was compared to the secretome of isolated rat adipocytes, previously published by Chen et al (2005) (Chen, Cushman et al. 2005). Only 21 common proteins were detected which included proteins known to be secreted from adipose tissue – adiponectin, SPARC, gelsolin and adipsin (Fig. 6). These data confirm that adipocytes alone are not the principal source of secreted proteins. It is possible that other cell types in the stromovascular fraction such as macrophages and neurons may be the source of secreted proteins, however as the adipose tissue used in the study came from lean animals, the expected number of adipose tissue macrophages should be low. An alternative explanation is that the secretome of whole adipose tissue is the result of a complex paracrine interaction between the multiple cell types within the adipose tissue and that the adipose tissue secretome is not merely the sum of the secretomes of each of its component parts.

Figure 6 – Venn diagram showing overlap of protein secretion from WAT explants, 3T3-L1 adipocytes and isolated rat adipocytes (from Chen et al 2005). The 12 proteins detected in all three samples were adiponectin, adipsin, angiotensinogen (SerpinA8), cathepsin B, cathepsin D, collagen α-1(IV), collagen α-2(IV), complement C1s, haptoglobin, laminin subunit β-2, osteonectin, and thrombospondin-1. Diagram composed using 3-Venn applet (Chow and Rodgers 2005).

Discussion

In this study, three important observations were made. Firstly, it was found that the overall secretory capacity of visceral adipose tissue is considerably higher than that of subcutaneous adipose tissue and secondly, that this enhanced secretory capacity of the visceral depot extended to cells of the stromovascular fraction – preadipocytes and microvascular endothelial cells. Thirdly, adipose tissue as a whole secretes more proteins than its individual component parts. This suggests it is inappropriate to consider the adipocyte *per se* to be the principal secretory component of adipose tissue in isolation. It is more likely that the secretome of adipose tissue is a function of the complex interplay of the component cell types. Therefore, when studying the physiology of adipose tissue it is important to interrogate the tissue as a whole, rather than isolated adipocytes alone, in order to preserve this important cross-talk which dictates the physiological functions of adipose tissue.

To interrogate the adipose tissue secretome, two previously published techniques were combined, CILAIR (Roelofsen, Dijkstra et al. 2009) and LAC (Crowe, Wu et al. 2009) as a streamlined method to exclude contaminating proteins from entrapped serum, including highly abundant proteins such as albumin, and intracellular contents from damaged cells. Metabolic labelling has been validated as a tool to reliably identify the source of proteins in conditioned media (Alvarez-Llamas, Szalowska et al. 2007). Proteins that incorporate the label are newly synthesized by the tissue under analysis and not derived from contaminants. LAC selectively enriches for proteins targeted for secretion, thus overcoming contamination from dead or damaged cells. Abundant serum proteins, such as albumin, that are non-glycosylated are

removed. This obviates the need for multiple washing steps to dilute these contaminating serum proteins, decreasing sample processing time and the negative impact of prolonged tissue handling on results. The use of LAC may overlook the identification of non-glycosylated proteins and indeed leptin was not detected in this analysis. In comparing this study to previous studies of the whole adipose tissue secretome 25 common proteins were identified. These included adiponectin, adipsin, complement C3 and gelsolin (Kratchmarova, Kalume et al. 2002; Wang, Mariman et al. 2004; Alvarez-Llamas, Szalowska et al. 2007). Therefore the technique of LAC-CILAIR is a useful and valid tool for interrogation of the adipose tissue secretome.

Visceral adipose tissue explants secreted proteins at a greater rate than subcutaneous adipose tissue (59% vs. 21% of proteins upregulated more than 2-fold). This upregulation of protein secretion from the visceral depot was consistent across whole adipose tissue explants and cells of the stromovascular fraction – preadipocytes and microvascular endothelial cells. Preadipocytes and microvascular endothelial cells were cultured *in-vitro* for at least one week prior to the application of labelled media, thus overriding potential paracrine influences from their depot of origin. This suggests that the up-regulation of protein secretion is an intrinsic characteristic of components of the visceral adipose depot. A smaller number of proteins were secreted in greater abundance from subcutaneous adipose tissue explants, so these results cannot be confounded by the technique used here, which may selectively detect protein secretion from the visceral depot.

Cluster analysis of proteins secreted in greater abundance from visceral adipose tissue revealed members of the acute phase response and proteins involved in the innate immune system. These data raise two interesting hypotheses. The first is that visceral adipose tissue is more pro-

angiogenic than subcutaneous adipose tissue, as many members of the acute phase response, for example haptoglobin (Park, Baek et al. 2009) and complement pathway proteins (Rohrer, Long et al. 2009), are involved in angiogenesis. The capacity for angiogenesis is a crucial requirement for adipose tissue expansion. The second hypothesis is that visceral adipose tissue secretes pro-inflammatory cytokines. This is consistent with recent data that visceral adipose tissue, particularly in obesity, develops chronic low-grade inflammation with macrophage infiltration, which in turn leads to insulin resistance.

The up-regulation of protein secretion observed in visceral whole adipose tissue, also held true in visceral compared with subcutaneous preadipocytes (68% vs. 0%) and endothelial cells (62% vs. 15%, respectively). These data are summarised in Table 4. Cluster analysis of the 14 proteins secreted more abundantly from visceral preadipocytes revealed proteins involved in extracellular matrix production. This, together with the finding that visceral adipose tissue secretes pro-angiogenic factors, these data suggest that visceral preadipocytes are better adapted for rapid adipose tissue expansion than subcutaneous preadipocytes. Of the 21 proteins secreted in greater abundance from visceral microvascular endothelial cells, many were involved in extracellular matrix production and macrophage recruitment. These data support the adipose tissue explant and preadipocyte data that visceral adipose depots are primed for expansion compared with subcutaneous depots. It also suggests that adipose tissue microvascular endothelial cells play a pivotal role in adipose tissue inflammation by enticing circulating blood macrophages into the adipose tissue.

	WAT explants	Endothelial cells	Preadipocytes
incorporated label	146	66	23
signal peptide	86	34	22
signal peptide, visceral / subcutaneous ratio > 2	50	21	11
signal peptide, subcutaneous / visceral ratio > 2	19	5	0
no signal peptide, visceral / subcutaneous ratio > 2	23	10	1
no signal peptide, subcutaneous / visceral ratio > 2	22	14	0
% of proteins identified with signal peptide	62%	52%	96%
% of total ion score from signal peptide containing proteins	88%	76%	99%

Table 4. Summary of numbers of proteins detected, and relative abundance between visceral and subcutaneous adipose tissue samples.

This study represents the first survey of the endothelial cell secretome. In comparing endothelial cells from visceral and subcutaneous adipose tissue depots, significant differences in protein secretion were demonstrated. Among the endothelial secretome, were known endothelial secretory proteins like thrombospondins 1, 2 and 3, as well as a number of proteins not previously documented as endothelial secreted factors. Surprisingly, many were known adipocyte secretory proteins, including growth arrest specific 6 (GAS6), plasminogen activator inhibitor-1 (PAI-1), periostin, pentraxin-related protein 3 (PTX3) and SPARC. Of particular interest was the identification of adipocyte enhancer binding protein 1 (AEBP1), a secreted protein that has been proposed to act as a transcriptional repression factor through binding of the enhancer sequence of the aP2/FABP4 gene in adipocytes, as well as PPARγ and LXR sites in macrophages (He, Muise et al. 1995; Majdalawieh, Zhang et al. 2006). Preadipocytes deficient in AEBP1 are hyperproliferative, with enhanced adipogenesis (Ro, Zhang et al. 2007). AEBP1 can be detected in whole WAT samples, but when adipocytes are purified from adipose tissue, AEBP1 cannot be detected (Ro, Kim et al. 2001). Considering the discovery of AEBP1 secretion from endothelial cells, it is considered likely that AEBP1 is principally derived from the endothelial component of adipose tissue. As was the case for other secretory proteins, AEBP1 was secreted in greater abundance from visceral than subcutaneous depots. This observation could be important for explaining the deleterious effects of visceral adipose tissue.

This study interrogated the secretome of whole adipose tissue explants and subsequently the secretome of cells of the stromovascular fraction, preadipocytes and microvascular endothelial cells, to determine which component of adipose tissue was principally responsible for adipokine secretion. A total of 115 proteins were identified from these three samples, of which 67 were

unique to adipose tissue explants, 16 were unique to endothelial cells, and 7 were unique to preadipocytes. There were 8 proteins identified across all samples, including members of the collagen family, osteonectin, metalloproteinase inhibitor 1, C1 esterase inhibitor, plasminogen activator inhibitor-1 and cathepsin B. When the secretome of whole adipose tissue was compared with the secretomes of differentiated 3T3-L1 adipocytes and primary rat adipocytes, relatively few common proteins were identified. These data infer that adipocytes are not the principal source of secreted proteins in adipose tissue. Given that adipose tissue explants utilised in this study were obtained from young, lean animals, the number of macrophages within the adipose tissue explants used should be low. Therefore, it is unlikely that macrophages made a significant contribution to the adipose tissue secretome in this study. This leads to the conclusion that the secretome of whole adipose tissue is not the sum of the secretomes of each of its component parts, but is the result of an interaction between the multiple cell types within the adipose tissue. This means that studying adipocytes or cells of the stromovascular fraction in isolation is disadvantageous, as the complex nature of adipose tissue is disrupted and key elements may be missed. This has significant implications for the future study of adipose tissue.

Chapter 5

The role of fatty acid binding protein 4 in the adipo-insular axis

Lindsay Wu

Isolation and stimulation of islets were performed in collaboration with Dr. James Cantley, Garvan Institute of Medical Research. Data from this chapter were accepted as an abstract, "Non-classical secretion of adipocyte fatty acid binding protein" Wu LE, Cantley J, Burchfield JG, James DE for the 2010 Hunter Cell Biology Meeting, Hunter Valley, NSW, Australia. Supplementary mass spectrometry data for this chapter are provided in the attached DVD-ROM.

Abstract

Adiposity correlates closely with fasting insulin levels and β cell mass, though it is not necessarily associated with insulin resistance or type 2 diabetes. This implies the existence of inter-organ communication between adipose tissue and the β cell, which may involve a secretory component. Rapid expansion of white adipose tissue results in hypoxia due to insufficient vascularisation. It was postulated that hypoxia leads to the secretion of a factor from the adipocyte to enhance β cell function and insulin release, to support adipose tissue expansion, tissue remodelling and angiogenesis. To test this, adipocytes were cultured under hypoxic conditions, and conditioned media from these cells was used to treat primary islets. Whereas conditioned media from normoxic cells had no effect on glucose - stimulated insulin secretion (GSIS) from islets, conditioned media from hypoxic adipocytes increased glucose - stimulated insulin secretion by 70%. Using quantitative mass spectrometry, FABP4 was identified as a major hypoxia-inducible adipocyte secretory factor. Purified FABP4 enhanced GSIS in a manner similar to hypoxic adipocyte conditioned media. It is concluded that FABP4 is a hypoxia-inducible adipokine that plays a key role in the adipo-insular axis to enhance insulin secretion in response to the prevailing needs of adipose tissue.

Introduction

Within the past fifteen years, there has been an intense focus on the role of adipose tissue as an endocrine organ, due to its ability to regulate distal organs via adipose secretory proteins, termed adipokines (Galic, Oakhill et al. 2009). The most well studied of these is leptin, which influences appetite via an interaction with its cognate receptor in the hypothalamus of the brain (Friedman and Halaas 1998). Other adipokines include adiponectin, which mediates whole body insulin sensitivity (Kadowaki, Yamauchi et al. 2006), and retinol binding protein 4 (RBP4), which decreases insulin sensitivity in skeletal muscle (Yang, Graham et al. 2005). Although adipose tissue influences a number of distal processes, there is a paucity of data surrounding its interaction with the insulin producing β-cells of the pancreas.

There is good reason to believe that adipose tissue interacts with pancreatic β cells. It has long been known that adiposity is closely linked to fasting insulin levels, irrespective of peripheral insulin resistance (Bagdade, Bierman et al. 1967). The half-life of insulin in the circulation is 4-6 minutes (Duckworth, Bennett et al. 1998), and fasting insulin levels are measured after at least 10 hours of fasting, which precludes the effect of increased meal loads or delayed response to insulin after a meal, due to insulin resistance. This is a critical observation, as it is widely held that obesity-induced hyperinsulinaemia is due to β-cell compensation for insulin resistance. In addition, adiposity is closely linked to β-cell mass (Ferrannini, Camastra et al. 2004). The existence of a so called "adipo-insular axis" to explain the correlation between increased adiposity and β cell function has previously been proposed (Huypens 2007). Although explaining the correlation between adiposity and β-cell function, the proposed mechanism relies on the

adipokine leptin to mediate this interaction. Although leptin interacts with β-cells, it does so in an inhibitory rather than potentiating manner (Kieffer and Habener 2000). This is reflected by the enlarged β-cells of ob/ob mice, which lack leptin (Bock, Pakkenberg et al. 2003). Furthermore, the circulating concentrations of leptin, which inhibit β-cell function, increase with obesity (Considine, Sinha et al. 1996). In the absence of a mechanism for the adipo-insular axis, this study sought to identify the molecular player, which was assumed to be an adipocyte secretory protein, which may mediate a positive interaction between adipose tissue and β-cell function.

Numerous studies have used proteomics to identify adipocyte secretory proteins (Kratchmarova, Kalume et al. 2002; Wang, Mariman et al. 2004; Chen, Cushman et al. 2005; Alvarez-Llamas, Szalowska et al. 2007; Zvonic, Lefevre et al. 2007; Roelofsen, Dijkstra et al. 2009). While successful at identifying secretory proteins under non-stimulated conditions, there have been no attempts to quantitate changes in adipokine secretion during treatment with insults physiologically relevant to obesity. It is important to note that many metabolic insults previously used on adipocytes are relevant to insulin resistance, but not necessarily obesity. In this study, hypoxia was used to simulate obesity.

Adipose tissue hypoxia has come to light as an important phenomenon in obesity. During obesity, white adipose tissue expands in size through a combination of hypertrophy and hyperplasia. This expansion is accompanied by an increase in angiogenesis in this highly vascularised organ (Christiaens and Lijnen 2009), which is unique in the plasticity of its vasculature. The only instances of angiogenesis that occur in an adult human are during tumour

growth, obesity or tissue repair. Adipose tissue hypoxia is proposed to occur during obesity when fat depots expand faster than angiogenesis can occur, resulting in areas of insufficient vascularisation. This has been reported in genetic models of obesity (Yin, Gao et al. 2009), dietary-induced models of obesity (Ye, Gao et al. 2007), and in obese humans (Trayhurn, Wang et al. 2008). Hypoxia may result in insulin signalling defects (Yin, Gao et al. 2009), endoplasmic reticulum stress, mitochondrial dysfunction, low grade inflammation with accompanying macrophage infiltration, decreased adipokine secretion and cell necrosis (Ye 2009). As has been suggested in the case of hyperinsulinaemia, adipose tissue hypoxia results from obesity, and is not necessarily related to insulin resistance or type 2 diabetes. A link between adipose tissue hypoxia and β cell function, as mediated by the release of a humoural factor from adipose tissue, is herein proposed.

In this study, the effects of normal and hypoxic adipocyte conditioned media on β-cell function were investigated. Conditioned media from hypoxic adipocytes enhanced glucose-stimulated insulin secretion from β-cells. The filtration of conditioned media with a 10 kDa molecular weight cut-off filter did not affect the ability of hypoxic adipocyte conditioned media to potentiate glucose-stimulated insulin secretion, indicating that the factor(s) responsible for this effect on β-cells is either a protein or a protein bound molecule. Using a quantitative mass spectrometry approach, a screen for hypoxia-regulated adipocyte secretory proteins revealed fatty acid binding protein 4 (FABP4) as one of the few proteins whose secretion was increased during hypoxia. Physiologically relevant doses of FABP4 enhance β-cell function to a similar degree as observed in the serum of high fat fed animals. The secretion of this protein is of interest, as fatty acid binding protein does not possess an N-terminal signal peptide necessary for

classical protein secretion. These data provide an insight into non-classical protein secretion, which may be useful in understanding the secretion of other non-classically secreted proteins such as FGF-1 and IL-1. A key role for FABP4 in the adipo-insular axis is herein proposed.

Methods

SILAC labelling

All isotopes were from Cambridge laboratories. The "heavy" isotope of arginine was U-^{13}C6 U-^{15}N4 arginine (catalogue number CNLM-539), "heavy" lysine was U-^{13}C6 U-^{15}N2 lysine (catalogue number CNLM-291). "Light" (non-labelled) arginine and lysine were from Sigma. Growth media was low glucose Dulbecco's modified eagle media (DMEM) deficient in leucine, arginine, lysine and phenol red from Sigma (catalogue number D9443). Glucose was adjusted to 4.5 g/L, leucine was added to a concentration of 0.105 g/L, and phenol red was added to 0.0159 g/L. Arginine and lysine were added at 25% of normal concentration in DMEM to avoid conversion of excess isotopes into proline (O'Quinn, Knabe et al. 2002; Ong, Kratchmarova et al. 2003). Arginine isotopes were added back at a concentration of 0.021 g/L, lysine isotopes were added back at a concentration of 0.0365 g/L. After addition of all ingredients, media was passed through a 0.20 μm filter. 3T3-L1 adipocytes were cultured for at least 12 rounds of division in this media to achieve at least 80% labelling. Adipocytes were then seeded at 50% confluence and differentiated as described previously (MacDougald and Lane 1995).

Mass spectrometry

Samples were subjected to mass spectrometry as previously described (Larance, Ramm et al. 2005; Crowe, Wu et al. 2009). Samples were separated by SDS-PAGE on a 10% acrylamide gel. Lanes were excised and cut into 12 equal sized pieces, which were further cut into ~1 mm^3 cubes. Samples were treated with 50% acetonitrile in 500 mM ammonium bicarbonate for 30 min, then 100% acetonitrile for 10 min. Trypsin was added at 12.5 ng/µl in 100 mM ammonium bicarbonate and incubated overnight at 37°C. Tryptic peptides were extracted by addition of 100 µL of 5% formic acid for one hour at 37°C, followed by addition of 100 µL of acetonitrile for 1 h at 37°C, and an additional 500 µL of acetonitrile for 2 h. Samples were dried under vacuum, resuspended in 20 µL formic acid and subjected to mass spectrometry using a Waters Ultima quadrupole time of flight (QTOF) coupled to liquid chromatography. Peak picking and protein identification was performed using Mascot Distiller software package, version 2.3.1.0. MDRO 2.3.1.0 (Matrix Sciences). The SwissProt database on Mascot Server 2.2 was used for searches. Taxonomy was restricted to *Mus musculus*. MS mass tolerance was set to 0.5 Da, MSMS mass tolerance was set to 0.05 Da. Variable modifications selected were oxidation (M), propionamide and carbamidomethyl. Trypsin was set as cleavage enzyme after arginine or lysine and a maximum of 2 missed cleavages were permitted. Quantitation method was as follows. Method: constrain search – yes, protein ratio type – weighted, protein score type – standard, report detail – yes, minimum peptides – 1. Protocol: precursor, allow mass time match – yes, allow elution shift – no, all charge states – no. Component "light" was mode – exclusive, unmodified site – K, position – anywhere, unmodified site – R, position – anywhere. Component "heavy" was mode – exclusive, modification – Label: 13C(6)15N(2) (K), modification – Label: 13(6)15N(4) (R). Integration – trapezium, integration source – survey, precursor range – envelope. Quality:

minimum precursor charge – 1, isolated precursor – No, Minimum a(1) – 0.0, peptide threshold type – minimum score. Outlier – auto. For all ratios measured, numerators and denominators were set to 1.00.

Hypoxia

At day 8, adipocytes were washed extensively with PBS and changed to serum free media containing isotopes of arginine and lysine and supplemented with 1 nM insulin. "Heavy" labelled adipocytes were placed in a sealed chamber and a gas containing 1% oxygen, 5% CO_2 and 94% N_2 was pumped through the chamber for 5 min before being sealed. The chamber was placed in a 37°C incubator alongside "light" labelled adipocytes, which were left at atmospheric oxygen concentration (21% O_2). After 16 h, conditioned media was collected from adipocytes, centrifuged at 2,000 *g* for 10 min to pellet cell debris, and subjected to glycoprotein affinity purification, as described in chapters 1, 3 and in (Crowe, Wu et al. 2009). For subsequent experiments (all western blots), conditioned media was collected and subjected to TCA protein precipitation. TCA was added to samples at 25% of total volume, inverted, and left at -20°C for at least 30 min. Samples were centrifuged at 16,000 *g* at 4°C for 15 min, and pellets were subsequently washed twice by addition of 100% acetone cooled to -20°C, centrifuged at 16,000 *g* for 5 min at 4°C. Pellets were dried, and resuspended in laemli buffer supplemented with 50 mM TCEP.

Conditioned media experiments

Adipocytes at 8 days post differentiation were washed extensively with PBS and changed to RPMI1640 media supplemented with penicillin, streptomycin and glutamine and 1 nM insulin. Adipocytes were kept under normoxic or hypoxic conditions as described above for 16 hours. Conditioned media was collected and passed through a 0.22 µm filter to remove cell debris. For dialysed samples, conditioned media was dialysed extensively against RPMI1640 with PSG and concentrated to using an Amicon ultra centrifugal concentrating device with a molecular weight cut-off of 10,000 Da (Millipore cat. no. UFC901024). Concentrated media was resuspended to one third original volume in RPMI1640 with HEPES buffer, 10% FCS and PSG before application to islets.

Islet isolation

Primary islets were isolated from C57BL6 mice as previously described (Cantley, Selman et al. 2009), and this method is modified and reproduced here. Islets were treated for 18 h with adipocyte conditioned media, then incubated in low glucose RPMI1640 prior to stimulation with 20 mM glucose. Mice were sacrificed by cervical dislocation, and the common bile duct was cannulated and its duodenal end occluded by clamping. Liberase solution (2 ml at 0.25 mg/ml in HBSS) was injected into the duct to distend the pancreas. The pancreas was excised, incubated at 37°C for 15 min, and mechanically disrupted in 10 ml of HBSS (supplemented with 1% BSA). Cellular components were collected by centrifugation (201 *g* for 1 min), washed, and resuspended in 10 ml of KRBH (Krebs-Ringer buffer containing 2 mmol/l D-glucose and 10 mmol/l HEPES). Islets were hand-picked under a microscope and washed once in KRBH. Prior

to DNA or protein extraction, islets were collected by centrifugation at 5,724 *g* for 2 min and stored at –80°C. For insulin secretion studies, isolated islets were cultured overnight in RPMI1640, followed by overnight culture with adipocyte conditioned media diluted with 10% FCS, PSG and HEPES. Medium was replaced with KRBH 1 h prior to study. Dynamic insulin release was then assessed using a multichamber perifusion system at 37°C in a temperature-controlled environment. Insulin was measured in perifusate samples by radioimmunoassay, as previously described. Static insulin release was assessed using batch cultures of 5 islets in 150 µl KRBH plus additional D-glucose, 25 mmol/l KCl, or 10 mmol/l ketoisocaproic acid (Sigma-Aldrich) for 1 h at 37°C. Insulin release was measured by ELISA.

RT-PCR

Expression of FABP4 and GLUT1 from normoxic and hypoxic 3T3-L1 adipocytes was measured using Taqman probes Mm00445880_m1 and Mm00441473_m1 as according to manufacturer's instructions.

Antibodies, ELISA

Insulin secretion was measured with an insulin radioimmunoassay as previously described (Cantley, Selman et al. 2009). FABP4 was measured from serum using the FABP4 ELISA kit from MBL (cat. no. CY-8077). Extracellular histone bound DNA was measured by ELISA using a Cell Death Detection ELISA^{PLUS} kit from Roche. FABP4 antibody (D25B3) and cytochrome C antibody (4272) were from Cell Signaling Technologies, MA, USA. Tubulin antibody (DM1A) and adiponectin antibody (A6354) were from Sigma (Australia). Complement C3 antibody

(ICN55444) was from Aurora, OH, USA. Collagen (VI) antibody (610407) and 14-3-3 antibody (sc-629) were from Santa Cruz, CA, USA. Caveolin antibody was from BD Biosciences, CA, USA. FABP5 antibody was generated in the immunology department of the Garvan Institute, and was a kind gift from Ms. Heidi Schilter.

Results

Hypoxic adipocyte conditioned media potentiates GSIS

To probe a link between obese, hypoxic adipose tissue and β cell function, conditioned media experiments using cultured 3T3-L1 adipocytes and primary pancreatic islets were conducted. White adipose tissue contains adipocytes, preadipocytes, endothelial cells, macrophages and other cell types. Initially it was decided to focus on adipocytes alone. To do this, 3T3-L1 adipocytes were employed. These cells behave similarly to endogenous adipocytes *in vivo*, as they have similar rates of insulin-stimulated glucose uptake and insulin-stimulated suppression of lipolysis and they express most adipocytes-specific genes, including fatty acid synthase, GLUT4 and adiponectin (MacDougald and Lane 1995). They are, however, not a perfect model for *in vivo* adipocytes, as they express very low levels of the adipokine leptin (MacDougald, Hwang et al. 1995).

To simulate adipose tissue hypoxia, 3T3-L1 adipocytes were kept under an atmosphere of 1% oxygen for 18 hr. Conditioned media from these adipocytes was applied to primary islets, both unmodified and as filtered media. Filtered media had been dialysed against a 10 kDa molecular weight cut-off to remove small non-protein molecules, such as fatty acids and ions that may affect pH, and to retain protein and protein bound molecules only. Unmodified and filtered conditioned media samples were used to treat primary murine islets. After 18 hr of treatment, glucose - stimulated insulin secretion was measured. Conditioned media from control adipocytes had no statistically significant effect on insulin secretion from islets, however conditioned media from hypoxic adipocytes enhanced glucose-stimulated insulin secretion by around 70% (Fig. 1). This increase in insulin secretion occurred after treatment with both unmodified and filtered

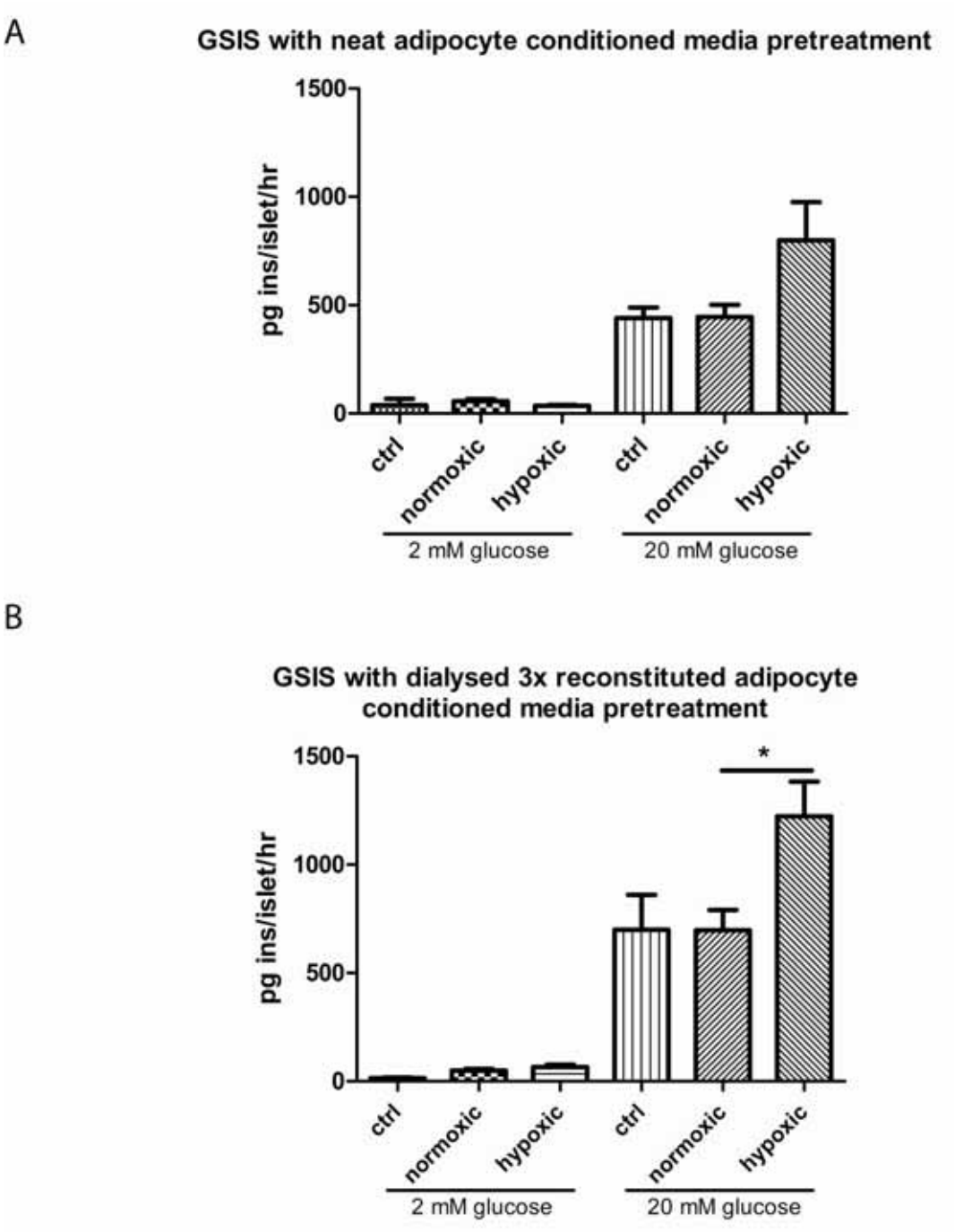

Figure 1 Hypoxic adipocyte conditioned media enhances GSIS from islets. A) Neat adipocyte conditioned media was applied to primary islets for 16 hours, and insulin release with glucose stimulation was measured. B) To exclude the effects of small (non-protein) molecules, conditioned media was dialysed against a 10 kDa amicon filter, and concentrated three times. Concentrated media was applied to primary islets for 16 hours, and insulin release with glucose stimulation was measured. Experiment repeated four times. *$p < 0.05$ by two-tailed *t*-test

conditioned media, indicating that the factor(s) responsible for enhanced insulin secretion are most likely protein, or protein bound.

Identification of FABP4 as an hypoxia regulated secretory protein

To identify the adipocyte secretory factor responsible for enhanced GSIS, quantitative mass spectrometry using the recently established technique of stable isotope labelling of amino acids in cell culture (SILAC) (Ong, Blagoev et al. 2002) was performed, as described in methods and in previous chapters. After cells had been subcultured in SILAC media, a label incorporation rate of 80% was observed. "Light" and "heavy" labelled adipocytes were incubated with serum free media for 18 h under either normoxic or hypoxic (1% O_2) conditions. Conditioned media was collected, mixed, and purified proteins were enriched by glycoprotein affinity purification as previously described (Crowe, Wu et al. 2009). Samples were subjected to tandem mass spectrometry, and isotopic ratios measured to obtain relative differences in protein abundance (Table 1). Overall, hypoxia led to a reduction in the secretion of most protein species. Adiponectin was decreased with hypoxia, an observation that is consistent with previous studies (Chen, Lam et al. 2006; Hosogai, Fukuhara et al. 2007). Notably, the secretion of few proteins was up-regulated with hypoxia (highlighted in grey, Table 1). Of the proteins that were increased with hypoxia, two of these were fatty acid binding proteins. They were adipocyte fatty acid binding protein (FABP4 – also known as ap2) and epithelial fatty acid binding protein (FABP5 – also known as Mal1). The fatty acid binding protein family shows some homology and the expression of the members of this family is tissue specific (Fig. 2).

Accession	Score	Hypoxia / normoxia	SD (geo)	# peptides	Description
P01027|CO3_MOUSE	4720	0.2352		55	Complement C3
Q01149|CO1A2_MOUSE	4001	0.3925		39	Collagen alpha-2(I) chain
P04117|FABP4_MOUSE	1560	1.296		11	Fatty acid-binding protein, adipocyte
P20152|VIME_MOUSE	1505	0.8417		15	Vimentin
P20029|GRP78_MOUSE	1468	0.6169		15	78 kDa glucose-regulated protein
P11499|HS90B_MOUSE	1458	0.9496		17	Heat shock protein HSP 90-beta
P63017|HSP7C_MOUSE	1401	1.352	5.195	16	Heat shock cognate 71 kDa protein
P11087|CO1A1_MOUSE	1239	0.4178		16	Collagen alpha-1(I) chain
Q60994|ADIPO_MOUSE	1050	**0.171**	**4.02**	**8**	Adiponectin
P07901|HS90A_MOUSE	964	1.04		8	Heat shock protein HSP 90-alpha
P56480|ATPB_MOUSE	889	0.7963		10	ATP synthase subunit beta, mitochondrial
P08121|CO3A1_MOUSE	837	0.4326		14	Collagen alpha-1(III) chain
P17156|HSP72_MOUSE	802	1.103	10.02	10	Heat shock-related 70 kDa protein 2
P48678|LMNA_MOUSE	781	0.5092		16	Lamin-A/C
P28653|PGS1_MOUSE	694	0.5006		7	Biglycan
Q02788|CO6A2_MOUSE	633	0.3557		11	Collagen alpha-2(VI) chain
P70663|SPRL1_MOUSE	633	0.295		13	SPARC-like protein 1
P09405|NUCL_MOUSE	598	0.6709	33.01	8	Nucleolin
Q61646|HPT_MOUSE	588	**0.295**	**1.416**	**5**	Haptoglobin
Q04857|CO6A1_MOUSE	584	0.5924		11	Collagen alpha-1(VI) chain
Q9Z2U0|PSA7_MOUSE	580	0.9762	1.208	6	Proteasome subunit alpha type-7
P11152|LIPL_MOUSE	569	0.2183		7	Lipoprotein lipase
Q9R1E6|ENPP2_MOUSE	546	0.3145	9.342	12	Ectonucleotide pyrophosphatase/ phosphodiesterase family member 2
P08003|PDIA4_MOUSE	545	0.6063		10	Protein disulfide-isomerase A4
P16627|HS71L_MOUSE	521	0.9969	6.664	5	Heat shock 70 kDa protein 1L
P40142|TKT_MOUSE	464	1.121	10.15	8	Transketolase
P35700|PRDX1_MOUSE	426	1.102		6	Peroxiredoxin-1
P11859|ANGT_MOUSE	419	0.3344	8.214	3	Angiotensinogen
P21460|CYTC_MOUSE	392	0.3603		3	Cystatin-C
P19096|FAS_MOUSE	350	0.08798	14.18	7	Fatty acid synthase
P08113|ENPL_MOUSE	343	0.914		4	Endoplasmin
Q9CQN1|TRAP1_MOUSE	343	0.09174	168.8	3	Heat shock protein 75 kDa, mitochondrial
P49722|PSA2_MOUSE	338	0.04047	427.3	6	Proteasome subunit alpha type-2
Q9DD06|RARR2_MOUSE	338	0.2709		5	Retinoic acid receptor responder protein 2
P26041|MOES_MOUSE	337	0.7244	1.639	8	Moesin
P10493|NID1_MOUSE	319	0.7337	1.213	4	Nidogen-1
Q05816|FABP5_MOUSE	94	1.936	1.076	2	Fatty acid-binding protein, epidermal

Table 1. MS quantitation of secreted protein abundance during hypoxia. SILAC labelled 3T3-L1 adipocytes were left in serum free media for 16 hours under hypoxic (1% O_2) or normoxic conditions. Conditioned media was collected, mixed in equal proportions, glycoprotein affinity purification performed and proteins subjected to quantitative mass spectrometry. The ratio of hypoxic to normoxic protein abundance is shown. All proteins upregulated during hypoxia are shown in grey. Experiment performed twice, with inversion of isotopes between experiments.

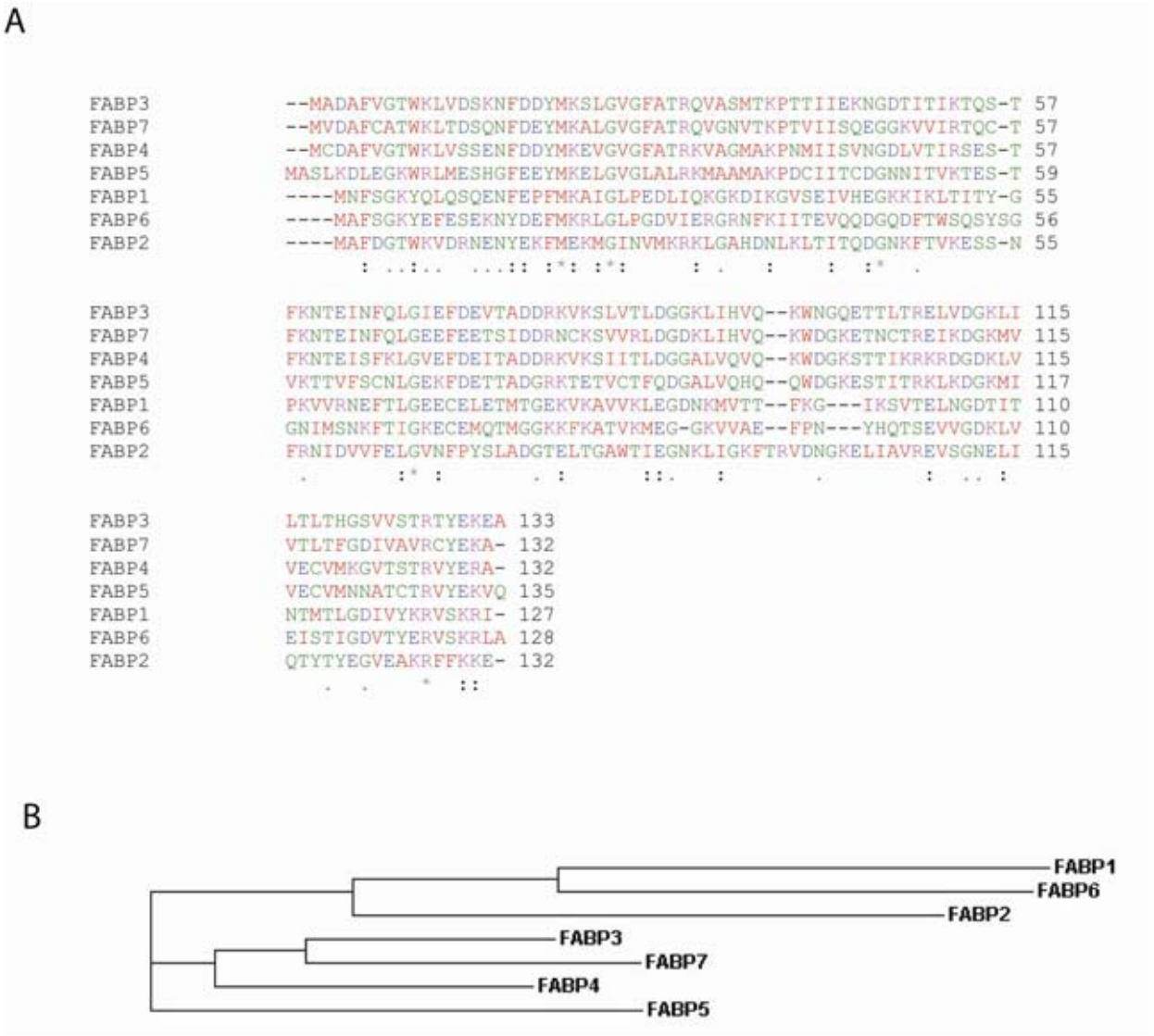

Figure 2. Alignment and phylogeny of fatty acid binding proteins. A) Sequence alignment of members of the fatty acid binding protein family. B) Phylogram of relationships between members of the fatty acid binding protein family. Alignments and pylogeny calculated using ClustalW (Larkin, Blackshields et al. 2007).

In this study, it was decided to focus on FABP4 rather than FABP5. While FABP4 is expressed almost exclusively in adipose tissues, FABP5 is also expressed in epithelia and in macrophages. The adipose tissue expression specificity of FABP4 compared to FABP5 is shown in Fig. 3. FABP4, also known as aP2, is abundantly expressed in adipocytes, and its promoter is often used to drive the expression of white adipose tissue specific knockout animals. FABP4 expression levels are influenced by hypoxia in human trophoblasts (Biron-Shental, Schaiff et al. 2007). To confirm the increased secretion of FABP4 during hypoxia seen by mass spectrometry, precipitated protein from conditioned media samples were immunoblotted using FABP4 specific antisera (Fig. 4a). This was further confirmed through the ELISA measurements of FABP4 concentrations in adipocyte conditioned media (Fig. 4b). These data confirm the increased secretion of FABP4 during hypoxia. There may be several possible mechanisms for this increase. FABP4 secretion alone may be specifically regulated, in which case a depletion of intracellular FABP4 might be observed. In Fig. 4a, no change in intracellular FABP4 levels were observed. In Fig. 5, 1.25% of the conditioned media released over 18 hours was immunoblotted alongside 0.3% of total cell lysates. A similar amount of FABP4 was observed in hypoxic adipocyte cell lysates and hypoxic conditioned media. Given the amount loaded, extracellular FABP4 equated to approximately 30% intracellular levels. If this 30% were not replaced through new protein synthesis, a 30% difference should have been observed between normoxic and hypoxic cell lysates. No difference was observed, indicating secreted FABP4 must be replaced in the adipocyte through new protein synthesis. To replenish the intracellular levels of FABP4, hypoxia must result in an increased level of gene transcription and/or protein synthesis. To measure transcription, FABP4 mRNA was measured using real-time PCR (Fig. 5). The expression of the basal glucose transporter GLUT1 was also measured as a control for the effects of hypoxia. The

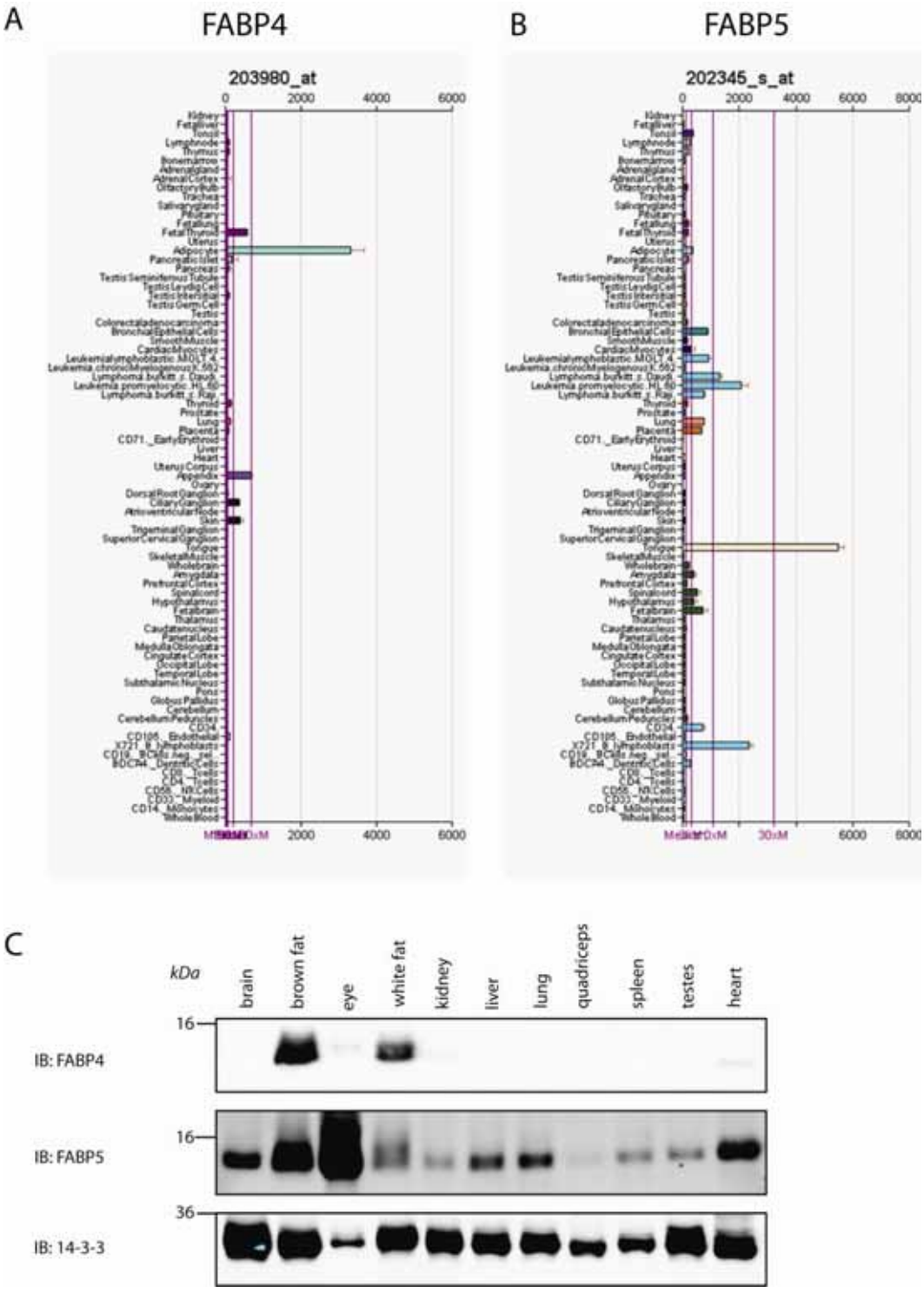

Figure 3. FABP4 is more adipose-specific than FABP5. Gene expression data for A) FABP4 and B) FABP5. C) Tissues were obtained from C57BL6 mouse and 5 µg protein immunoblotted with FABP4 and FABP5 specific antibodies. Gene expression data obtained previously (Su, Wiltshire et al. 2004) and compiled using BioGPS database biogps.gnf.org

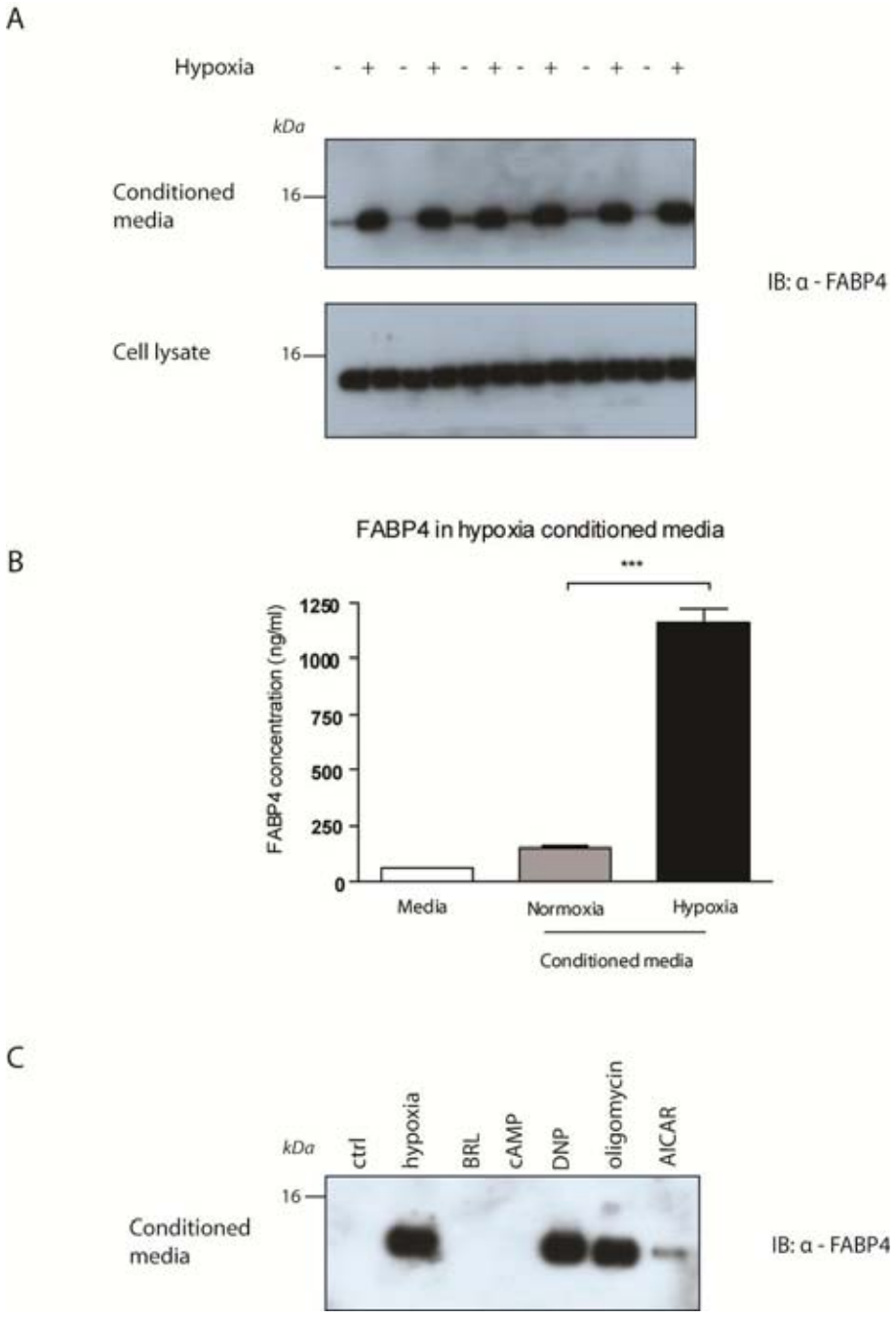

Figure 4. FABP4 is released from adipocytes under conditions of hypoxia and mitochondrial stress. A) 3T3-L1 adipocytes were left in serum free media under an atmosphere of 1% oxygen to stimulate hypoxia. Conditioned media was collected and proteins precipitated using TCA precipitation. Corresponding cell lysates were obtained, and 10 µg protein loaded. Samples were immunoblotted with FABP4 specific antibody. B) ELISA measurement of FABP4 concentration in filtered conditioned media samples used in figure 1. C) Adipocytes were left under normal conditions (ctrl), hypoxia (1% O_2), or incubated with β-3-adrenergic receptor ligand BRL, dibutryl cyclic AMP, di-nitrophenol (DNP) (10 µM) or oligomycin (5 µM) for 16 hr in serum free media. Conditioned media was collected, proteins precipitated using TCA precipitation. Samples were immunoblotted with FABP4 specific antibody. *** $p<0.001$ by two tailed *t*-test. Figure A) repeated 5 times, figure C) repeated 3 times.

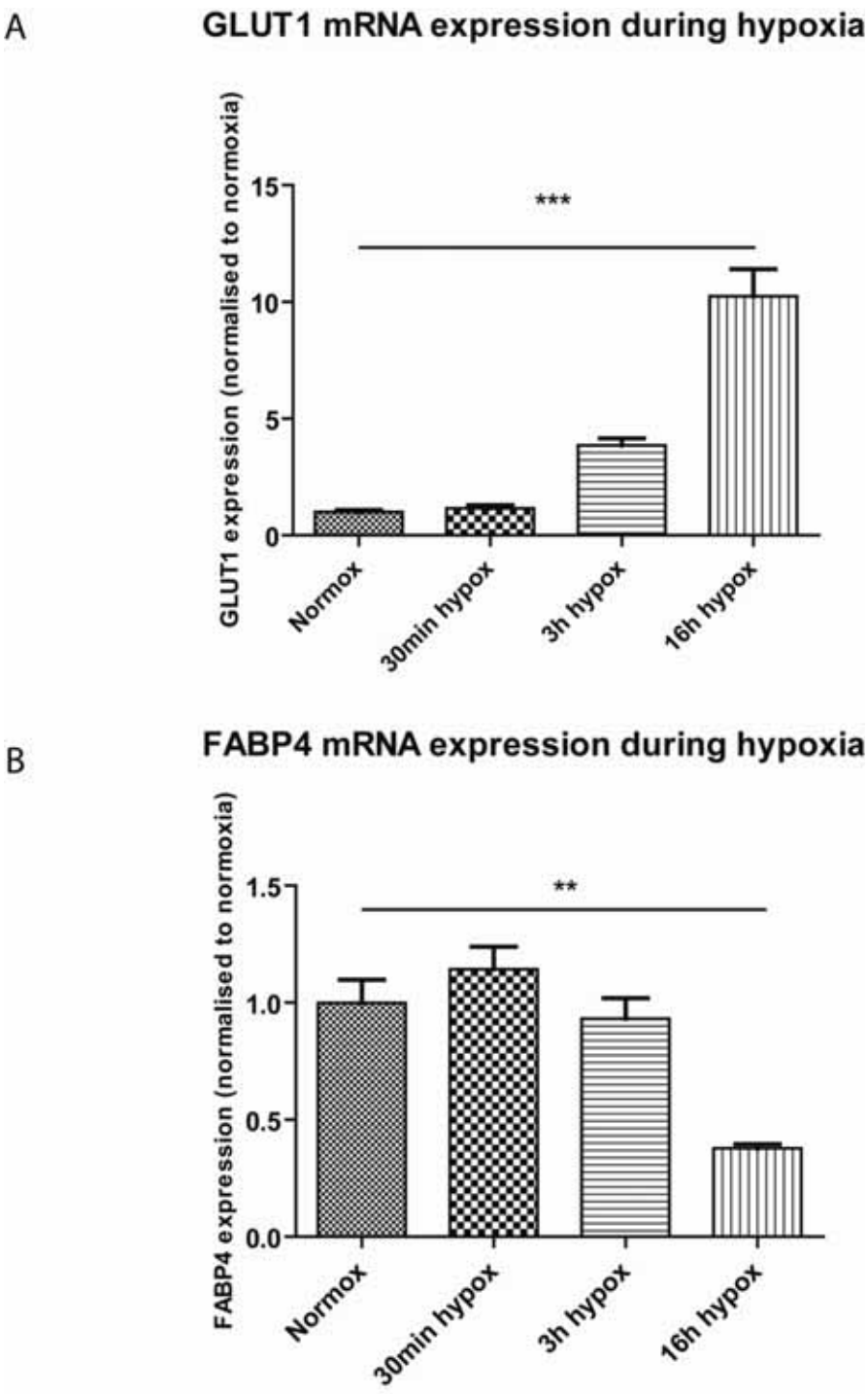

Figure 5. Expression of FABP4 is decreased during hypoxia. 3T3-L1 adipocytes were scraped, and RNA was extracted after indicated periods of hypoxia. Gene expression was subsequently measured by RT-PCR. A) Expression of HIF1α target gene GLUT1 was increased during hypoxia. B) Expression of FABP4 was decreased during hypoxia. **p<0.005, ***p<0.0001 by two-tailed *t*-test.

expression of this gene increases during hypoxia, as it is a target of the hypoxia responsive transcription factor HIF1α (Chen, Pore et al. 2001). Unexpectedly, a decrease in FABP4 expression was observed. The final possibility indicated by this is that FABP4 synthesis from existing mRNA must be increased, and it is possible that there is some form of negative feedback signalling to the nucleus to decrease FABP4 transcription.

One possible explanation for increased extracellular FABP4 is that this protein, which is a cytosolic protein, is non-specifically released from damaged or necrotic hypoxia-sensitive cells. If this were the case, one would anticipate the presence of other cytosolic proteins in the media. To test this, conditioned media samples and cell lysates were immunoblotted with antibodies specific for a range of extracellular and intracellular markers (Fig. 6). Hypoxia did result in an increase in the extracellular presence of cytosolic markers β-tubulin and the plasma membrane marker caveolin. However, when the amount of extracellular protein was compared to the amount of intracellular protein, FABP4 was released to a much greater extent (Fig. 6c). The extracellular to intracellular ratio during hypoxia of FABP4 was around 1.3, whereas the same ratio for tubulin was around 0.2, and for caveolin was around 0.05. Decreased extracellular presence of the secreted proteins complement C3 and adiponectin during hypoxia was also observed, confirming data obtained by SILAC/mass spectrometry (Table 1). Interestingly, very little complement C3 was observed in cell lysates when compared to conditioned media, indicating constitutive secretion of complement C3, rather than intracellular storage and regulated release. This is to be contrasted with adiponectin, which primarily resides in the ER where it is retained through disulfide bonding to the ER chaperone ERp44 (Wang, Schraw et al. 2007).

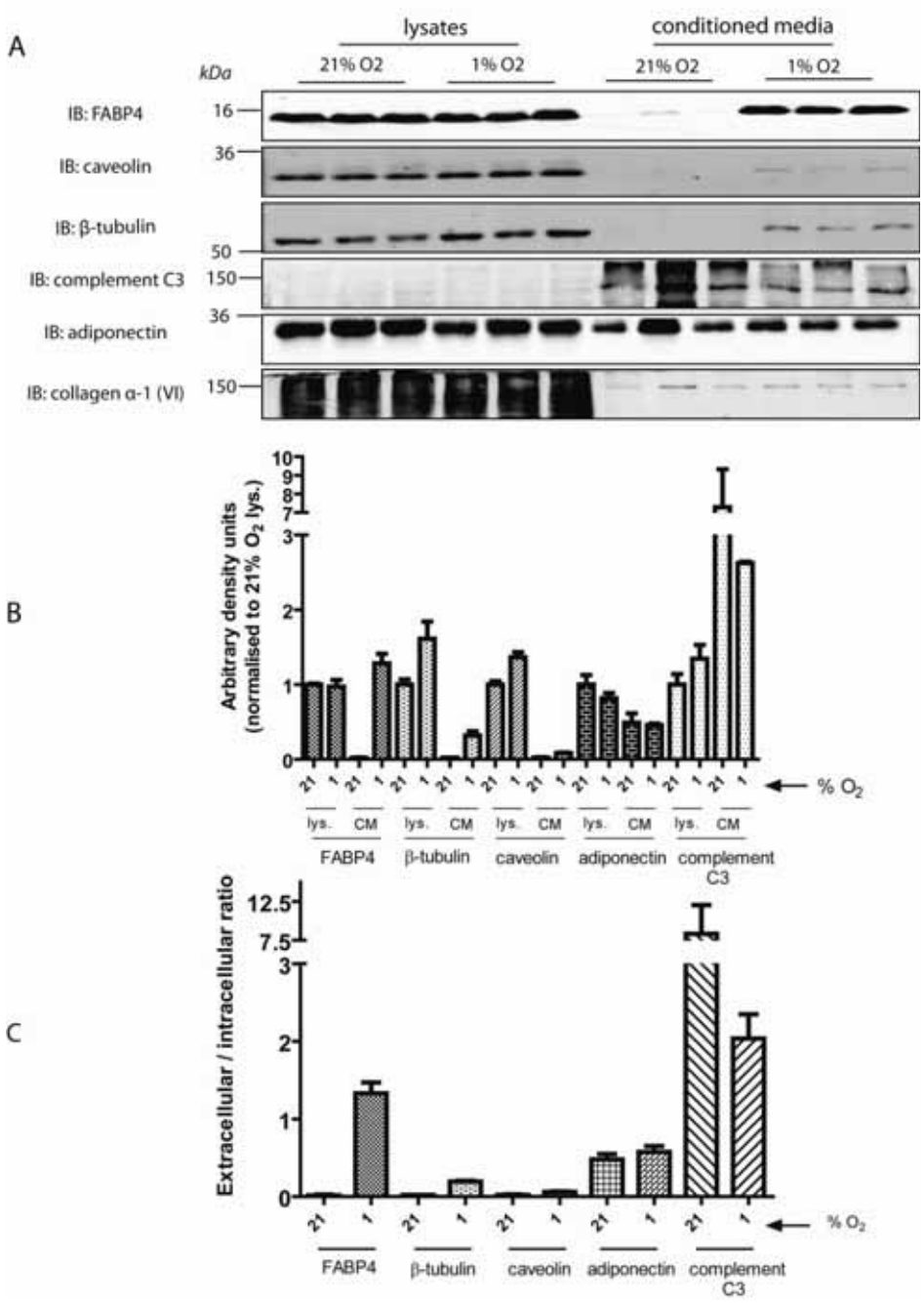

Figure 6. FABP4 is not released via general cell necrosis. A) 3T3-L1 adipocytes were kept under normoxic (21% O_2) or hypoxic (1% O_2) conditions for 16 hours. Cells were scraped to generate cell lysates, and conditioned media were TCA precipitated. Cell lysates (10 µg), or 0.3% of total protein, were loaded alongside 1.25% of the total proteins secreted from adipocytes in 16 hours. Samples were immunoblotted as indicated. B) Quantitation of immunoblot. C) Ratio of extracellular to intracellular protein abundance. FABP4 had a significantly higher extracellular to intracellular abundance ratio during hypoxia than the cytosolic protein β-tubulin and the plasma membrane protein caveolin.

To measure the health of adipocytes during hypoxia, aliquots of conditioned media were tested for extracellular DNA bound histones, a measure of cellular necrosis (Fig. 7). Whilst hypoxia did result in a significant increase in necrosis compared to normoxic control adipocytes, the magnitude of this increase (30%) was not sufficient to explain the degree of extracellular FABP4 appearance during hypoxia. Taken together, these data point towards regulated secretion of FABP4 during hypoxia, rather than non-specific release from necrotic cells.

FABP4 enhances β-cell function

High fat feeding did not affect blood glucose concentrations, consistent with observations that while high fat fed mice may undergo peripheral insulin resistance, they do not undergo β cell failure to become frankly diabetic. High fat fed animals had increased circulating insulin levels, which were raised approximately 2.3 fold over chow fed animals. High fat feeding also increased the circulating levels of FABP4, by approximately 3-fold, to around 800 ng/ml (Fig. 8). These data are consistent with the hypothesis of a positive modulation of β-cell function and insulin release by FABP4.

While correlations between FABP4 and insulin in conditioned media or serum had been observed, direct causation between these parameters has not been shown. To address this, recombinant FABP4 was obtained (Cayman chemicals), and incubated with primary islets in the presence of the fatty acids palmitate or linoleate (Fig. 9). FABP4 has previously been shown to have affinity for a menagerie of fatty acid species, including palmitate and linoleate, however FABP4 displays the highest affinity for linoleate out of the 16 fatty acid species that have been tested, as measured by the displacement of the fluorescent lipid analogue 1-anilinonapthalene-8-

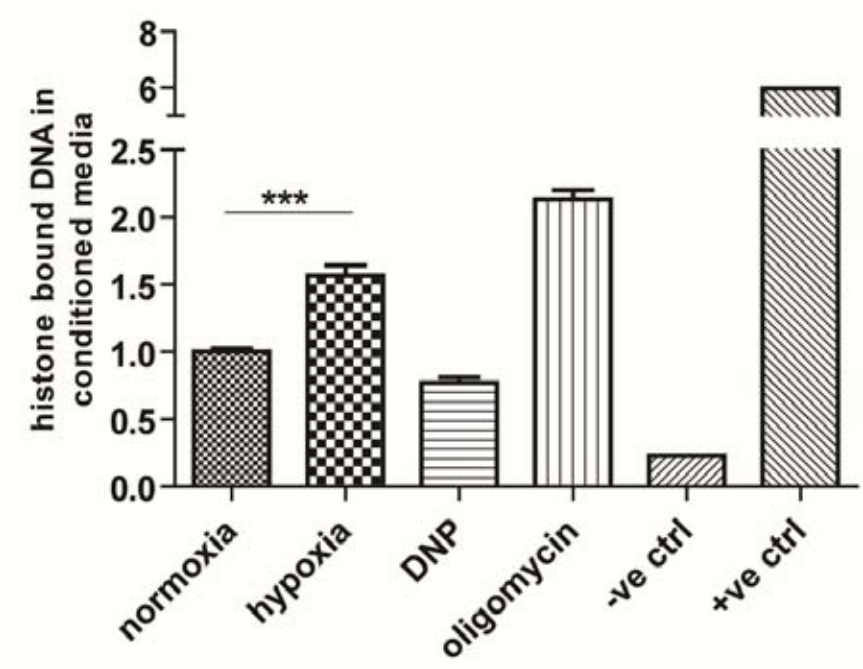

Figure 7. Hypoxia increases cell necrosis. 3T3-L1 adipocytes were incubated in serum free media supplemented with 1 nM insulin for 18 hours under normoxic or hypoxic (1% O_2) conditions or treated with the metabolic poisons DNP or oligomycin. Aliquots of conditioned media were obtained, and extracellular histone bound DNA indicative of necrosis was measured by ELISA. Negative control was unconditioned media, positive control was histone bound DNA standard. ***$p<0.0001$, two tailed *t*-test.

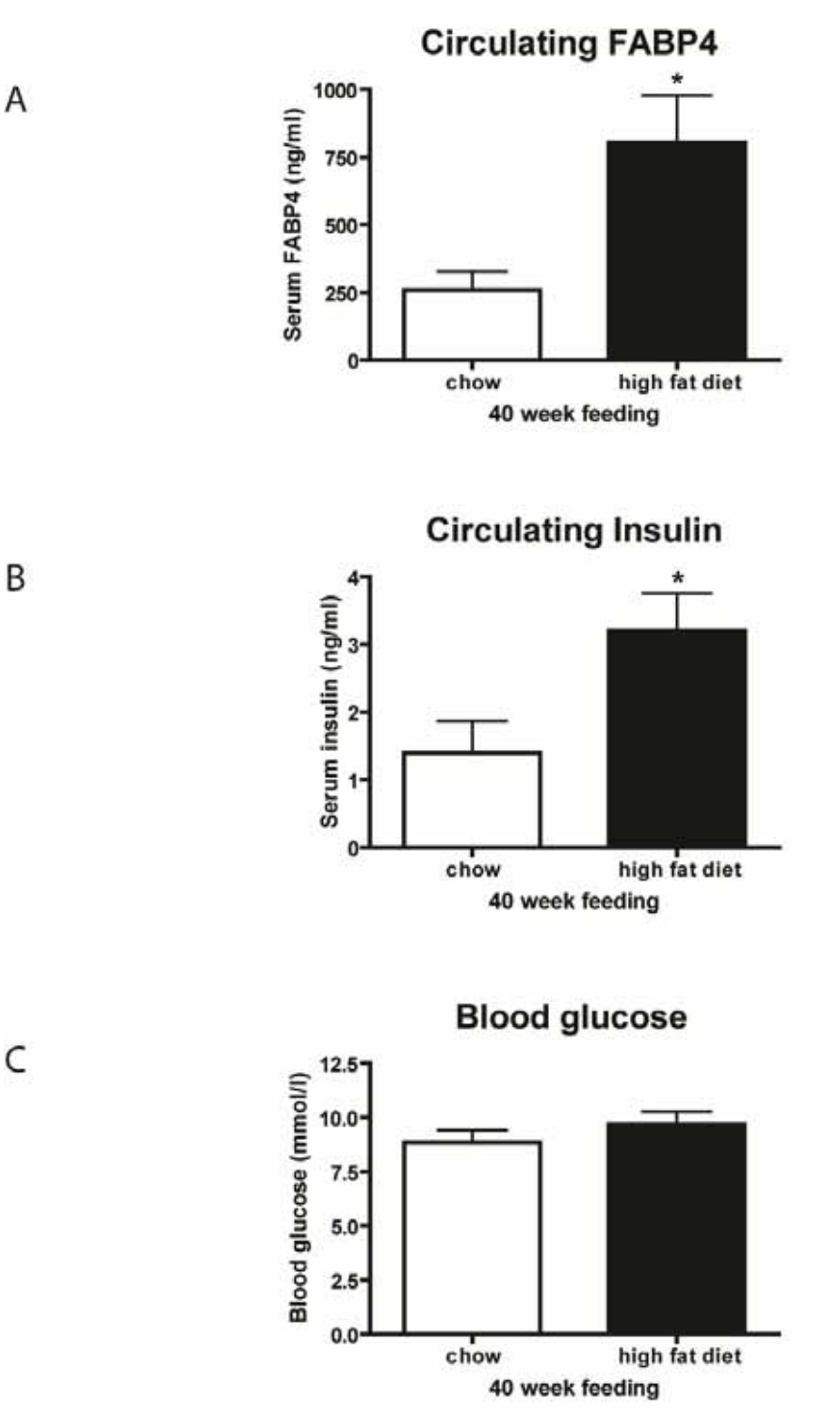

Figure 8. Fasting levels of FABP4 and insulin are elevated during high fat feeding, despite maintaining normoglycaemia. C57BL6 mice were fed a high fat diet for 40 weeks, fasted overnight, and serum levels of A) FABP4, B) insulin and C) glucose were measured. (*$p<0.05$ unpaired two tailed *t*-test)

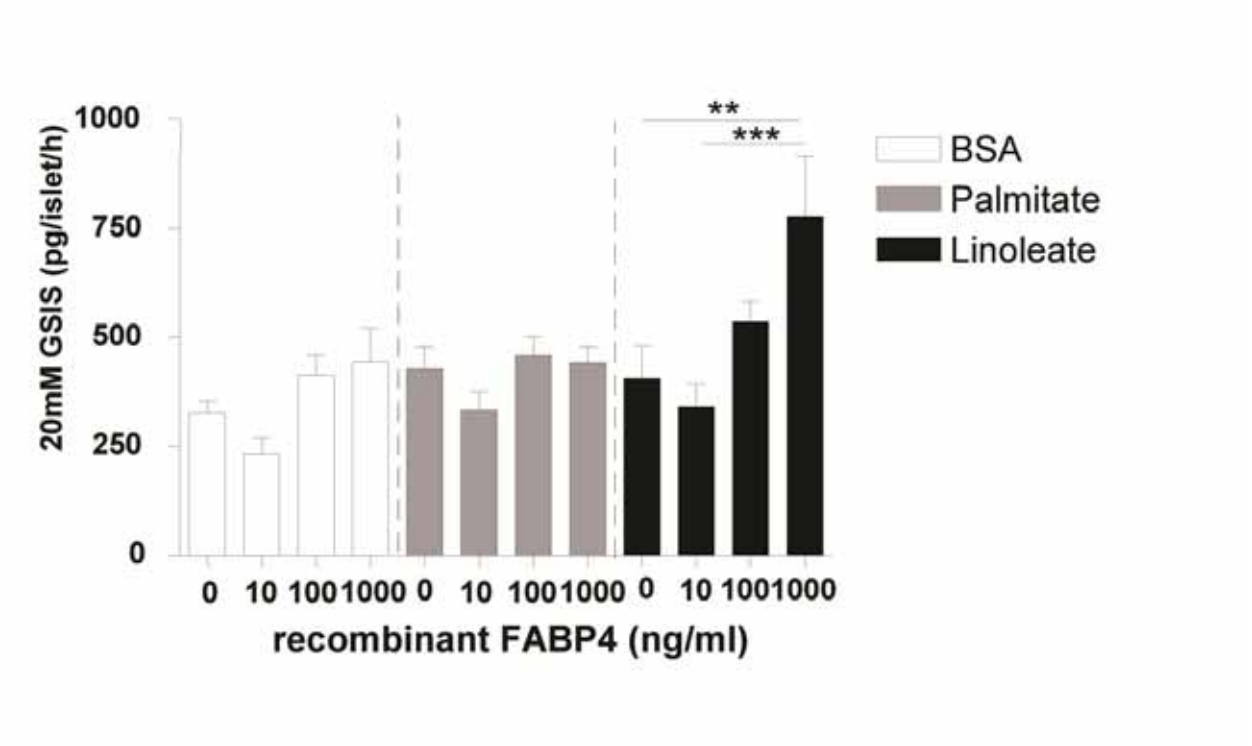

Figure 9. Physiological doses of purified recombinant FABP4 enhance glucose-stimulated insulin secretion from islets in the presence of linoleate. Recombinant FABP4 (Cayman chemicals) was preincubated with BSA, 400 µM palmitate or 400 µM linoleate and added to islets at the indicated concentration for 16 hours. Glucose stimulated insulin secretion was subsequently assessed. A significant increase in GSIS was observed in the presence of 1000 ng/ml FABP4 preincubated with linoleate. This concentration is physiological, and is similar to levels of FABP4 observed in high fat fed animals, and in adipocyte conditioned media experiments (Fig. 4 and Fig. 8). (**p<0.01, *** p<0.001 by two-tailed *t*-test)

sulfonic acid (Simpson, LiCata et al. 1999). When recombinant FABP4 was used to pre-treat islets, 1 μg/ml FABP4 pre-treated with linoleate resulted in a significant increase in GSIS. These data confirm the hypothesis that FABP4 is able to enhance β cell function. Importantly, the dose of FABP4 needed to enhance β cell function (1 μg/ml) *in vitro* was similar to the physiological concentrations of FABP4 observed in the serum of high fat fed animals (800 ng/ml) (Fig. 8), and the concentrations of FABP4 observed in adipocyte conditioned media used for *in vitro* experiments (Fig. 4b). These doses of FABP4 were accompanied by a similar degree of enhancement of insulin secretion, with an ~80% increase with the administration of exogenous FABP4 (Fig. 9), a 70% increase for *in vitro* conditioned media experiments (Fig. 1) and a ~100% increase in the serum of high fat fed animals (Fig. 8).

Metabolic poisons stimulate FABP4 secretion

In the absence of oxygen, ATP synthesis shifts from oxidative phosphorylation to anaerobic glycolysis. In the presence of sufficient oxygen to make oxidative phosphorylation possible, 32 molecules of ATP may be produced for every molecule of glucose that enters the cell. During anaerobic glycolysis, only 2 molecules of ATP are produced per molecule of glucose, making this process metabolically inefficient. It was proposed that the shift away from oxidative phosphorylation to anaerobic glycolysis would result in an energy crisis for the cell. To ameliorate this energy crisis, the adipocyte may secrete FABP4 to enhance insulin secretion, causing increased glucose uptake into cells and improved energy availability. To investigate this hypothesis, adipocytes were treated with the mitochondrial poisons dinitrophenol and oligomycin, as well as aminoimidazole carboxamide ribonucleotide (AICAR), which is an

activator of AMP kinase, the central energy regulator of the cell (Corton, Gillespie et al. 1995; Merrill, Kurth et al. 1997). Treatment of adipocytes with these compounds stimulated release of FABP4 (Fig. 4c), indicating that the mechanism of release possibly relies on the energy status of the cell.

Non-classical secretion of FABP4

FABP4 plays a role in adipocyte differentiation, and is involved in shuttling fatty acids from the cytosol to the nucleus (Makowski, Brittingham et al. 2005). Its presence has also been reported in the serum, with serum concentrations correlating closely with adiposity (Xu, Wang et al. 2006). To determine whether this protein is a secretory protein or a cytosolic protein, the murine FABP4 sequence was submitted to the SecretomeP algorithm (Bendtsen, Jensen et al. 2004). A signal peptide was not predicted, however secretion was predicted (NN score = 0.755, scores higher than 0.5 indicate likely secretion) (Fig. 10). This indicates the likely non-classical secretion of FABP4 via an ER-Golgi independent pathway. To test this, adipocytes were treated with the inhibitor of classical secretion Brefeldin A (BFA) (Dinter and Berger 1998) (Fig. 11). While inhibiting secretion of classically secreted proteins such as adiponectin and complement C3, BFA did not inhibit the hypoxia-stimulated secretion of FABP4. This confirms that the secretion of FABP4 occurs via a non-classical pathway. Much mystery surrounds non-classical protein secretion, with FGF proteins and IL-1 being the most well studied non-classically secreted proteins (Prudovsky, Mandinova et al. 2003; Nickel and Rabouille 2009). There is evidence showing that non-classical protein secretion is dependent on Cu^{2+} or Ca^{2+} dependent S100A proteins (Prudovsky, Mandinova et al. 2003). FGF and IL-1α secretion is dependent on

A

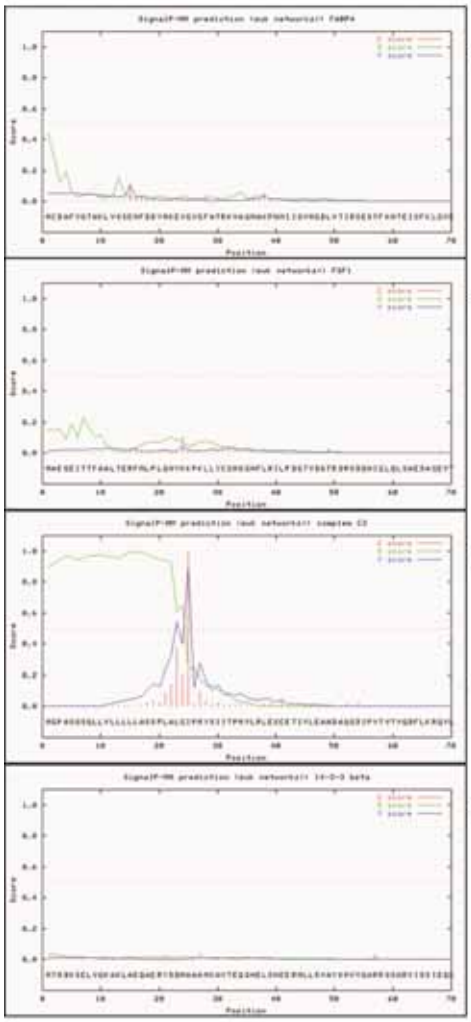

```
>FABP4                    length = 70
# Measure  Position  Value  Cutoff  signal peptide?
  max. C     15       0.119   0.32   NO
  max. Y     15       0.102   0.33   NO
  max. S      1       0.440   0.87   NO
  mean S     1-14     0.112   0.48   NO
       D     1-14     0.107   0.43   NO
```

```
>FGF1                     length = 70
# Measure  Position  Value  Cutoff  signal peptide?
  max. C     24       0.106   0.32   NO
  max. Y     32       0.043   0.33   NO
  max. S      7       0.227   0.87   NO
  mean S     1-31     0.085   0.48   NO
       D     1-31     0.064   0.43   NO
```

```
>complem_C3               length = 70
# Measure  Position  Value  Cutoff  signal peptide?
  max. C     25       0.995   0.32   YES
  max. Y     25       0.905   0.33   YES
  max. S     16       0.996   0.87   YES
  mean S     1-24     0.931   0.48   YES
       D     1-24     0.918   0.43   YES
# Most likely cleavage site between pos. 24 and 25:
  ALG-IP
```

```
>14-3-3_beta              length = 70
# Measure  Position  Value  Cutoff  signal peptide?
  max. C     57       0.037   0.32   NO
  max. Y     27       0.014   0.33   NO
  max. S      2       0.034   0.87   NO
  mean S     1-26     0.017   0.48   NO
       D     1-26     0.016   0.43   NO
```

B

```
# SecretomeP 1.0f predictions

# Name         NN-score Odds    Weighted   Warning
#                            by prior
#=============================================================================
14-3-3_beta     0.352   0.660     0.001    -
FABP4           0.755   2.687     0.005    -
FGF1            0.847   4.271     0.009    -
complement_C3   0.534   1.144     0.002    signal peptide predicted by SignalP
#
#=============================================================================
```

Figure 10. FABP4 is not predicted to have a classical signal peptide, but is predicted to be released via a non-classical route. A) SignalP 3.0 does not predict a classical signal peptide for FABP4, the non-classically released FGF1, or the cytoplasmic protein 14-3-3, but does predict a signal peptide for the classically released complement C3. B) SecretomeP 2.0 predicts non-classical secretion of FABP4 as well as the known non-classically secreted protein FGF1, but not for the known cytosolic protein 14-3-3. NN-scores above 0.500 indicate likely secretion.

the Cu^{2+} dependent protein S100A13, and their secretion from cells can be blocked with the copper inhibitor tetrathiomolybdate (TTM) (Mandinova, Soldi et al. 2003). To test this pathway for FABP4 secretion from adipocytes, adipocytes were treated with TTM (Fig. 11). No inhibition of FABP4 release was observed with TTM treatment. It is possible that FABP4 release is dependent on another member of the S100A family. There is data, for example, showing an interaction between FABP5 and S100A7 (Hagens, Masouye et al. 1999; Hagens, Roulin et al. 1999; Ruse, Broome et al. 2003), which is a Ca^{2+} but not Cu^{2+} dependent member of the S100A protein family (Santamaria-Kisiel, Rintala-Dempsey et al. 2006).

Various explanations have been proposed for non-classical protein secretion. Some of these explanations rely on the regulated transport of a membrane bound vesicle or exosome. To investigate the sub-cellular localisation of FABP4, differential centrifugation was performed to fractionate adipocytes into plasma membrane, high density microsomes (golgi, ER, lysosomes), low density microsomes (vesicles) and cytosol. These fractions were immunoblotted for FABP4 (Fig. 12). FABP4 primarily resides in the cytoplasmic fraction, however a substantial portion of FABP4 exists in the high density microsome fraction, indicating a possible reliance on a membrane bound organelle for secretion. Immunofluorescence microscopy was performed, and a punctate staining pattern was observed for FABP4 in adipocytes (Fig. 13). These punctae display a vesicular – like staining pattern, however further studies will be needed to confirm the identity of FABP4 in vesicles.

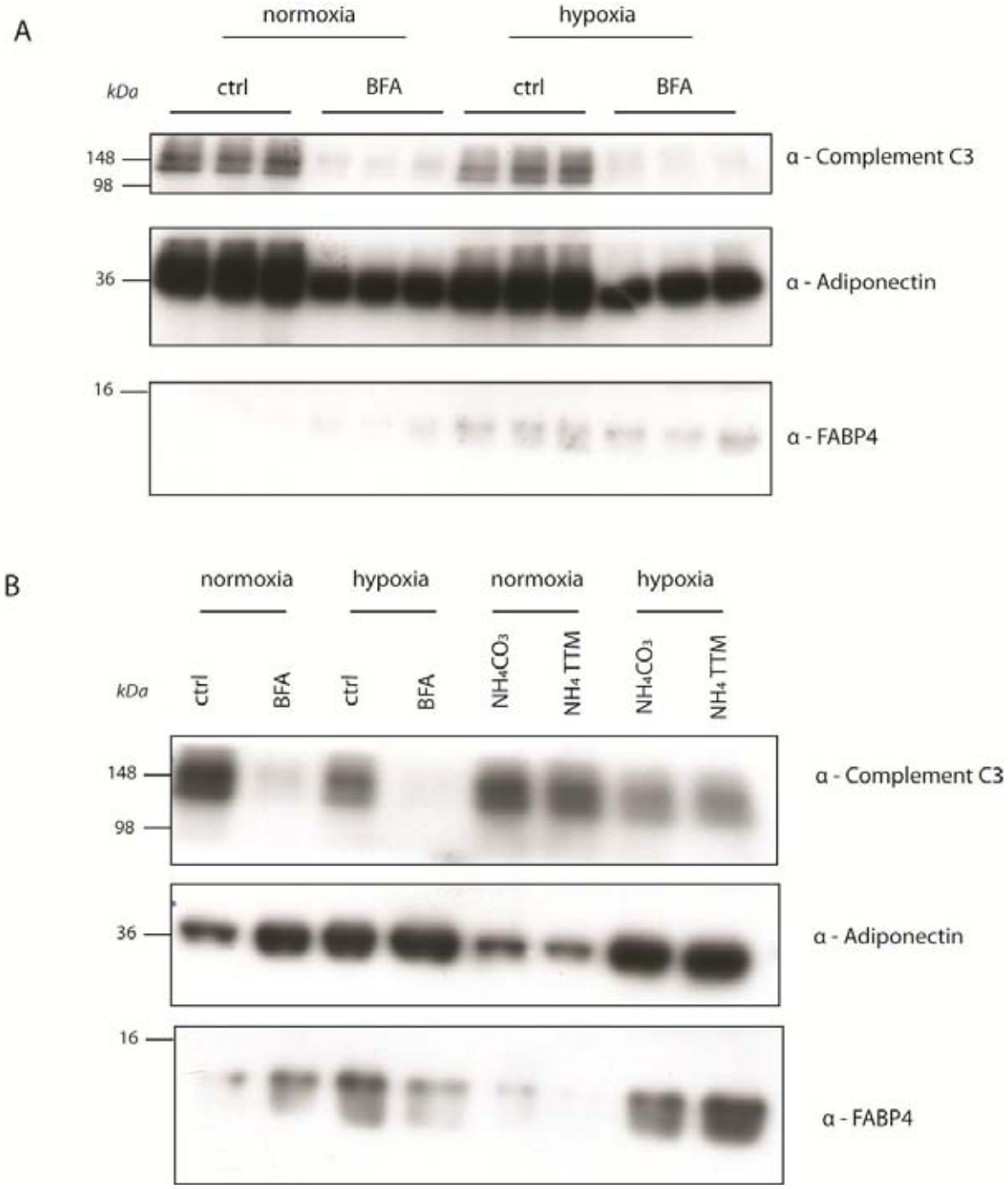

Figure 11. FABP4 release occurs via a BFA and Cu^{2+} insensitive pathway. A) Normoxic and hypoxic 3T3-L1 adipocytes were treated with Brefeldin A (2 μg/ml), an inhibitor of classical secretion, conditioned media was collected, proteins precipitated using TCA protein precipitation and immunoblotted with a FABP4 specific antibody. Non-classical secretion of FGF and IL-1 occurs via a S100A protein dependent pathway. Several of these proteins are Cu^{2+} dependent. B) Normoxic and hypoxic 3T3-L1 adipocytes were treated with the Cu^{2+} chelator tetrathiomolybdate (TTM), conditioned media collected, proteins precipitated and immunoblotted with FABP4 specific antibody.

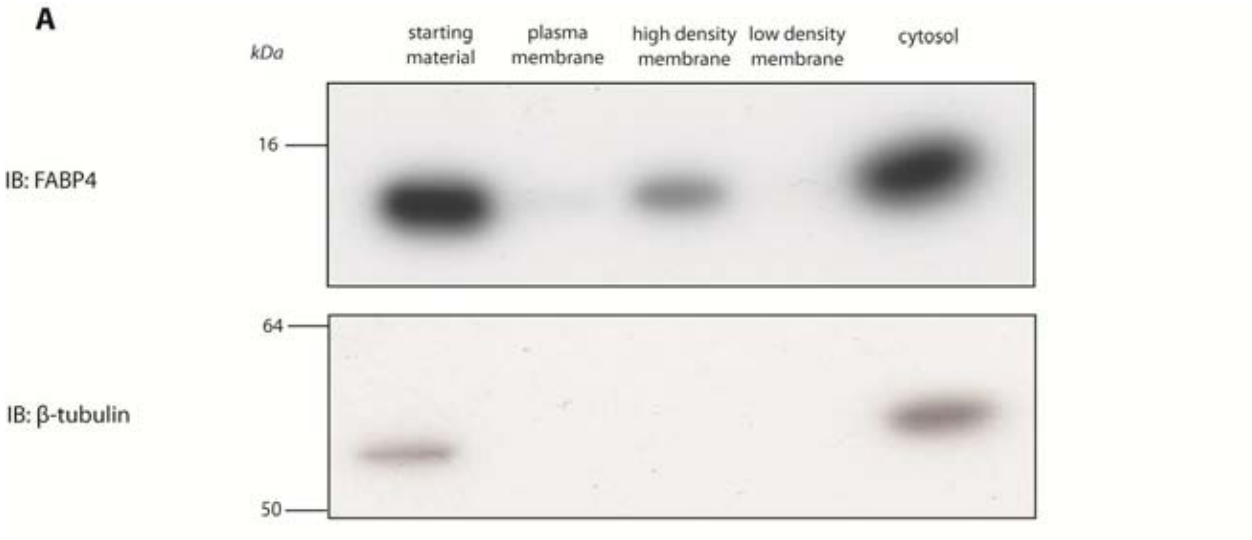

Figure 12. FABP4 resides primarily in the cytosol, with a substantial pool in the high density membrane fraction. A) 3T3-L1 adipocytes were fractionated as described in methods. Equal amounts of protein were immunoblotted for FABP4 and the cytosol marker beta tubulin. B) Low density microsomes from 3T3-L1 adipocytes were subjected to glycerol gradient fractionation, and immunoblotted for FABP4 as well as plasma membrane marker caveolin, classical secretory proteins complement C3 and adiponectin, plasma membrane glucose transporter GLUT4, golgi marker sortilin and cytosolic marker beta tubulin. FABP4 localises primarily with the cytosolic marker beta tubulin.

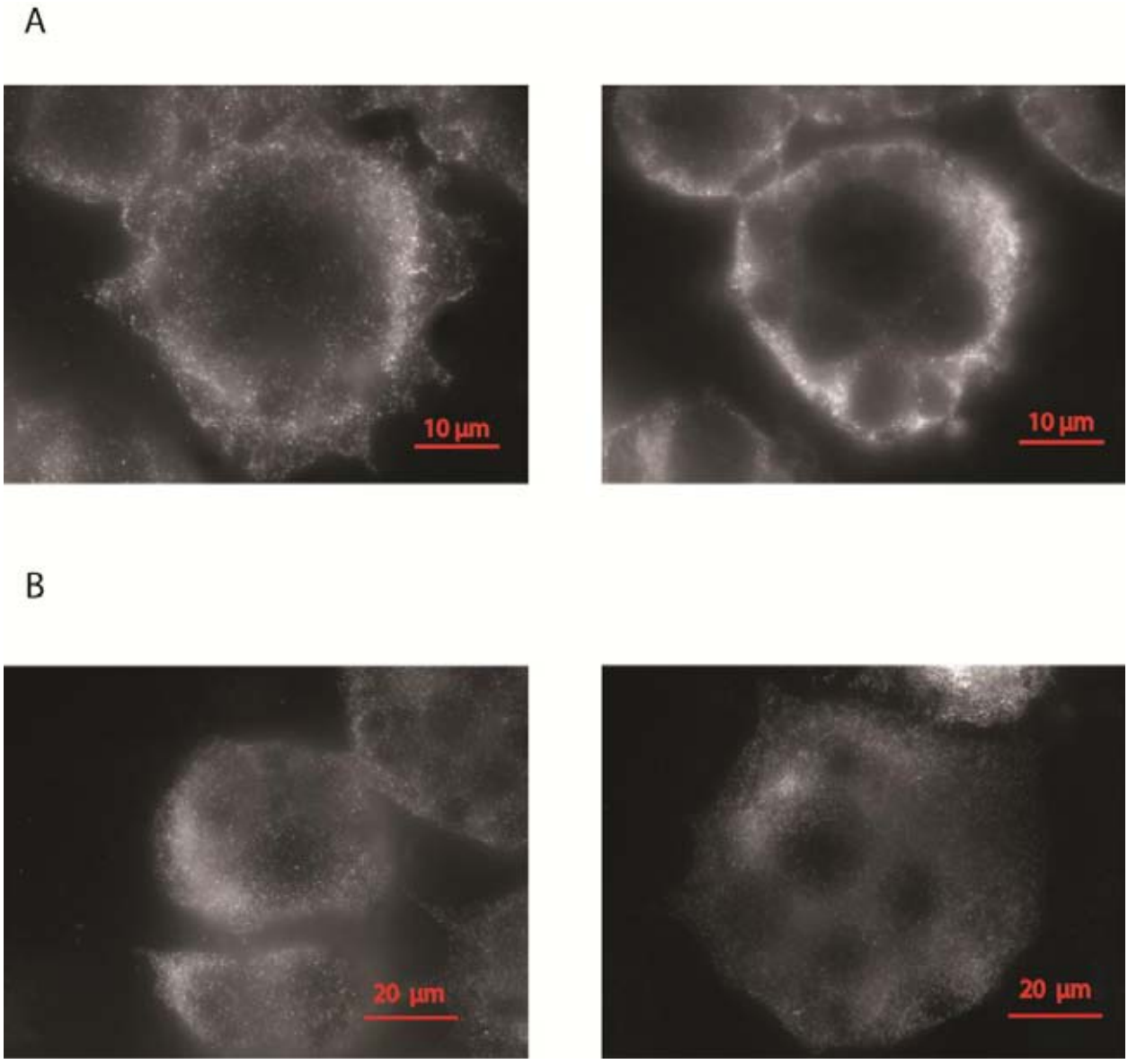

Figure 13. FABP4 localises to punctuate structures in adipocytes. A) Normoxic and B) hypoxic 3T3-L1 adipocytes were fixed in paraformaldehyde and stained for FABP4 using a FABP4 specific antibody followed by Cy5 conjugated secondary antibody staining. Confocal images of cells were obtained on a Zeiss upright confocal microscope. Diffuse staining is observed around the periphery of hypoxic adipocytes, this may reflect an interaction between FABP4 and the extracellular matrix.

Potential modification of FABP4 by 4-hydroxynonenal

Apart from causing an energy crisis, hypoxia, dinitrophenol and oligomycin all cause an increase in reactive oxygen species (ROS). Reactive oxygen species cause lipid peroxidation, particularly in lipid rich adipocytes. One common product of this lipid peroxidation is the reactive aldehyde 4-hydroxynonenal (4-HNE), which is formed from degradation and peroxidation of linoleate (Fig. 14) (Schaur 2003). Proteins may be modified by 4-hydroxynonenal on cysteine and lysine residues. There is evidence for modification of FABP4 and FABP5 by 4-hydroxynonenalation on a cysteine residue, Cys117 in FABP4 and Cys120 in FABP5 (Bennaars-Eiden, Higgins et al. 2002; Grimsrud, Picklo et al. 2007). These residues lie within the lipid binding pockets of the proteins. Modification of these residues by 4-hydroxynonenal decreases fatty acid binding by at least 10-fold, as measured by displacement of the fluorescent fatty acid analogue 1-anilonapthalene-8-sulfonate (Bennaars-Eiden, Higgins et al. 2002; Grimsrud, Picklo et al. 2007). To test for possible modification of FABP4 by 4-HNE, cell lysates were immunoblotted with 4-HNE specific antiserum (Fig. 14). Hypoxia, dinitrophenol and oligomycin treatment all resulted in an increase in the appearance of multiple bands on the immunoblot, including one species at the same molecular weight as FABP4. This species is proposed to be FABP4. Further experiments are needed to confirm this modification by 4-hydroxynonenal, as well as its physiological importance.

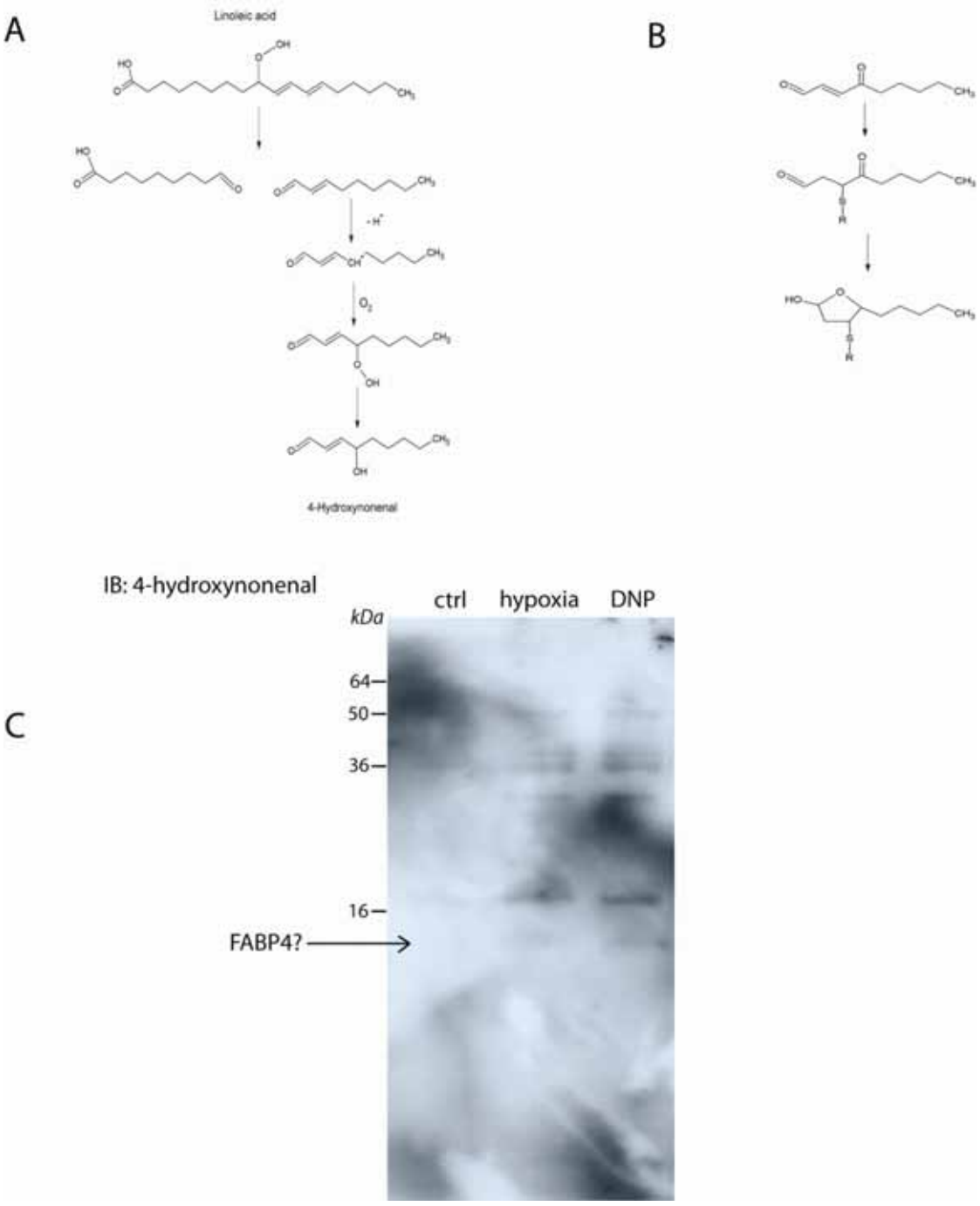

Figure 14. Lipid peroxidation leads to 4-hydroxynonenal formation and modification or proteins. A) Hydroperoxide lyase catalyses a hock cleavage of linoleic acid, leading to the formation of 9-oxo-nonanic acid and nonenal. Nonenal is peroxidated, resulting in the formation of 4-hydroxynonenal (Schneider, Tallman et al. 2001; Schaur 2003). B) Proteins may be modified by 4-hydroxynonenal on cysteine residues. Hemiacetal cyclisation of cysteine bound 4-hydroxynonenal may subsequently occur (Schaur 2003). C) Lysates from untreated, hypoxic or DNP treated 3T3-L1 adipocytes were immunoblotted with a 4-hydroxynonenal specific antibody. An hypoxia and DNP sensitive protein species of a similar electrophoretic mobility to FABP4 was identified (indicated by arrow).

Discussion

White adipose tissue is a highly vascularised organ, and is dense in micro capillaries that supply oxygen to adipocytes. In obesity, white adipose tissue expansion may exceed the necessary blood supply, resulting in insufficient vasculature and oxygenation to all adipocytes and consequent adipose tissue hypoxia (Trayhurn, Wang et al. 2008). Adipose tissue hypoxia may be associated with insulin resistance, but importantly, it is not a consequence of insulin resistance, and is instead primarily related to obesity. This is a similar situation to that observed for fasting insulin levels. While fasting insulin levels are elevated in obese individuals, they are not necessarily dependent on peripheral insulin resistance, with one study identifying insulin resistance as explaining only 38% of the variance associated with fasting insulin levels (Laakso 1993). During fasting, and in the absence of peripheral insulin resistance, there should be no reason for elevated insulin levels, as the half-life of insulin is 4-6 minutes (Duckworth, Bennett et al. 1998). The reason for this increase in fasting insulin during obesity has remained a mystery for over 40 years, since the first measurements of immunoreactive fasting insulin were obtained by Bagdade and co-workers (1967). In the present study, a link between obese (and consequently hypoxic) adipose tissue and β cell function through the release of a humoral factor was proposed. Conditioned media from hypoxic adipocytes enhanced β cell function, and this effect was preserved when conditioned media was filtered to remove non-protein molecules smaller than 10 kDa. In itself, this finding is an important addition to the understanding of whole body glucose homeostasis. This is the first time that adipose tissue has been demonstrated to enhance β cell function through an endocrine mechanism, and this adds an important dimension to the understanding of the role of white adipose tissue in the endocrine system. While the existence of

an "adipo-insular" axis has been proposed (Kieffer and Habener 2000; Huypens 2007), these data represent the first direct evidence of positive regulation of β cell function by adipose tissue, as opposed to the negative regulation of β cell function by adipocytes through leptin that has been proposed (Kieffer and Habener 2000). The hypothesis proposed by Huypens (2007) for positive regulation of β cell function through adiposity relies on adiponectin and leptin to increase β cell mass to compensate for increased insulin demands that exist during obesity. However, there are two potential problems with this hypothesis. Firstly, leptin negatively, not positively, regulates β cell function. Ob/ob mice, genetically deficient in leptin, have enlarged β cell mass (Bock, Pakkenberg et al. 2003), consistent with the negative regulation of leptin on β cell function. Adiponectin is a highly studied adipokine with pro-metabolic effects (Kadowaki, Yamauchi et al. 2006). However, despite being secreted from adipose tissue, serum levels decrease with obesity (Arita, Kihara et al. 1999), and so adiponectin is unlikely to be the factor that is responsible for increased β cell mass and fasting insulin levels during obesity. One would expect the serum levels of the adipocyte secretory protein adiponectin to increase with obesity. The unexpected decrease in the serum levels of adiponectin that occurs during obesity may be explained by the results of this study, which confirms the findings of others (Ye, Gao et al. 2007). These data show a decrease in adiponectin production and release from adipocytes under hypoxic conditions, again underscoring the importance of adipose tissue hypoxia in understanding obesity.

A mass spectrometric screen for secreted proteins up-regulated during hypoxia identified the non-classically secreted protein FABP4, which was confirmed by western blotting to be secreted in greater amounts during hypoxia. Addition of recombinant FABP4 with linoleate to islets at

physiological doses enhanced insulin secretion. Apart from these data, there are good reasons to believe that FABP4 is the factor responsible for the enhanced β cell function, which was observed in this study. One recent study examined the effects of FABP3 and FABP4 in cardiac myocytes (Lamounier-Zepter, Look et al. 2009). FABP3 was found to increase cell size in cardiac myocytes (Burton, Hogben et al. 1994). This observation is important in the context of the findings of this study. β-cell mass increases during obesity (Ferrannini, Camastra et al. 2004), and this may be due to the same trophic effects of FABP4 that were observed in cardiac myocytes. In addition to increased cell size, administration of FABP3 and FABP4 to cardiac myocytes caused decreased systolic Ca^{2+} signalling (Lamounier-Zepter, Look et al. 2009). This again is an important observation in terms of the current findings, as insulin granules are released from β cells in a Ca^{2+} dependent manner (Rorsman 2005).

One important question raised by the interaction of FABP4 with cardiac myocytes, and for the possible interaction of FABP4 with β cells, is the mechanism of interaction with these cells. FABP4, as its name suggests, is a carrier of fatty acids. In this study, evidence is provided for 4-hydroxynonelation of FABP4 during hypoxia. Modification of this residue reduces the ability of FABP4 to bind fatty acids by over 10-fold, as measured by binding of the fluorescent lipid analogue 1-anilinonapthalene-8-sulfonic acid (Grimsrud, Picklo et al. 2007). The existence of this 4-hydroxynonenal modification in extracellular FABP4 makes it unlikely that FABP4 functions in the endocrine system as simply a carrier, or chaperone, of fatty acids. This role in the circulation is more likely played by proteins such as albumin, which is by several orders of magnitude the most abundant protein in serum, present at concentrations of 35-55 grams per litre. In contrast, FABP4 is present in the serum at concentrations of only 20-32 nanograms per

litre (Xu, Wang et al. 2006). This concentration is more indicative of a signalling role than a fatty acid chaperone role, which in the serum is fulfilled by albumin. This signalling role is observed in the important role FABP4 plays in macrophage activation and inflammation. Considerable effort has been devoted towards the development of a small molecule drug to inhibit the lipid binding ability of FABP4. This drug, and FABP4 deletion, results in a strong reduction in the chronic inflammation observed during high fat feeding (Furuhashi, Tuncman et al. 2007). FABP4 plays an important intracellular role, and it is possible that these effects are a result of the intracellular, as opposed to the extracellular, role of FABP4.

The model proposed here of adipocyte communication to the β cell was entirely *in vitro*, so the influence of other cell or tissue types in this interplay can be discounted. This would have to involve some sort of physical interaction between FABP4 and the β cell. An early study by Burton and co-workers (1994) identified ^{125}I labelled FABP binding to cardiac myocytes in a saturable manner (Burton, Hogben et al. 1994). That this binding was saturable indicates that the interaction is most likely via some form of cell surface receptor or binding site, and not via uptake into the cell. The identity of this cell surface binding protein remains a mystery, and further work is needed to identify it, as well as the possible downstream signalling cascades that mediate the effects of FABP. One clue possibly exists from the knowledge that FABP4 interacts with cardiac myocytes to decrease Ca^{2+} signalling (Lamounier-Zepter, Look et al. 2009), while also interacting with β cells to increase insulin release, which occurs via an increase in cytosolic Ca^{2+}. Increased circulating glucose is transported into the β cell via GLUT2, and is metabolised into ATP. This increased ATP concentration blocks the ATP-sensitive K^+ channels, causing membrane depolarisation and opening of voltage dependent Ca^{2+} channels (Rorsman 2005). In β

cells, the ATP sensitive K^+ channel sits at the cell membrane. Inhibition of this channel would in theory cause excessive polarisation, subsequently resulting in Ca^{2+} entry into the cell via the voltage dependent Ca^{2+} channel and insulin exocytosis. In cardiac myocytes, the Na^+-K^+ ATPase pump also sits at the surface, and inhibition of this channel should instead result in decreased systolic Ca^{2+} signalling and contraction. Although decreased Ca^{2+} signalling in cardiac myocytes may seem disparate to increased Ca^{2+} signalling in β cells, both of these effects may occur if the upstream cell surface ATP sensitive K^+ channels is inhibited. It is considered here that this cell surface ATP sensitive K^+ channel is a candidate for the cell surface receptor by which FABP4 mediates its effects.

Perhaps one ideal experiment to confirm the role of FABP4 in β cell function in this investigation would have been to compare the effects of adipocyte conditioned media from wild type and FABP4 -/- mice on β cells. At the time of writing, access had kindly been granted to FABP4 -/- and FABP5 -/- mice. Access to these mice will hopefully allow further confirmation of the role of FABP4 in potentiating β-cell function. Nonetheless, one instructive experiment for this investigation has already been performed. Mice that are homozygous for deletion of FABP4 and FABP5 display an improved metabolic phenotype, with animals fed a high fat diet showing decreased signs of inflammation and increased insulin sensitivity when compared to wild-type littermates (Maeda, Cao et al. 2005). In a study by Maeda and co-workers, fasting insulin and fasting glucose concentrations in FABP4 -/- FABP5 -/- and wild type mice were compared. When knockout and wild-type littermates were fed a high fat diet both groups displayed equal body weight and fat mass. However, the knockout animals displayed a 70% reduction in fasting insulin levels. These animals also displayed improved peripheral insulin sensitivity, and so it is

difficult to conclude whether the observed decreased insulin levels were a result of improved insulin sensitivity in peripheral tissues or a result of an FABP4 stimulus to the β cell. It would be instructive to know whether β cell mass was influenced in these animals, as it is proposed in this study that FABP4 is responsible for the β cell hypertrophy observed in obesity. However, this type of experiment is still hostage to improved peripheral insulin sensitivity as a result of decreased inflammation during high fat feeding.

Perhaps the most relevant study performed in relation to the present investigation is a study by Scheja and co-workers (Scheja, Makowski et al. 1999). They found that FABP4 -/- animals have decreased insulin levels when administered with agents that stimulate insulin release, including β adrenergic agonists (Susulic, Frederich et al. 1995). Acute administration of β-3-adrenergic agonists lead to an increase (>100-fold) in circulating insulin (Susulic, Frederich et al. 1995). Whereas wild-type mice respond to β adrenergic receptor agonists by increasing their circulating insulin, these effects were not observed in FABP -/- animals (Scheja, Makowski et al. 1999). FABP4 is not expressed in the β cell, eliminating the possibility of a β cell defect. It was theorised that this β cell phenotype was a result of defective lipid trafficking, however a definitive role for FABP4 in the extracellular space had at the time of publishing not yet been defined. In addition, other work has shown that the effect of increased insulin secretion in response to β adrenergic receptor agonists occurs independently of free fatty acids (Togashi 2002). FABP4 is an extremely abundant protein in the adipocyte, making up around 1% of total adipocyte protein weight, and this abundance makes RNA interference experiments very hard to achieve. The most ideal experiment for further investigations still remains to compare the effects of conditioned media from FABP4 -/- animals on β cell function.

The data in this study point towards an intriguing possible paradigm shift in our understanding of glucose homeostasis. In this study, hypoxia and mitochondrial poisons increased FABP4 secretion. In response to these stimuli, adipocytes are likely to undergo an energy crisis, as they shift from oxidative phosphorylation to anaerobic glycolysis. FABP4 secretion was then shown to potentiate β cell function. One possible interpretation of this is that cells sense the energy crisis, and attempts to alleviate it by increasing insulin levels and consequent glucose transporter translocation and glucose uptake. This interpretation is intriguing, because the current thinking of glucose homeostasis revolves around a "supply" based model, whereby tissues are supplied with glucose only in the presence of elevated glucose associated with a meal, which leads to insulin release and consequent glucose uptake. Insulin release and glucose uptake is primarily viewed in terms of preventing hyperglycaemia and its associated complications. The problem with this "supply" based model, which has pervaded the current thinking of glucose homeostasis for some decades, is that it is without a "demand" element. When tissues require energy, it is conceivable that there are mechanisms to increase glucose uptake. It has been described that AMP activated kinase (AMPK) acts as a central energy sensor of the cell, and when the AMP to ATP ratio reaches a certain threshold, AMPK induces the translocation of glucose transporters from an intracellular storage location to the plasma membrane, increasing glucose uptake (Merrill, Kurth et al. 1997). AMPK activates the translocation of a shared pool as well as a distinct pool of GLUT4 glucose transporters that is independent of the pool of GLUT4 that is translocated to the surface in response to insulin (Fazakerley, Holman et al. 2009). It may be that when cells have a strong requirement for energy, FABP4 is released to stimulate insulin secretion and reinforce glucose uptake in addition to the glucose uptake that will occur with activation of AMPK during

an energy crisis. Glucose transport in adipocytes is not confined to GLUT4. Basal glucose transport may occur through GLUT1, however during insulin stimulation, GLUT4 is rate limiting in glucose transport. During hypoxia, the transcription factor HIF1α increases transcription of GLUT1 (Chen, Pore et al. 2001). The kinetics of GLUT1 gene transcription, translation, protein folding and transport are such that it is likely to take hours for functional GLUT1 to increase glucose transport. In contrast, secreted FABP4 might act as a faster way of increasing glucose transport, through increased circulating and GLUT4 translocation. Another possible interpretation of the "supply and demand" model for glucose homeostasis proposed here is that adipocytes release FABP4 and stimulate insulin release not to alleviate an energy crisis in the adipocyte, but to provide energy to distal tissues, such as skeletal muscle. Under hyperinsulinaemic euglycaemic clamp conditions, skeletal muscle is responsible for the majority of insulin stimulated glucose clearance, accounting for around 80% of clearance in the lean state (DeFronzo, Jacot et al. 1981), however defects in stimulated glucose clearance into muscle occurs during type 2 diabetes and obesity (Reaven 1995). This reflects the greater need of energy-hungry muscle for readily utilised carbohydrate, as opposed to adipose tissue, which uses carbohydrate for conversion into lipids and consequent storage. Energy deprivation to muscle has far more dire consequences than energy deprivation in adipocytes, which carry significant stores of energy in the form of lipids. Prior to this study, the only physiological stimuli known to increase insulin secretion independently of increased blood glucose concentration is exposure to cold temperature (Smith 1984). Exposure to cold temperature activates β-3 adrenergic receptors, which increase lipolysis, shivering response and non-shivering (brown adipose tissue) thermogenesis. Activation of β-3 adrenergic receptors by pharmacological agents also dramatically increases serum insulin levels (Susulic, Frederich et al. 1995). During cold

exposure, the shivering response is essentially a form of strenuous exercise, as the body attempts to use muscle to metabolise energy to provide heat. The accompanying release of insulin may be an example of "demand" driven glucose homeostasis. It is important to note that exposure to cold temperatures activates transcription of heart type FABP (FABP3) in brown adipose tissue (Daikoku, Shinohara et al. 1997), indicating a possible role for multiple members of the FABP family to interact with the β cell.

One problem with this concept of “demand” driven glucose homeostasis is that insulin is likely to suppress hepatic glucose output, thus depriving distal tissues of the glucose that increased insulin stimulated glucose transport seeks. The effects of FABP4 on hepatic glucose output are not known, and should be subjected to further investigation. It is possible that glucose transport, and not suppression of hepatic glucose output, is the rate limiting step in overall glucose uptake into peripheral tissues.

The proposed concept of “demand” driven insulin release is somewhat paradoxical, in that energy excess actually leads to an energy deficiency in adipocytes, which seek to ameliorate this through additional insulin release and subsequent glucose uptake. This occurs through the expansion of adipose tissue, which subsequently results in adipose tissue hypoxia and a switch to metabolically inefficient glycolysis. When considering this concept, the history of human evolution must be considered, as it is only within the past 100 years that humans have had access to sufficient nutrients to suffer from obesity and its accompanying adipose tissue hypoxia. There have been no strong evolutionary pressures to deal with adipose tissue hypoxia and its accompanying paradox of energy deficiency within obese adipose tissue.

Regardless of this concept of "demand" driven glucose homeostasis, these data are an important advance in the understanding of the pathology of obesity, and in particular, fulfil the mystery of elevated fasting insulin levels during obesity, which may occur independently of peripheral insulin resistance. The finding that hypoxic or energy deficient adipocytes enhance β cell function through the release of a circulating factor (FABP4) is important for understanding data from the HOMA-IR measurement (Matthews, Hosker et al. 1985), a widespread clinical and research tool that uses fasting glucose and insulin levels to assess insulin sensitivity. Controversy surrounds the use of the HOMA-IR measurement (Ferrara and Goldberg 2001), which has only been properly validated for determining peripheral insulin sensitivity in non-diabetic children (Gungor, Saad et al. 2004). Elevated FABP4 secreted from obese adipose tissue causing increased insulin secretion represents another potential cause of elevated circulating insulin that may occur during insulin resistance to compensate for the inability of tissues to lower blood glucose, as the HOMA-IR measurement assumes. One study (Laakso 1993) indicated that insulin resistance may only account for 38% of the variance associated with fasting insulin levels. It may be that the HOMA-IR measurement is really a function of both obesity (and its accompanying adipose tissue hypoxia) as well as insulin sensitivity, rather than a measure purely of insulin sensitivity. In light of these data, use of the HOMA-IR measurement should be re-assessed to so as to properly interpret epidemiological work that has utilised this measurement.

FABP4 is a highly abundant protein in adipocytes. According to one study this protein alone makes up 1.8 - 8.1% of total protein secretion from human adipocytes (Lamounier-Zepter, Look et al. 2009). Despite this, there has been little work into the mechanism of FABP4 release.

FABP4 is one of a growing class of proteins that is secreted from cells in a non-classical manner. Other non-classically secreted proteins include fibroblast growth factor 1, IL-1, CNTF, Y-box protein 1, and macrophage migration inhibitory factor 1 (Reiness, Seppa et al. 2001; Flieger, Engling et al. 2003; Prudovsky, Mandinova et al. 2003; Frye, Halfter et al. 2009). One possible explanation for the observation of FABP4 release is that FABP4 is released into the media non-specifically due to necrosis and/or mechanical damage to the cell. Several pieces of evidence argue against this. If simple mechanical damage were the main cause of non-classical protein secretion, non-regulated secretion of all cytosolic proteins should occur. Instead, only a small amount of other cytosolic proteins was evident in the conditioned media. In contrast, FABP4 is found at near equimolar amounts within and outside of adipocytes (Fig. 6 and (Xu, Wang et al. 2006)). Interestingly, one study using "inside out" plasma membrane vesicles has shown secretion of two non-classically secreted proteins directly across the plasma membrane in a regulated, temperature-dependent manner (Schafer, Zentgraf et al. 2004). This temperature-dependence argues against the possibility that non-classical protein release is merely a result of leakage of proteins from necrotic or mechanically damaged cells. These non-classically secreted proteins do fulfil an important role in the extracellular space, as evidenced by the existence of cell surface tyrosine kinase transmembrane receptors that are specifically activated by non-classically secreted proteins. These receptors include the CNTF receptor, FGF receptor and IL-1 receptor (Stahl and Yancopoulos 1994; O'Neill 2000; Ornitz and Itoh 2001).

Non-classical protein secretion occurs via a fairly poorly defined pathway. In the case of FGF1, IL-1, CNTF, MMP-1 and Y-box protein 1, release is increased with cell stresses including inflammation, heat shock, low serum concentrations and hypoxia (Jackson, Friedman et al. 1992;

Shin, Opalenik et al. 1996; Mouta Carreira, Landriscina et al. 2001; Prudovsky, Mandinova et al. 2003). One common mechanism that has been proposed for non-classical protein secretion involves activation of caspase-1, which is activated by the inflammasome (Keller, Ruegg et al. 2008). Activation of the inflammasome and caspase-1 is dependent on cell stress, and inhibition of caspase-1 activation was found to block the secretion of several pro-survival and pro-inflammatory non-classical secretory proteins. It is possible that these cytokines are released to alleviate situations of physiological stress and reinforce cell growth. Insulin is a strong pro-survival protein hormone, and FABP4 mediated enhancement of its secretion may be part of the mechanism to alleviate cell stress, or to reinforce adiposity by promoting differentiation of adipocytes.

In one study, FABP4 was found at near equimolar concentrations inside and outside of the adipocyte (Xu, Wang et al. 2006), a finding that was not dissimilar to the findings of this study (Fig. 6). For FABP4 to be found at equimolar concentrations inside and outside of the cell is interesting, as it possibly points towards a diffusive mode of transport. If this were the case, there would have to be a channel specific to FABP4 that only opens during hypoxia, or only allows hypoxia-modified FABP4 to be released. This concept is supported by analogy with one possible mode of transport for the non-classically secreted protein FGF2. It has been shown that secretion of FGF2 relies on an immediate extracellular to intracellular concentration gradient of FGF2 for release by either direct, unassisted translocation through the membrane, or across an as yet unidentified plasma membrane channel (Nickel and Rabouille 2009). Once through the channel, FGF2 is bound by carbohydrate modifications of heparan sulphate proteoglycans in the extracellular matrix, leading to an accumulation on the extracellular side of the plasma

membrane that diminishes the extracellular to intracellular concentration gradient, which would otherwise slow subsequent secretion (Zehe, Engling et al. 2006). In the case of FABP4, no transporter for this protein has been identified. One possibility comes from data here showing possible modification of FABP4 by the reactive aldehyde 4-hydroxynonenal. 4-hydroxynonenal is a toxic product of lipid peroxidation, and is neutralised by GSTA4 mediated conjugation with glutathione, and subsequently exported from the cell (Ishikawa, Esterbauer et al. 1986; Awasthi, Yang et al. 2004). Subsequent work has shown this export to occur via the cell surface channel RLIP76, also known as Ral-1 interacting protein (Cheng, Sharma et al. 2001). It is possible that RLIP76 or a similar detoxifying channel could be involved in the export of 4-hydroxynonenalated FABP4 from the adipocyte. FABP4 is a small protein, of molecular weight 14.5 kDa. This small size might mean that conjugation to 4-hydroxynonenal and export of a cytosolic protein is an efficient way for detoxification. Without modification from 4-hydroxynonenal, FABP4 may be unable to leave the cell via a detoxifying channel such as RLIP76.

If, like FGF2, FABP4 secretion across a cell surface channel relies upon a concentration gradient between the extracellular and intracellular space, the nature of the extracellular matrix would be of importance, as FGF2 has been shown to be sequestered by heparan sulphate proteoglycan extracellular matrix proteins. In this study, a quantification of relative ratios of adipocyte secretory proteins from normoxia to hypoxia (Table 1) was performed. Many of the proteins detected were extracellular matrix proteins, and the secretion of these decreased with hypoxia (Table 2), with collagens, biglycan and laminin found in a hypoxia : normoxia ratio of around 0.4. This decrease in the abundance of extracellular matrix proteins might result in a decrease in

FABP4 concentration at the immediate extracellular periphery near the plasma membrane, resulting in a sharpening of the extracellular to intracellular concentration gradient. This sharpened gradient might then encourage release of FABP4 through a membrane channel. This proposed scheme for FABP4 secretion is shown in Fig. 15.

An interaction between FABP4 and an extracellular matrix protein might explain the initial detection of FABP4. The mass spectrometric screen used in this study relies on glycoprotein affinity purification to obtain secretory proteins (Crowe, Wu et al. 2009), as secretory proteins typically undergo N-glycosylation as they enter the endoplasmic reticulum and pass through the secretory pathway (Lodish 2003). Non-secretory proteins do not undergo glycosylation and should not bind the lectin Concanavalin A, or should be removed by high salt washes that take place during glycoprotein affinity purification. There is no evidence for the N-glycosylation of FABP4, it does not contain a signal peptide for entry into the ER, and is not predicted by appropriate algorithms to have N-glycosylation or O-glycosylation sites (Blom, Sicheritz-Ponten et al. 2004; Julenius, Molgaard et al. 2005). As such, FABP4 should not have been detected in this screen. The detection of FABP4 (11 peptides) means either high salt (0.5M NaCl) washing was not enough to remove cytoplasmic contaminants, or FABP4 can bind an adipocyte derived glycosylated secretory protein. If the proposed mechanism for FABP4 secretion is true, FABP4 will be bound to an extracellular matrix protein. As classical secretory proteins, these extracellular matrix proteins (e.g. collagens) are N-glycosylated. It may be that the initial detection of FABP4 in this study occurred as a result of an extracellular matrix protein forming a "bridge" between concanavalin A and non-glycosylated FABP4.

Accession	Score	Mass	Hypoxia / Normoxia	# peptides	Description
CO1A2_MOUSE	4000	129478	0.3274	39	Collagen alpha-2(I) chain
CO1A1_MOUSE	1237	137948	0.2321	16	Collagen alpha-1(I) chain
CO3A1_MOUSE	825	138858	0.4809	14	Collagen alpha-1(III) chain
CO6A2_MOUSE	631	110266	0.9343	11	Collagen alpha-2(VI) chain
CO6A1_MOUSE	584	108422	2.167	11	Collagen alpha-1(VI) chain
CO4A2_MOUSE	189	167220	0.6334	6	Collagen alpha-2(IV) chain
CO2A1_MOUSE	53	141886	0.05441	3	Collagen alpha-1(II) chain

Table 2. Extracellular matrix proteins are downregulated during hypoxia. Extracellular matrix proteins from data in table 1 show a decrease in abundance during hypoxia.

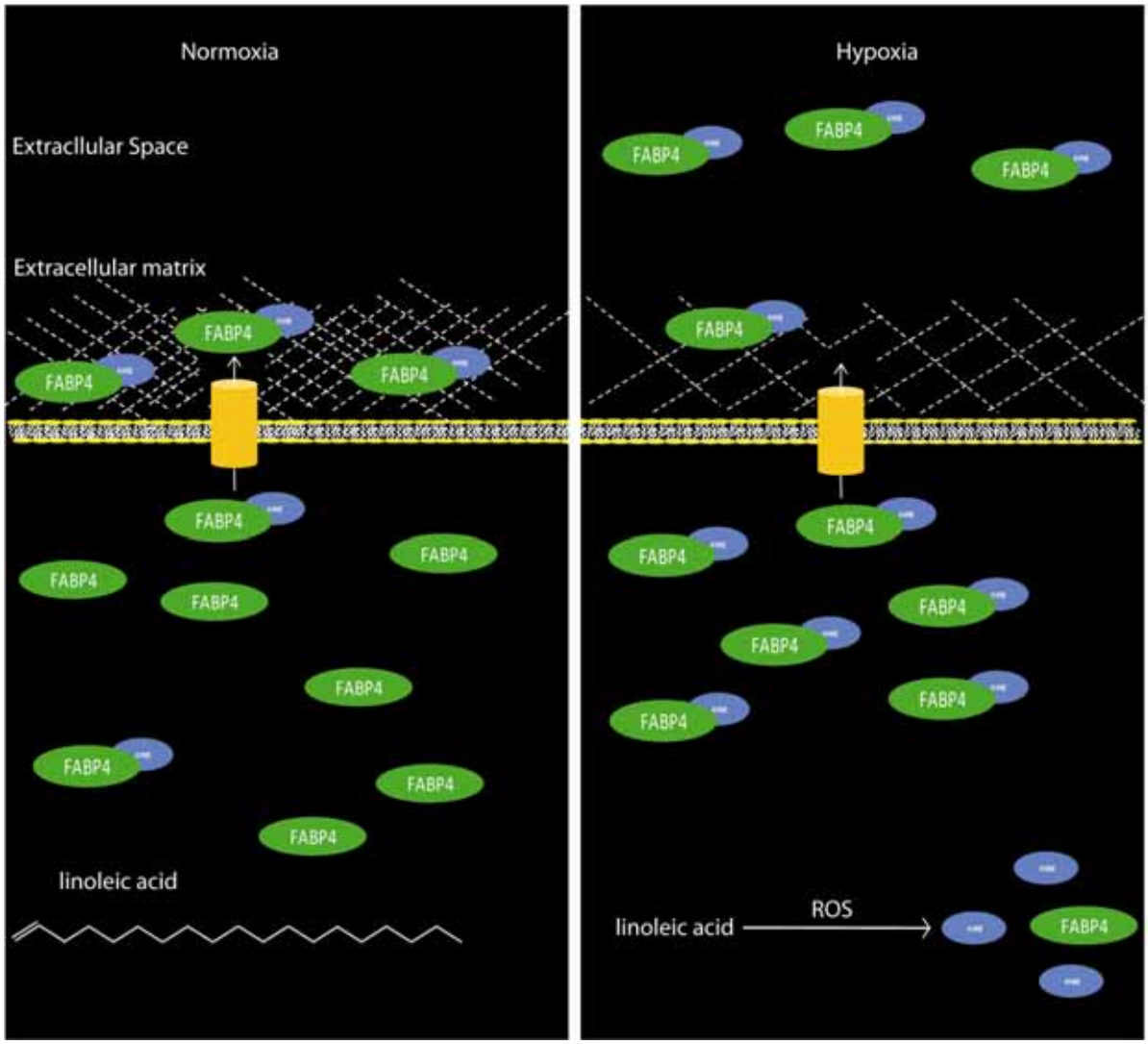

Figure 15. Model for hypoxia mediated non-classical secretion of FABP4. Under conditions of normoxia, 4-hydroxynonenal (4HNE) levels are low, modification of FABP4 does not occur, and FABP4 is not exported through a 4-HNE detoxifying channel. The pool of FABP4 that is modified by 4-HNE is exported and caught in the extracellular matrix in the environment immediately outside the cell. Further secretion becomes thermodynamically unfavourable as the extracellular concentration is equal or greater than the intracellular concentrations. During hypoxia, increased levels of reactive oxygen species result in lipid peroxidation and the formation of 4HNE, which modifies FABP4. Once modified, FABP4 may be exported from the cell through 4-HNE detoxifying channels. Hypoxia decreases the secretion of extracellular matrix proteins (table 2). With a diminished extracellular matrix, FABP4 can no longer accumulate in the environment proximal to the channel through which FABP4 is secreted. Without accumulation of FABP4 proximal to the plasma membrane, diffusion of FABP4 from the cytosol to the extracellular space becomes thermodynamically favourable.

The idea of an interaction between FABP4 and the extracellular matrix is supported by the immunofluorescence staining pattern observed in Fig. 13. While punctate structures are observed within the adipocyte, there is diffuse staining of FABP4 in the area surrounding the adipocyte. Cover-slips were thoroughly washed during staining, and the presence of extracellular FABP4 in these images may indicate some kind of retention of FABP4 in the area surrounding the adipocyte.

Data from this study shows strong release of FABP4 during hypoxia, which similarly causes the release of FGF1 (Mouta Carreira, Landriscina et al. 2001). In addition, this study demonstrates the release of FABP4 upon treatment of adipocytes with metabolic poisons. Hypoxia and these metabolic poisons are linked together through reactive oxygen species (ROS), and this link was supported by the observation that hypoxia induced FABP4 release was inhibited by treatment with anti-oxidants. In addition to demonstrating a link between hypoxic adipose tissue and β cell function, this study provides a new angle for dissecting the mechanism of non-classical protein release.

Chapter 6

General Discussion

Lindsay Wu

Glycoprotein purification and quantitative mass spectrometry for investigating secretory changes during disease

In this study, glycoprotein enrichment was successfully used to purify secretory proteins from conditioned media samples to the exclusion of cytoplasmic proteins, allowing deeper proteomic detection of low abundance secretory proteins. The ability to detect secretory proteins was combined with the use of quantitative mass spectrometry, primarily through the use of SILAC. This allowed comparisons of protein secretion between treatments. In chapter 2, SILAC allowed the relative quantitation of hepatocyte secretory proteins during simulated models of fatty liver disease as well as hepatitis C infection, both of which lead to a higher risk of insulin resistance and type 2 diabetes. Partial labelling was also used to explore the temporal dynamics of protein synthesis and secretion from 3T3-L1 adipocytes, in an important adaptation of the traditional ^{35}S methionine based "pulse – chase" type experiment. In chapter 4, partial SILAC labelling was used in primary tissue explants and primary cell cultures. This allowed for the relative quantitation of protein secretion from two different adipose tissue depots. These data will hopefully provide an insight into the nature of adipose tissue depots, and in particular, will aid in the understanding of visceral- but not subcutaneous- adipose tissue mediated peripheral insulin resistance. In chapter 5, complete SILAC labelling was used to measure differences in protein secretion from 3T3-L1 adipocytes under control or low oxygen conditions. This experiment led to the identification of FABP4 as an hypoxia regulated adipocyte secretory protein, which was later found to play a key role in enhancing the function of insulin producing β-cells. These data provided a novel insight into the mechanism behind obesity induced hyperinsulinaemia.

Future applications of technique

The ability to quantitatively measure secretion of proteins between two samples leads to the ability to perform a range of important experiments. For any intervention of a tissue through either disease or therapeutic treatment, where an effect is observed distal to the target tissue, secreted proteins may be yielding an effect. To identify the secretory proteins that mediate distal effects, a quantitative mass spectrometry based approach such as this is ideal. As an example of future experiments that could be performed, little is known of the effects of anti-diabetic drugs on protein secretion. One future experiment might aim to measure secretion of proteins from adipose tissue or muscle in the presence of an anti-diabetic drug such as metformin. A similar approach might be taken to identify secretory protein upregulated from adipocytes during treatment with the clinically used PPARγ agonists thiazolidinediones. In addition to identifying proteins that may mediate effects distal to a perturbed tissue, identification of secreted proteins is also important for diagnosis of disease through serum markers. One future experiment might be to perform an experiment similar to the investigation in chapter 4, where tissues were dissected out of an animal and incubated in media containing SILAC isotopes. Rather than comparing two healthy tissues to examine endogenous differences in secretion, the secretory ability of a healthy tissue might be compared to a perturbed state of that same tissue. As an example, the secretory ability of healthy mammary tissue might be compared to that of a mammary carcinoma. Differences in protein secretion might lead to the identification of serum markers for breast cancers, and this experimental approach could be adopted for other cancer types.

Future developments of technique

Although glycoprotein purification enriches for secretory proteins to the exclusion of cytosolic proteins, experiments with whole tissue explants are plagued by the existence of serum proteins not secreted by the tissue of interest. One approach used to address this issue is to incubate tissues in media containing amino acid isotopes, as was performed in chapter 4 and in a previous study (Alvarez-Llamas, Szalowska et al. 2007). The incorporation of isotope amino acids allows for the differentiation of proteins synthesised and secreted from the tissue of interest from contaminating serum proteins. Conditioned media samples from tissue explants typically contain a high protein concentration, only a small percentage of which are secretory proteins from the tissue of interest. Although purification of glycoproteins minimises the contribution of cytosolic proteins, a high concentration of serum proteins still exist in the sample, and will still dilute the detection of low abundance proteins secreted from the tissue explants. Ideally, these serum proteins would also be removed from samples prior to mass spectrometry. One future development of the technique used in this study would be to isolate newly synthesised glycoproteins only. This could be performed by the addition of a synthetic moiety to the carbohydrates that are incorporated into glycoproteins. This unnatural carbohydrate could be added into culture media, and incorporated into newly synthesised glycoproteins. Covalent reaction of glycoproteins to immobilised substrates via their synthetic moieties could then be used as a basis for the purification of newly synthesised glycoproteins, which would exclude both cytoplasmic and serum proteins from a conditioned media sample. As an example, N_3 (azide) can be covalently added to carbohydrates, resulting in the incorporation of azide molecules into glycosylated proteins. Azide can undergo highly specific covalent reactions.

Azide can covalently bond to triarylphosphines in a process known as the Staudinger ligation, originally discovered over 80 years ago (Saxon, Luchansky et al. 2002; Kohn and Breinbauer 2004). Phosphines that react with azide containing sugars can be covalently conjugated to a common purification tag such as biotin, which can later be removed with sepharose immobilised streptavidin. The azide containing carbohydrate is tolerated by the cell, well incorporated into glycoproteins and has been used with Staudinger chemistry as a method for identification of O-linked glycoproteins from cell lysates (Vocadlo, Hang et al. 2003). Rather than reacting azide-carbohydrates with phosphines, triple-bonded alkynes similarly undergo highly specific covalent reactions with azides (Zeng, Ramya et al. 2009). This is known as a "click" ligation. Alkynes are cheaper and less complicated to synthesise than phosphines. At the time of writing, azide labelling of glycoproteins followed by labelling or purification of glycoproteins proteins with tags or reporter molecules using click chemistry has become more feasible. Click chemistry reagents are now commercially available under the trade name of "Click –iT" reagents (Invitrogen).

3T3-L1 adipocytes versus white adipose tissue explants

In chapter 2 of this investigation, the secretory repertoire of 3T3-L1 adipocytes was surveyed. 3T3-L1 adipocytes form an adherent two dimensional monolayer in culture. In contrast, adipose tissue explants of the type surveyed in chapter 4 of this investigation exist in a three dimensional extracellular matrix. Whereas adherent 3T3-L1 adipocytes usually contain multiple lipid droplets and a large cytoplasm, adipocytes from animal adipose tissue explants contain a single large lipid droplet that take up the majority of the cell, leaving only a small space for cytoplasmic contents.

Both cell types are insulin responsive. In light of the differences between cultured 3T3-L1 adipocytes and adipocytes from animals, one obvious question is whether they display a similar secretory profile. This question is important, as it validates the use of 3T3-L1 cells as a model for adipocytes of the sort found in animal adipose tissue. A total of 108 secretory proteins were identified from 3T3-L1 adipocytes, whereas 90 secretory proteins were identified from adipose tissue explants. When the lists of secretory proteins identified from 3T3-L1 adipocytes and mouse adipose tissue explants are compared, 26 proteins were found in common. Examination of the lists of proteins identified in both cases shows members of the complement pathway, haptoglobin, adiponectin and serine protease inhibitors are abundantly secreted from both. The greatest differences observed between the two samples were in the detection of extracellular matrix proteins. Whereas for 3T3-L1 adipocytes members of the collagen family featured prominently on the list of secreted proteins detected, collagens did not feature as prominently on the list of proteins secreted from WAT explants. Laminin proteins were instead the most abundant extracellular matrix proteins secreted from explants. This difference may reflect differences in the architecture of 3T3-L1 adipocytes, which grow in an adherent 2-dimensional monolayer, compared to adipose tissue explants, which exist in a three dimensional arrangement. Collagens form the "skeleton" of the three dimensional extracellular matrix, whereas laminins form the basis of inter-cellular bonding interactions (Colognato and Yurchenco 2000). 3T3-L1 adipocytes might be secreting collagens in an attempt to build a three dimensional extracellular matrix, whereas white adipose tissue explants, which already exist in such a matrix, have no need for additional collagen. The secretion of laminins from white adipose tissue explants may be a response to the shearing of whole depots into smaller pieces and breakage of inter-cellular bonds that occurs during sample preparation of explants. Despite differences in secretion of

extracellular matrix proteins, 3T3-L1 adipocytes and white adipose tissue explants secreted similar signalling and regulatory proteins. It is concluded that despite differences in secretion of paracrine factors involved in regulation of the extracellular matrix, cultured 3T3-L1 adipocytes are representative of primary adipocytes with respect to their endocrine regulatory ability. This suggests that 3T3-L1 adipocytes are a reliable representative model for *in vivo* adipocytes.

Notable absences from the adipocyte secretome

Several proteins were notable in their absence from this investigation. Across all the experiments performed, not one single peptide corresponding to either leptin or TNFα was detected. Leptin is the most important and well studied of all adipokines, due to its ability to interact with the hypothalamus and suppress appetite (Friedman and Halaas 1998). Leptin is one of the few secretory proteins that is not N-glycosylated (Cohen, Halaas et al. 1996), and this could account for its absence in the present screen. However, other studies that used mass spectrometry to identify adipose secretory proteins also failed to identify leptin (Kratchmarova, Kalume et al. 2002; Wang, Mariman et al. 2004; Chen, Cushman et al. 2005; Alvarez-Llamas, Szalowska et al. 2007; Zvonic, Lefevre et al. 2007; Roelofsen, Dijkstra et al. 2009). Leptin is expressed at extremely low levels in 3T3-L1 adipocytes (MacDougald, Hwang et al. 1995), although even other studies that have utilised human adipose tissue explants were unable to detect leptin (Alvarez-Llamas, Szalowska et al. 2007; Roelofsen, Dijkstra et al. 2009). Also notable in its absence from this study was TNFα, which is extensively studied in the literature as an important adipose secretory protein (Hotamisligil, Shargill et al. 1993; Galic, Oakhill et al. 2009). Like leptin, TNFα has also not been detected in other studies of the adipocytes secretome. TNFα is N-

glycosylated, and so it should have been enriched like other glycoproteins in this screen. 3T3-L1 adipocytes do not express TNFα, and studies into the mechanism of TNFα secretion from 3T3-L1 adipocytes have relied on TNFα overexpression (Xu, Uysal et al. 2002). Although TNFα secretion from isolated primary adipocytes has been detected, the process of primary isolation in itself induces TNFα expression (Ruan, Zarnowski et al. 2003). TNFα is abundantly secreted from macrophages (Locksley, Killeen et al. 2001). One possibility that has not been addressed in the literature is that TNFα is not secreted by adipocytes *per se* but rather by macrophages that infiltrate adipose tissue particularly of obese individuals (Xu, Barnes et al. 2003). Indeed one study has suggested that TNFα secretion from white adipose tissue is almost entirely a result of non-adipocyte secretion (Fain, Bahouth et al. 2004). Publicly available gene expression data for TNFα would also suggest that it is unlikely that TNFα is secreted from adipocytes (Fig. 1). Of course, it may be possible that TNFα secretion from adipocytes is only induced under certain physiological conditions that occur during obesity or insulin resistance. The present study surveyed the secretome of adipocytes under a wide range of perturbed conditions, including chronic insulin treatment, chronic TNFα treatment, hypoxia, and in visceral versus subcutaneous white adipose tissue explants. Despite these stimuli, this study failed to identify one single peptide corresponding to TNFα. Based on these data, it is speculated that TNFα is in fact not an adipokine, and if it is present in the secretome of adipose tissue it is likely derived from activated macrophages that may infiltrate adipose tissue.

Another protein prominently described in the literature as an adipokine is retinol binding protein 4 (RBP4). This protein was not detected from adipose tissue in this study. RBP4 was originally identified as a factor secreted from adipose tissue that induced insulin resistance in skeletal muscle tissue in adipose tissue specific GLUT4 knockout animals (Yang, Graham et al. 2005).

Later reports suggested that RBP4 expression is specific to visceral adipose tissue (Kloting, Graham et al. 2007), an important finding for elucidating the role of visceral adiposity in the onset of peripheral insulin resistance. RBP4 is glycosylated, and so should have been detected during the screens in this study. Interestingly, RBP4 secretion was only detected from hepatocytes. Publicly available tissue distribution data (Fig. 1) in fact shows abundant expression of RBP4 from liver, and comparatively little expression from adipocytes. From these data, greater emphasis should be placed on RBP4 as an hepatocyte secretory factor, as opposed to an adipocyte secretory factor. In light of the abundant difference in RBP4 expression between adipose tissue and the liver, it is unlikely that adipose tissue makes a sufficient contribution to the circulating levels of RBP4 in rodents. Consistent with this, several reports have started to question the role of RBP4 in insulin resistance.

In contrast to previous reports, Phillip Kern and colleagues have reported that there is no correlation between adiposity and RBP4, and there is in fact an increase in RBP4 levels during treatment with the insulin sensitising agent rosiglitazone (Yao-Borengasser, Varma et al. 2007). Chemical inhibition or genetic deletion of RBP-4 has no detectable effects on insulin sensitivity in both the chow fed and high fat fed situation (Motani, Wang et al. 2009). Moreover, it was reported at the 2009 Scientific Sessions of the American Diabetes Association by that earlier findings of increased RBP4 with insulin resistance, visceral adipose tissue specific expression of RBP4, and induction of insulin resistance with exogenous RBP4 administration could not be reproduced (Kern 2009).

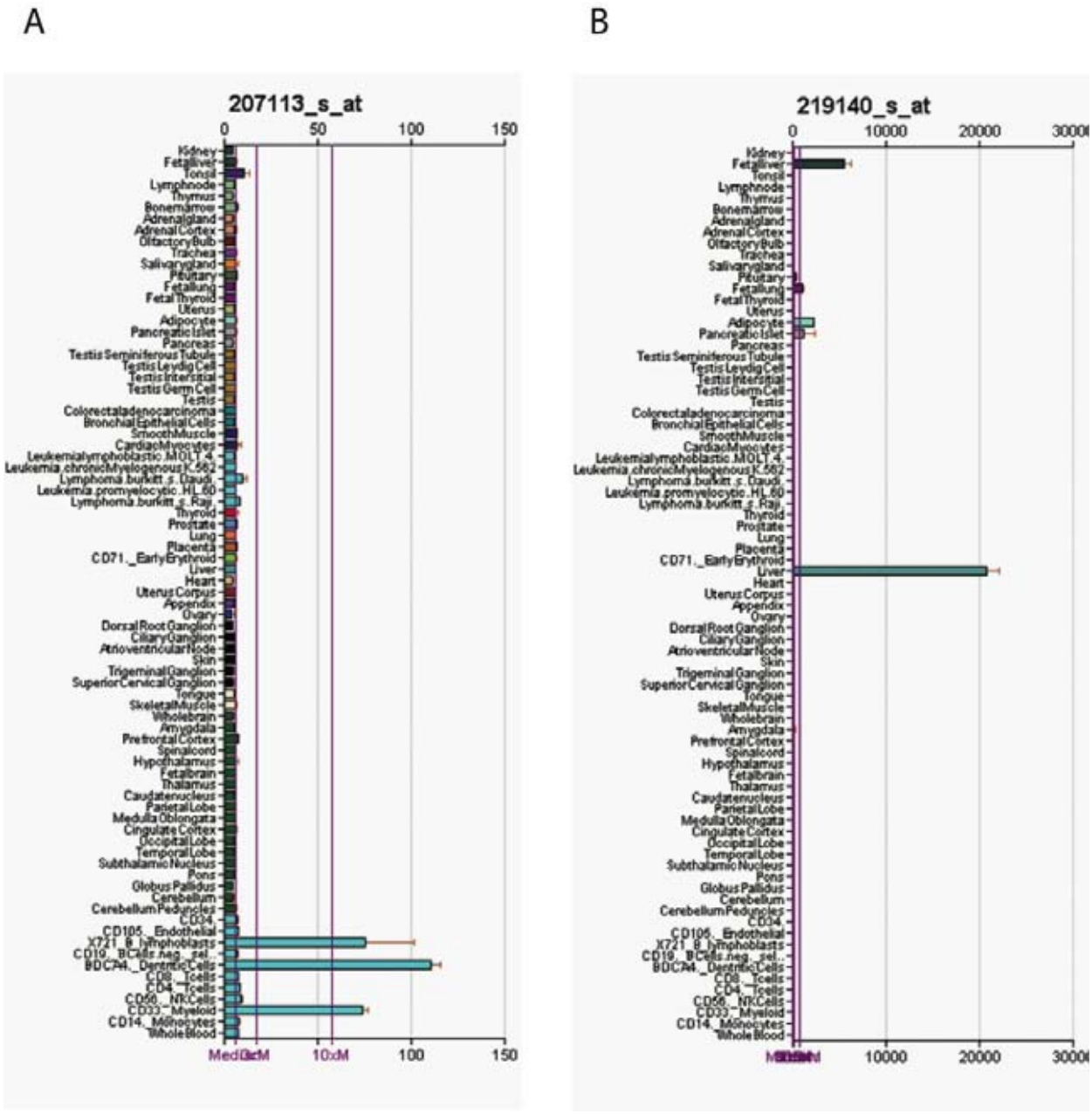

Figure 1. Gene expression data illustrating the tissue specific expression of A) TNFα and B) RBP4. Comparatively little expression of these secretory proteins was observed in adipocytes. Data from BioGPS biogps.gnf.org

Angiogenesis in adipogenesis

Early in this investigation, a mass spectrometry screen for novel adipocyte secretory proteins identified pigment epithelial derived factor. This protein has potent anti-angiogenic activity. Serum levels of PEDF were elevated in high fat fed obese insulin resistant mice. Injection of purified PEDF into the serum of lean insulin sensitive mice led to insulin resistance, whilst injection of a neutralising antibody against PEDF into high fat fed obese mice restored insulin sensitivity. The expression of PEDF was upregulated in 3T3-L1 cells during adipogenesis. Much like PEDF, one secretory protein that was identified from TNFα treated adipocytes was PRLTS. This protein bears significant identity to the ligand binding extracellular domain of the PDGF receptor. It was proposed here that PRLTS acts a soluble form of the PDGF receptor, chelating and inhibiting the angiogenic signalling effects of PDGF. Much like PEDF, PRLTS is upregulated during adipogenesis. In contrast to the known and proposed anti-angiogenic effects of PEDF and PRLTS, the expression of pro-angiogenic molecules such as VEGF, PDGF and PDGF receptor were measured. Interestingly, expression of these pro-angiogenic molecules decreased with adipogenesis. These data point towards a regulation of angiogenesis during adipogenesis, with a need for adipogenesis during the formation of adipose tissue, and a down-regulation of angiogenesis once adipose tissue has matured. During obesity, expansion of existing adipose tissue may exceed existing vasculature, leading to adipose tissue hypoxia. In Chapter 5, hypoxia in 3T3-L1 adipocytes induced the secretion of FABP4. This molecule potentiated glucose stimulated insulin secretion from β-cells. Dysregulation of PEDF and PRLTS secretion during obesity may play a role in the insufficient vascularisation that leads to adipose tissue hypoxia. As a result of investigations in Chapter 5, adipose tissue hypoxia now

can be shown to play an important role in regulation of β-cell function, with potential consequences for insulin resistance and glucose homeostasis.

In the present investigation, a number of pro- and anti- angiogenic secretory molecules were identified from adipocytes, and the expression of these molecules varied dramatically during the course of adipogenesis. These molecules included PEDF, VEGF, PDGF receptor, VEGF receptor, and PRLTS. Interestingly, a number of other adipocyte secretory proteins identified here have been shown to play a role in the regulation of angiogenesis. These include haptoglobin, multiple members of the complement pathway, angiotensinogen, and lipocalin-2 (Lees, MacFadyen et al. 1993; Venkatesha, Hanai et al. 2006; Park, Baek et al. 2009; Rohrer, Long et al. 2009). Insulin-like growth factor binding proteins have been implicated in suppression of angiogenesis (Liu, Lee et al. 2007). In addition, the receptor for the adipocyte secretory protein GAS6 is the receptor tyrosine kinase Axl, which is important for angiogenesis (Li, Ye et al. 2009). Collectively, these data indicate that adipose tissue has the capacity to orchestrate a finely tuned angiogenic regulatory system. Secretion of angiogenic regulatory molecules was not observed for other cell types that were examined, including hepatocytes and myotubes indicating that this system of angiogenic regulation is quite specific to the adipocyte. What is it about adipose tissue, as opposed to other tissues such as the liver or muscle, which requires such careful regulation of angiogenesis? One of the most unique features of adipose tissue is its capacity for expansion, which involves cellular hypertrophy and hyperplasia. For other tissues, such as skeletal muscle, to expand, hyperplasia but not hypertrophy may occur (Heineke and Molkentin 2006). Intriguingly, in situations where cellular hypertrophy is a prevailing mechanism as in the case of cardiac hypertrophy this often leads to disease possibly due to the inability of a concomitant angiogenic response. The ability of adipose tissue to rapidly

expand has most likely evolved with the capacity to supply adipocytes with oxygen and nutrients, as exemplified by adipose tissue angiogenesis. While other organs do not normally expand and contract in size during the life of an adult, adipose tissue does expand and contract in size. This is accompanied by expansion in vasculature. With the exceptions of pregnancy and tumour growth, obesity is the only circumstance under which vasculature may expand. Inhibition of adipose tissue angiogenesis by selective apoptosis of adipose tissue endothelium through the unique surface marker Prohibitin has in fact been shown to limit obesity (Kolonin, Saha et al. 2004). The unique need for expansion of adipose tissue vasculature may explain the tight angiogenic regulatory system of angiogenesis from adipocytes.

Although organs such as the liver contain a greater vascular density than fat, these organs do not expand and contract in size. In contrast, adipose tissue undergoes large fluctuations in size. A complex network of microvasculature is required to maintain blood supply to adipose tissue, which requires careful, localised regulation. Also worth considering is the endocrine nature of white adipose tissue. From this investigation it would appear that adipose tissue is by no means extraordinary in its secretory ability, particularly when compared to other insulin sensitive tissue such as liver. There are, however, still important adipose secretory proteins, such as leptin, adiponectin and from the current work, FABP4 that are needed to mediate distal endocrine roles. A complex network of microvasculature may be necessary to evacuate adipocyte secretory proteins to distal sites in the circulatory network.

FABP4 – future investigations

Perhaps the most exciting part of this investigation was evidence for the existence of an adipo - insular axis, as mediated by FABP4. Several questions remain regarding this. FABP4 is without an N-terminal signal peptide needed for secretion via the classical pathway, so what precisely is the molecular itinerary of interactions necessary for its secretion? Does this interaction represent a parallel secretory pathway that applies to other non-signal peptide containing secreted proteins, such as FGF2 and IL-1? Identification of the "classical" secretory pathway led to the award of a Nobel Prize to Professor Gunther Blöbel, and perhaps one of the next great challenges in cell biology will be to fully elucidate this "non-classical" secretory pathway. Elucidation of this pathway may afford an opportunity to intervene in diseases such as cancer, which is in part mediated by FGF proteins. Equally important to identifying the mechanism of FABP4 secretion is identifying its mode of action. Further challenges regarding FABP4 secretion and its mechanism of action are discussed.

Non-classical protein secretion

This investigation began with the premise that proteins without signal peptides were located in the cytosol only, and the existence of these proteins in the extracellular space was only possible due to lysis of necrotic cells. A strategy was developed to enrich for proteins that enter the secretory pathway, based on the N-glycosylation of these proteins. In chapter 5 of this investigation, a quantitative mass spectrometry approach was used to identify adipocyte

secretory proteins upregulated during hypoxia that could mediate the effects of hypoxic adipocyte conditioned media on β-cell function. The primary candidate that was identified for this effect was fatty acid binding protein 4. This protein is without an N-terminal signal peptide needed for entry into the secretory pathway and classical secretion. Despite this, FABP4 seems to be abundantly secreted from adipocytes in a coordinated fashion. From this, it would appear that FABP4 can be added to a growing list of proteins that are secreted from cells in the absence of an N-terminal signal peptide. Unlike classically secreted proteins that were originally targeted in this investigation, non-classical secretory proteins do not have any known defining features that can be used for purification. They are also without a defining characteristic that can be used to differentiate between cytosolic and secreted, as is the case with the signal peptide and classical secretory proteins. Based on the sequence characteristics of known non-classically secreted proteins, an algorithm (SecretomeP) has been developed to score the likelihood of non-classical secretion of a proteins based on their amino acid sequence (Bendtsen, Jensen et al. 2004). Despite the existence of this algorithm, sequence patterns that are conserved within non-classically secreted proteins are very poorly defined, and little is known of the non-classical secretory pathway. Intriguingly, non-classically secreted proteins are not thought to undergo N-glycosylation, and so it is fortuitous that this protein was detected in the present screen. One distinct possibility is that FABP4 is bound to a classically secreted protein, such as an extracellular matrix protein, accounting for its detection as a result of co-precipitation. This idea was explored in relation to possible interactions with the extracellular matrix in chapter 5. One possibility is that FABP4 is O-glycosylated, however no O-glycosylation site is predicted using the appropriate algorithm (Blom, Sicheritz-Ponten et al. 2004). It may also be that the detection of FABP4 only occurred through impure glycoprotein purification. The sheer abundance of

FABP4 in conditioned media combined with a possibly impure glycoprotein purification may have been the only reasons for identification of this protein.

A common secretory mechanism for classically secreted proteins is known, and this pathway can be targeted with interventions such as Brefeldin A to differentiate between secretory and non-secretory proteins (Wang, Mariman et al. 2004). In contrast, non-classical secretion is poorly defined, and a common mechanism for secretion has not been defined well enough to experimentally target. This may be changing, with the recent identification of the role of the inflammasome and caspase-1 in non-classical protein secretion (Keller, Ruegg et al. 2008; Nickel and Rabouille 2009). Inhibition of caspase 1 was used in one of these studies to survey the existence of caspase-1 sensitive secretory proteins, but further confirmation of the secretion of proteins identified using this approach is needed to validate this approach. Targeting of common non-classical secretion mechanisms is being used as a strategy to initially identify novel non-classically secreted proteins. Unfortunately, even if validated, this technique cannot be scaled up to survey the entire "non-classical secretome" of cells to the proteomic depth used here to survey the "classical secretome". This is still due to the pervasive presence of dysregulated cytosolic protein release from necrotic cells. These contaminating proteins will still dilute the detection of proteins of interest, until such time as a common feature to non-classically secreted proteins (such as a sequence motif or post-translational modification) can be identified and exploited for purification.

Non-classical protein secretion is a fairly poorly defined process. The majority of non-classical protein secretion studies have been performed on just two proteins, interleukin-1 and fibroblast growth factor 2. Due to the small number of non-secretory proteins known, the non-classical secretory mechanisms that are known for these proteins might not necessarily define a single

pathway for multiple non-classically secreted proteins. In chapter 5, a novel secretory mechanism for FABP4 is proposed. This mechanism adds a new dimension to non-classical protein secretion as it depends on levels of reactive oxygen species. It proposes a role for these species in formation of a FABP4 post-translational modification, 4-hydroxynonenalation, which would play a role in targeting of the protein for secretion. 4-Hydroxynonenal is formed as a result of lipid peroxidation, and can modify proteins through cysteine and lysine residues. There are no known signalling roles for 4-hydroxynonenal. It is proposed here that 4-hydroxynonenal provides the signal for protein export, via a detoxifying channel such as RLIP76. This channel is known to transport glutathione bound 4-HNE. This molecule, consisting of a tripeptide and 4HNE, would be very small, compared to macromolecular proteins. How does a 14.5 kDa protein such as FABP4 pass through this channel? One possibility is that the channel is large enough to allow this protein to pass through in a fully folded state. Another possibility is that FABP4 must unfold, and the polypeptide chain fed through to the other side of the plasma membrane, where it may refold. FABP4 is modified by 4HNE on a single residue (Cys117), which lies on the interior of the barrel shaped structure of FABP4. It can be conceived that this modification disrupts the tertiary structure of FABP4, possibly catalysing the unfolding that may allow FABP4 to be exported from the cell via a channel such as RLIP76. If this proposed mechanism does prove to be true, 4-hydroxynonenalation of proteins might be the unique characteristic of non-classically secreted proteins that can be exploited for purification and screening by mass spectrometry.

Mechanism of action for FABP4

In this investigation, FABP4 exerted effects on pancreatic β-cells. Another investigation has identified an effect of FABP4 on cardiac myocytes (Lamounier-Zepter, Look et al. 2009). In each case, the question remains: how does FABP4 interact with these cells? Is it purely via an interaction with the cell surface, or does some kind of endocytic event occur? In Chapter 5, it was shown that FABP4 on its own has no effect on glucose-stimulated insulin secretion. Treatment of islets with recombinant FABP4 pre-incubated with linoleate, but not palmitate, recapitulated the effects of hypoxic adipocyte conditioned media on glucose-stimulated insulin secretion. This suggests that either fatty acids somehow alter the properties of FABP4, possibly via an allosteric change, or that fatty acids themselves are specially delivered by FABP4 to alter β-cell function. If it is the fatty acids carried by FABP4 that mediate the effect on β-cells, do they need to be in complex with FABP4 to exert their effects or is dissociation necessary? How does this dissociation occur?

To answer these questions, a number of experiments must be performed. Firstly, it must be determined whether FABP4 binding to β-cells is saturable. Binding of ^{125}I labelled FABP4 to β-cells in a saturable manner would indicate the presence of a cell surface receptor that specifically interacts with FABP4. If binding is non-saturable, this would indicate endocytic uptake of FABP4. In either case, there must be a specific cell surface binding protein to mediate this effect. The identity of this protein could be elucidated through co-immunoprecipitation combined with mass spectrometry. To determine whether the fatty acid cargo of FABP4 is of importance for an interaction with β-cells, the same binding studies should be performed comparing control and linoleate pre-incubated FABP4. Knowing whether linoleate stays in complex with or dissociates

away from FABP4 into the cell is important. If FABP4 is found to bind to a cell surface receptor, then recombinant FABP4 could be pre-incubated with ^{14}C labelled linoleate and used to treat β-cells. FABP4 carrying ^{14}C linoleate could be dissociated away from islets by competitive binding with "cold" (i.e. non-radioisotopic) FABP4-linoleate. If, after competitive binding and washing, radioactivity can be measured from β-cell lysates, then this indicates a dissociation of FABP4 from linoleate, which may be transported into the cell most likely via a cell surface channel. Data from these experiments will be essential in understanding the mechanism by which FABP4 exerts its effects. In particular, identification of the receptor for FABP4 and its tissue distribution will allow further elucidation of other physiological effects, as well as the signalling events that occur downstream of the receptor.

Adipose tissue as an endocrine organ?

As discussed earlier, extensive focus has been devoted to the role of adipose tissue as an endocrine organ. This focus is perhaps unjustified given the similar number of protein species that are secreted from other cell types measured here, including hepatocytes and endothelial cells. Production of adipokines is regulated at the level of transcription, whereas protein secretion from other "traditional" endocrine cell types is regulated at the level of the storage granule, which can be released in a matter of seconds. Cells that are traditionally viewed as having an endocrine role are professional secretors, and have an extensive ER-Golgi network. In light of this, the classification of adipose tissue as an endocrine organ is unusual. One exception to this conclusion is FABP4. As shown in Chapter 5 its secretion is regulated dynamically in a

manner not relying on changes in transcription. In fact, transcription of FABP4 was reduced during hypoxia, while secretion increased. This is evidence of FABP4 release in a temporal, regulated manner. This secretion occurs independently of the ER-Golgi pathway. FABP4 is an abundant protein in adipocytes, accounting for over 1% of total protein. In light of these data, it is possible that adipocytes are indeed “endocrine” in nature, principally due to their ability to regulate the secretion of fatty acid binding proteins from a readymade intracellular pool in a dynamic, temporal manner via this non classical secretory pathway. However, several facets of FABP regulation need to be clarified as described above before this conclusion can be made. , they can be stimulated to secrete a protein that acts distally to its tissue of origin from a readymade intracellular pool in a dynamic, temporal manner. Although adipocytes do not have the extensive ER-Golgi network of professional secretory cells, secretion of FABP4 occurs independently of these organelles. In light of these data, perhaps adipocytes can after all be considered an endocrine cell type.

Final conclusions

This study has shown that purification of N-glycosylated proteins from conditioned media is an ideal method for removing contaminating proteins and detecting low abundance secretory proteins. This method was used to survey the secretome of adipocytes to a greater depth than previous studies. The first ever screen of the hepatocyte and skeletal muscle secretome was performed. One of the proteins identified from the adipocyte screen, PEDF, is an anti-angiogenic adipocyte secretory protein that was found to play a role in obesity mediated insulin resistance.

Perhaps the most exciting part of this work was the observation that conditioned media from hypoxic adipocytes was able to enhance β cell function. The factor that was responsible for these effects was unknown. To probe this question, quantitative proteomics was used to identify this factor as fatty acid binding protein 4. The identification of FABP4 as a factor that was able to potentiate glucose stimulated insulin secretion from β-cells provided the first molecular details of why circulating insulin and β-cell mass correlate so strongly with adiposity. Taken as a whole, these data have led to novel and important insights into insulin resistance and obesity, and provide a resource of data for future investigations.

List of References

Adams, M., C. T. Montague, et al. (1997). "Activators of peroxisome proliferator-activated receptor gamma have depot-specific effects on human preadipocyte differentiation." J Clin Invest **100**(12): 3149-53.

Aebersold, R. and M. Mann (2003). "Mass spectrometry-based proteomics." Nature **422**(6928): 198-207.

Aguirre, V., T. Uchida, et al. (2000). "The c-Jun NH(2)-terminal kinase promotes insulin resistance during association with insulin receptor substrate-1 and phosphorylation of Ser(307)." J Biol Chem **275**(12): 9047-54.

Ahmed, A. M. (2002). "History of diabetes mellitus." Saudi Med J **23**(4): 373-8.

Alberdi, E., M. S. Aymerich, et al. (1999). "Binding of pigment epithelium-derived factor (PEDF) to retinoblastoma cells and cerebellar granule neurons. Evidence for a PEDF receptor." J Biol Chem **274**(44): 31605-12.

Alessi, M. C., M. Poggi, et al. (2007). "Plasminogen activator inhibitor-1, adipose tissue and insulin resistance." Curr Opin Lipidol **18**(3): 240-5.

Alter, L. L. L. T. G. L. E. L. J. E. H. D. N. J. D. A. (2007). "Thiazolidinediones and Cardiovascular Outcomes in Older Patients With Diabetes." Journal of the American Medical Association **298**(22): 2634-2643.

Alvarez-Llamas, G., E. Szalowska, et al. (2007). "Characterization of the Human Visceral Adipose Tissue Secretome." Mol Cell Proteomics **6**(4): 589-600.

Apte, R. S., R. A. Barreiro, et al. (2004). "Stimulation of neovascularization by the anti-angiogenic factor PEDF." Invest Ophthalmol Vis Sci **45**(12): 4491-7.

Arateus (1856). The Capadocian, the extant works. London.

Arita, Y., S. Kihara, et al. (1999). "Paradoxical decrease of an adipose-specific protein, adiponectin, in obesity." Biochem Biophys Res Commun **257**(1): 79-83.

Arkan, M. C., A. L. Hevener, et al. (2005). "IKK-beta links inflammation to obesity-induced insulin resistance." Nat Med **11**(2): 191-8.

Auth, D. and G. Brawerman (1992). "A 33-kDa polypeptide with homology to the laminin receptor: component of translation machinery." Proc Natl Acad Sci U S A **89**(10): 4368-72.

Aviles-Santa, L., J. Sinding, et al. (1999). "Effects of metformin in patients with poorly controlled, insulin-treated type 2 diabetes mellitus. A randomized, double-blind, placebo-controlled trial." Ann Intern Med **131**(3): 182-8.

Awasthi, Y. C., Y. Yang, et al. (2004). "Regulation of 4-hydroxynonenal-mediated signaling by glutathione S-transferases." Free Radic Biol Med **37**(5): 607-19.

Ayodele, O. E., C. O. Alebiosu, et al. (2004). "Diabetic nephropathy--a review of the natural history, burden, risk factors and treatment." J Natl Med Assoc **96**(11): 1445-54.

Bagdade, J. D., E. L. Bierman, et al. (1967). "The significance of basal insulin levels in the evaluation of the insulin response to glucose in diabetic and nondiabetic subjects." J Clin Invest **46**(10): 1549-57.

Bajaj, M., S. Suraamornkul, et al. (2005). "Effect of a sustained reduction in plasma free fatty acid concentration on intramuscular long-chain fatty Acyl-CoAs and insulin action in type 2 diabetic patients." Diabetes **54**(11): 3148-53.

Banting, F. G. (1937). "Early Work on Insulin." Science **85**(2217): 594-596.

Banting, F. G., C. H. Best, et al. (1991). "Pancreatic extracts in the treatment of diabetes mellitus: preliminary report. 1922." CMAJ **145**(10): 1281-6.

Barker, J. M. (2006). "Clinical review: Type 1 diabetes-associated autoimmunity: natural history, genetic associations, and screening." J Clin Endocrinol Metab **91**(4): 1210-7.

Barsky, S. H., C. N. Rao, et al. (1984). "Characterization of a laminin receptor from human breast carcinoma tissue." Breast Cancer Res Treat **4**(3): 181-8.

Bendtsen, J. D., L. J. Jensen, et al. (2004). "Feature-based prediction of non-classical and leaderless protein secretion." Protein Eng Des Sel **17**(4): 349-56.

Bendtsen, J. D., H. Nielsen, et al. (2004). "Improved prediction of signal peptides: SignalP 3.0." J Mol Biol **340**(4): 783-95.

Bennaars-Eiden, A., L. Higgins, et al. (2002). "Covalent modification of epithelial fatty acid-binding protein by 4-hydroxynonenal in vitro and in vivo. Evidence for a role in antioxidant biology." J Biol Chem **277**(52): 50693-702.

Bergenstal, R. M., C. Wysham, et al. "Efficacy and safety of exenatide once weekly versus sitagliptin or pioglitazone as an adjunct to metformin for treatment of type 2 diabetes (DURATION-2): a randomised trial." Lancet **376**(9739): 431-9.

Bernard, A., J. Gao-Li, et al. (2009). "Laminin receptor involvement in the anti-angiogenic activity of pigment epithelium-derived factor." J Biol Chem **284**(16): 10480-90.

Biron-Shental, T., W. T. Schaiff, et al. (2007). "Hypoxia regulates the expression of fatty acid-binding proteins in primary term human trophoblasts." Am J Obstet Gynecol **197**(5): 516 e1-6.

Bjorbaek, C., K. El-Haschimi, et al. (1999). "The role of SOCS-3 in leptin signaling and leptin resistance." J Biol Chem **274**(42): 30059-65.

Bjorntorp, P. (1990). "Abdominal obesity and risk." Clin Exp Hypertens A **12**(5): 783-94.

Bjorntorp, P. (1990). ""Portal" adipose tissue as a generator of risk factors for cardiovascular disease and diabetes." Arteriosclerosis **10**(4): 493-6.

Blobel, G. and B. Dobberstein (1975). "Transfer of proteins across membranes. I. Presence of proteolytically processed and unprocessed nascent immunoglobulin light chains on membrane-bound ribosomes of murine myeloma." J Cell Biol **67**(3): 835-51.

Blobel, G. and B. Dobberstein (1975). "Transfer of proteins across membranes. II. Reconstitution of functional rough microsomes from heterologous components." J Cell Biol **67**(3): 852-62.

Blom, N., T. Sicheritz-Ponten, et al. (2004). "Prediction of post-translational glycosylation and phosphorylation of proteins from the amino acid sequence." Proteomics **4**(6): 1633-49.

Bock, T., B. Pakkenberg, et al. (2003). "Increased islet volume but unchanged islet number in ob/ob mice." Diabetes **52**(7): 1716-22.

Boden, G. and X. Chen (1995). "Effects of fat on glucose uptake and utilization in patients with non-insulin-dependent diabetes." J Clin Invest **96**(3): 1261-8.

Boden, G., X. Chen, et al. (1995). "Effects of a 48-h fat infusion on insulin secretion and glucose utilization." Diabetes **44**(10): 1239-42.

Boden, G. and G. I. Shulman (2002). "Free fatty acids in obesity and type 2 diabetes: defining their role in the development of insulin resistance and beta-cell dysfunction." Eur J Clin Invest **32 Suppl 3**: 14-23.

Bolinder, J., L. Kager, et al. (1983). "Differences at the receptor and postreceptor levels between human omental and subcutaneous adipose tissue in the action of insulin on lipolysis." Diabetes **32**(2): 117-23.

Bost, F., M. Aouadi, et al. (2005). "The extracellular signal-regulated kinase isoform ERK1 is specifically required for in vitro and in vivo adipogenesis." Diabetes **54**(2): 402-11.

Boucher, J., D. Quilliot, et al. (2005). "Potential involvement of adipocyte insulin resistance in obesity-associated up-regulation of adipocyte lysophospholipase D/autotaxin expression." Diabetologia **48**(3): 569-77.

Brakenhielm, E. and Y. Cao (2008). "Angiogenesis in adipose tissue." Methods Mol Biol **456**: 65-81.

Brunt, E. M. "Pathology of nonalcoholic fatty liver disease." Nat Rev Gastroenterol Hepatol **7**(4): 195-203.

Bruun, J. M., A. S. Lihn, et al. (2004). "Higher production of IL-8 in visceral vs. subcutaneous adipose tissue. Implication of nonadipose cells in adipose tissue." Am J Physiol Endocrinol Metab **286**(1): E8-13.

Bruun, J. M., A. S. Lihn, et al. (2005). "Monocyte chemoattractant protein-1 release is higher in visceral than subcutaneous human adipose tissue (AT): implication of macrophages resident in the AT." J Clin Endocrinol Metab **90**(4): 2282-9.

Burns, T. W., B. E. Terry, et al. (1979). "Insulin inhibition of lipolysis of human adipocytes: the role of cyclic adenosine monophosphate." Diabetes **28**(11): 957-61.

Burton, P. B., C. E. Hogben, et al. (1994). "Heart fatty acid binding protein is a novel regulator of cardiac myocyte hypertrophy." Biochem Biophys Res Commun **205**(3): 1822-8.

Caballero, B. (2007). "The global epidemic of obesity: an overview." Epidemiol Rev **29**: 1-5.

Campfield, L. A., F. J. Smith, et al. (1995). "Recombinant mouse OB protein: evidence for a peripheral signal linking adiposity and central neural networks." Science **269**(5223): 546-9.

Cantley, J., C. Selman, et al. (2009). "Deletion of the von Hippel-Lindau gene in pancreatic beta cells impairs glucose homeostasis in mice." J Clin Invest **119**(1): 125-35.

Cao, Y. (2007). "Angiogenesis modulates adipogenesis and obesity." J Clin Invest **117**(9): 2362-8.

Carey, D. G., A. B. Jenkins, et al. (1996). "Abdominal fat and insulin resistance in normal and overweight women: Direct measurements reveal a strong relationship in subjects at both low and high risk of NIDDM." Diabetes **45**(5): 633-8.

Carey, D. G., T. V. Nguyen, et al. (1996). "Genetic influences on central abdominal fat: a twin study." Int J Obes Relat Metab Disord **20**(8): 722-6.

Celis, J. E., P. Gromov, et al. (2004). "Proteomic characterization of the interstitial fluid perfusing the breast tumor microenvironment: a novel resource for biomarker and therapeutic target discovery." Mol Cell Proteomics **3**(4): 327-44.

Chen, B., K. S. Lam, et al. (2006). "Hypoxia dysregulates the production of adiponectin and plasminogen activator inhibitor-1 independent of reactive oxygen species in adipocytes." Biochem Biophys Res Commun **341**(2): 549-56.

Chen, C., N. Pore, et al. (2001). "Regulation of glut1 mRNA by hypoxia-inducible factor-1. Interaction between H-ras and hypoxia." J Biol Chem **276**(12): 9519-25.

Chen, X., S. W. Cushman, et al. (2005). "Quantitative proteomic analysis of the secretory proteins from rat adipose cells using a 2D liquid chromatography-MS/MS approach." J Proteome Res **4**(2): 570-7.

Cheng, J. Z., R. Sharma, et al. (2001). "Accelerated metabolism and exclusion of 4-hydroxynonenal through induction of RLIP76 and hGST5.8 is an early adaptive response of cells to heat and oxidative stress." J Biol Chem **276**(44): 41213-23.

Chisholm, D. J., L. V. Campbell, et al. (1997). "Pathogenesis of the insulin resistance syndrome (syndrome X)." Clin Exp Pharmacol Physiol **24**(9-10): 782-4.

Chow, S. and P. Rodgers (2005). Extended Abstract: Constructing Area-Proportional Venn and Euler Diagrams with Three Circles. Euler Diagrams Workshop. Paris.

Christiaens, V. and H. R. Lijnen (2009). "Angiogenesis and development of adipose tissue." Mol Cell Endocrinol.

Chung, C., J. A. Doll, et al. (2008). "Anti-angiogenic pigment epithelium-derived factor regulates hepatocyte triglyceride content through adipose triglyceride lipase (ATGL)." J Hepatol **48**(3): 471-8.

Cinti, S., G. Mitchell, et al. (2005). "Adipocyte death defines macrophage localization and function in adipose tissue of obese mice and humans." J Lipid Res **46**(11): 2347-55.

Cohen, S. L., J. L. Halaas, et al. (1996). "Human leptin characterization." Nature **382**(6592): 589.

Colognato, H. and P. D. Yurchenco (2000). "Form and function: the laminin family of heterotrimers." Dev Dyn **218**(2): 213-34.
Considine, R. V., M. K. Sinha, et al. (1996). "Serum immunoreactive-leptin concentrations in normal-weight and obese humans." N Engl J Med **334**(5): 292-5.
Cook, K. S., H. Y. Min, et al. (1987). "Adipsin: a circulating serine protease homolog secreted by adipose tissue and sciatic nerve." Science **237**(4813): 402-5.
Corton, J. M., J. G. Gillespie, et al. (1995). "5-aminoimidazole-4-carboxamide ribonucleoside. A specific method for activating AMP-activated protein kinase in intact cells?" Eur J Biochem **229**(2): 558-65.
Crowe, S., S. M. Turpin, et al. (2008). "Metabolic remodeling in adipocytes promotes ciliary neurotrophic factor-mediated fat loss in obesity." Endocrinology **149**(5): 2546-56.
Crowe, S., L. E. Wu, et al. (2009). "Pigment epithelium-derived factor contributes to insulin resistance in obesity." Cell Metab **10**(1): 40-7.
Curat, C. A., V. Wegner, et al. (2006). "Macrophages in human visceral adipose tissue: increased accumulation in obesity and a source of resistin and visfatin." Diabetologia **49**(4): 744-7.
Daikoku, T., Y. Shinohara, et al. (1997). "Dramatic enhancement of the specific expression of the heart-type fatty acid binding protein in rat brown adipose tissue by cold exposure." FEBS Lett **410**(2-3): 383-6.
DeFronzo, R. A., E. Jacot, et al. (1981). "The effect of insulin on the disposal of intravenous glucose. Results from indirect calorimetry and hepatic and femoral venous catheterization." Diabetes **30**(12): 1000-7.
Dennis, G., Jr., B. T. Sherman, et al. (2003). "DAVID: Database for Annotation, Visualization, and Integrated Discovery." Genome Biol **4**(5): P3.
DiGirolamo, M., J. B. Fine, et al. (1998). "Qualitative regional differences in adipose tissue growth and cellularity in male Wistar rats fed ad libitum." Am J Physiol **274**(5 Pt 2): R1460-7.
Dinter, A. and E. G. Berger (1998). "Golgi-disturbing agents." Histochem Cell Biol **109**(5-6): 571-90.
Donath, M. Y., J. A. Ehses, et al. (2005). "Mechanisms of beta-cell death in type 2 diabetes." Diabetes **54 Suppl 2**: S108-13.
Drucker, D. J. (2006). "The biology of incretin hormones." Cell Metab **3**(3): 153-65.
Drucker, D. J. and M. A. Nauck (2006). "The incretin system: glucagon-like peptide-1 receptor agonists and dipeptidyl peptidase-4 inhibitors in type 2 diabetes." Lancet **368**(9548): 1696-705.
Duckworth, W. C., R. G. Bennett, et al. (1998). "Insulin degradation: progress and potential." Endocr Rev **19**(5): 608-24.
Duh, E. J., H. S. Yang, et al. (2002). "Pigment epithelium-derived factor suppresses ischemia-induced retinal neovascularization and VEGF-induced migration and growth." Invest Ophthalmol Vis Sci **43**(3): 821-9.
Engfeldt, P. and P. Arner (1988). "Lipolysis in human adipocytes, effects of cell size, age and of regional differences." Horm Metab Res Suppl **19**: 26-9.
Engstrom, G., B. Hedblad, et al. (2005). "Complement C3 is a risk factor for the development of diabetes: a population-based cohort study." Diabetes **54**(2): 570-5.
Fain, J. N., S. W. Bahouth, et al. (2004). "TNFalpha release by the nonfat cells of human adipose tissue." Int J Obes Relat Metab Disord **28**(4): 616-22.
Fain, J. N. and A. K. Madan (2005). "Regulation of monocyte chemoattractant protein 1 (MCP-1) release by explants of human visceral adipose tissue." Int J Obes (Lond) **29**(11): 1299-307.
Fain, J. N., A. K. Madan, et al. (2004). "Comparison of the release of adipokines by adipose tissue, adipose tissue matrix, and adipocytes from visceral and subcutaneous abdominal adipose tissues of obese humans." Endocrinology **145**(5): 2273-82.

Fazakerley, D. J., G. D. Holman, et al. (2009). "Kinetic evidence for unique regulation of GLUT4 trafficking by insulin and AMPK activators in l6 myotubes." J Biol Chem.

Febbraio, M. A. and B. K. Pedersen (2002). "Muscle-derived interleukin-6: mechanisms for activation and possible biological roles." FASEB J **16**(11): 1335-47.

Ferrannini, E., S. Camastra, et al. (2004). "beta-cell function in obesity: effects of weight loss." Diabetes **53 Suppl 3**: S26-33.

Ferrara, C. M. and A. P. Goldberg (2001). "Limited value of the homeostasis model assessment to predict insulin resistance in older men with impaired glucose tolerance." Diabetes Care **24**(2): 245-9.

Ferry, G., E. Tellier, et al. (2003). "Autotaxin is released from adipocytes, catalyzes lysophosphatidic acid synthesis, and activates preadipocyte proliferation. Up-regulated expression with adipocyte differentiation and obesity." J Biol Chem **278**(20): 18162-9.

Filleur, S., T. Nelius, et al. (2009). "Characterization of PEDF: a multi-functional serpin family protein." J Cell Biochem **106**(5): 769-75.

Flieger, O., A. Engling, et al. (2003). "Regulated secretion of macrophage migration inhibitory factor is mediated by a non-classical pathway involving an ABC transporter." FEBS Lett **551**(1-3): 78-86.

Flier, J. S., K. S. Cook, et al. (1987). "Severely impaired adipsin expression in genetic and acquired obesity." Science **237**(4813): 405-8.

Freeze, H. H. (2001). "Lectin affinity chromatography." Curr Protoc Protein Sci **Chapter 9**: Unit 9 1.

Fried, S. K., C. D. Russell, et al. (1993). "Lipoprotein lipase regulation by insulin and glucocorticoid in subcutaneous and omental adipose tissues of obese women and men." J Clin Invest **92**(5): 2191-8.

Friedman, J. M. and J. L. Halaas (1998). "Leptin and the regulation of body weight in mammals." Nature **395**(6704): 763-70.

Fruhbeck, G. (2008). Overview of Adipose Tissue and Its Role in Obesity and Metabolic Disorders. Adipose Tissue Protocols. K. Yang, Humana Press.

Fruhbeck, G., J. Gomez-Ambrosi, et al. (2001). "The adipocyte: a model for integration of endocrine and metabolic signaling in energy metabolism regulation." Am J Physiol Endocrinol Metab **280**(6): E827-47.

Frye, B. C., S. Halfter, et al. (2009). "Y-box protein-1 is actively secreted through a non-classical pathway and acts as an extracellular mitogen." EMBO Rep **10**(7): 783-9.

Fujiwara, Y., H. Ohata, et al. (1995). "Isolation of a candidate tumor suppressor gene on chromosome 8p21.3-p22 that is homologous to an extracellular domain of the PDGF receptor beta gene." Oncogene **10**(5): 891-5.

Fukuhara, A., M. Matsuda, et al. (2005). "Visfatin: a protein secreted by visceral fat that mimics the effects of insulin." Science **307**(5708): 426-30.

Furuhashi, M., G. Tuncman, et al. (2007). "Treatment of diabetes and atherosclerosis by inhibiting fatty-acid-binding protein aP2." Nature **447**(7147): 959-65.

Gabriely, I., X. H. Ma, et al. (2002). "Removal of visceral fat prevents insulin resistance and glucose intolerance of aging: an adipokine-mediated process?" Diabetes **51**(10): 2951-8.

Gale, E. A. (2001). "Lessons from the glitazones: a story of drug development." Lancet **357**(9271): 1870-5.

Galic, S., J. S. Oakhill, et al. (2009). "Adipose tissue as an endocrine organ." Mol Cell Endocrinol.

Galuska, D., J. Ryder, et al. (1998). "Insulin signaling and glucose transport in insulin resistant skeletal muscle. Special reference to GLUT4 transgenic and GLUT4 knockout mice." Adv Exp Med Biol **441**: 73-85.

Gan, S. K., A. D. Kriketos, et al. (2003). "Insulin action, regional fat, and myocyte lipid: altered relationships with increased adiposity." Obes Res **11**(11): 1295-305.

Gao, Z., D. Hwang, et al. (2002). "Serine phosphorylation of insulin receptor substrate 1 by inhibitor kappa B kinase complex." J Biol Chem **277**(50): 48115-21.
Gesta, S., M. Bluher, et al. (2006). "Evidence for a role of developmental genes in the origin of obesity and body fat distribution." Proc Natl Acad Sci U S A **103**(17): 6676-81.
Green, H. and M. Meuth (1974). "An established pre-adipose cell line and its differentiation in culture." Cell **3**(2): 127-33.
Grimsrud, P. A., M. J. Picklo, Sr., et al. (2007). "Carbonylation of adipose proteins in obesity and insulin resistance: identification of adipocyte fatty acid-binding protein as a cellular target of 4-hydroxynonenal." Mol Cell Proteomics **6**(4): 624-37.
Gualillo, O., J. R. Gonzalez-Juanatey, et al. (2007). "The emerging role of adipokines as mediators of cardiovascular function: physiologic and clinical perspectives." Trends Cardiovasc Med **17**(8): 275-83.
Guilherme, A., J. V. Virbasius, et al. (2008). "Adipocyte dysfunctions linking obesity to insulin resistance and type 2 diabetes." Nat Rev Mol Cell Biol **9**(5): 367-77.
Gungor, N., R. Saad, et al. (2004). "Validation of surrogate estimates of insulin sensitivity and insulin secretion in children and adolescents." J Pediatr **144**(1): 47-55.
Haffner, S. M. (2000). "Sex hormones, obesity, fat distribution, type 2 diabetes and insulin resistance: epidemiological and clinical correlation." Int J Obes Relat Metab Disord **24 Suppl 2**: S56-8.
Hagens, G., I. Masouye, et al. (1999). "Calcium-binding protein S100A7 and epidermal-type fatty acid-binding protein are associated in the cytosol of human keratinocytes." Biochem J **339 (Pt 2)**: 419-27.
Hagens, G., K. Roulin, et al. (1999). "Probable interaction between S100A7 and E-FABP in the cytosol of human keratinocytes from psoriatic scales." Mol Cell Biochem **192**(1-2): 123-8.
Halaas, J. L., K. S. Gajiwala, et al. (1995). "Weight-reducing effects of the plasma protein encoded by the obese gene." Science **269**(5223): 543-6.
Harman-Boehm, I., M. Bluher, et al. (2007). "Macrophage infiltration into omental versus subcutaneous fat across different populations: effect of regional adiposity and the comorbidities of obesity." J Clin Endocrinol Metab **92**(6): 2240-7.
He, G. P., A. Muise, et al. (1995). "A eukaryotic transcriptional repressor with carboxypeptidase activity." Nature **378**(6552): 92-6.
He, L., A. Sabet, et al. (2009). "Metformin and insulin suppress hepatic gluconeogenesis through phosphorylation of CREB binding protein." Cell **137**(4): 635-46.
Heineke, J. and J. D. Molkentin (2006). "Regulation of cardiac hypertrophy by intracellular signalling pathways." Nat Rev Mol Cell Biol **7**(8): 589-600.
Helenius, A. and M. Aebi (2004). "Roles of N-linked glycans in the endoplasmic reticulum." Annu Rev Biochem **73**: 1019-49.
Hennige, A. M., H. Staiger, et al. (2008). "Fetuin-A induces cytokine expression and suppresses adiponectin production." PLoS One **3**(3): e1765.
Hevener, A. L., W. He, et al. (2003). "Muscle-specific Pparg deletion causes insulin resistance." Nat Med **9**(12): 1491-7.
Hirosumi, J., G. Tuncman, et al. (2002). "A central role for JNK in obesity and insulin resistance." Nature **420**(6913): 333-6.
Hoehn, K. L., C. Hohnen-Behrens, et al. (2008). "IRS1-independent defects define major nodes of insulin resistance." Cell Metab **7**(5): 421-33.
Hoehn, K. L., A. B. Salmon, et al. (2009). "Insulin resistance is a cellular antioxidant defense mechanism." Proc Natl Acad Sci U S A **106**(42): 17787-92.
Holland, W. L., J. T. Brozinick, et al. (2007). "Inhibition of ceramide synthesis ameliorates glucocorticoid-, saturated-fat-, and obesity-induced insulin resistance." Cell Metab **5**(3): 167-79.

Horowitz, J. F., S. W. Coppack, et al. (1999). "Effect of short-term fasting on lipid kinetics in lean and obese women." Am J Physiol **276**(2 Pt 1): E278-84.
Hosogai, N., A. Fukuhara, et al. (2007). "Adipose tissue hypoxia in obesity and its impact on adipocytokine dysregulation." Diabetes **56**(4): 901-11.
Hotamisligil, G. S., P. Peraldi, et al. (1996). "IRS-1-mediated inhibition of insulin receptor tyrosine kinase activity in TNF-alpha- and obesity-induced insulin resistance." Science **271**(5249): 665-8.
Hotamisligil, G. S., N. S. Shargill, et al. (1993). "Adipose expression of tumor necrosis factor-alpha: direct role in obesity-linked insulin resistance." Science **259**(5091): 87-91.
Huang da, W., B. T. Sherman, et al. (2009). "Systematic and integrative analysis of large gene lists using DAVID bioinformatics resources." Nat Protoc **4**(1): 44-57.
Huppertz, C., C. Schwartz, et al. (1996). "Comparison of the effects of insulin, PDGF, interleukin-6, and interferon-gamma on glucose transport in 3T3-L1 cells: lack of cross-talk between tyrosine kinase receptors and JAK/STAT pathways." Diabetologia **39**(12): 1432-9.
Huse, D. M., G. Oster, et al. (1989). "The economic costs of non-insulin-dependent diabetes mellitus." JAMA **262**(19): 2708-13.
Huypens, P. R. (2007). "Leptin and adiponectin regulate compensatory beta cell growth in accordance to overweight." Med Hypotheses **68**(5): 1134-7.
Hyams, J. S., D. E. Carey, et al. (1986). "Type 1 procollagen as a biochemical marker of growth in children with inflammatory bowel disease." J Pediatr **109**(4): 619-24.
Ingalls, A. M., M. M. Dickie, et al. (1950). "Obese, a new mutation in the house mouse." J Hered **41**(12): 317-8.
Ishikawa, T., H. Esterbauer, et al. (1986). "Role of cardiac glutathione transferase and of the glutathione S-conjugate export system in biotransformation of 4-hydroxynonenal in the heart." J Biol Chem **261**(4): 1576-81.
Jackson, A., S. Friedman, et al. (1992). "Heat shock induces the release of fibroblast growth factor 1 from NIH 3T3 cells." Proc Natl Acad Sci U S A **89**(22): 10691-5.
James, D. E., M. Strube, et al. (1989). "Molecular cloning and characterization of an insulin-regulatable glucose transporter." Nature **338**(6210): 83-7.
Jenkins, A., S. X. Zhang, et al. (2008). "Increased serum pigment epithelium derived factor levels in Type 2 diabetes patients." Diabetes Res Clin Pract **82**(1): e5-7.
Jenkins, A. J., S. X. Zhang, et al. (2007). "Increased serum pigment epithelium-derived factor is associated with microvascular complications, vascular stiffness and inflammation in Type 1 diabetes." Diabet Med **24**(12): 1345-51.
Julenius, K., A. Molgaard, et al. (2005). "Prediction, conservation analysis, and structural characterization of mammalian mucin-type O-glycosylation sites." Glycobiology **15**(2): 153-64.
Jung, K., W. Cho, et al. (2009). "Glycoproteomics of plasma based on narrow selectivity lectin affinity chromatography." J Proteome Res **8**(2): 643-50.
Kadowaki, T., T. Yamauchi, et al. (2006). "Adiponectin and adiponectin receptors in insulin resistance, diabetes, and the metabolic syndrome." J Clin Invest **116**(7): 1784-92.
Kaji, H., H. Saito, et al. (2003). "Lectin affinity capture, isotope-coded tagging and mass spectrometry to identify N-linked glycoproteins." Nat Biotechnol **21**(6): 667-72.
Keller, M., A. Ruegg, et al. (2008). "Active caspase-1 is a regulator of unconventional protein secretion." Cell **132**(5): 818-31.
Kern, P. (2009). The RBP4 controversy. 69th Annual Sessions of the American Diabetes Association. New Orleans, LO, USA.
Khan, T., E. S. Muise, et al. (2009). "Metabolic dysregulation and adipose tissue fibrosis: role of collagen VI." Mol Cell Biol **29**(6): 1575-91.

Kieffer, T. J. and J. F. Habener (2000). "The adipoinsular axis: effects of leptin on pancreatic beta-cells." Am J Physiol Endocrinol Metab **278**(1): E1-E14.
Kim, Y. B., S. E. Nikoulina, et al. (1999). "Normal insulin-dependent activation of Akt/protein kinase B, with diminished activation of phosphoinositide 3-kinase, in muscle in type 2 diabetes." J Clin Invest **104**(6): 733-41.
Kissebah, A. H., N. Vydelingum, et al. (1982). "Relation of body fat distribution to metabolic complications of obesity." J Clin Endocrinol Metab **54**(2): 254-60.
Klein, S., L. Fontana, et al. (2004). "Absence of an effect of liposuction on insulin action and risk factors for coronary heart disease." N Engl J Med **350**(25): 2549-57.
Kloting, N., T. E. Graham, et al. (2007). "Serum retinol-binding protein is more highly expressed in visceral than in subcutaneous adipose tissue and is a marker of intra-abdominal fat mass." Cell Metab **6**(1): 79-87.
Kobayashi, K., T. M. Forte, et al. (2000). "The db/db mouse, a model for diabetic dyslipidemia: molecular characterization and effects of Western diet feeding." Metabolism **49**(1): 22-31.
Kohn, M. and R. Breinbauer (2004). "The Staudinger ligation-a gift to chemical biology." Angew Chem Int Ed Engl **43**(24): 3106-16.
Kolonin, M. G., P. K. Saha, et al. (2004). "Reversal of obesity by targeted ablation of adipose tissue." Nat Med **10**(6): 625-32.
Komiya, A., H. Suzuki, et al. (1997). "PRLTS gene alterations in human prostate cancer." Jpn J Cancer Res **88**(4): 389-93.
Kou, B., Y. Li, et al. (2004). "In vivo inhibition of tumor angiogenesis by a soluble VEGFR-2 fragment." Exp Mol Pathol **76**(2): 129-37.
Kovsan, J., A. Osnis, et al. (2009). "Depot-specific adipocyte cell lines reveal differential drug-induced responses of white adipocytes--relevance for partial lipodystrophy." Am J Physiol Endocrinol Metab **296**(2): E315-22.
Kraegen, E. W., D. E. James, et al. (1983). "In vivo insulin sensitivity in the rat determined by euglycemic clamp." Am J Physiol **245**(1): E1-7.
Kratchmarova, I., D. E. Kalume, et al. (2002). "A proteomic approach for identification of secreted proteins during the differentiation of 3T3-L1 preadipocytes to adipocytes." Mol Cell Proteomics **1**(3): 213-22.
Laakso, M. (1993). "How good a marker is insulin level for insulin resistance?" Am J Epidemiol **137**(9): 959-65.
Lago, F., C. Dieguez, et al. (2007). "The emerging role of adipokines as mediators of inflammation and immune responses." Cytokine Growth Factor Rev **18**(3-4): 313-25.
Lamounier-Zepter, V., C. Look, et al. (2009). "Adipocyte fatty acid-binding protein suppresses cardiomyocyte contraction: a new link between obesity and heart disease." Circ Res **105**(4): 326-34.
Langin, D., A. Dicker, et al. (2005). "Adipocyte lipases and defect of lipolysis in human obesity." Diabetes **54**(11): 3190-7.
Lara-Castro, C., N. Luo, et al. (2006). "Adiponectin multimeric complexes and the metabolic syndrome trait cluster." Diabetes **55**(1): 249-59.
Larance, M., G. Ramm, et al. (2005). "Characterization of the role of the Rab GTPase-activating protein AS160 in insulin-regulated GLUT4 trafficking." J Biol Chem **280**(45): 37803-13.
Larkin, M. A., G. Blackshields, et al. (2007). "Clustal W and Clustal X version 2.0." Bioinformatics **23**(21): 2947-8.
Lees, K. R., R. J. MacFadyen, et al. (1993). "Role of angiotensin in the extravascular system." J Hum Hypertens **7 Suppl 2**: S7-12.

Leng, Y., H. K. Karlsson, et al. (2004). "Insulin signaling defects in type 2 diabetes." Rev Endocr Metab Disord **5**(2): 111-7.
Li, Y., X. Ye, et al. (2009). "Axl as a potential therapeutic target in cancer: role of Axl in tumor growth, metastasis and angiogenesis." Oncogene **28**(39): 3442-55.
Li, Z. Z., M. Berk, et al. (2009). "Hepatic lipid partitioning and liver damage in nonalcoholic fatty liver disease: role of stearoyl-CoA desaturase." J Biol Chem **284**(9): 5637-44.
Lihn, A. S., J. M. Bruun, et al. (2004). "Lower expression of adiponectin mRNA in visceral adipose tissue in lean and obese subjects." Mol Cell Endocrinol **219**(1-2): 9-15.
Lindenbach, B. D., M. J. Evans, et al. (2005). "Complete replication of hepatitis C virus in cell culture." Science **309**(5734): 623-6.
Lis, H. and N. Sharon (1993). "Protein glycosylation. Structural and functional aspects." Eur J Biochem **218**(1): 1-27.
Liu, B., K. W. Lee, et al. (2007). "Insulin-like growth factor-binding protein-3 inhibition of prostate cancer growth involves suppression of angiogenesis." Oncogene **26**(12): 1811-9.
Locksley, R. M., N. Killeen, et al. (2001). "The TNF and TNF receptor superfamilies: integrating mammalian biology." Cell **104**(4): 487-501.
Lodish, H. (2003). Molecular Cell Biology. New York, WH Freeman.
Lokker, N. A., J. P. O'Hare, et al. (1997). "Functional importance of platelet-derived growth factor (PDGF) receptor extracellular immunoglobulin-like domains. Identification of PDGF binding site and neutralizing monoclonal antibodies." J Biol Chem **272**(52): 33037-44.
Luft, R. (1989). "Oskar Minkowski: discovery of the pancreatic origin of diabetes, 1889." Diabetologia **32**(7): 399-401.
Lumeng, C. N., S. M. Deyoung, et al. (2007). "Increased inflammatory properties of adipose tissue macrophages recruited during diet-induced obesity." Diabetes **56**(1): 16-23.
MacDougald, O. A., C. S. Hwang, et al. (1995). "Regulated expression of the obese gene product (leptin) in white adipose tissue and 3T3-L1 adipocytes." Proc Natl Acad Sci U S A **92**(20): 9034-7.
MacDougald, O. A. and M. D. Lane (1995). "Adipocyte differentiation. When precursors are also regulators." Curr Biol **5**(6): 618-21.
MacDougald, O. A. and M. D. Lane (1995). "Transcriptional regulation of gene expression during adipocyte differentiation." Annu Rev Biochem **64**: 345-73.
Maeda, K., H. Cao, et al. (2005). "Adipocyte/macrophage fatty acid binding proteins control integrated metabolic responses in obesity and diabetes." Cell Metab **1**(2): 107-19.
Maeda, N., I. Shimomura, et al. (2002). "Diet-induced insulin resistance in mice lacking adiponectin/ACRP30." Nat Med **8**(7): 731-7.
Majdalawieh, A., L. Zhang, et al. (2006). "Adipocyte enhancer-binding protein 1 is a potential novel atherogenic factor involved in macrophage cholesterol homeostasis and inflammation." Proc Natl Acad Sci U S A **103**(7): 2346-51.
Makowski, L., K. C. Brittingham, et al. (2005). "The fatty acid-binding protein, aP2, coordinates macrophage cholesterol trafficking and inflammatory activity. Macrophage expression of aP2 impacts peroxisome proliferator-activated receptor gamma and IkappaB kinase activities." J Biol Chem **280**(13): 12888-95.
Mandinova, A., R. Soldi, et al. (2003). "S100A13 mediates the copper-dependent stress-induced release of IL-1alpha from both human U937 and murine NIH 3T3 cells." J Cell Sci **116**(Pt 13): 2687-96.
Matthews, D. R., J. P. Hosker, et al. (1985). "Homeostasis model assessment: insulin resistance and beta-cell function from fasting plasma glucose and insulin concentrations in man." Diabetologia **28**(7): 412-9.
Maury, E. and S. M. Brichard "Adipokine dysregulation, adipose tissue inflammation and metabolic syndrome." Mol Cell Endocrinol **314**(1): 1-16.

Merrill, G. F., E. J. Kurth, et al. (1997). "AICA riboside increases AMP-activated protein kinase, fatty acid oxidation, and glucose uptake in rat muscle." Am J Physiol **273**(6 Pt 1): E1107-12.
Milner, K. L., D. van der Poorten, et al. (2009). "Chronic Hepatitis C is Associated with Peripheral rather than Hepatic Insulin Resistance." Gastroenterology.
Miyagi, M. and K. C. Rao (2007). "Proteolytic 18O-labeling strategies for quantitative proteomics." Mass Spectrom Rev **26**(1): 121-36.
Molina, H., Y. Yang, et al. (2009). "Temporal profiling of the adipocyte proteome during differentiation using a five-plex SILAC based strategy." J Proteome Res **8**(1): 48-58.
Mori, Y., Y. Murakawa, et al. (1999). "Effect of troglitazone on body fat distribution in type 2 diabetic patients." Diabetes Care **22**(6): 908-12.
Motani, A., Z. Wang, et al. (2009). "Identification and characterization of a non-retinoid ligand for retinol-binding protein 4 which lowers serum retinol-binding protein 4 levels in vivo." J Biol Chem **284**(12): 7673-80.
Mouta Carreira, C., M. Landriscina, et al. (2001). "The comparative release of FGF1 by hypoxia and temperature stress." Growth Factors **18**(4): 277-85.
Nakabayashi, H., K. Taketa, et al. (1982). "Growth of human hepatoma cells lines with differentiated functions in chemically defined medium." Cancer Res **42**(9): 3858-63.
Nathan, D. M. (2002). "Clinical review 146: The impact of clinical trials on the treatment of diabetes mellitus." J Clin Endocrinol Metab **87**(5): 1929-37.
Ng, Y., G. Ramm, et al. (2008). "Rapid activation of Akt2 is sufficient to stimulate GLUT4 translocation in 3T3-L1 adipocytes." Cell Metab **7**(4): 348-56.
Nickel, W. and C. Rabouille (2009). "Mechanisms of regulated unconventional protein secretion." Nat Rev Mol Cell Biol **10**(2): 148-55.
Nielsen, S., Z. Guo, et al. (2004). "Splanchnic lipolysis in human obesity." J Clin Invest **113**(11): 1582-8.
Nisbet, J. C., J. M. Sturtevant, et al. (2004). "Metformin and serious adverse effects." Med J Aust **180**(2): 53-4.
Notari, L., V. Baladron, et al. (2006). "Identification of a lipase-linked cell membrane receptor for pigment epithelium-derived factor." J Biol Chem **281**(49): 38022-37.
O'Neill, L. A. (2000). "The interleukin-1 receptor/Toll-like receptor superfamily: signal transduction during inflammation and host defense." Sci STKE **2000**(44): re1.
O'Quinn, P. R., D. A. Knabe, et al. (2002). "Arginine catabolism in lactating porcine mammary tissue." J Anim Sci **80**(2): 467-74.
Ogata, N., M. Matsuoka, et al. (2007). "Plasma concentration of pigment epithelium-derived factor in patients with diabetic retinopathy." J Clin Endocrinol Metab **92**(3): 1176-9.
Ogden, C. L., M. D. Carroll, et al. (2006). "Prevalence of overweight and obesity in the United States, 1999-2004." JAMA **295**(13): 1549-55.
Okada, T., H. Nishizawa, et al. (2008). "URB is abundantly expressed in adipose tissue and dysregulated in obesity." Biochem Biophys Res Commun **367**(2): 370-6.
Ong, S. E., B. Blagoev, et al. (2002). "Stable isotope labeling by amino acids in cell culture, SILAC, as a simple and accurate approach to expression proteomics." Mol Cell Proteomics **1**(5): 376-86.
Ong, S. E., I. Kratchmarova, et al. (2003). "Properties of 13C-substituted arginine in stable isotope labeling by amino acids in cell culture (SILAC)." J Proteome Res **2**(2): 173-81.
Ornitz, D. M. and N. Itoh (2001). "Fibroblast growth factors." Genome Biol **2**(3): REVIEWS3005.
Ort, T., A. A. Arjona, et al. (2005). "Recombinant human FIZZ3/resistin stimulates lipolysis in cultured human adipocytes, mouse adipose explants, and normal mice." Endocrinology **146**(5): 2200-9.
Ostrowski, K., T. Rohde, et al. (1998). "Evidence that interleukin-6 is produced in human skeletal muscle during prolonged running." J Physiol **508 (Pt 3)**: 949-53.

Pajvani, U. B., X. Du, et al. (2003). "Structure-function studies of the adipocyte-secreted hormone Acrp30/adiponectin. Implications fpr metabolic regulation and bioactivity." J Biol Chem **278**(11): 9073-85.

Park, S. J., S. H. Baek, et al. (2009). "Enhancement of angiogenic and vasculogenic potential of endothelial progenitor cells by haptoglobin." FEBS Lett **583**(19): 3235-40.

Plomgaard, P., C. P. Fischer, et al. (2008). "Tumor necrosis factor-alpha modulates human in vivo lipolysis." J Clin Endocrinol Metab **93**(2): 543-9.

Poitout, V. and R. P. Robertson (2002). "Minireview: Secondary beta-cell failure in type 2 diabetes--a convergence of glucotoxicity and lipotoxicity." Endocrinology **143**(2): 339-42.

Prudovsky, I., A. Mandinova, et al. (2003). "The non-classical export routes: FGF1 and IL-1alpha point the way." J Cell Sci **116**(Pt 24): 4871-81.

Quillen, D. M. and L. Kuritzky (2002). "Type 2 diabetes management: a comprehensive clinical review of oral medications." Compr Ther **28**(1): 50-61.

Rabe, K., M. Lehrke, et al. (2008). "Adipokines and insulin resistance." Mol Med **14**(11-12): 741-51.

Reaven, G. M. (1995). "Pathophysiology of insulin resistance in human disease." Physiol Rev **75**(3): 473-86.

Rebuffe-Scrive, M., M. Bronnegard, et al. (1990). "Steroid hormone receptors in human adipose tissues." J Clin Endocrinol Metab **71**(5): 1215-9.

Recklies, A. D., H. Ling, et al. (2005). "Inflammatory cytokines induce production of CHI3L1 by articular chondrocytes." J Biol Chem **280**(50): 41213-21.

Reiness, C. G., M. J. Seppa, et al. (2001). "Chick ciliary neurotrophic factor is secreted via a nonclassical pathway." Mol Cell Neurosci **17**(6): 931-44.

Revollo JR, K. A., Mills KF, Satoh A, Wang T, Garten A, Dasgupta B, Sasaki Y, Wolberger C, Townsend RR, Milbrandt J, Kiess W, Imai S (2007). "Nampt/PBEF/Visfatin regulates insulin secretion in beta cells as a systemic NAD biosynthetic enzyme." Cell Metabolism **6**(5): 363-75.

Reynisdottir, S., K. Ellerfeldt, et al. (1994). "Multiple lipolysis defects in the insulin resistance (metabolic) syndrome." J Clin Invest **93**(6): 2590-9.

Ro, H. S., S. W. Kim, et al. (2001). "Gene structure and expression of the mouse adipocyte enhancer-binding protein." Gene **280**(1-2): 123-33.

Ro, H. S., L. Zhang, et al. (2007). "Adipocyte enhancer-binding protein 1 modulates adiposity and energy homeostasis." Obesity (Silver Spring) **15**(2): 288-302.

Roelofsen, H., M. Dijkstra, et al. (2009). "Comparison of isotope-labeled amino acid incorporation rates (CILAIR) provides a quantitative method to study tissue secretomes." Mol Cell Proteomics **8**(2): 316-24.

Rohrer, B., Q. Long, et al. (2009). "A targeted inhibitor of the alternative complement pathway reduces angiogenesis in a mouse model of age-related macular degeneration." Invest Ophthalmol Vis Sci **50**(7): 3056-64.

Rorsman, P. (2005). "Insulin Secretion: Function and Therapy of Pancreatic Beta-Cells in Diabetes." British Journal of Diabetes and Vascular Disease **187**(5): 187-191.

Rosen, E. D. and B. M. Spiegelman (2006). "Adipocytes as regulators of energy balance and glucose homeostasis." Nature **444**(7121): 847-53.

Ross, P. L., Y. N. Huang, et al. (2004). "Multiplexed protein quantitation in Saccharomyces cerevisiae using amine-reactive isobaric tagging reagents." Mol Cell Proteomics **3**(12): 1154-69.

Ruan, H., M. J. Zarnowski, et al. (2003). "Standard isolation of primary adipose cells from mouse epididymal fat pads induces inflammatory mediators and down-regulates adipocyte genes." J Biol Chem **278**(48): 47585-93.

Ruse, M., A. M. Broome, et al. (2003). "S100A7 (psoriasin) interacts with epidermal fatty acid binding protein and localizes in focal adhesion-like structures in cultured keratinocytes." J Invest Dermatol **121**(1): 132-41.

Ryden, M. and P. Arner (2007). "Tumour necrosis factor-alpha in human adipose tissue -- from signalling mechanisms to clinical implications." J Intern Med **262**(4): 431-8.

Said, G. (2007). "Diabetic neuropathy--a review." Nat Clin Pract Neurol **3**(6): 331-40.

Saltiel, A. R. and C. R. Kahn (2001). "Insulin signalling and the regulation of glucose and lipid metabolism." Nature **414**(6865): 799-806.

Santamaria-Kisiel, L., A. C. Rintala-Dempsey, et al. (2006). "Calcium-dependent and -independent interactions of the S100 protein family." Biochem J **396**(2): 201-14.

Savage, D. B., K. F. Petersen, et al. (2007). "Disordered lipid metabolism and the pathogenesis of insulin resistance." Physiol Rev **87**(2): 507-20.

Saxon, E., S. J. Luchansky, et al. (2002). "Investigating cellular metabolism of synthetic azidosugars with the Staudinger ligation." J Am Chem Soc **124**(50): 14893-902.

Schafer, T., H. Zentgraf, et al. (2004). "Unconventional secretion of fibroblast growth factor 2 is mediated by direct translocation across the plasma membrane of mammalian cells." J Biol Chem **279**(8): 6244-51.

Schaur, R. J. (2003). "Basic aspects of the biochemical reactivity of 4-hydroxynonenal." Mol Aspects Med **24**(4-5): 149-59.

Scheel, T. K., J. M. Gottwein, et al. (2008). "Development of JFH1-based cell culture systems for hepatitis C virus genotype 4a and evidence for cross-genotype neutralization." Proc Natl Acad Sci U S A **105**(3): 997-1002.

Scheele, G., B. Dobberstein, et al. (1978). "Transfer of proteins across membranes, Biosynthesis in vitro of pretrypsinogen and trypsinogen by cell fractions of canine pancreas." Eur J Biochem **82**(2): 593-9.

Scheja, L., L. Makowski, et al. (1999). "Altered insulin secretion associated with reduced lipolytic efficiency in aP2-/- mice." Diabetes **48**(10): 1987-94.

Schmitz-Peiffer, C., D. L. Craig, et al. (1999). "Ceramide generation is sufficient to account for the inhibition of the insulin-stimulated PKB pathway in C2C12 skeletal muscle cells pretreated with palmitate." J Biol Chem **274**(34): 24202-10.

Schneider, C., K. A. Tallman, et al. (2001). "Two distinct pathways of formation of 4-hydroxynonenal. Mechanisms of nonenzymatic transformation of the 9- and 13-hydroperoxides of linoleic acid to 4-hydroxyalkenals." J Biol Chem **276**(24): 20831-8.

Shental-Bechor, D. and Y. Levy (2008). "Effect of glycosylation on protein folding: a close look at thermodynamic stabilization." Proc Natl Acad Sci U S A **105**(24): 8256-61.

Shi, H., A. D. Strader, et al. (2007). "The effect of fat removal on glucose tolerance is depot specific in male and female mice." Am J Physiol Endocrinol Metab **293**(4): E1012-20.

Shin, J. T., S. R. Opalenik, et al. (1996). "Serum-starvation induces the extracellular appearance of FGF-1." Biochim Biophys Acta **1312**(1): 27-38.

Silha, J. V., M. Krsek, et al. (2005). "Angiogenic factors are elevated in overweight and obese individuals." Int J Obes (Lond) **29**(11): 1308-14.

Simpson, M. A., V. J. LiCata, et al. (1999). "Biochemical and biophysical analysis of the intracellular lipid binding proteins of adipocytes." Mol Cell Biochem **192**(1-2): 33-40.

Smith, O. L. (1984). "Insulin response in rats acutely exposed to cold." Can J Physiol Pharmacol **62**(8): 924-7.

Snijder, M. B., J. M. Dekker, et al. (2003). "Associations of hip and thigh circumferences independent of waist circumference with the incidence of type 2 diabetes: the Hoorn Study." Am J Clin Nutr **77**(5): 1192-7.

Snijder, M. B., J. M. Dekker, et al. (2003). "Larger thigh and hip circumferences are associated with better glucose tolerance: the Hoorn study." Obes Res **11**(1): 104-11.
Spiegelman, B. M. (1998). "PPAR-gamma: adipogenic regulator and thiazolidinedione receptor." Diabetes **47**(4): 507-14.
Stahl, N. and G. D. Yancopoulos (1994). "The tripartite CNTF receptor complex: activation and signaling involves components shared with other cytokines." J Neurobiol **25**(11): 1454-66.
Steensberg, A., C. Keller, et al. (2002). "IL-6 and TNF-alpha expression in, and release from, contracting human skeletal muscle." Am J Physiol Endocrinol Metab **283**(6): E1272-8.
Stefan, N., A. M. Hennige, et al. (2006). "Alpha2-Heremans-Schmid glycoprotein/fetuin-A is associated with insulin resistance and fat accumulation in the liver in humans." Diabetes Care **29**(4): 853-7.
Steinberg, G. R., B. E. Kemp, et al. (2007). "Adipocyte triglyceride lipase expression in human obesity." Am J Physiol Endocrinol Metab **293**(4): E958-64.
Steppan, C. M., S. T. Bailey, et al. (2001). "The hormone resistin links obesity to diabetes." Nature **409**(6818): 307-12.
Stratton, I. M., A. I. Adler, et al. (2000). "Association of glycaemia with macrovascular and microvascular complications of type 2 diabetes (UKPDS 35): prospective observational study." BMJ **321**(7258): 405-12.
Su, A. I., T. Wiltshire, et al. (2004). "A gene atlas of the mouse and human protein-encoding transcriptomes." Proc Natl Acad Sci U S A **101**(16): 6062-7.
Susulic, V. S., R. C. Frederich, et al. (1995). "Targeted disruption of the beta 3-adrenergic receptor gene." J Biol Chem **270**(49): 29483-92.
Takahashi, K., K. Miyakawa, et al. (1998). "Effects of granulocyte/macrophage colony-stimulating factor on the development and differentiation of CD5-positive macrophages and their potential derivation from a CD5-positive B-cell lineage in mice." Am J Pathol **152**(2): 445-56.
Taniguchi, C. M., B. Emanuelli, et al. (2006). "Critical nodes in signalling pathways: insights into insulin action." Nat Rev Mol Cell Biol **7**(2): 85-96.
Thorne, A., F. Lonnqvist, et al. (2002). "A pilot study of long-term effects of a novel obesity treatment: omentectomy in connection with adjustable gastric banding." Int J Obes Relat Metab Disord **26**(2): 193-9.
Tiidus, P. (2008). Skeletal muscle damage and repair.
Tilg, H. and A. R. Moschen (2006). "Adipocytokines: mediators linking adipose tissue, inflammation and immunity." Nat Rev Immunol **6**(10): 772-83.
Togashi, M. S., H; Iwamoto, Y (2002). "Insulin Secretion in Response to .BETA.3-Adrenergic Receptor Agonist AJ-9677 Is Mainly Stimulated by the Factor other than Free Fatty Acids." Biomed Res **23**(1): 23-28.
Tombran-Tink, J. and C. J. Barnstable (2003). "PEDF: a multifaceted neurotrophic factor." Nat Rev Neurosci **4**(8): 628-36.
Trayhurn, P., B. Wang, et al. (2008). "Hypoxia in adipose tissue: a basis for the dysregulation of tissue function in obesity?" Br J Nutr **100**(2): 227-35.
Trujillo, M. E. and P. E. Scherer (2006). "Adipose tissue-derived factors: impact on health and disease." Endocr Rev **27**(7): 762-78.
Unger, R. H. (2003). "Minireview: weapons of lean body mass destruction: the role of ectopic lipids in the metabolic syndrome." Endocrinology **144**(12): 5159-65.
Vague, J. (1956). "The degree of masculine differentiation of obesities: a factor determining predisposition to diabetes, atherosclerosis, gout, and uric calculous disease." Am J Clin Nutr **4**(1): 20-34.
Van Harmelen, V., S. Reynisdottir, et al. (1998). "Leptin secretion from subcutaneous and visceral adipose tissue in women." Diabetes **47**(6): 913-7.

Vaziri, C. and D. V. Faller (1996). "Down-regulation of platelet-derived growth factor receptor expression during terminal differentiation of 3T3-L1 pre-adipocyte fibroblasts." J Biol Chem **271**(23): 13642-8.

Venkatesha, S., J. Hanai, et al. (2006). "Lipocalin 2 antagonizes the proangiogenic action of ras in transformed cells." Mol Cancer Res **4**(11): 821-9.

Vocadlo, D. J., H. C. Hang, et al. (2003). "A chemical approach for identifying O-GlcNAc-modified proteins in cells." Proc Natl Acad Sci U S A **100**(16): 9116-21.

Voros, G., E. Maquoi, et al. (2005). "Modulation of angiogenesis during adipose tissue development in murine models of obesity." Endocrinology **146**(10): 4545-54.

Wajchenberg, B. L. (2000). "Subcutaneous and visceral adipose tissue: their relation to the metabolic syndrome." Endocr Rev **21**(6): 697-738.

Wakita, T., T. Pietschmann, et al. (2005). "Production of infectious hepatitis C virus in tissue culture from a cloned viral genome." Nat Med **11**(7): 791-6.

Wang, P., E. Mariman, et al. (2004). "Profiling of the secreted proteins during 3T3-L1 adipocyte differentiation leads to the identification of novel adipokines." Cell Mol Life Sci **61**(18): 2405-17.

Wang, Y., K. S. Lam, et al. (2007). "Lipocalin-2 is an inflammatory marker closely associated with obesity, insulin resistance, and hyperglycemia in humans." Clin Chem **53**(1): 34-41.

Wang, Z. V., T. D. Schraw, et al. (2007). "Secretion of the adipocyte-specific secretory protein adiponectin critically depends on thiol-mediated protein retention." Mol Cell Biol **27**(10): 3716-31.

Watt, M. J., A. G. Holmes, et al. (2006). "Regulation of HSL serine phosphorylation in skeletal muscle and adipose tissue." Am J Physiol Endocrinol Metab **290**(3): E500-8.

Wei, Y., D. Wang, et al. (2006). "Saturated fatty acids induce endoplasmic reticulum stress and apoptosis independently of ceramide in liver cells." Am J Physiol Endocrinol Metab **291**(2): E275-81.

Weigle, D. S., A. M. Hutson, et al. (1998). "Leptin does not fully account for the satiety activity of adipose tissue-conditioned medium." Am J Physiol **275**(4 Pt 2): R976-85.

Weisberg, S. P., D. McCann, et al. (2003). "Obesity is associated with macrophage accumulation in adipose tissue." J Clin Invest **112**(12): 1796-808.

Wellen, K. E. and G. S. Hotamisligil (2005). "Inflammation, stress, and diabetes." J Clin Invest **115**(5): 1111-9.

Wessel, D. and U. I. Flugge (1984). "A method for the quantitative recovery of protein in dilute solution in the presence of detergents and lipids." Anal Biochem **138**(1): 141-3.

Wolfe, R. R., E. J. Peters, et al. (1987). "Effect of short-term fasting on lipolytic responsiveness in normal and obese human subjects." Am J Physiol **252**(2 Pt 1): E189-96.

Xu, A., Y. Wang, et al. (2006). "Adipocyte fatty acid-binding protein is a plasma biomarker closely associated with obesity and metabolic syndrome." Clin Chem **52**(3): 405-13.

Xu, H., G. T. Barnes, et al. (2003). "Chronic inflammation in fat plays a crucial role in the development of obesity-related insulin resistance." J Clin Invest **112**(12): 1821-30.

Xu, H., K. T. Uysal, et al. (2002). "Altered tumor necrosis factor-alpha (TNF-alpha) processing in adipocytes and increased expression of transmembrane TNF-alpha in obesity." Diabetes **51**(6): 1876-83.

Yamada S, O. P., Kennedy DL, Whayne TF (1979). "The effects of dexamethasone on metabolic activity of hepatocytes in primary monolayer culture." In Vitro Cellular & Developmental Biology - Plant **16**(7): 559-570.

Yamagishi, S., H. Adachi, et al. (2006). "Elevated serum levels of pigment epithelium-derived factor in the metabolic syndrome." J Clin Endocrinol Metab **91**(6): 2447-50.

Yamauchi, T., J. Kamon, et al. (2003). "Cloning of adiponectin receptors that mediate antidiabetic metabolic effects." Nature **423**(6941): 762-9.

Yamauchi, T., J. Kamon, et al. (2002). "Adiponectin stimulates glucose utilization and fatty-acid oxidation by activating AMP-activated protein kinase." Nat Med **8**(11): 1288-95.

Yan, Q. W., Q. Yang, et al. (2007). "The adipokine lipocalin 2 is regulated by obesity and promotes insulin resistance." Diabetes **56**(10): 2533-40.

Yang, Q., T. E. Graham, et al. (2005). "Serum retinol binding protein 4 contributes to insulin resistance in obesity and type 2 diabetes." Nature **436**(7049): 356-62.

Yao-Borengasser, A., V. Varma, et al. (2007). "Retinol binding protein 4 expression in humans: relationship to insulin resistance, inflammation, and response to pioglitazone." J Clin Endocrinol Metab **92**(7): 2590-7.

Ye, J. (2009). "Emerging role of adipose tissue hypoxia in obesity and insulin resistance." Int J Obes (Lond) **33**(1): 54-66.

Ye, J., Z. Gao, et al. (2007). "Hypoxia is a potential risk factor for chronic inflammation and adiponectin reduction in adipose tissue of ob/ob and dietary obese mice." Am J Physiol Endocrinol Metab **293**(4): E1118-28.

Yin, J., Z. Gao, et al. (2009). "Role of hypoxia in obesity-induced disorders of glucose and lipid metabolism in adipose tissue." Am J Physiol Endocrinol Metab **296**(2): E333-42.

Yoneda, M., S. Saito, et al. (2007). "Hepatitis C virus directly associates with insulin resistance independent of the visceral fat area in nonobese and nondiabetic patients." J Viral Hepat **14**(9): 600-7.

Yu, C., Y. Chen, et al. (2002). "Mechanism by which fatty acids inhibit insulin activation of insulin receptor substrate-1 (IRS-1)-associated phosphatidylinositol 3-kinase activity in muscle." J Biol Chem **277**(52): 50230-6.

Zehe, C., A. Engling, et al. (2006). "Cell-surface heparan sulfate proteoglycans are essential components of the unconventional export machinery of FGF-2." Proc Natl Acad Sci U S A **103**(42): 15479-84.

Zeng, Y., T. N. Ramya, et al. (2009). "High-efficiency labeling of sialylated glycoproteins on living cells." Nat Methods **6**(3): 207-9.

Zhang, H., X. J. Li, et al. (2003). "Identification and quantification of N-linked glycoproteins using hydrazide chemistry, stable isotope labeling and mass spectrometry." Nat Biotechnol **21**(6): 660-6.

Zhong, J., P. Gastaminza, et al. (2005). "Robust hepatitis C virus infection in vitro." Proc Natl Acad Sci U S A **102**(26): 9294-9.

Zhou, G., R. Myers, et al. (2001). "Role of AMP-activated protein kinase in mechanism of metformin action." J Clin Invest **108**(8): 1167-74.

Zvonic, S., M. Lefevre, et al. (2007). "Secretome of primary cultures of human adipose-derived stem cells: modulation of serpins by adipogenesis." Mol Cell Proteomics **6**(1): 18-28.